RCA Engineer

Vol. 27 No. 5 Sept./Oct. 1982

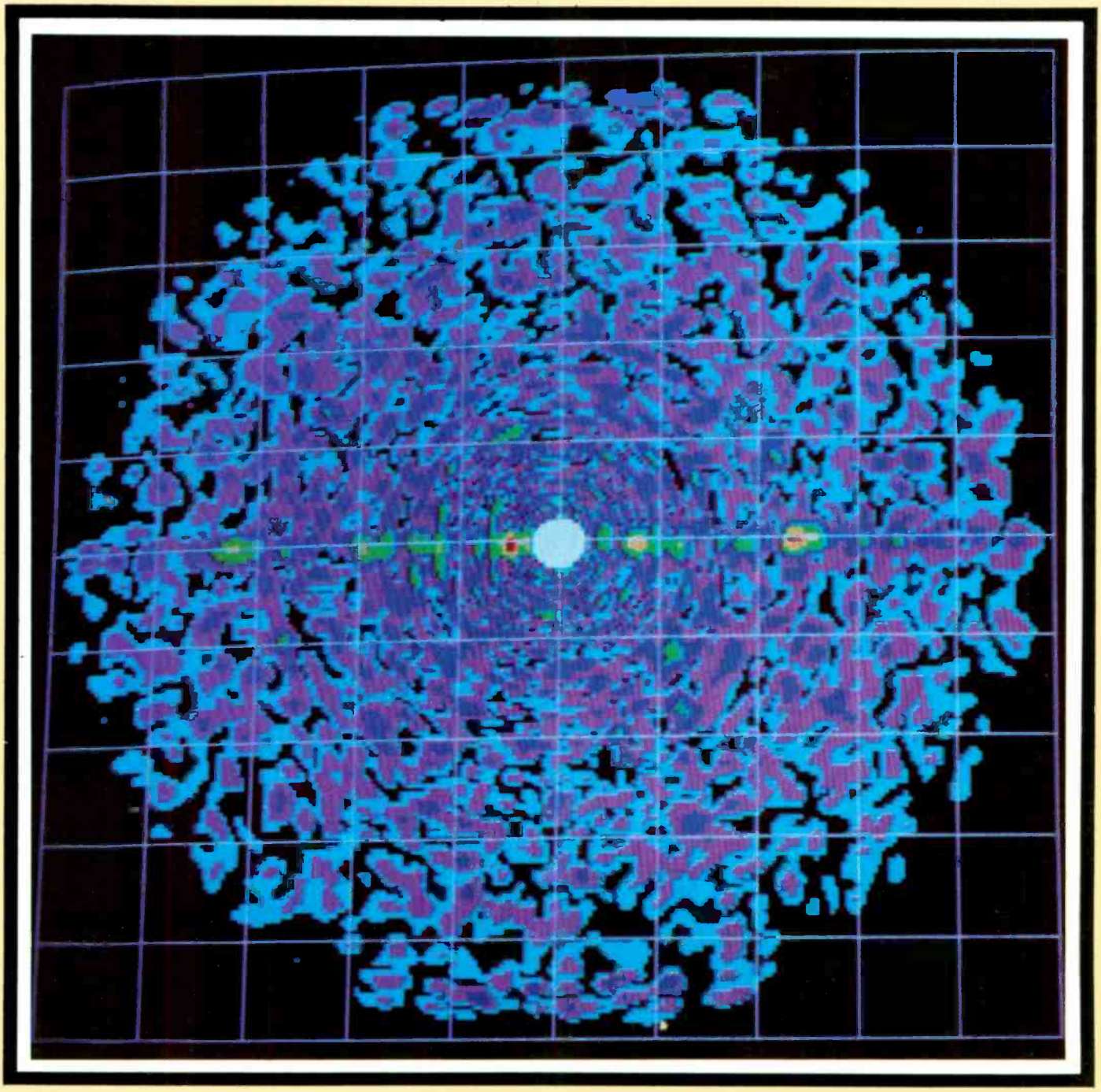

Microwave Technology

Cover photo by Ken Kleindienst

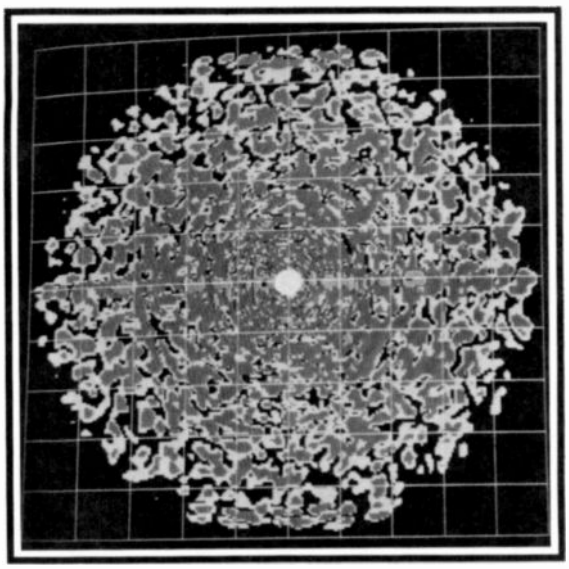

Use of color displays for presentation of phased-array radar pattern contours was initiated and developed in Missile and Surface Radar's Advanced Antenna and Microwave Technology organization by Dr. William J. Graham. Bill describes the display shown on the cover in the following paragraphs:

"This is an eight-color contour display of the computed radiation pattern over an entire hemisphere in front of a large planar phased array. The elements of the array have been given signal levels in accordance with a Taylor weighting function together with random amplitude and phase errors. The horizontal and vertical coordinates are direction cosines aligned with the X and Y axes of the plane of the array. The color gives a measure of the sidelobe radiation relative to the peak of the main beam (seen in the center of the pattern in white). The sidelobe levels, in decreasing order, are designated by red, yellow, green, blue, pink, turquoise, and black. Each color represents a quantization range of 3 to 5 dB.

"This contour was generated from a grid of 256 × 256 points computed on an IBM 370 computer and stored on magnetic tape. Quantization was performed by an HP-1000 minicomputer. A high-resolution Hitachi 2719 color monitor was used for the display, which was then photographed.

"The pattern-contour display permits easy interpretation of a huge amount of data (up to 262,144 points) with respect to sidelobe structure and the localization of peak sidelobes (seen as red). This information was previously presented by a computer point-by-point plot of sidelobe peaks only, suppressing much of the data to save plotting time and preserve legibility."

RCA Engineer

A technical journal published by
RCA Research and Engineering
Bldg. 204-2
Cherry Hill, NJ 08358
TACNET: 222-4254 (609-338-4254)

RCA Engineer Staff

Tom King	Editor
Mike Sweeny	Associate Editor
Louise Carr	Art Editor
Frank Strobl	Contributing Editor
Betty Gutchigian	Composition
Dorothy Berry	Editorial Secretary

Editorial Advisory Board

Jay Brandinger	Division Vice-President and General Manager, "SelectaVision" VideoDisc Operations
John Christopher	Vice-President, Technical Operations, RCA Americom
Hans Jenny	Manager, Engineering Information
Arch Luther	Division Vice-President, Engineering and Product Assurance, Commercial Communications Systems Division
Howie Rosenthal	Staff Vice-President, Engineering
Ed Troy	Director, Operations Planning and Support, Solid State Division
Bill Underwood	Director, Engineering Professional Programs
Bill Webster	Vice-President, Laboratories

Consulting Editors

Ed Burke	Administrator, Marketing Information and Communications, Government Systems Division
Walt Dennen	Manager, Naval Systems Department Communications and Information, Missile and Surface Radar
Charlie Foster	Manager, Systems and Procedures, RCA Laboratories
John Phillips	Manager, Business Development and Planning, RCA Service Company

• To disseminate to RCA engineers technical information of professional value • To publish in an appropriate manner important technical developments at RCA, and the role of the engineer • To serve as a medium of interchange of technical information between various groups at RCA • To create a community of engineering interest within the company by stressing the interrelated nature of all technical contributions • To help publicize engineering achievements in a manner that will promote the interests and reputation of RCA in the engineering field • To provide a convenient means by which the RCA engineer may review his professional work before associates and engineenng management • To announce outstanding and unusual achievements of RCA engineers in a manner most likely to enhance their prestige and professional status.

F. Sterzer

Microwave technology at RCA

Microwaves are vital to modern civilizations. Our air traffic is controlled with the help of microwave radars, most of our telecommunications are transmitted on microwave carriers, the television shows we watch are usually distributed by terrestrial or satellite microwave links, many of us cook our food in microwave ovens, our armed forces use microwaves to detect hostile intruders, to guide weapons, to provide secure communications, and so on.

Because of the great importance of microwaves, there is a large, worldwide effort to advance the body of knowledge and techniques that constitute microwave technology. RCA engineers and scientists have made many distinguished contributions to this worldwide effort. Their contributions have ranged from original work on many types of microwave tubes and microwave solid-state devices to large phased-array radars for fleet defense and geostationary satellites that relay communication signals carried at microwave frequencies.

Two major RCA businesses depend heavily on modern microwave technology. The Government Systems Division uses the latest in microwave technology in products such as radars, satellites, satellite ground stations, and electronic countermeasure systems. RCA Communications, Inc., sells communications services that are carried principally by microwaves. They own and operate several geostationary communications satellites built for them by the Government Systems Division. These satellites make use of some of the most recent advances in microwave technology.

The future of microwave technology at RCA looks bright. The worldwide demand for microwave products and microwave-based services promises to increase substantially during the 1980s. RCA is well positioned to take advantage of this projected increase in demand. In addition to important growth in our present microwave-based businesses, we expect to participate in such major new microwave-based business opportunities as Direct Broadcast Satellites, advanced tactical radars, millimeter-wave satellite ground terminals, and so on. Major goals for our microwave technology efforts in the 1980s include transistors that can operate efficiently at millimeter-wave frequencies, high-power antenna arrays populated with solid-state power sources, miniaturized high-Q filters, multigigabit logic circuits, and low-cost manufacturing techniques for thin-film microwave circuits.

Fred Sterzer
Director, Microwave Technology Center
RCA Laboratories

RCA Engineer

Vol. 27 | No. 5 Sept. | Oct. 1982

microwave business history

4 Microwave components research at RCA
M. Nowogrodzki

microwave technology applications

7 Solid-state power amplifiers replacing TWTs in C-band satellites
H.J. Wolkstein | J.N. LaPrade

17 Medical applications of microwave energy
R.W. Paglione

21 The Engineer's Notebook: A high-power *pin* diode
P.J. Stabile

23 Radar instruments: Sensors for industrial applications
M. Nowogrodzki | D.D. Mawhinney | R.W. Kipp

31 Low-sidelobe antennas for tactical phased-array radars
W.T. Patton

37 Wideband receivers for communications satellites
H. Goldberg

43 Shaped-beam reflector antennas for communications satellites
C.E. Profera | G.L. Rosol | H.H. Soule | J. Kara

microwave components

50 Active and passive microwave components
E.J. Denlinger

58 A review of GaAs microwave monolithic integrated circuits
H.C. Huang | L.C. Upadhyayula | M. Kumar

64 Automated assembly of lumped-element GaAs FET power amplifiers
J.B. Klatskin | D. Haggis | R.L. Camisa | B.T. Joyce

71 Computer-aided manufacture of precision microwave components for phased-array radar GaAs MESFET power amplifiers
M.E. Breese | R.J. Mason

microwave design and test

76 Computer-aided design and testing of microwave circuits
B.S. Perlman | D.L. Rhodes | J.L. Schepps

87 Computer design and testing of a microwave antenna-feed manifold
G.P. Bolger | V.D. Holaday

departments

Patents, **91** | Pen and Podium, **94** | News and Highlights, **95**

Copyright © 1982 RCA Corporation
All rights reserved

in this issue ...
microwave technology

■ **Nowogrodzki:** *"It may be instructive to recall at least some of the RCA contributions to the technology as it is practiced today."*

■**Wolkstein/LaPrade:** *"The SSPA can replace the C-band TWT with demonstrated improvements in rf performance and projected improvements in reliability and operating life."*

■**Paglione:** *"The future holds promising approaches to diagnosis, treatment, and monitoring in every aspect of the medical profession."*

■**Stabile:** *"RCA high-frequency high-voltage power* pin *diodes provide low-frequency performance formerly available only in the UHF region."*

■**Nowogrodzki/Mawhinney/Kipp:** *"The two instruments offer unique, effective and reliable solutions to industrial control problems . . . ."*

■**Patton:** *"The results indicate that dramatic system-performance improvement in a jamming environment can be obtained with only a moderate increase in antenna cost and weight."*

■**Goldberg:** *"This unit is a wide-bandwidth receiver covering the full communication spectrum assigned to the satellite, and it amplifies all of the signals of a transponder simultaneously."*

■**Profera, *et al.*:** *"The Satcom F dual-reflector assembly is the first completely designed by RCA Astro-Electronics and is an excellent example of an advanced offset-reflector design."*

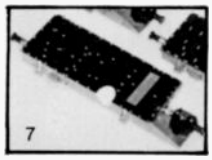

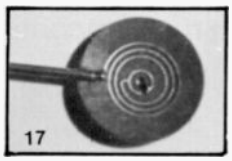

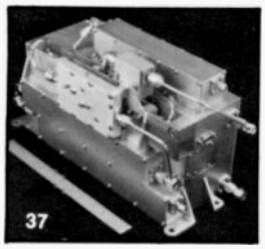

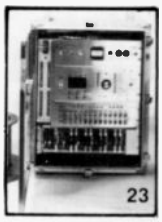

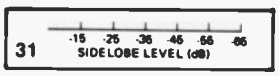

■**Denlinger:** *"Emphasis, here, has been placed on describing briefly the work that has recently been done within RCA."*

■**Huang/Upadhyayula/Kumar:** *"The promising attributes of the monolithic technology are the potential reduction of fabrication costs, the improved reliability and reproducibility, and reduced size and weight."*

■**Klatskin, *et al.*:** *"This paper describes a joint effort undertaken by RCA Laboratories and RCA Automated Systems to develop techniques for automated fabrication of wideband, lumped-element matched GaAs MESFET power amplifiers."*

■**Breese/Mason:** *"The fabrication of microwave components has taken a step forward since the introduction of modern numerically controlled (NC) machine tools."*

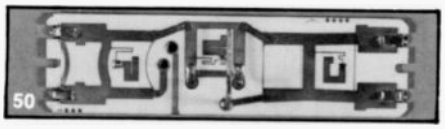

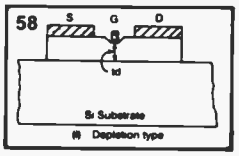

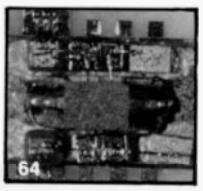

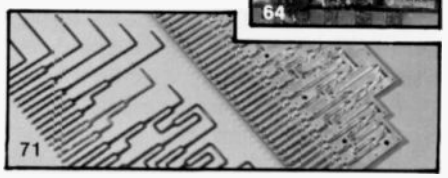

■**Perlman/Rhodes/Schepps:** *"Such computer aids are helping produce superior products with greater reliability and yields."*

■**Bolger/Holaday:** *"Test programs have been developed to control all performance measurements using the HP8409 automatic network analyzer . . . ."*

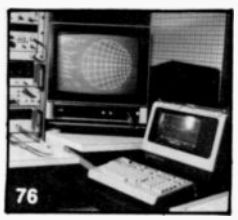

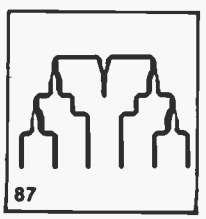

---

in future issues...

modeling, simulation and analysis
engineering productivity: tools and techniques
space technology

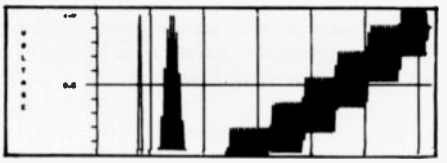

M. Nowogrodzki

Microwave components research at RCA

Microwave technology owes some of its successes to RCA research and development. Here are some of the milestones in the component area.

Abstract: *The important and varied contributions of RCA engineers to microwave technology, surveyed here from the personal point of view of the author, show RCA's technology since World War II. Landmarks along the road to the technological developments of today, described in this issue of the* RCA Engineer, *include: the commercial magnetron oscillator and traveling-wave tube; pencil triodes; tubes for microwave-relay service; solid-state components; GaAs power FETs; and more.*

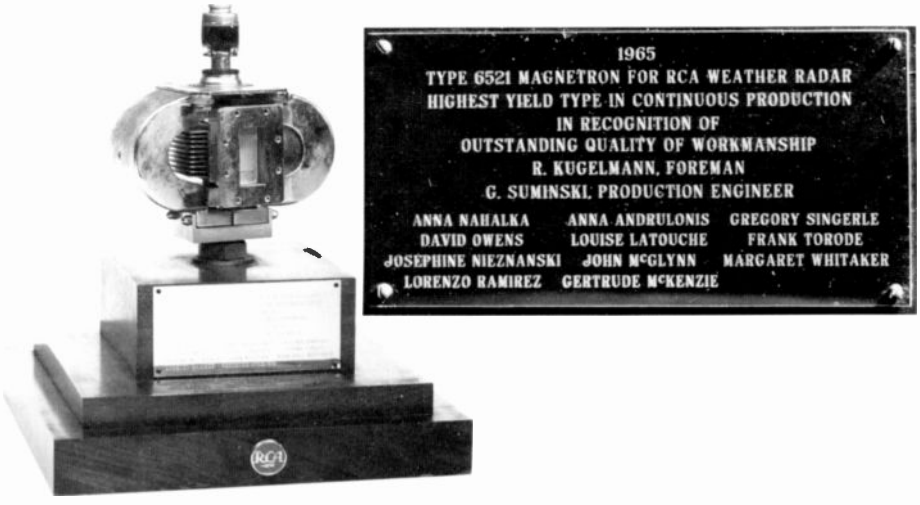

The Type-6521 magnetron was developed at RCA for specific use in the RCA AVQ-10 weather radar, used by most of the commercial airlines for many years. Both the magnetron and the weather radar itself were pioneering RCA achievements. Operating in C-band, the magnetron was one of the first mass-produced tubes of this kind for commercial use. The photograph shows a unit that was mounted as an award for the production group and displayed in the entrance lobby of RCA Bldg. 55 in Harrison, N.J., the home of RCA Microwave Tube Operations, where the magnetron was manufactured.

The publication of a compilation of technical papers devoted to a single technology usually serves as a milestone, a time to look back to the technology's start and to look forward to where it is heading. And so, with this issue of the *RCA Engineer* devoted to the microwave technology, one is tempted to reach back to the days of World War II, when microwaves as a practical technology were born both in the university laboratories established to further the war effort and at industrial laboratories, RCA Laboratories included. I shall resist this temptation and leave this mammoth task to future historians of science.*

Yet it may be instructive to recall at least some of the RCA contributions to the technology as it is practiced today—both to jog the memory of the older RCA engineers and to provide some insight for the younger ones.

*All dates cited in this review are approximate. The date of publication of a paper or patent may be preceded by several years of research and development.

©1982 RCA Corporation
Final manuscript received July 12, 1982.
Reprint RE-27-5-1

After the war

RCA emerged from the classified R&D efforts during World War II with solid positions in both microwave power devices of interest in those days: the magnetron oscillator and the traveling-wave tube (TWT).

The establishment, soon after the war, of an RCA microwave tube department that was part of the RCA Tube Division spurred microwave tube research there (at Lancaster, Pa., and then Harrison, N.J.) and at RCA Laboratories (Princeton, N.J.). In the magnetron field, the Type 6521, developed for the RCA airborne weather radar, remained a prime example of a mass-produced magnetron for nongovernment use for many years. Also, pioneering work was done by RCA engineers in the cavity tuning of magnetrons, for FM modulation purposes (Jenny, 1952), and for wideband tuning of high-power tubes (Vaccaro, 1956).

Early work on traveling-wave tubes (Lindenblad, late-1930s; Shulman, 1947) paced the ramified developments of these tubes in the 1950s. In the low-noise area, these were exciting days: Time after time, practical designs based on pioneering theoretical work (Peter, 1952; Bloom and Peter, 1954) showed results below the then accepted "theoretical limit." For many years RCA's commercial Type 6861, designed for S-band operation, was the industry's standard.

In more conventional tubes, RCA's pencil triodes are still being used. Developed in the mid-forties for operation in L-band, pencil triodes continue to be mass-produced by automatic techniques to this day (in Lancaster, Pa.). They are used primarily in radiosonde (a miniature radio transmitter

carried aloft with instruments for broadcasting humidity, temperature, and pressure) weather-monitoring equipment, in a version that includes an integral cavity.

Many of the techniques used in modern TWTs were invented or perfected at RCA. One of the first tubes for microwave-relay service (Siekanowicz, 1954) was followed by the concept of periodic permanent-magnet (PPM) focusing (Chang, 1955) and depressed-collector operation for efficiency improvement (Wolkstein, Sterzer, 1958). The first PPM-focused tube in space was an RCA design flying in an RCA spacecraft (Relay, 1962), while frequency-memory loops used in present-day electronic-warfare systems are based on fundamental RCA investigations of signal suppression and limiting in TWTs (Wolkstein, 1961).

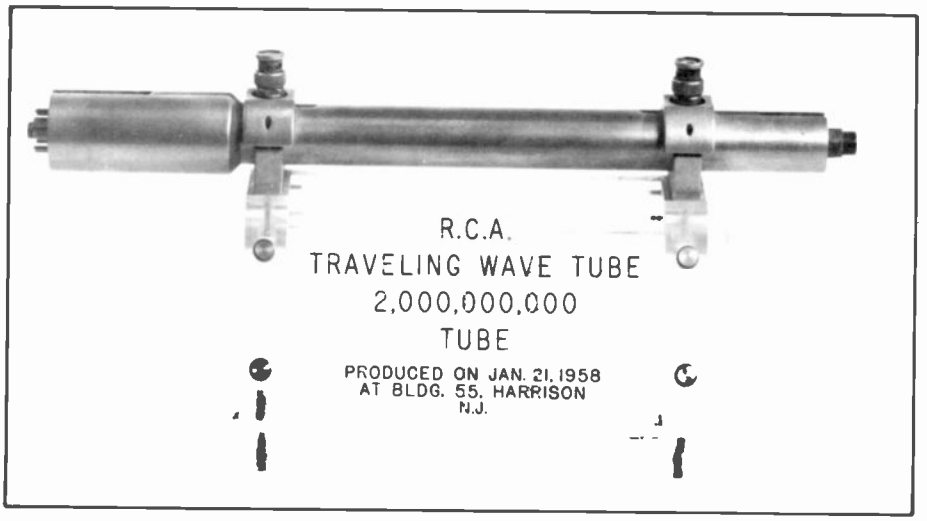

The 2-billionth vacuum tube produced in the RCA complex of tube-making facilities in Harrison, N.J. was a traveling-wave tube (TWT) designed for service in a C-band radio-relay system manufactured by RCA Ltd. in Montreal, Canada. The Microwave Tube Operations activity in Harrison reported through the Power Tube Operations in Lancaster, Pa., but was nevertheless closely tied to the extensive RCA tube-making plant in Harrison, and used many of the technical and support services available at this major RCA facility. The TWT, one of two types used in the RCA radio-relay system, used technologies quite advanced for that time, including periodic permanent-magnet (PPM) electron-beam focusing, a high-precision convergent-beam cathode, and tightly controlled exhaust-and-processing techniques.

Microwave solid-state components

Meanwhile, significant research was going on at RCA in microwave solid-state components. The forerunners of today's experimental gigabit logic used parametric subharmonic oscillators (Sterzer, 1959). Early work on ferrites led to a millimicrosecond microwave modulator (Solomon, Sterzer, 1959) and ultimately to the ferrite circulator (Hershenov, 1967). Tunnel-diode amplifiers were manufactured commercially by RCA in the mid-sixties.

While working with avalanche diodes (present-day IMPATTs), the high-efficiency "anomalous mode" was discovered at RCA Laboratories in 1967 (Prager, Chang, Weissbrod), and later its theory of operation was developed (Clorfeine, 1969). In a paper considered a milestone in the understanding of microwave solid-state device operation, basic frequency-power relationships were developed (Johnson, 1965). Nergaard (1967) proposed the use of integrated solid-state microwave amplifiers in a phased-array antenna—a concept still not fully implemented today. Another powerful early concept, which is only now coming into its own in conjunction with the impedance matching of power FETs, was the use of lumped-element matching of bipolar transistors, used for batch-fabricating 3-GHz amplifiers (Caulton, 1971). The "anomalous-mode" devices, renamed TRAPATTs, became respectable microwave oscillators for pulsed service. IMPATTs were pushed into the millimeter-wave range, while the use of transferred-electron devices, originally limited to oscillator service, was extended by RCA to amplifiers (Perlman, Walsh, 1969).

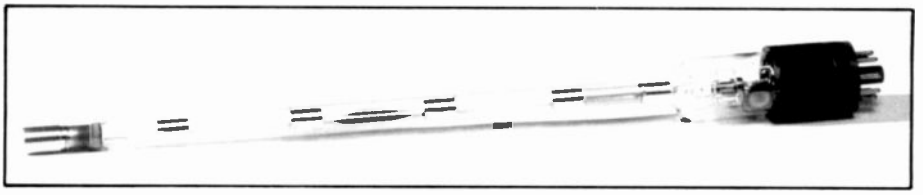

The Type-6861 traveling-wave tube marked a milestone in the understanding of low-noise phenomena and design in traveling-wave tubes. Extensive research at RCA Laboratories, combined with meticulous engineering at RCA's Microwave Tube Operations, produced a design which consistently provided performance better than the "theoretical limits" formulated only a few years previously. The tube, which used a carefully processed oxide cathode and a parallel-flow electron beam, was processed on special equipment designed and built by RCA, and provided an unprecedented 4.5-dB noise figure in S-band. It was used with a separate solenoid for focusing the beam.

The RCA tunnel-diode amplifier is an example of fast-turnaround engineering. Tunnel diodes were still in the relatively early stages of development when the amplifier was developed and introduced into commercial production for communications and radar systems. The amplifiers used diodes developed and manufactured at the RCA Somerville, N.J., plant. The model shown was used as a retrofit in the C-band RCA weather radar, and served to increase the operating range of the system by substantially decreasing the receiver's noise figure.

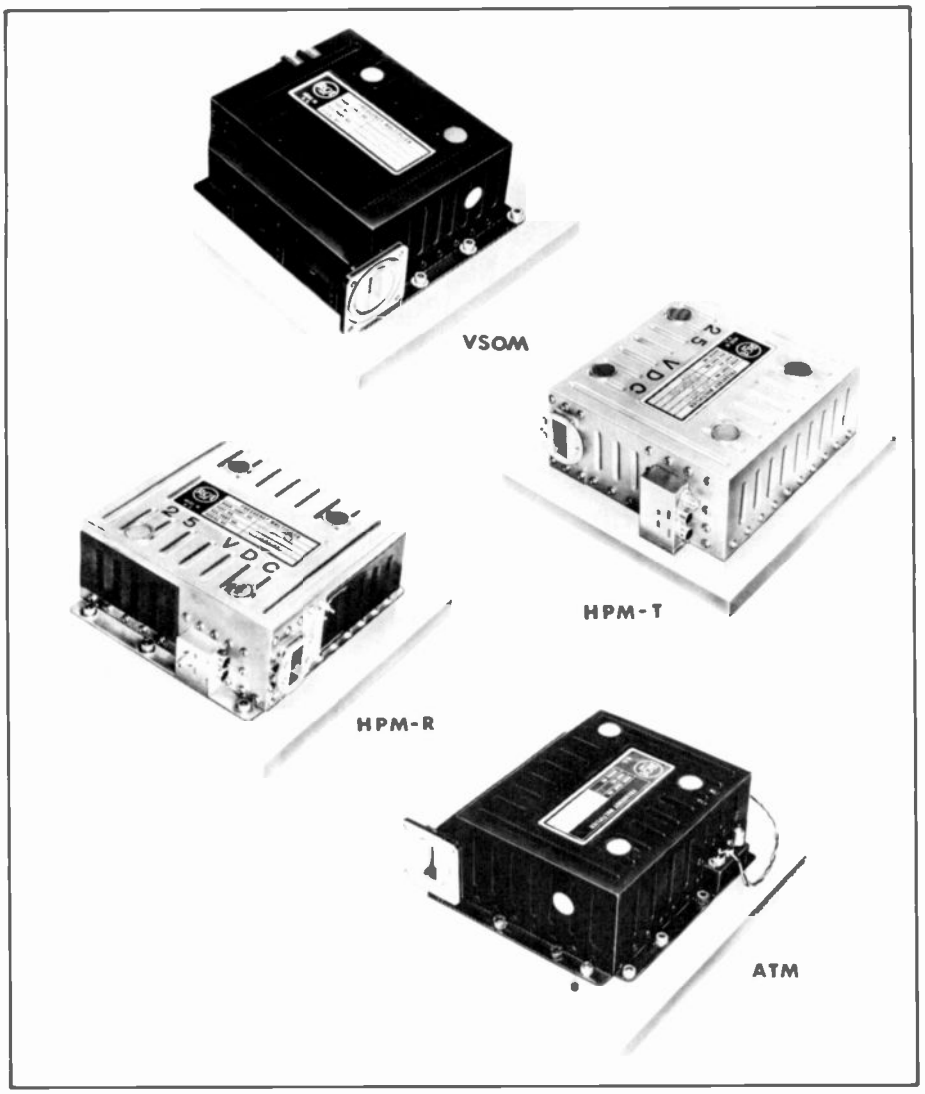

The Lunar Excursion Module (LEM) landing, rendezvous, and docking systems—essential elements in the successful Apollo mission for the landings on the moon—were the responsibility of RCA's Aerospace Communications and Control Division, as it was then called, in Burlington, Mass. The four units shown, which mark the first use of microwave solid-state radar components in space, were built at the Microwave Tube Operations activity in Harrison, N.J. The velocity sensor oscillator multiplier (VSOM) and altimeter (ATM) units were used for landing. The high-power multiplier-transponder (HPM-T) and high-power multiplier-responder (HPM-R) were used in the rendezvous and docking operations of the LEM. All units operated in the X-band frequency range.

Gallium arsenide power FETs

If the 1950s were the decade of microwave tubes and the 1960s saw the expansion of solid-state devices into the microwave field, the 1970s were the days when the gallium arsenide field-effect transistor (GaAs FET) emerged from the laboratory and created a new industry, a phenomenon which future historians of science may compare to the development of the klystron in the thirties and forties. The microwave power FET, proposed and demonstrated by RCA Laboratories, is having a profound effect on the directions of the microwave systems business.

Early work at RCA Laboratories on Schottky-barrier GaAs transistors dates to the late 1960s. With the invention of the self-aligned gate technology, device performance as a gigabit-rate modulator was demonstrated in 1971 (Napoli, *et al.*), and a 150-mW device operating at 6 GHz was described in 1973 (Napoli, *et al.*). The rest, as the saying goes, is history . . . .

Conclusion

As previously stated, I wanted to offer a brief perspective against which to place the papers in this special issue. I extend my apologies to the many contributors to the rich RCA heritage in the microwave technology who are not mentioned herein. This introduction is not a documented and exhaustive history of microwave engineering at RCA—only a personal memoir of one RCA microwave engineer.

Markus Nowogrodzki was graduated with the degrees of Bachelor of Electrical Engineering, *cum laude*, in 1948, and Master of Electrical Engineering, in 1951, both from the Polytechnic Institute of Brooklyn. In 1955, he joined RCA and was engaged in the development and manufacture of magentrons, microwave triodes, traveling-wave tubes, and solid-state subsystems. As Manager, Traveling-Wave Tube Operation, he supervised a department comprising design, manufacturing, applications, and program-control activties.

Mr. Nowogrodzki left RCA in 1967, and returned in January 1973, as Manager, Division Liaison, at RCA Laboratories' Microwave Technology Center. He is now in charge of the Center's Subsystems and Special Projects group. Mr. Nowogrodzki has written more than twenty papers on various aspects of microwave component design and applications. He holds six patents.

Contact him at:
RCA Laboratories
Princeton, N.J.
TACNET: 226-2521

H.J. Wolkstein | J.N. LaPrade

Solid-state power amplifiers replacing TWTs in C-band satellites

Over 1000 operating traveling-wave tube (TWT) amplifiers have been used in space, but now RCA solid-state power amplifiers, with enhanced system performance and reliability, are replacing TWTs in downlink commercial communications satellites.

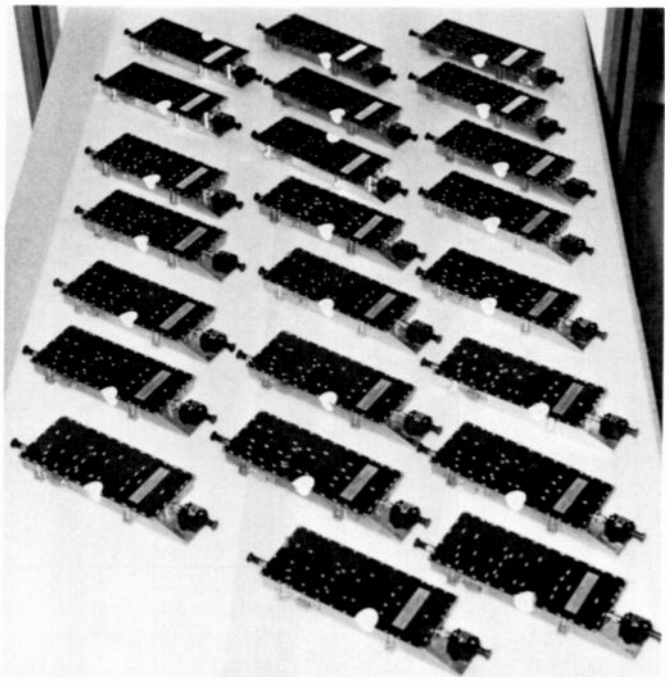

Fig. 1. *The 23 amplifiers shown are assembled and flight tested for use in the Satcom F communications satellite.*

Abstract: *Traveling-wave tubes—the preferred means for downlink amplification since the start of satellite communications—are now being replaced by solid-state amplifiers that have superior performance, greatly enhanced reliability characteristics, and potentially lower fabrication costs. This paper describes the 8.5-watt, 60-dB gain, solid-state GaAs FET power amplifier that is now being fabricated and tested in flight quantities for C-band operation in RCA Satcom and other satellite communications systems. The inherent differences in performance between the traveling-wave tube and the advanced solid-state amplifier are described in detail. Data presented for the amplifier, which is constructed in modular fashion, illustrate the degree of reproducibility between amplifiers for the first 24 units fabricated and flight-acceptance tested for the Satcom program. Typical performance parameters of the solid-state amplifier are covered. Computer-controlled test facilities, designed for automated testing, setup and evaluation of the amplifier in all stages of construction, are also described.*

Although the traveling-wave tube (TWT) spaceborne, downlink power amplifier has rendered outstanding performance in the past, its role in providing microwave power in advanced satellite systems is now being challenged. The superior performance and reliability of the field-effect-transistor (FET) solid-state power amplifier (SSPA), recently introduced and demonstrated within RCA, is now apparent. This unique SSPA, developed at RCA Laboratories[1] and RCA Astro-Electronics, has been "space qualified" and is now being manufactured by RCA Astro in flight quantities for Satcom and other related satellite-communications systems.

© 1982 RCA Corporation
Final manuscript received August 16, 1982
Reprint RE-27-5-2

The solid-state power amplifier

The SSPA, several of which are shown in Fig. 1, has been designed to provide an rf power-output level of 8.5 W for C-band service with a dc-to-rf efficiency of approximately 35 percent and an operating gain of 60 dB. The amplifier, which covers an instantaneous bandwidth of 160 MHz selectable within the 3.7- to 4.2-GHz band, operates with a nominal input potential of 8.7 V and weighs less than 13 oz. Twenty-four SSPA units and four spares have been recently built, assembled, and flight tested for use in the Satcom Flight-F satellite scheduled for launch for RCA Americom during the fourth quarter of 1982. This is the first of an all-solid-state commercial-communications satellite series that will be placed in orbit for conventional video and voice traffic.

The advantages of the SSPA

The SSPA provides improved reliability and system performance over the TWT in several important areas.

- Cathode wear-out and the various failure mechanisms associated with thermionic electron emission for the TWT are entirely eliminated with the SSPA.
- Outgassing and vacuum-tube contamination sometimes experienced with TWTs, leading to catastrophic failure during heater turn-off and turn-on, are no longer an operational consideration with SSPAs.
- Low-voltage operation of the SSPA, with a benign requirement for less than 10 V, replaces the high-voltage electronic power converter for the TWT. This eliminates the voltage breakdown and arc-over failure commonly experienced with the TWT and the electronic power conditioner at operating potentials typically greater than 2500 V.
- High-voltage potting and/or stand-off capability are no longer problems. Failure mechanisms such as ionization breakdown, and microdischarges in the Paschens high-voltage breakdown region due to the inherent outgassing of components, have been removed.
- Heater-cathode warm-up time, and the necessity to keep the cathode active (hot) during long standby periods, have been eliminated.

Accelerated life and stress tests conducted

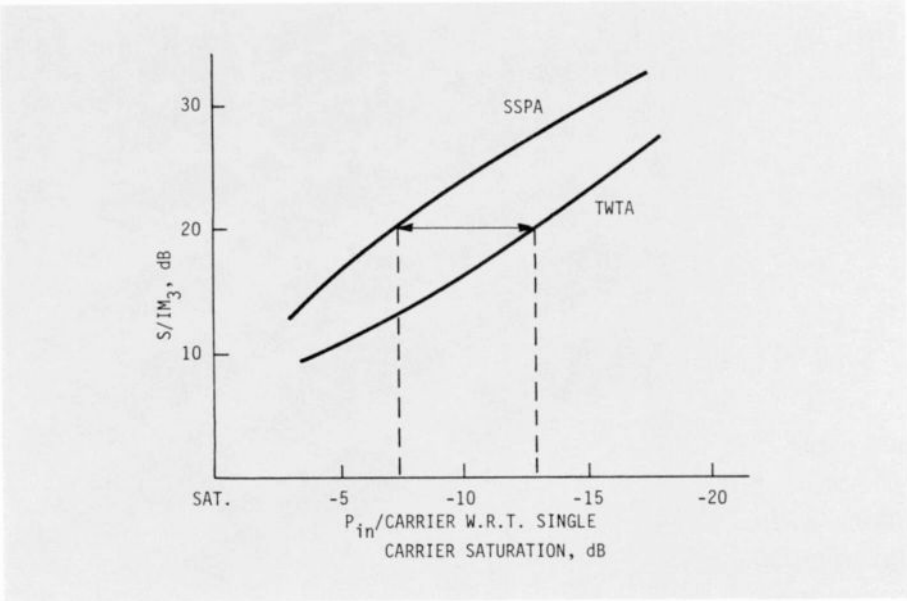

Fig. 2. *The effect of power amplifier linearity on channel capacity. The third-order intermodulation distortion product for the SSPA is typically -13 dBc, an improvement of approximately 5 dB over the conventional TWTA.*

at RCA indicated that routinely screened and selected FETs for flight operation have demonstrated a failure rate, for the entire 8.5-W SSPA and power conditioner, that is half that of a competitive TWTA. The SSPA can indeed sustain rf performance in continuous space service for ten years. The improvement in active channel availability for the SSPA over the TWTA is two-to-one for the designated 10-year mission life. A redundancy plan is used whereby each lot of seven SSPAs provides for six active operating channels. In the redundancy plan, four standby SSPAs are used to support twenty-four working SSPAs in the Satcom spacecraft.

Improvements in SSPA performance over the TWTA as a downlink amplifier cover several important transmission parameters.

- The SSPA is inherently more linear than the TWTA. The typical operating point for the SSPA, which provides for an rf output power of 8.5 W, occurs at a small-signal gain compression of approximately 2 dB. In contrast, a TWT typically operates at a small-signal gain compression of 6 dB.

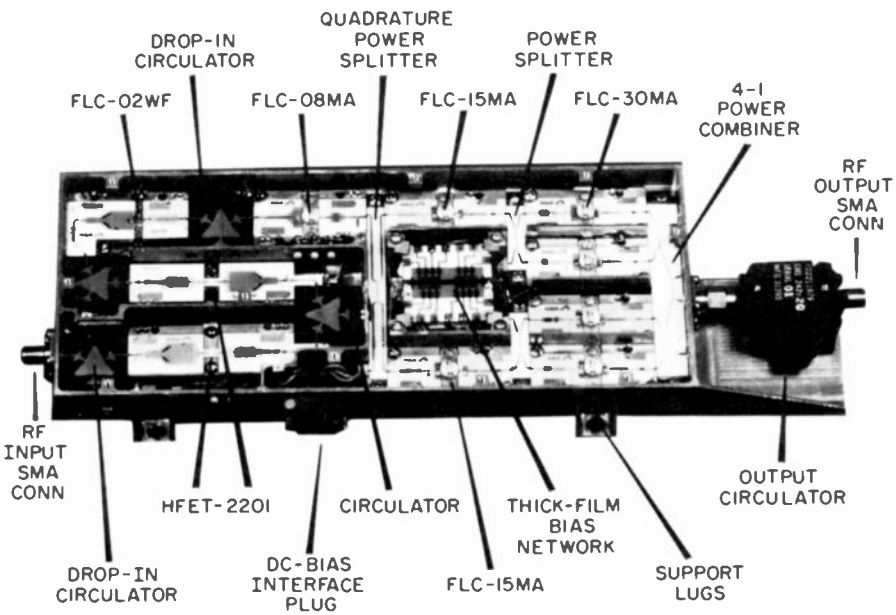

Fig. 3. *A detailed portrait of microstrip technology used in the SSPA design.*

- The third-order intermodulation-distortion (IMD) product for the SSPA is typically 13-dB down from either of two equal carriers at the operating output-power level. This is typically 5-dB better than the IMD of the TWT at saturation. Moreover, the carrier-to-IMD separation improves significantly for the SSPA over the TWT as the two-tone carriers are backed off in amplitude. This factor provides for increased channel capacity, as shown in Fig. 2.
- The SSPA has a total differential phase shift generally less than 22° over a 30-dB drive range extending from a small signal to the specified power-output operating point. The TWT, in contrast, typically undergoes at least a 45° phase change over the same drive range. Similarly, the amplitude-modulation-to-phase-modulation (AM/PM) conversion ratio for the SSPA is less than 2° per dB, while the TWT has a conversion ratio of 5° per dB. These improved phase characteristics reduce link distortion for both analog and digital quadraphase-shift-key (QPSK) modulation.
- The SSPA, when properly matched, has demonstrated a small-signal gain contour and fine grain almost devoid of any perturbations or cyclic gain changes. This is in contrast to the TWT, which sometimes exhibits fine-grain spikes due to periodic rf reflections caused by helix distortion.
- The noise figure of the SSPA is under 10 dB. This is in contrast to the 25-dB noise figure that an 8.5-W TWT typically provides. Although the noise figure of the transponder channel is set by the 6-GHz low-noise front-end receiver, the improved noise figure for the SSPA provides additional margin.

The SSPA thus has reduced distortion and improved performance in a satellite link and accommodates an increased traffic density and channel capability without the degree of input rf power backoff normally required for TWTs. For example, with a typical test-tone-to-noise ratio of 46 dB, 5000 channels with single sideband modulation can be accommodated by the TWT; while under the same conditions, the SSPA can handle 10,000 channels. This can mean improved bandwidth use and more revenue.

Figure 3 illustrates the microstrip integrated circuitry of the solid-state power amplifier for the RCA Satcom satellite. Discrete, hermetically sealed GaAs FET devices are used for each of the amplifier

stages with associated microstrip matching and interconnecting circuitry on alumina substrates. The amplifier weighs less than 13 oz., approximately one-half the weight of the TWT it replaces, and measures 7″ × 3″ × 0.75″. This significant weight differential may be used in the spacecraft solar-power supply to offset the slightly lower dc-to-rf power efficiency of the SSPA compared to the efficiency of the two-collector TWT (typically 33% versus 38%).

The SSPA design

A block diagram of the FET amplifier and the gain distribution is shown in Fig. 4. Six cascaded amplifier stages were designed with CAD circuit techniques for optimum performance using microstrip matching circuits. The design technique and related data associated with FET characterization, circuit optimization, power splitting and combining, and so on, have been covered in a previous paper.[1] Each individual FET amplifier unit has been designed to be built and tested as a stand-alone module with input- and output-matching impedances of 50 ohms. Bias voltages and operating parameters are initially established during module evaluation and tests. As illustrated, the six-stage amplifier consists of four low-level, single-ended amplifier stages operated under Class A conditions, followed by two sets of balanced amplifier stages operated to obtain maximum output-power and efficiency while maintaining acceptable IMD performance.

Three separate input voltages used for the SSPA are obtained from the electronic power converter (EPC). These voltages are the drain potential (+3.5 V) for the first two low-level stages, a high-level drain potential (+8.7 V) for the remaining stages, and a common negative gate-bias potential (−3.7 V). The gate potential is distributed to individual stages at the proper selected bias levels to meet rf and dc performance requirements by means of a unique thick-film-resistance divider network[2] developed at RCA Laboratories.

The low-level input amplifier

The first four amplifier sections comprising the low-level input amplifier chain are designed to use interstage, drop-in microstrip circulators to reduce ripples in the passband and to keep the gain slope below 0.025 dB/MHz. The low-level driver chain is tested in a stand-alone testable integrated assembly (Fig. 5). The SMA output-connector assembly is removed after the unit undergoes "tuning" by means of parasitic capacitors to obtain the prerequisite gain flatness and frequency response under swept small-signal conditions.

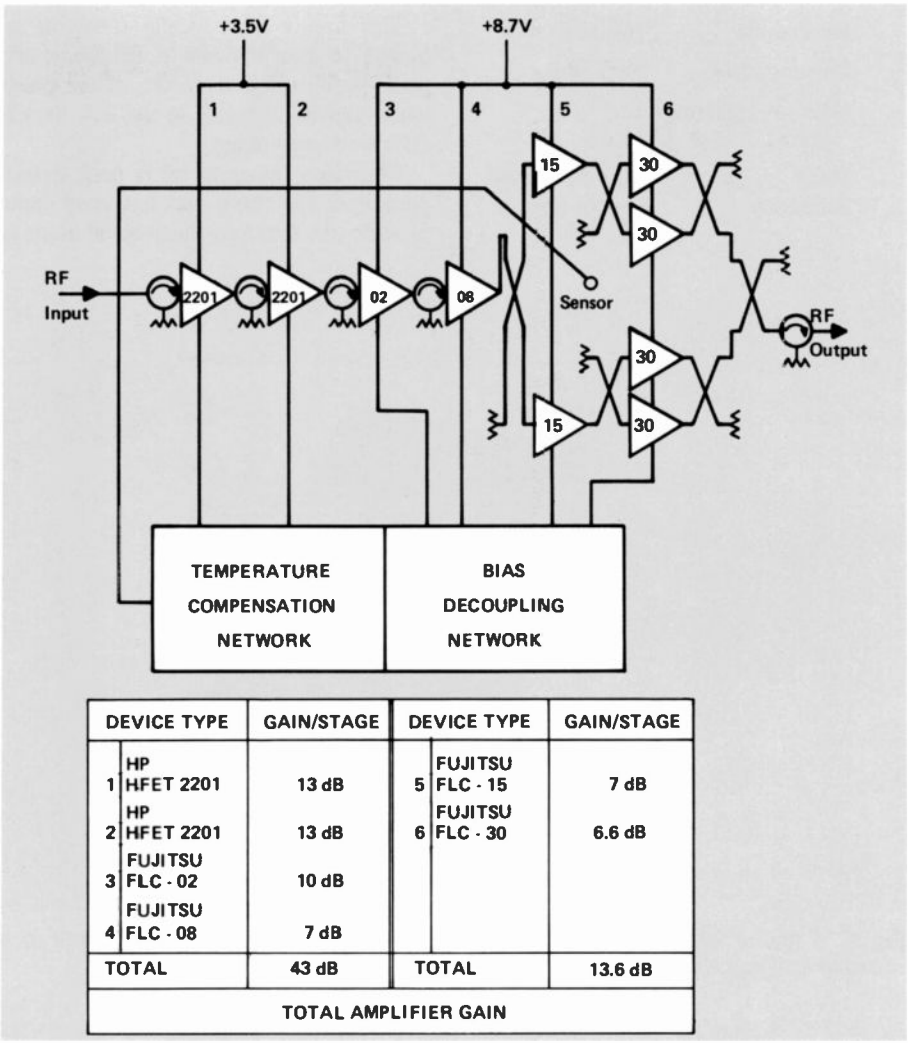

DEVICE TYPE	GAIN/STAGE	DEVICE TYPE	GAIN/STAGE
1 HP HFET 2201	13 dB	5 FUJITSU FLC - 15	7 dB
2 HP HFET 2201	13 dB	6 FUJITSU FLC - 30	6.6 dB
3 FUJITSU FLC - 02	10 dB		
4 FUJITSU FLC - 08	7 dB		
TOTAL	43 dB	TOTAL	13.6 dB
TOTAL AMPLIFIER GAIN			

Fig. 4. *The solid-state power amplifier. The microwave and dc bias circuitry are represented. Gains at full power output are tabulated on a per-stage basis. Gain variation because of temperature is compensated for by a sensing bias-control network.*

Typical performance parameters of this low-power-level assembly, which covers the entire 500-MHz 3.7- to 4.2-GHz bandwidth, are:

Power Output	0.5 watts
Gain	45 dB
Gain Flatness	0.3 dB
IMD	−22 dBc C/IM_3

The output-power section

The drive for the output-power section is obtained by splitting the output rf power of the low-level driver section into two equal components by means of quadrature power splitters. This output is then amplified by two balanced amplifiers (type FLC-15), schematically shown in Fig. 4. The output rf power of these two amplifiers is then split again to power four final output FET stages (type FLC-30). The outputs of the four final power amplifiers are summed by means of a four-way interdigitated quadrature power combiner. Since these output stages operate past the linear range with the onset of gain compression, assumptions of linearity are invalid; hence, the conventionally measured, small-signal S-parameters used to design the first four low-level stages are not used for the design of the output stages. The output impedances of these power FETs are instead matched by use of an automatic load-pull system, a unique computer-controlled instrument developed by RCA Laboratories that allows the determination of the optimal load impedance as a function of output power. A complete output-power module, shown in Fig. 6, comprises a separate testable pallet and provides for the following salient performance parameters:

Bandwidth	160 MHz
Power output	39.5 dBm
Gain (at operating point)	15 dB
IMD	−13 dBc C/IM_3
Efficiency	~ 35% (power added)

This unit is parasitically tuned, if required, to meet the power, efficiency, and gain specifications over any of the designated 160-MHz bands in the 3.7- to 4.2-GHz frequency range.

Obtaining the required rf performance parameters for both the low-level input module (the first four stages stand alone in a testable configuration) and the high-power output module (Fig. 6) permits the total integration and assembly of the complete SSPA unit, as previously shown in Fig. 3. The complete amplifier assembly requires extensive testing, although optimization of performance by tuning and final adjustment of the operating bias has been minimized by alignment of the subassembly amplifier modules.

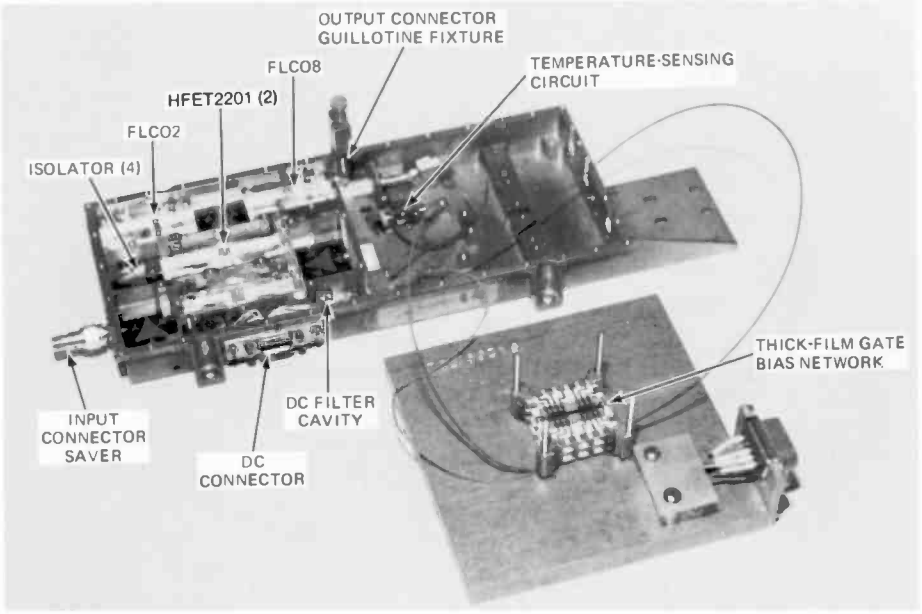

Fig. 5. *A layout of the low level assembly. The first-four stages stand alone in a testable configuration.*

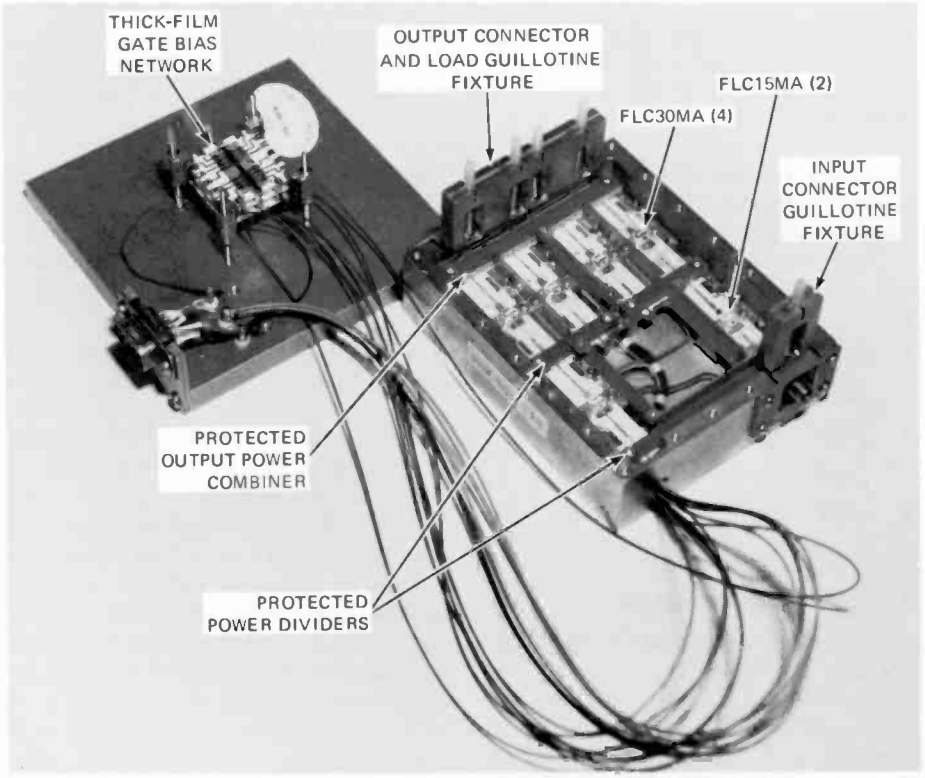

Fig. 6. *A complete output assembly stands alone as a testable unit when mounted in a test housing and connected with a thick-film bias network.*

Technology Transfer Program

The Technology Transfer Program carried out by RCA Laboratories provided RCA Astro-Electronics with the proper skills, procedures, standards and controls to make possible the fabrication, assembly, parts procurement, integration and test of the SSPA. The ultimate requirement has been production of the SSPA to meet the performance capability, production-yield potential, service life, and reliability needed to replace TWTs for the Satcom commercial satellite mission.

The transfer program, a cooperative effort between the two divisions, involved voluminous information flow, the training of personnel, and the establishment and implementation of microcircuit fabrication and test facilities. The documentation and reliability requirements exceeded those required for previous land-based or airborne equipment. To ensure that the amplifier design was compatible with Astro's background and assembly practices for satellite-borne systems, the prototype flight models undergoing final "productization" were made by use of the engineering skills at Astro[3] and RCA Laboratories.[4] This involved the mechanical and electrical optimization of the associated rf ground planes and various rf interconnections, appropriate shielding, EMI proofing, and overall amplifier packaging to meet rigid environmental specification requirements of the SSPA.

Fabrication facilities/practices

Astro-Electronics established a clean-room facility for microcircuit fabrication and assembly of the SSPA and related transponder and beacon components. This room houses space for 8 independent fabrication work areas and 10 rf test technicians, and includes all types of appropriate welding, bonding, soldering, cleaning, rf test, and inspection equipment required for SSPA and related fabrications.[5] The room is pressurized, air conditioned, and controlled for a "Class 10,000" room with a dust count of less than 10,000 particles per cubic

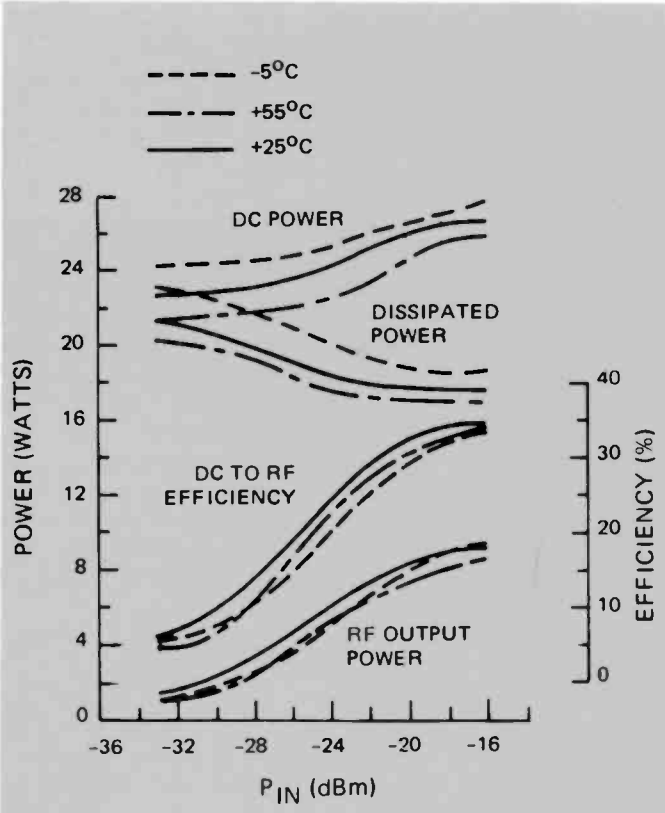

Fig. 7. SSPA power distribution as a function of input power and temperature is shown. The rf power and efficiency for frequencies covering 3.7 to 3.9 GHz meet specifications established for the SSPA, with a minimum of 8.5 W and an efficiency of approximately 33 percent. At channel mid-band frequency, with an input level of −20 dBm, the saturated output rf power is typically 40 dBm (10 W) with an efficiency of 37.2 percent at 40°C. Moreover, the output-power variation across the bandwidth shown is less than 0.3 dB.

The typical dc power requirements for this performance are also shown. As indicated, the dc power required at 3.7 GHz is 26.0 W at 25°C with full drive, and approximately 22 W at no drive. The maximum power dissipation is 23 W from the EPC and the maximum dc power required (under worst-case conditions) is 28.0 W at 3.7 GHz at a temperature of −5°C ambient.

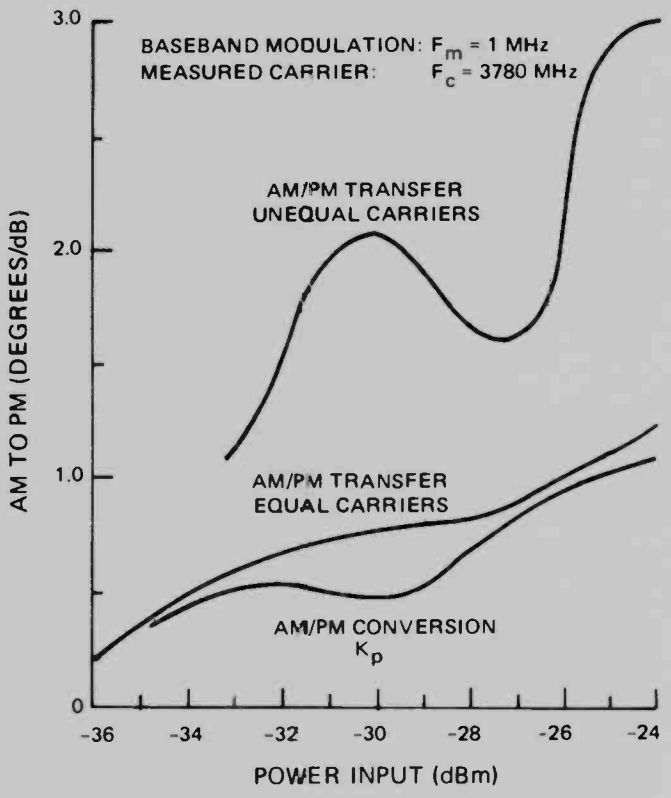

Fig. 8. AM/PM conversion for a single carrier and AM/PM transfer between equal carriers and unequal carriers amplified by the SSPA. The measurement shows a significant decrease in phase distortion for the SSPA when compared to a typical TWT. Additional measurements were also made of the AM/PM transfer coefficient K_T, which is an equally important parameter relating to modulation transfer between carriers in multicarrier operation. For these measurements, shown above, a common modulation frequency of 1 MHz was detected in each case using a communications receiver with 3.3-MHz IF bandwidth. For each AM/PM transfer measurement, a carrier separation of 40 MHz was maintained.

foot. Rigid controls are followed for each of the FET modules fabricated.

The automated test facility

A complete production rf test facility, developed by RCA Laboratories and based on the pioneering use of the HP-1000 Executive Computer and related software, has been installed at Astro-Electronics for automated and routine testing of the solid-state power amplifier[6] and its component rf modules. Four individual test stations of the facility are under computer control. Each of the stations has a stand-alone terminal, printer, plotter, as well as computer-controlled microwave sensing and measuring equipment. Two of the stations operate in conjunction with appropriate phase-locked, automatic-network analyzers to measure the phase shift versus the amplitude and voltage standing-wave ratio, while the additional test stations are used to measure gain versus frequency, power-transfer characteristics (P_{in} versus P_{out}), spurious signals, and intermodulation distortion.

This automated test equipment provides excellent reproducibility and accuracy of measurements, highlights all specified test conditions and out-of-specification measurements, and maintains a continuous record of performance for control and assessment purposes in disc memory and tape backup. The data, printed out in a specified format, are included in the documentation folder that accompanies each SSPA. This equipment is now routinely used for flight-model thermal-vacuum and acceptance testing, with appropriate printed readout and related data plotted for most operating parameters. As a result of this automatic testing facility, the testing time for the SSPA in manufacturing has been reduced by more than 50% from the old manual testing methods.

Typical SSPA rf performance characteristics

Typical performance characteristics were obtained from SSPA units made under

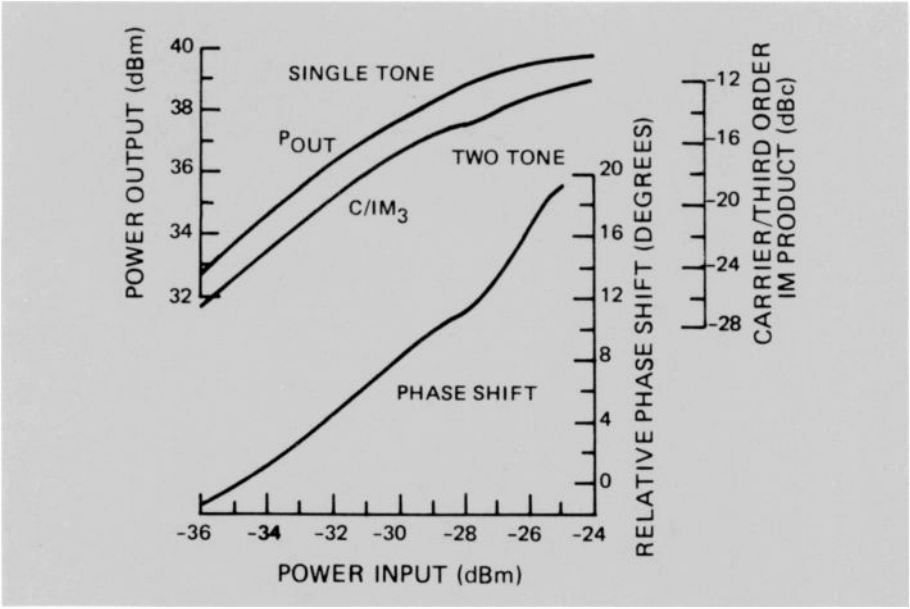

Fig. 9. *The power output for single-tone input and the level of the third-order-intermodulation products is shown, together with the relative phase shift as a function of input power.*

standardized production control for satellite operation. The power-transfer characteristics, the rf power output as a function of rf input drive, and the efficiency of the typical SSPA are shown in Fig. 7.

Since the maximum power dissipation of a single FLC-30 output-power FET is about 3 W under normal operating conditions, and its typical thermal resistance is 11°C/W, the temperature rise of the FET is only 33°C for an ambient operating temperature of 40°C. This assumes a 10°C temperature drop between the FET and spacecraft. A low junction temperature is extremely important for reliable, long-term operation of the FET amplifier.

Nonlinearities inherent in an amplifier produce distortion of the signal-modulated rf carrier. This distortion, a function of rf-input-drive level, causes two distinct types of nonlinearities relating to amplitude and phase distortion. Amplitude nonlinearities can be measured by gain compression, which is apparent by the reduction in gain from the small-signal value as drive increases. Phase nonlinearities, which have more significance than amplitude nonlinearities in an FM-modulated system, can be determined from the amplitude-modulation-to-phase-modulation (AM/PM) conversion factor

$$K_p = \frac{\Delta \phi}{\Delta P_1 / P_1}.$$

Measurement of AM/PM conversion (K_p) of a typical SSPA is shown in Fig. 8. The AM/PM performance of the SSPA is important because transmission distortions such as crosstalk and an increase in bit-error-rate arise in part from these AM/PM effects. The SSPA, as the dominant nonlinear element within the transponder, will determine the overall signal quality at the downlink earth receiver. Our measurements show significant decreases in phase distortion for the SSPA when compared to a TWT.

Intermodulation between multiple carriers sharing the same amplifier in a satellite causes distortion, which is another indicator of amplifier nonlinearity. To evaluate this characteristic, measurements are typically made of the two-tone third-order-intermodulation products that occur at frequencies $2f_{1,2} \pm f_{2,1}$ (sum and difference frequencies) relating to the input carriers.

One of the outstanding features of the SSPA is its linearity and gain flatness. As an indication of operating linearity for a typical SSPA, Fig. 9 illustrates the single-tone power output, the two-tone third-order-intermodulation product levels, and the relative phase shift, all as a function of the input drive level.

Power output and phase shift were measured at the centerband frequency of 3780 MHz, and the IMD was characterized for two equal carriers at 3760 and 3780 MHz. Third-order-intermodulation distortion measurements for two equal signals meet specified system requirements under the various rf drive back-off conditions. The total phase shift for the amplifier over a 10-dB drive range, starting at the 8.5-W operating points, is well below the specified limit of 22° cited for the amplifier.

A computer-controlled stepped-frequency small-signal-gain plot and the related tabulated gain data are shown in Fig. 10 for the typical SSPA. At 23°C, the amplifier is required to have gain flatness within a 0.3-dB/40-MHz window across the full 160-MHz operating bandwidth and a gain slope that never exceeds 0.025 dB/MHz. Gain slope is critical since frequency-modulated multicarrier inputs will be amplitude modulated by the gain slope with the subsequent AM/PM effects, inducing crosstalk between the carriers. The output from an automated test of gain versus frequency provides precise documentation of gain slope and gain variation parameters. As indicated in the tabulated computer data, performance is well within the designated SSPA specification.

As gain changes with varying temperature in the SSPA, a thermistor bias circuit controlling the gate bias to the first two stages of the amplifier compensates. Compensation circuitry has been designed to operate from 0°C to 40°C. Actually, the SSPA operating temperature range is 17°C to 40°C for the Satcom system based on the location of the amplifiers within the satellite. All amplifiers are compensated to within a 1.3 dB p-p maximum gain change over this temperature range. Figure 10 shows relative gain change for a typical SSPA, which is illustrated as 1.03 dB from 17°C to 40°C.

Group delay or linear envelope delay is another key performance characteristic specified and evaluated for the SSPA. Semi-automatic data are obtained by integrating an HP 9845T desk-top calculator with a Rantec group-delay test setup. A more sophisticated approach to group-delay measurement uses the phase versus frequency data

$$t_d = \frac{d\phi}{df}$$

from a phase-locked automated network analyzer (PLANA) measurement and derives the group-delay characteristic numerically. Preliminary results show good correlation between the Rantec and PLANA techniques. The maximum group-delay variation as a function of frequency for the amplifiers tested is typically 0.2 ns/10 MHz, well within a specification of 0.5 ns/10 MHz for the channel. This low value for group delay relates to the excellent fine-grain gain that the SSPA typically provides.

All-transistor-amplifier subassemblies, which are cascaded to make the SSPA amplifier chain, have been designed for

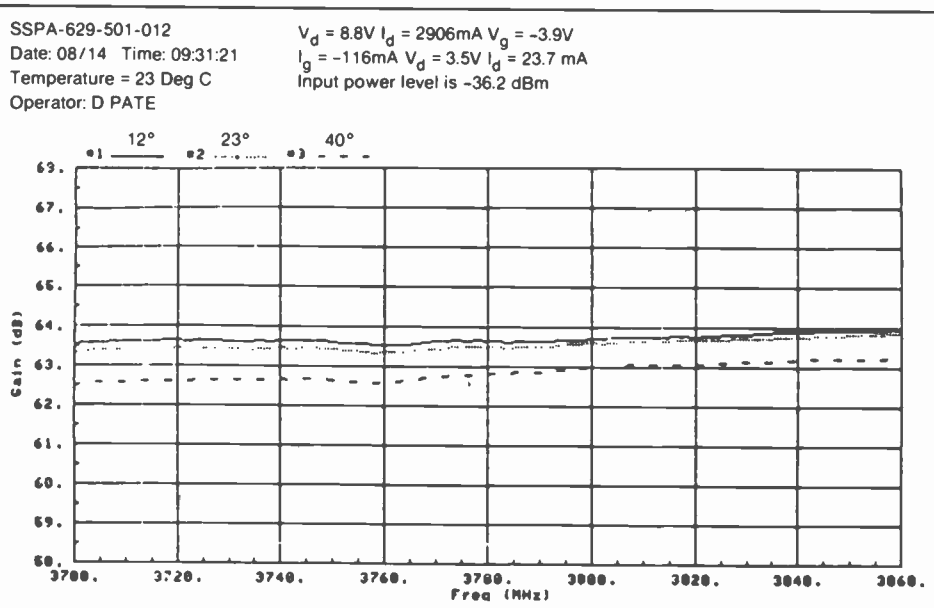

Freq (MHz)	Gain (dB)
3700.	63.33
3706.	63.40
3712.	63.41
3718.	63.44
3724.	63.43
3730.	63.42
3736.	63.44
3742.	63.45
3748.	63.45
3754.	63.39
3760.	63.35
3766.	63.41
3772.	63.47
3778.	63.51
3780.	63.49
3784.	63.48
3790.	63.52
3796.	63.57
3802.	63.59
3808.	63.64
3814.	63.65
3820.	63.67
3826.	63.70
3832.	63.73
3838.	63.76
3844.	63.79
3850.	63.81
3856.	63.83

Fig. 10. *The output from an automated test of gain versus frequency provides precise documentation of gain slope and gain variation parameters. Gain is automatically measured at discrete temperature levels. Following the temperature testing, data files are recalled and automatically plotted in this overlay fashion to reveal amplifier gain variation as a function of temperature.*

unconditional stability in a system with a 50-ohm characteristic impedance. However, because of the potential for distortion and/or disruption of communications traffic, measurements of spurious emissions are routinely taken on each SSPA.

To better understand SSPA performance, interaction with the electronic power conditioner (EPC) must be considered. The sensitivity or pushing factors for the SSPA are given in Table I.

The companion EPC has been designed[7] with ripple voltage held to 8 mV p-p for the gate bias and +3.5 V low-voltage drain and 20 mV p-p for the high-voltage drain potential. Tests involving SSPA/EPC under interface conditions in the spacecraft have been performed to ensure that the combination EPC and SSPA provide the required overall integrated performance (Fig. 11).

Although the amplifier is characterized as an 8.5-W device, power output and efficiency of the SSPA are a function of the high current-drain potential. A test was performed to characterize power output and efficiency with the drain potential varied from 8.7 to 10.1 V. Results, which are given in Fig. 12, indicate that an rf power output of 10.0 W can be obtained at 3.78 GHz with a 9.3-V drain at an efficiency of approximately 33%. The data shows that a power-output increase of 0.85 W/V was observed along with an efficiency degradation of approximately 1.5%/V as the drain voltage was increased. For reliability reasons, the amplifier has been restricted to operation below 9.3 V (9.0 V at the FET drain lead) for extended periods of time.

Acceptance test data

Table II summarizes acceptance test data taken on Flight Models for each of the specific amplifiers that provide frequency coverage over the 3.7- to 4.2-GHz downlink band in seven 160-MHz overlapping bands. The individual frequency bands cited

Table I. *Satcom 8.5-W SSPA drain-bias sensitivity.*

	+8.7-V Drain			+3.5-V Drain		
	10%	*-10%*	*Worst Case Δ Δ*	*+10%*	*-10%*	*Worst Case Δ/Δ*
Small-signal gain	0	0.1dB	0.12dB	-0.4 dB	+0.2 dB	1.15 dB/V
Output power	1.03 W	-1.17 W	1.38 W/V	+0.03 W	0	0.086 W/V
Output phase	2.3°	5°	5.9°/V	2.2°	1.7°	6.3°/V

Gate-bias sensitivity.

	Vg = -3.7/V		
	+10%	*10%*	*Worst Case Δ/Δ*
Small-signal gain	-0.6 dB	+0.8 dB	1.67 dB/V
Output power	-0.26 W	+0.1 W	0.87 W/V
Output phase	+4.2°	-8.2°	27.34°/V

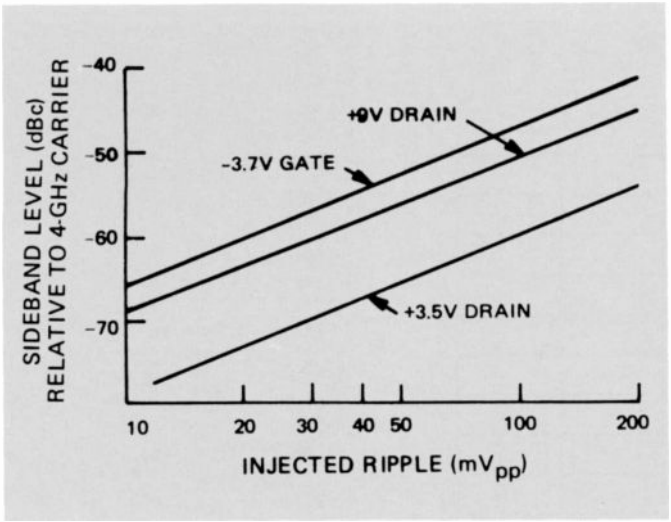

Fig. 11. *One of the tests carried out subjected three out of four SSPA amplifiers to a carrier with 95% rf amplitude modulation, while monitoring the sideband levels induced on the fourth SSPA. Both sinusoidal and square-wave modulation from 500 Hz to 10 kHz were investigated.*

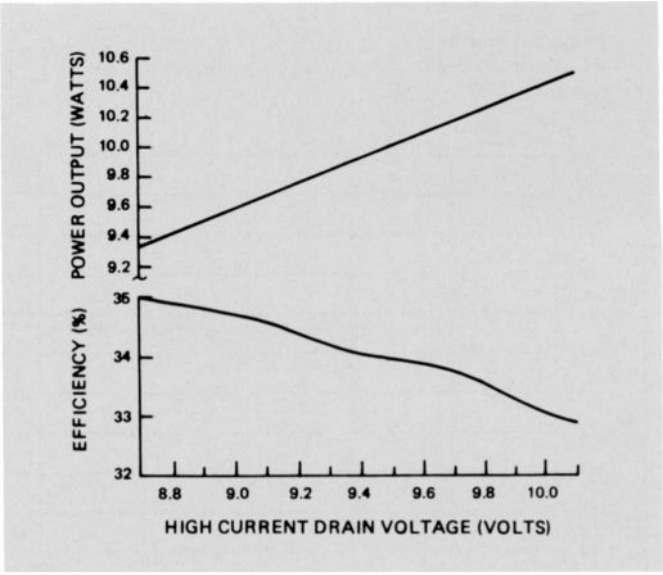

Fig. 12. *The SSPA is operated at a nominal drain voltage of 8.7 V. As drain voltage is increased, power-output capability increases, but efficiency decreases.*

for each of the seven distinct SSPA types ensure that each SSPA will operate over the primary channel designated, as well as in an alternately designated channel if an initially operating SSPA is eliminated and a spare switched in during satellite operation. Twenty-eight amplifiers are used on the Advanced Satcom F spacecraft; twenty-four amplifiers are active, with four on standby for redundancy.

In addition to measures of the previously mentioned features, gain flatness and line-

Table II. *SSPA performance spanning 3.7–4.2 GHz.*

	Type		*501*	*502*	*503*	*504*	*505*	*506*	*507*
Specification	Limit	Units	3.7–3.76	3.76–3.92	3.82–3.98	3.88–4.04	3.94–4.10	4.0–4.16	4.04–4.2
Operating-point drive		dBm	–26.0	–25.0	–19.0	–26.2	–23.1	–25.1	–25.2
Output power	39.2 8.3	(dBm) Watts	39.4	39.4	39.2	39.3	39.4	39.4	39.4
Large-signal gain	58–68	dB	65.2	64.6	58.2	65.5	62.6	64.6	64.5
Small-signal gain flatness	0.3	dB/40MHz	0.216	0.30	0.16	0.19	0.25	0.16	0.17
Gain slope	0.025	dB/MHz	0.010	0.010	0.008	0.017	0.015	0.000	0.013
Gain variation (0–40° C)	1.3	dBpp	0.64	0.53	0.90	1.20	0.75	0.81	0.93
Amplitude linearity									
–3 dB	–12	dBc	12.8	13.7	12.1	15.2	13.1	12.9	12.1
–10 dB	–20	dBc	21.0	26.2	21.7	30.5	23.5	27.0	22.9
–17 dB	–30	dBc	38.4	45.0	35.1	42.6	42.3	40.8	42.0
Phase shift									
0 dB	22	degrees	19.2	14.9	18.0	8.9	18.2	15.9	16.4
–3 dB	17	degrees	12.2	10.1	15.0	7.2	12.0	15.4	8.2
–6 dB	14	degrees	6.2	4.7	11.0	3.7	9.4	7.6	3.9
–10 dB	7	degrees	1.1	1.2	3.6	0.1	3.6	2.5	0.7
Group delay variation	0.7	ns	0.7	0.4	0.5	0.3	0.3	0.6	0.6
Slope	0.5	ns/10MHz	0.4	0.2	0.5	0.2	0.1	0.5	0.2
VSWR input	1.25:1		1.22:1	1.118:1	1.14:1	1.181:1	1.046:1	1.24:1	1.068:1
output	1.15:1		1.054:1	1.099:1	1.10:1	1.045:1	1.118:1	1.08:1	1.102:1
Spurious (dc–12.4611)	–10	dBm/ 10/MHz	none	none	none	none	none	none	none
Harmonics 2nd	–12	dBc	–53	–52	–58	–41	–49	–49	–41
3rd	–21	dBc	–36	–43	–36	–44	–33	–36	–30
Power (dc) 40° C			25.9	24.9	24.8	24.4	23.8	24.2	24.0
23° C	27.5	Average	25.0	25.6	25.4	25.1	24.3	26.9	24.7
17° C	28.5	peak watts	25.2	25.9	25.7	25.2	24.7	27.0	24.8
Worst-case efficiency (dc/rf)	30 percent	Minimum	33.7	33.6	32.3	33.7	35.30	32.3	35.1

arity, extensive tests have been routinely made on each amplifier for spurious output covering the 0.01- to 12.4-GHz frequency range. These tests clearly indicate that the SSPA is unequivocally stable.

Reliability of the SSPA

Operational reliability and long service life are among the most important requirements for a satellite-borne communications system. Therefore, a comprehensive stress and life-test program was initiated. As a prelude to reliability tests, preliminary assessment and evaluation of various GaAs field-effect transistors for the critical final output stages of the SSPA was undertaken. This selection, as indicated previously, was based on the high level of power-added efficiency, and basic reliability data supplied by the manufacturer under the operating conditions required. Consistent with this selection, generically identical Fujitsu FLC-type transistors with common processing, reduced gate periphery, and lower power rating, were also selected for most of the remaining lower power stages in the chain.

To substantiate this selection, a comprehensive characterization and accelerated life-test program were initiated to qualify the selected FETs and to provide sufficient data to enable a prediction of the mean-time-to-failure for the FETs and the integrated SSPA.[8] The power FETs were operated at elevated channel temperature. This test was performed to obtain an estimate of the failure rate and wearout life consistent with a 10-year objective operating period and to determine whether any inherent failure mechanism existed. The tests carried out under rf drive conditions were implemented by using FLC-30 output-power modules consisting of appropriate microstrip circuitry and passive matching components. Although actual SSPA operating-channel temperature for the FLC-30 has been estimated to be ~90°C, based on an SSPA maximum base-plate-mounting temperature of 45°C in the spacecraft, two separate levels of elevated channel temperature (190°C and 215°C) were used for life tests.

The results of the accelerated life-testing program pursued are highlighted in Table III.

During the life test, no catastrophic failures occurred that could be assigned to FET malfunction. Consistent with worst-case design analysis in the SSPA, the failure criteria due to wearout were based on an output gain reduction of 0.3 dB with fixed rf drive.

The resulting failure rates for the FETs based on the aforementioned tests predict less than two failures in 10^9 device hours. Using a failure rate for each of the FETs within the SSPA, parts count data, and a recognized failure rate of 10 FITs (failures in 10^9 hours) for each passive component, a reliability prediction of 457 FITs can be substantiated for the SSPA. This is in contrast to ~1500-2000 FITs for comparable TWTs.

During the course of the SSPA technology transfer program, comprehensive specifications were developed to assure a continued supply of FET devices with reproducible electrical characteristics capable of consistently meeting established performance criteria. During the manufacturing cycle, both failed parts and parts with discrepant performance are thoroughly analyzed. This permits a prompt response if difficulties are encountered with devices that might lead to long-term reliability degradation. At this point in time, an engineering model SSPA has been tested under rf drive (output power, 7.8 W) at an ambient temperature of 55°C for more than 12,000 hours with no detectable degradation in rf performance. These tests will be augmented by additional life tests as the manufacturing process continues.

Table III. *Testing under these conditions provides the necessary acceleration factors and related failure rates by establishing a linear Arrhenius function between temperature of operation and mean-time-to-failure. Using this relationship, a prediction has to be made of expected life performance at operating temperature for the FETs on the basis of data collected at elevated temperature over greatly reduced time spans.*

Operating channel temperature	*Test unit hours at operating rf power*	*Total amplifier modules tested*	*Maximum operating test time without failure*
190°C	100,882	19	2 units with 6,680 hrs 1 unit with 8,091 hrs
215°C	24,686	8	1 unit with >6,000 hrs

Table IV. *A performance comparison of the solid-state power amplifier versus the traveling-wave-tube amplifier.*

	SSPA	*TWT*
RF power	8.5 W	same
Frequency	3.7 to 4.2 GHz	same
Bandwidth	160 MHz	100 MHz
Power gain	>58 dB	same
Gain compression (at high-level operating power)	~2 dB	6 dB
Gain flatness	0.3 dB/10 MHz	same
Amplitude linearity (3rd-order IMD)	-12 dBc	-8 dBc
Phase conversion (AM/PM)	2°/dB	5°/dB
Total phase shift (final 10-dB drive range)	22°	45°
Harmonics	-35 dBc	-12 dBc
Efficiency	~33%	38%
Maximum operating voltage	10 V	2500 V
Thermal cathode-heater assembly	none	required
Weight — SSPA Weight — EPC	13 oz. 18 oz.	25 oz. 36 oz.
Projected life	10 yrs.	7 yrs.
Failures in 10^9 hours	<500	>2000

Conclusion

The SSPA can replace the C-band TWT with demonstrated improvements in rf performance and projected improvements in

Authors LaPrade (standing) and Wolkstein.

Nick LaPrade is a Member of the Technical Staff, Microwave Design and Engineering, RCA Astro-Electronics. He joined RCA in 1978 after completion of his BSEE. He received the MSEE from Drexel University in June, 1982, and is now a doctoral candidate there. He was involved in the original development work on the SSPA, including the first high-gain 5-W SSPA, which laid the groundwork for the 8.5-W development program. He currently supports production efforts on the SSPA, in addition to his engineering design responsibilities.
Contact him at:
RCA Astro-Electronics
Princeton, N.J.
TACNET: 229-2567

Herb Wolkstein joined Microwave Operations in 1955, after seven years as Project Engineer in the Research Laboratories of National Union Electric Corporation. In 1961, he became Manager, TWT Design and Development. In 1964, as Manager of Microwave Advanced Product Development, Mr. Wolkstein directed a group in advanced development and applications work on TWTs and solid-state devices. In 1972, he was named Manager of the Advanced Programs and Application Engineering Group. He held that position until 1975; then he became a Member of Technical Staff of the Microwave Technology Center, RCA Laboratories, Princeton, N.J.

Today, as Manager, Space and Countermeasures Programs, Mr. Wolkstein develops and applies solid-state microwave devices and subsystems. Mr. Wolkstein has been awarded 12 patents in the electron-tube and solid-state fields. He has written numerous papers on microwave TWT and solid-state system designs.
Contact him at:
RCA Laboratories
Princeton, N.J.
TACENT: 226-2710

reliability and operating life. A comparison of the salient performance differences between the SSPA and TWT is given in Table IV. Improvements in all areas dependent on the linearity of power transfer characteristics will allow an increased number of rf subcarriers to be accommodated by each SSPA channel in multicarrier service and will result in more revenue. Efforts are now underway to increase rf power output and efficiency to give better equivalent isotropically radiated power and reduced spacecraft-solar-power system demands.

The benign operating potential of the SSPA eliminates voltage-breakdown failures, whether caused by self outgassing or by operation in the Paschens breakdown region typical of many TWTs. Moreover, the wear-out mechanism of the thermionic heater-cathode assembly, cathode positioning, and turn-off/turn-on constraints associated with TWT failure history are eliminated with the SSPA. These inherent improvements will lead to considerable reduction in the failure rate in contrast to the TWT. The SSPA will meet the required goal of ten years of operation in a communications satellite environment.

Acknowledgments

The authors acknowledge the foresight and confidence of P.E. Wright; the support and encouragement of F. Sterzer and J.E. Keigler; the insights supplied by P.F. Pelka, W.V. Allison, R.S. Wondowski, M.T. Cummings, B.R. Dornan, A.L. Stern, and W.J. Slusark in their respective fields of expertise. Thanks, also, to J.L. Mackin for his manufacturing and logistics acumen; and F.A. Pinelli, M.D. Bingert, and R.H. Carpenter for their manufacturing insight. In addition, the confidence of the Satcom Program Manager, A.W. Weinrich, and Payload Manager, H.J. Zelen, are gratefully acknowledged.

References

1. Doman, B., Slusark, W., Jr., Wu, Y.S., Pelka, P., Barton, R., Wolkstein, H., and Huang, H., "A 4-GHz FET Power Amplifier: An Advanced Transmitter for Satellite Down-Link Communications Systems," *RCA Review*; Vol. 41, No. 3, pp. 472-506 (September, 1980).
2. McEwan, K.J., Prahbu, A.N., Conlon, E.J., and Hitch, T.T., Private Communications: Thick Film Bias Network.
3. Allison, W., and Wondowski, R., Private Communications.
4. Cummings, M., Doman, B., and Pelka, P., Private Communications.
5. Pinelli, F., Bingert, M., Carpenter, R., Scoffone, R., and Ficken, R., Private Communications.
6. Perlman, B., Perlow, S., Paglione, R., and Schroeder, W., Private Communications: Automated Test Facility.
7. Schuster, R., Longeoy, D., Private Communications.
8. Slusark, W.J., McEwan, K., and Monshaw, V.R., Private Communications.

R.W. Paglione

Medical applications of microwave energy

Microwave energy has been effective in the solution of many biological problems. The Microwave Technology Center has developed equipment that has been used in some of these medical applications.

Abstract: *The Microwave Technology Center has been involved in the development of medically related microwave equipment for nearly ten years. These developments include microwave applicators for producing localized hyperthermia; a self-balancing microwave radiometer for noninvasively measuring tissue temperatures; microwave applicators used for "fixing" cells and for measuring blood flow; and a Doppler system for monitoring apnea.*

The use of microwaves in medically related applications dates back almost to the inception of microwave generators in the late 1930s and early 1940s. Researchers began to measure the dielectric properties of biological tissues at microwave frequencies in the late 1940s;[1] microwave diathermy[2] and medical uses of microwave ovens became prevalent in the 1950s.[3] Today, researchers are using microwaves for thawing frozen samples of blood, for detecting patient motion, for tomographic imaging,[4] for inducing localized hyperthermia as a cancer therapy, and in various other applications. The Microwave Technology Center of RCA has played an active role in the development of many of these medical applications, several of which will now be described.

Microwave hyperthermia

The most important of the medically related programs involves the use of localized radiofrequency and microwave heating for the treatment of cancer. This subject was treated thoroughly by Dr. F. Sterzer in the Jan./Feb. 1982 issue of the *RCA Engineer*. Since then, several new types of applicators have been developed: for example, a miniature coaxial applicator for interstitial heating, an applicator for treating cervical and uterine cancer, and an applicator for treating melanoma of the eye.

The miniature coaxial applicator, shown in Fig. 1, is made from a length of 0.86-mm-diameter, semi-rigid coaxial cable. The radiating end is formed by removing a small portion of the outer conductor of the cable, thereby exposing the insulated center conductor. The insulated center conductor is trimmed to a length that produces an efficient transfer of energy into the surrounding body tissues. This applicator operates at 2450 MHz and produces an ellipsoidal heating pattern about the junction of the outer conductor and the exposed center conductor. A copper-constantan thermocouple is attached to the outer conductor at this junction for monitoring temperature. The overall diameter of the applicator has been designed to fit inside a standard plastic brachytherapy tube.

This type of brachytherapy consists of inserting several radioactive pellets into one or more plastic tubes that have been placed within a tumor. A typical placement for breast cancer may be as sketched in Fig. 2. The plastic tubes are inserted into the breast with stainless-steel needles and then the needles are removed, leaving the tubes in place. The radioactive pellets are positioned in each tube so as to produce the desired radiation pattern and dosage. The microwave applicators are inserted into the same tubes prior to and after the ionizing radiation treatment. The usual microwave treatments consist of heating the tissues to approximately 43°C and maintaining them at that temperature for 45 minutes to one hour. These applicators are presently being used in animal and clinical experiments at the Montefiore Hospital, Bronx, New York, and at the St. Barnabas Hospital, Livingston, New Jersey.

A four-way power-splitter/controller was designed to supply and control the power to a system of four of the interstitial applicators. The entire unit is shown in Fig. 3. The power-split-

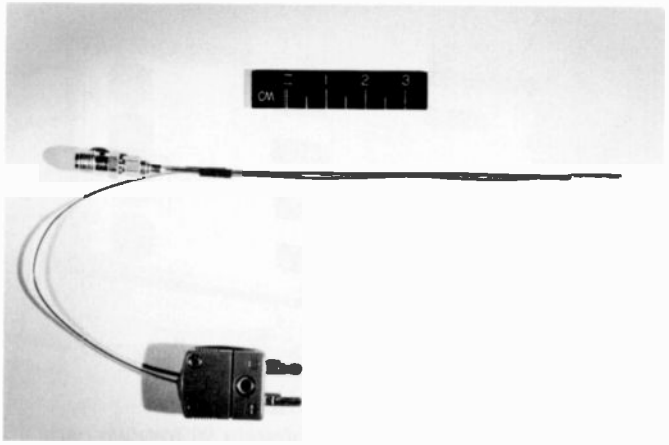

Fig. 1. *A miniature coaxial applicator used to produce interstitial microwave hyperthermia. The applicator is made from a length of 0.86-mm-diameter, semi-rigid coaxial cable. This applicator operates at a frequency of 2450 MHz.*

© 1982 RCA Corporation
Final manuscript received July 12, 1982
Reprint RE-27-5-3

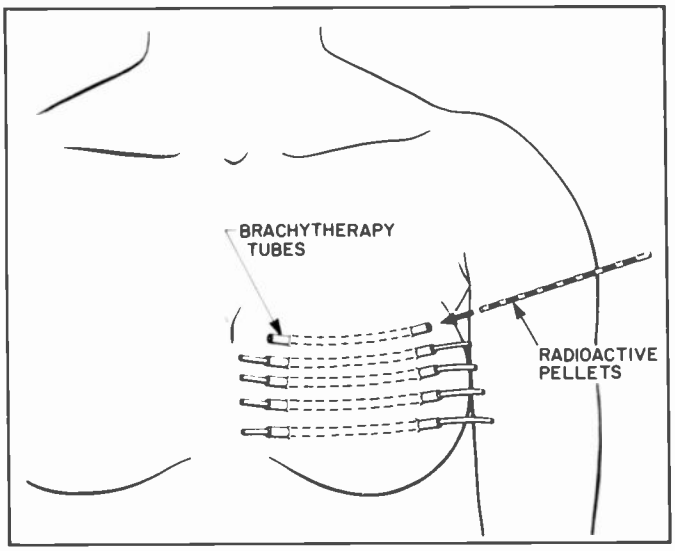

Fig. 2. *A typical placement of brachytherapy tubes for treating breast cancer. The microwave applicators are inserted into these tubes to heat the tissues prior to and after an ionizing radiation treatment.*

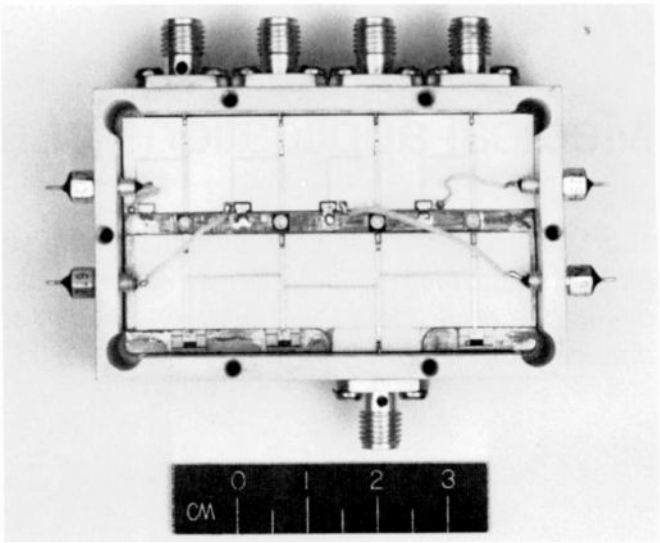

Fig. 3. *A four-way power-splitter/controller designed to supply and control the power to a system of four interstitial applicators. The microwave integrated circuit operates at a frequency of 2450 MHz at an input power of up to 50 watts.*

ter input circuit is a combination of 3-dB hybrid couplers, the first coupler splitting the input into two equal channels. A coupler on each of these channels produces four equal channels each with one-fourth the input power. A high-power *pin* diode is mounted across each of the output lines. These diodes have a very low impedance when they are forward biased and a very high impedance when they are reverse biased. Therefore, in the forward-biased case, the diodes will reflect the power back to the internal terminations; in the reverse-biased case, they will allow the power to be transmitted to the antennas. The bias to the *pin* diodes is generated by a comparator circuit (not shown in the figure) that dynamically compares the actual temperature to the desired temperature and then sets the bias accordingly.

The same four-way splitter/controller assembly and similar miniature coaxial applicators have been incorporated into a system for the National Institutes of Health in Bethesda, Maryland. This system, shown in Fig. 4, is based on a modified Fletcher-Suit applicator, shown in the foreground of Fig. 4. The modified Fletcher-Suit is shown in more detail in Fig. 5. The standard applicator, made entirely of stainless steel, is used to treat cancer of the cervix and uterus with ionizing radiation from radioactive pellets. To allow microwaves and ionizing radiation to be used, the stainless-steel ovoids were replaced with Teflon* and the tandem was replaced with fluorinated ethylene propylene (FEP). The positions of the microwave antennas are shown in the insets of Fig. 5. The heat-deposition patterns of this system are now being measured in tissue-equivalent materials at NIH, and some clinical trials are also being planned.

Figure 6 shows an applicator designed to treat melanoma of the eye with microwave hyperthermia. The radiating element is

* Trademark of E.I. duPont de Nemours & Co., Inc., Wilmington, Delaware.

Fig. 4. *The modified Fletcher-Suit system for treating cancer of the cervix and uterus with ionizing radiation and microwave hyperthermia. The system includes a 50-watt magnetron source, a four-way power-splitter/controller, and output attenuators.*

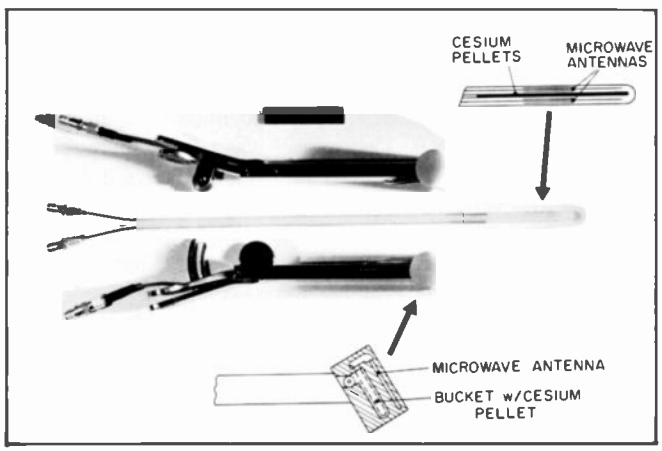

Fig. 5. *The modified Fletcher-Suit applicator. The applicator consists of a left and right colpostat and a center tandem. The ovoid on each colpostat contains a miniature coaxial applicator and a radioactive source. The tandem contains two miniature applicators and a radioactive source. The microwave applicators operate at 2450 MHz.*

a spiral inductor printed on a 0.79-mm-thick and 10 mm in diameter, bowl-shaped, RT Duroid* substrate fed by a 0.86-mm coaxial cable. The applicator operates at a frequency of 5800 MHz and is presently being used by researchers at the Brookhaven National Labs, Long Island, New York. The applicator is to be used in conjunction with an ionizing-radiation method that they have developed. This method uses a bowl-shaped gold plaque that is approximately 10 mm in diameter. The plaque is seeded with radioactive iodine and is sutured over the affected part of the eye and left in place for approximately 72 hours. The researchers' plan is to attach the microwave applicator between the plaque and the eye and heat while radiating. To date, they have been successful in heating a normal eye of a rabbit to 45°C, to a 5-mm depth beneath the applicator. Their next steps will be to determine the effect on an eye that has had a tumor transplanted into it, and then to determine the effects of the combination of heat and ionizing radiation.

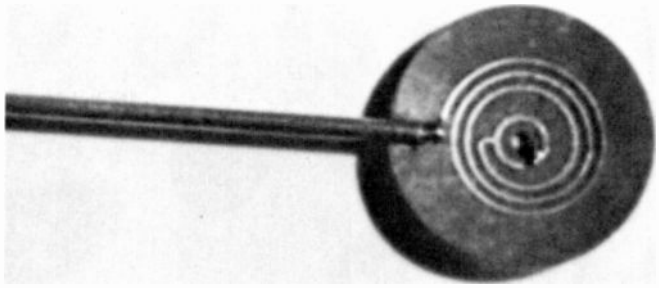

Fig. 6. *The applicator designed for treating melanoma of the eye. The radiating element is a spiral inductor that is printed on a bowl-shaped substrate. The energy is fed to the radiator through a 0.86-mm-diameter coaxial cable. The applicator operates at 5800 MHz.*

Microwave radiometer

A self-balancing microwave radiometer has also been developed by the Microwave Technology Center for noninvasively measuring the temperature of subcutaneous tissues.[5] Radiometers of the standard Dicke-switched type measure the thermal noise power received from a target and compare this to the thermal noise power received from a heat source at a known temperature.[6] The difference between these received powers is translated into a value for the temperature of the target. The temperature displayed is an average of the temperature over a depth determined by the frequency range of the components used in the radiometer. If the radiometer is filtered to receive radiation at for example, 5800 MHz, then the temperature displayed will be an average of the temperature over the first few millimeters of body tissue. However, if the frequency is 915 MHz, then the temperature would be an average over a depth of from 1 to 2 centimeters.

The temperature indicated by the radiometer not only depends on the tissue temperature but also on the mismatch between the antenna of the radiometer and the tissues. Self-balancing radiometers overcome the errors introduced by the applicator by automatically compensating for their mismatch. A schematic of a 2450-MHz radiometer is shown in Fig. 7. The reference radiation level is provided by a diode noise source, and the Dicke switch is a latching circulator.

The planned uses of the radiometer include the determination of the temperature-depth profile of body tissues during microwave hyperthermia and for the diagnoses of organic dysfunctions in routine or emergency situations.

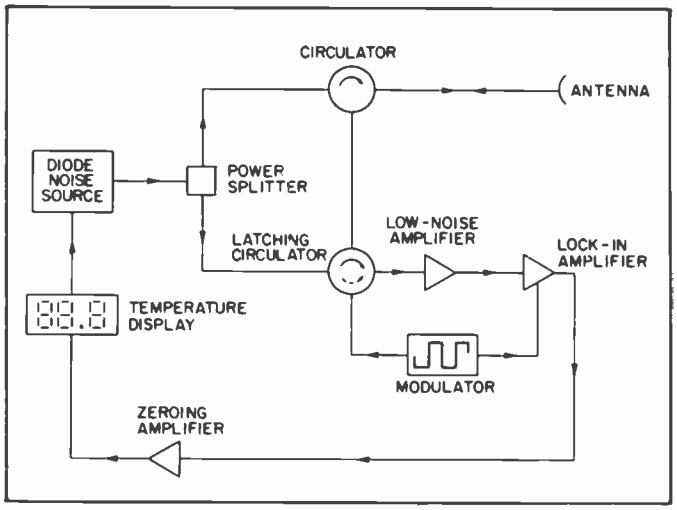

Fig. 7. *A 2450-MHz, self-balancing radiometer. The reference noise level is provided by a diode noise source, and the Dicke switch is a latching circulator.*

Microwave "fixing" of cells

Before cell cultures can be photographed in an electron microscope, the cells must not be growing or moving. This "fixing" procedure is normally done chemically with formaldehyde or other similar agents; however, these agents do add a certain degree of "artifact" (artificial structure) to the cells. It is believed that heat will have the same fixative effect on cells, but will produce little or no artifact. This theory is being tested by Structure Probe, Inc., West Chester, Pennsylvania. They are heating cells in agar, a culture medium, with a 2450-MHz applicator that was designed at the Microwave Technology Center. Figure 8a shows an electron micrograph of *E.-coli* bacteria cells in agar that have been heated with 10 watts of continuous power for 15 seconds and then "fixed" in the normal way with an aldehyde solution. In Fig. 8b, a similar cell culture has been heated with 10 watts for 30 seconds and "fixed" with the same solution. In Fig. 8a, the heat has had little effect and the cells have remained normal. In Fig. 8b, the cells were heated to the point where they exploded. Structure Probe is now trying to determine if cells heated with microwaves, as shown in Fig. 8a, are being "fixed" by the heat.

Microwave blood-flow measurement

Common techniques and equipments for measuring blood flow include the injection and monitoring of radioactive trace materials in the blood stream, angiograms, Doppler flowmeters, and the thermal washout technique. The thermal washout technique is certainly the least complicated of the above techniques since it only involves the generation and monitoring of heat—the decay rate of the tissue temperature after heating is proportional to blood flow. Using microwaves, the heat is generated in body tissues by the absorbed microwave energy and the temperature is measured by standard thermocouples or the previously mentioned radiometer. Figure 9 shows a coaxial applicator with an integral thermocouple that was designed to indicate the blood

* Trademark of Rogers Corporation, Chandler, Arizona.

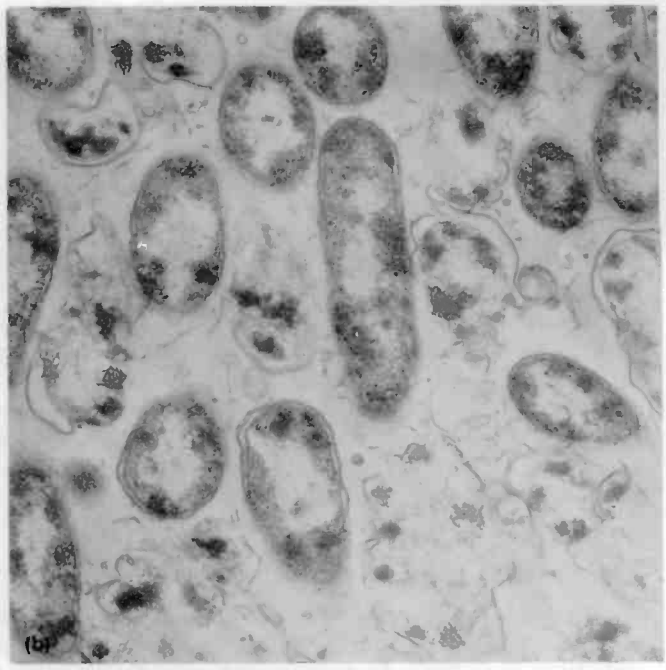

Fig. 8. *Electron micrographs (50,000X) of* ***(a)*** E.-coli *bacteria cells that were irradiated with 10 watts of microwave energy at a frequency of 2450 MHz for 15 seconds, and* ***(b)*** E.-coli *cells that were irradiated with 10 watts for 30 seconds. The cell structure in* ***(b)*** *is noticeably damaged. (Photomicrographs supplied by Structure Probe, Inc., West Chester, Pa.).*

flow of heart-muscle tissue on patients who are undergoing heart-bypass surgery. The center conductor of the coaxial line is a stainless-steel-sheathed thermocouple that is 0.51 mm in diameter. The center conductor is attached to a 90° coaxial connector and then it continues out through a shorted-stub tuner to a digital thermometer and strip-chart recorder. The microwave energy, at a frequency of 2450 MHz, is fed through the coaxial connector and is maximized in the direction of the body tissues by adjusting the tuner. To monitor blood flow, the open end of the applicator is placed against the tissues and approximately 1 watt of power is applied. The temperature, measured by the thermocouple-center-conductor, is displayed on a strip-chart recorder. The microwave power is shut off when the tissue temperature reaches 39 or 40°C, and the temperature decay is recorded. The process is repeated as often as desired and the decay curves are compared to determine the change in blood flow. This applicator was used in blood perfusion experiments performed on dogs by researchers in the Department of Physiology at Temple University.

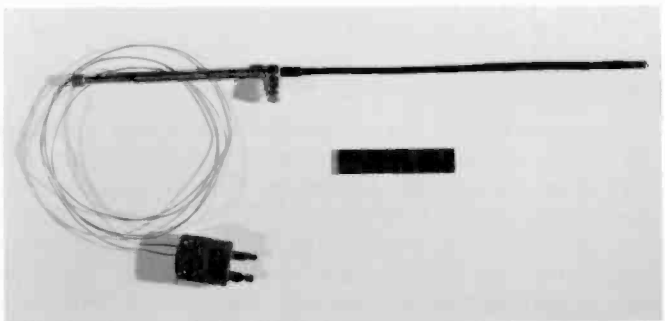

Fig. 9. *A coaxial applicator used to monitor blood flow. The applicator has a center conductor that is a stainless-steel-sheathed thermocouple for measuring the temperature of the tissues that have been heated with microwaves. The applicator operates at a frequency of 2450 MHz.*

Apnea monitor

The monitoring of apnea—the temporary loss of respiration—is particularly important in medical efforts to prevent sudden infant death (SID) syndrome. Most available apnea monitors are cumbersome in that they require a physical attachment of the sensing element to the body of the patient. Figure 10 is a photograph of an apnea monitoring system based on a microwave Doppler radar. The system was developed by the Microwave Technology Center for use as a remote monitor of respiration and heart rate. The unit on the right in Fig. 10 contains the antenna, transmitter, receiver, and signal processor. This unit can be mounted on or near the ceiling of a nursery for coverage of a crib, incubator, or playpen. The unit on the left in the figure contains an audible alarm that can be activated after the patient's respiration has

Fig. 10. *A Doppler radar used as a noncontacting apnea monitor. The unit on the right contains the antenna, transmitter, receiver, and signal processor; the unit on the left contains an audible alarm that can be activated when and if respiration ceases. The unit operates at a frequency of 10.525 GHz.*

stopped for a predetermined amount of time. The unit operates at 10.525 GHz and has an output power level of 0.1 milliwatts. If the patient-to-monitor distance is kept to a minimum of 1.8 m, then the power density at the patient is approximately 0.01 microwatts/cm^2, which is much less than the most conservative radiation-hazard standard. A miniaturized version of the apnea monitor has been proposed to the Army Medical Corps for an application involving the remote sensing of vital signs of personnel injured in battle.

Conclusion

The Microwave Technology Center has played a role in the development of microwave equipment for medical applications as evidenced by the projects that have been mentioned. The results of these ongoing projects, especially those relating to microwave hyperthermia, are continuing to show promise and acceptance. The future holds promising approaches to diagnosis, treatment, and monitoring in every aspect of the medical profession.

Acknowledgment

The author wishes to thank William Hittinger, Kerns Powers, Fred Sterzer, and William Webster for their continuing encouragement of this work.

References

1. England, T.S., and Sharples, N.A., "Dielectric Properties of the Human Body in the Microwave Region of the Spectrum," *Nature* Vol. 163, p. 487 (1949).
2. Krusen, F.H., "New Microwave Diathermy Director for Heating Large Regions of the Human Body," *Arch. of Phys. Med.*, Vol. 23, pp. 695-698 (1951).
3. Robert, J.F., and Cook, H.F., "Microwaves in Medical and Biological Research, *Brit. J. of Appl. Phys.*, Vol. 3, p. 33 (1952).
4. Rao, P.S., *et al.*, "Computer Tomography with Microwaves," *Radiology*, Vol. 135, No. 3, pp. 769-770 (June, 1980).
5. Sterzer, F., *et al.*, "A Self-Balancing Microwave Radiometer for Non-invasively Measuring the Temperature of Subcutaneous Tissues During Localized Hyperthermia Treatments of Cancer," *IEEE MTT-S Digest*, pp. 438-440 (1982).
6. Dicke, R.H., "The Measurement of Thermal Radiation at Microwave Frequencies," *Rev. Scient. Instr.*, Vol. 17, pp. 268-275 (July 1946).

Robert Paglione received the BSEE degree from New Jersey Institute of Technology (formerly Newark College of Engineering), Newark, New Jersey, in 1968, and the MSEE degree from Stevens Institute of Technology, Hoboken, New Jersey, in 1972. Mr. Paglione joined RCA Laboratories in 1967 and has been a Member of Technical Staff since 1970. He is currently affiliated with the Microwave Technology Center as a project engineer engaged in the development of rf and microwave heating equipment for industrial, medical, and scientific applications. Mr. Paglione has authored many publications in the microwave field and holds four U.S. patents. He is a member of the IEEE and the International Microwave Power Institute.

Contact him at:
RCA Laboratories
Princeton, N.J.
TACNET: 226-3167

The Engineer's Notebook

A high-power *pin* diode

Paul J. Stabile
RCA Laboratories
Princeton, N.J.

Longer carrier lifetimes have enabled *pin* diodes to operate at lower frequencies.[1] RCA high-frequency high-voltage power *pin* diodes provide low-frequency performance formerly available only in the UHF region. In the forward-bias mode, this high-lifetime *pin* diode will pass, distortion free, 4 kilowatts (kW) of high-frequency power into a 50-ohm load; and, in the reverse-bias mode, with only 0.1 milliwatts of dc power, one diode will block 4 kW of high-frequency power.

The *pin* diode was first proposed in the form of a fused germanium power rectifier.[2, 3] The intrinsic region allowed reverse-bias specifications to significantly exceed existing *p-n* junction reverse-bias capabilities. The *pin* was identified as a kilowatt device from its inception. In 1956, a diffused silicon *pin* power rectifier was introduced and shown to be superior to existing germanium or selenium rectifiers under higher ambient-temperature conditions (for example, 125°C).[4] The germanium and silicon diodes had an approximate upper-frequency limit, as efficient rectifiers, of 20 and 1 kHz, respectively.

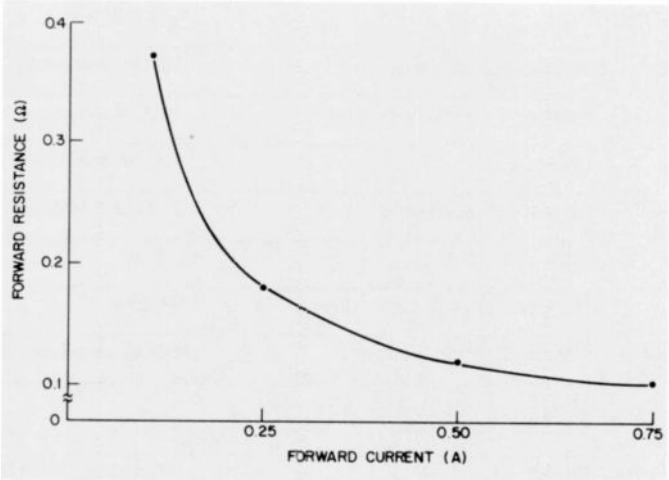

Fig. 1. *Forward resistance as a function of forward-bias current for two diodes packaged in series (MTC-P2).*

© 1982 RCA Corporation

Final manuscript received July 28, 1982
Reprint RE-27-5-4

Fig. 2. *A 10,000-volt package with 10 diodes in series.*

The next application considered for the *pin* diode was in the microwave-frequency range.[5] It was shown that the rf forward resistance of the *pin* depended on the level of the dc biasing current (Fig. 1). Also, the low capacitance in the zero-bias and especially the reverse-bias state enabled the diode to act as a high impedance to microwave signals. Microwave switching, transmission lines, attenuators, and limiters were suggested as applications for the *pin*. Even a monolithic traveling-wave diode amplifier, consisting of a sequence of alternate *p-n* and *pin* diodes, was proposed.[5] *Pin* diodes as protective microwave limiters were developed[6,7] and their peak protector levels approached the megawatt region at 9.0 GHz.[8]

Caulton *et al.*, Rosen *et al.*, and Basile *et al.* report the use of the *pin* diode as a high-power, low-loss switch at lower frequencies.[1,9,10] This was possible because the lifetime and the voltage breakdown of the diode were increased. Lifetimes of 15 to 50 μs allow the diode to operate at as low as 500 kHz. The only disadvantage at these low frequencies is that the diode must be reverse biased at the peak rf voltage for it to successfully remain off. This is due to drift transit-time effects.

To date, diodes have been packaged in various series combinations to provide greater voltage breakdown (Fig. 2). Specifications for typical *pin* diode packages are given in Table I.

References

1. Caulton, M., Rosen, A., Stabile, P., and Gombar, A., "*PIN* Diodes for Low-Frequency, High-Power Switching Applications," *IEEE Trans. Microwave Theory Tech.*, Vol. MTT-30, pp. 875-882 (June 1982).
2. Hall, R.N., "Power Rectifiers and Transistors," *Proc. IRE*, Vol. 40, pp. 1212-1218 (November 1952).
3. Hall, R.N. and Dunlap, W.C., "*P-N* Junctions Prepared for Impurity Diffusion," *Physical Review*, Vol. 80, No. 3, pp. 467-488 (November 1, 1950).
4. Prince, M.B., "Diffused *p-n* Junction Silicon Rectifiers," *Bell System Tech. J.*, Vol. 35, pp. 661-684 (May 1956).
5. Uhlir, A., Jr., "The Potential of Semiconductor Diodes in High-Frequency Communications," *Proc. IRE*, Vol. 46, pp. 1099-1115 (June 1958).
6. Cranna, N.G., "Diffused Silicon *PIN* diodes as Protective Limiters in Microwave Circuits," Tenth Interim Report on Microwave Solid-State Devices, Bell Telephone Laboratories, USAROL, Contract DA 36-039 sc 73224 (August 15, 1959).
7. Leenov, D., Forster, J.H., and Cranna, N.G., "*PIN* Diodes for Protective Limiter Applications," 1961 International Solid-State Circuits Conf., *Digest of Technical Papers*, pp. 84-85 (February 1961).
8. Leenov, D., "The Silicon *PIN* Diode as a Microwave Radar Protector at Megawatt Levels," *IEEE Trans. Elec. Dev.*, ED-11, pp. 53-61 (February 1964).
9. Rosen, A., Martinelli, R.U., Schwarzmann, A., Brucker, G.J., and Swartz, G.A., "High-Power, Low-Loss *PIN* Diodes for Phased-Array Radar," *RCA Review*, Vol. 40, pp. 22-58 (March 1979).
10. Basile, P.C., Erdmann, R.G., Caulton, M., Rosen, A., Stabile, P., and Gombar, A., "Solid-State Antenna Switching," *RCA Review*, Vol. 42, pp. 752-769 (December 1981).

Contacts: ***M. Caulton*** — **TACNET: 226-2929**
A. Rosen — **TACNET: 226-2927**
P. Stabile — **TACNET: 226-2594**

Table I.

	Type MTC-P1 (Single diode)	*Type MTC-P2 (Two diodes packaged in series)*
Lifetime	20 μs at I_F = 20 mA, I_R = 0.2 mA	20 μs at I_F = 20 mA I_R = 0.2 mA
Voltage breakdown	1000 V minimum	2000 V minimum
Heat-sink voltage isolation	1000 V minimum	2000 V minimum
Leakage	100 nA maximum at 1000 V	100 nA maximum at 2000 V
Forward rf resistance	0.1Ω at 2 MHz and 300 mA	0.1Ω at 2 MHz and 500 mA
Capacitance	2.5 pF	2 pF
Maximum forward HF current	9A rms	
Intermodulation distortion	50 dB, two-tone, third-order products	
Thermal resistance	6°C/W	6°C/W
Package	Interceram AV-178	

M. Nowogrodzki | D.D. Mawhinney | R.W. Kipp

Radar instruments: Sensors for industrial applications

A 30-percent increase in locomotive-hauled tonnage, and a pig-iron blast-furnace controller share a common bond—microwaves are doing the work.

Abstract: *Except in the airline industry, radar systems found very few nonmilitary applications in the years following World War II. During the last decade, industrial requirements for sensors operating in hostile environments brought about the development of specialized radar systems adapted to the peculiar operating conditions of a particular industry. In this paper we present a "progress report" on operating experiences with two special cw radars, one used for determining the speed of locomotives, the other employed inside steel blast furnaces for determining the range to the "burden" material.*

The radar speed sensor was developed in response to a need for providing a ground-speed reference for a locomotive, independent of wheel rotation. The blast-furnace radar, originally developed for Bethlehem Steel Co., is presently used by various steel companies in a number of installations in the United States and Canada. Proposed extensions of these designs, presently under consideration for different industrial applications, are described.

Although the military use of radar has drastically expanded since its introduction for modern warfare in World War II, nonmilitary developments have been less dramatic. At first, applications followed traditional wartime usage: airport and harbor surveillance, shipboard obstacle detection, commercial airborne weather radar, and radar altimeters—to cite the most obvious examples—all concentrated on the traditional radar measurement: that of distance. A more recent example of radar used in a nonmilitary instrument is designed to measure speed. The ubiquitous "radar trap" employed by law-enforcement agencies on the U.S. highways is a compact unit that spawned a nonmilitary "electronic warfare" mini-industry for jamming and deception devices of dubious legality.

Until recently, the industrial use of radar instruments, particularly those employed as the principal sensors for closed control loops in automated systems, has received relatively little attention. But new applications in this area can be expected. Modern computer-controlled systems, which have already penetrated traditionally conservative industries, require rapid and accurate on-line inputs for effective process control, and microwave radars have demonstrated their unique suitability for providing such data in hostile industrial environments.

Electromagnetic signals in the microwave range are practically unaffected by the environmental conditions encountered in industrial applications. Ultrasound systems perform poorly in the presence of thermal interfaces and gradients or mechanical noise; optical signals cannot penetrate dust, smoke, accumulated grime, and so on; mechanical systems are usually cumbersome, unreliable and slow; nuclear-measurement systems require continuous monitoring of personnel and are generally considered undesirable, if only for psychological reason By contrast, microwave systems are saf reliable and operable in adverse environments. Their main disadvantage is tha microwave signals cannot penetrate mos liquids, and significant moisture accumulations in their path must, therefore, b eliminated.

The two examples described in this article illustrate some of these features. In an instrument designed to perform range measurements inside a steel blast furnace, the microwave radar replaces a slow, cumbersome and unreliable arrangement of mechanical sensors (weights lowered to the surface of the "burden" in the furnace). The atmosphere inside the furnace is corrosive, with significant thermal gradients and clouds of gases and particulate matter obscuring the path of optical signals. The second RCA instrument, developed for placement underneath a locomotive, supplements the normal magnetic wheel speedometer to provide a comparison between the ground and wheel-rotation-derived speed. The signal travels through caked mud and grime, and the system performs with remarkable reliability and accuracy.

Blast-furnace radar

Modern pig-iron blast furnaces are automatically "charged"—the term refers to dumping specific amounts of ore, coke, limestone into the furnace—when the "burden," or material in the furnace, reaches a predetermined level. The material distribution within a blast furnace is important to

©1982 RCA Corporation
Final manuscript received June 8, 1982.
Reprint RE-27-5-5

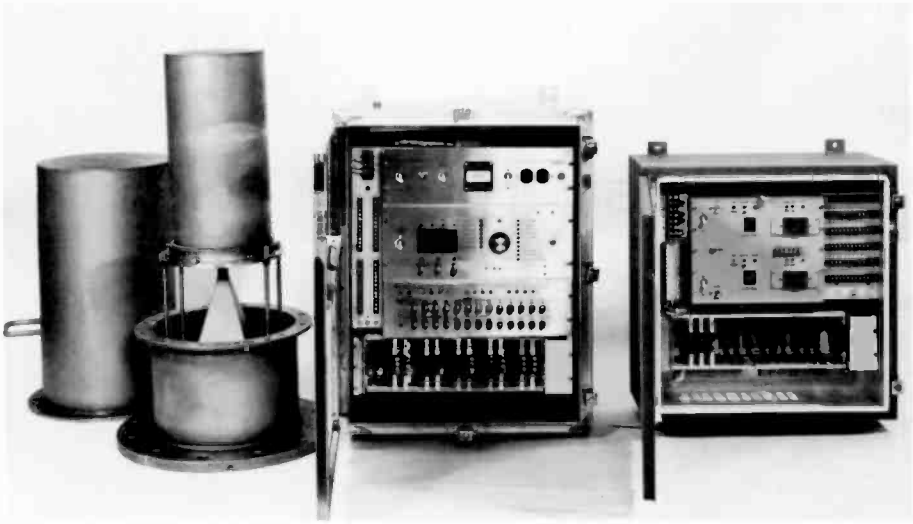

Fig. 1. *The components of the blast furnace radar. On the left is the microwave component subsystem (MCS); in the center is the processing electronics subsystem (PES), which controls the MCS and generates the range to the target; on the right is the display-interface subsystem, which interfaces the target-range information with the blast-furnace computer.*

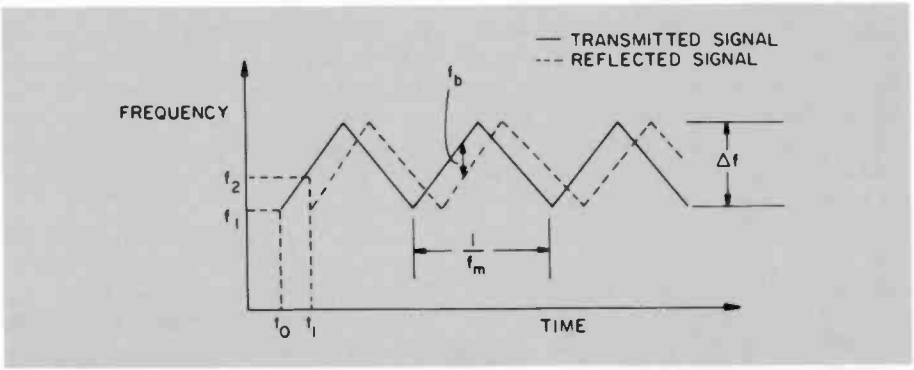

Fig. 2. *A graphic representation of an FM-cw radar that shows the relationship between beat frequency (f_b) and time. Therefore, f_b can be directly related to the distance to the target.*

the efficiency and consistency of the pig-iron produced, and for optimum furnace performance, it is desirable to predict and control the profiles of each of the ingredients. This is difficult to do in older furnaces, in which a charging bell is filled with the burden and its entire contents are dumped into the furnace, the only variable being the amount of material in the bell prior to dumping. In more modern furnaces, a rotating charging chute is used, and in addition to the amount of material accumulated for the charge, the chute angle and its speed of rotation can be adjusted for the various burden ingredients to optimize the profile. In either case, charging is periodic, its initiation being determined by the amount of material remaining in the furnace as molten metal is withdrawn from the bottom.

Since its original development in cooperation with Bethlehem Steel Company,[1] the RCA radar instrument has found wide acceptance in the United States and Canadian steel industries. A photograph of the three principal components of the instrument is shown as Fig. 1. The principle employed is that of an FM/cw radar. The frequency of a cw microwave signal (at approximately 10 GHz) is changed in triangular fashion, so that when the echo from the burden returns, the transmitter emits a frequency changed by an amount proportional to the time of two-way travel to (hence, the distance from) the burden surface (Fig. 2). This difference frequency is extracted and processed to provide range information. Important features of the system are its placement entirely outside the furnace, so that maintenance does not require a furnace shutdown; the use of existing pipes (formerly used for guiding the mechanical stockrods) as channels for the beam; and the incorporation of a self-calibrating feature, consisting of a microwave delay line of known electrical length, the return from which is used to correct the actual reading of the burden level. The circular chart of Fig. 3 provides a comparison between the distance measurements of the RCA radar (Fig. 3a) and those of a mechanical stockrod (Fig. 3b) taken in the same furnace and at the same time. Note, however, that the measurement locations are 90° apart.

The RCA radar instrument has changed both physically and electrically since the first prototype. Ten "production" systems have been installed, four are on order, and an additional two are expected to be ordered before this paper is published. The modifications to date have included improvements in the digital signal-processing circuits, a change of the window material (the original quartz was discovered to weaken as scratches developed in the surfaces due to bombardment by particles from within the furnace and handling of the window during installation), and a change in processing the return reflection signal, which is particularly useful for rotating-chute-type furnaces.

The instrument, originally developed for bell-type furnaces, emits a beam having a half angle of 2.5° to 3.5°, and the distance measurements are averaged from returns obtained from the burden area illuminated by this beam, that is, the antenna "footprint." It turns out that the angle of the burden surface, at the point of measurement with the vertical, may be very steep in rotating-chute furnaces. The steel engineers were concerned that the uncertainty as to which portion of the slanting burden surface was being measured by the radar (caused by the spreading antenna-beam footprint) may cause premature charging of the furnace. In response, we have developed a circuit which, under such circumstances, preferentially uses the shorter range("more material in furnace") for control purposes.

Figure 4 is a photograph of an RCA radar installation. The rf unit can be seen mounted atop the stockrod pipe; the piping system, used to keep the window dry by purging it with heated nitrogen or natural gas, is also clearly visible.

Future systems

Versions of the RCA radar may be useful for other applications, and considerable interest has been generated in its possible adaptations for lead-smelting furnaces, paper

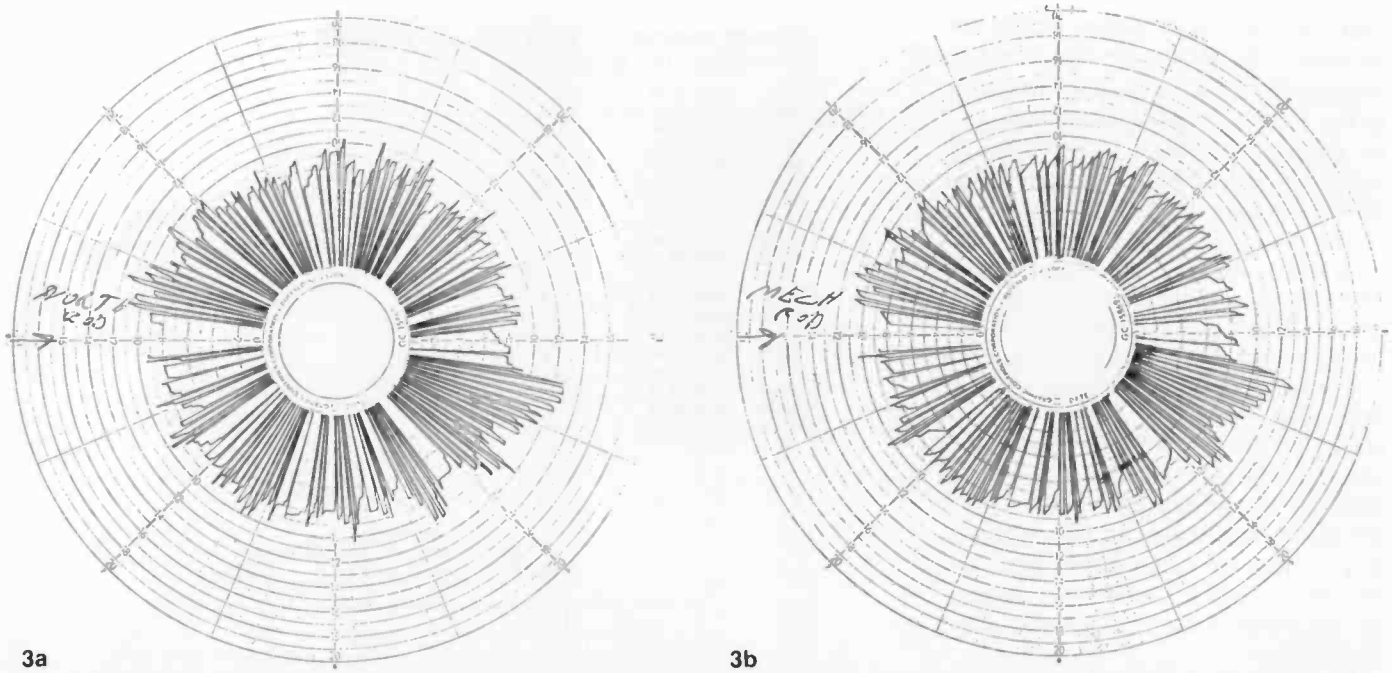

3a 3b

Fig. 3. *Figures* **3a** *and* **3b** *show a typical eight-hour shift at an actual blast furnace. Fig.* **3a** *is a circular chart of the radar stockrod. Fig.* **3b** *is a circular chart of the mechanical stockrod. Both charts start at the 9 o'clock position and then rotate clockwise. Increased furnace depth is shown by a radial lengthening of the line, and each furnace dump (adding of material) is signified by the traced inner circle. Figures* **3a** *and* **3b** *should be mentally overlapped. In overlapping these two figures, the furnace trends and fluctuations are clearly seen in the radar stockrod (Fig.* **3a***) and these conditions are mimicked by the mechanical stockrod (Fig.* **3b***).*

mills, casting ladles, and so on. Not only are the technical requirements different in each case—in terms, for example, of the acceptable range, accuracy, and beam size—but the environmental and economic constraints are usually also different for each proposed adaptation.

The most important future development based on the present radar is likely to be the profiling version of the instrument. As was previously mentioned, rotating-chute furnaces have the potential to optimize the surface profile of each burden ingredient. A radar that could measure and display these profiles after each charge would fill an important gap in modern steel-making instrumentation.

We have developed a concept for such an instrument, which would bounce the microwave beam off the back of the rotating chute, and we have performed initial feasibility measurements of such an approach.[2] More recently, computer simulations of such a radar have confirmed that a single-beam system would provide mapping of at least 60 percent of the burden surface, which is probably sufficient for a practical installation. Development of a full-scale prototype instrument is expected to begin, under contract, in the near future.

Figures 5 and 6 are computer simulations of the position of a radar scan beam as the beam traverses a fixed range or pla-

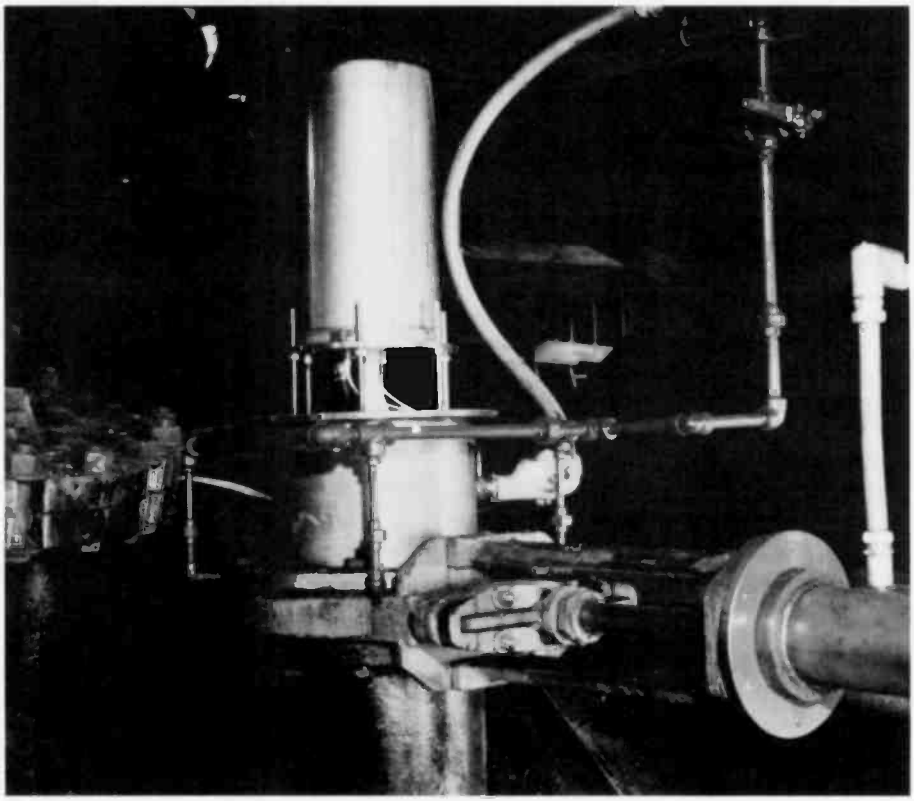

Fig. 4. *A photograph of a typical furnace installation. The cylinder houses the microwave component subsystem (MCS), and the flexible conduit line provides for the power and interconnections with the processing electronic subsystem (PES). Four vertical pipes (three are visible in the photograph) provide for nitrogen cleaning of the microwave window. The large horizontal object shown beneath the MCS outer housing is a slide-plate isolation valve that is used to protect the MCS.*

teau. The range to the plateau used in the program is 20 feet in both Figs. 5 and 6. Also specified by the programmer, as shown in Fig. 5, are the diameter of the surface to be scanned (30 feet) and the range of angles "theta two" θ_2 (02) through which the reflector is incremented $88° < 02 < 135°$.

The grid structure describes the plateau area in one-square-foot increments. The radar's horizontal beam is along the y axis, with the radar antenna positioned beyond the maximum negative y value.

The tabulated data of 02 and the corresponding 01 refer to the angle of the chute (02) and the angle of rotation of the chute (01) during the time when the beam intercepts this particular plateau. Of course, the inverse process may be accomplished; that is, given the range to the target surface, and knowing 01 and 02, the z parameter (the height or depth of material) may be calculated.

Note that 02 is stopped at the 135° (45°) point in Fig. 5. This is due to a physical limitation of the proposed reflector. By simulating an additional 22° increase in Fig. 6, the entire surface may be scanned. Redundancy and increased coverage can be added to the scanning radar system by adding another horizontal radar beam that is positioned in any of the other three quadrants of the furnace; thus, you might use two beams that are positioned 180° apart.

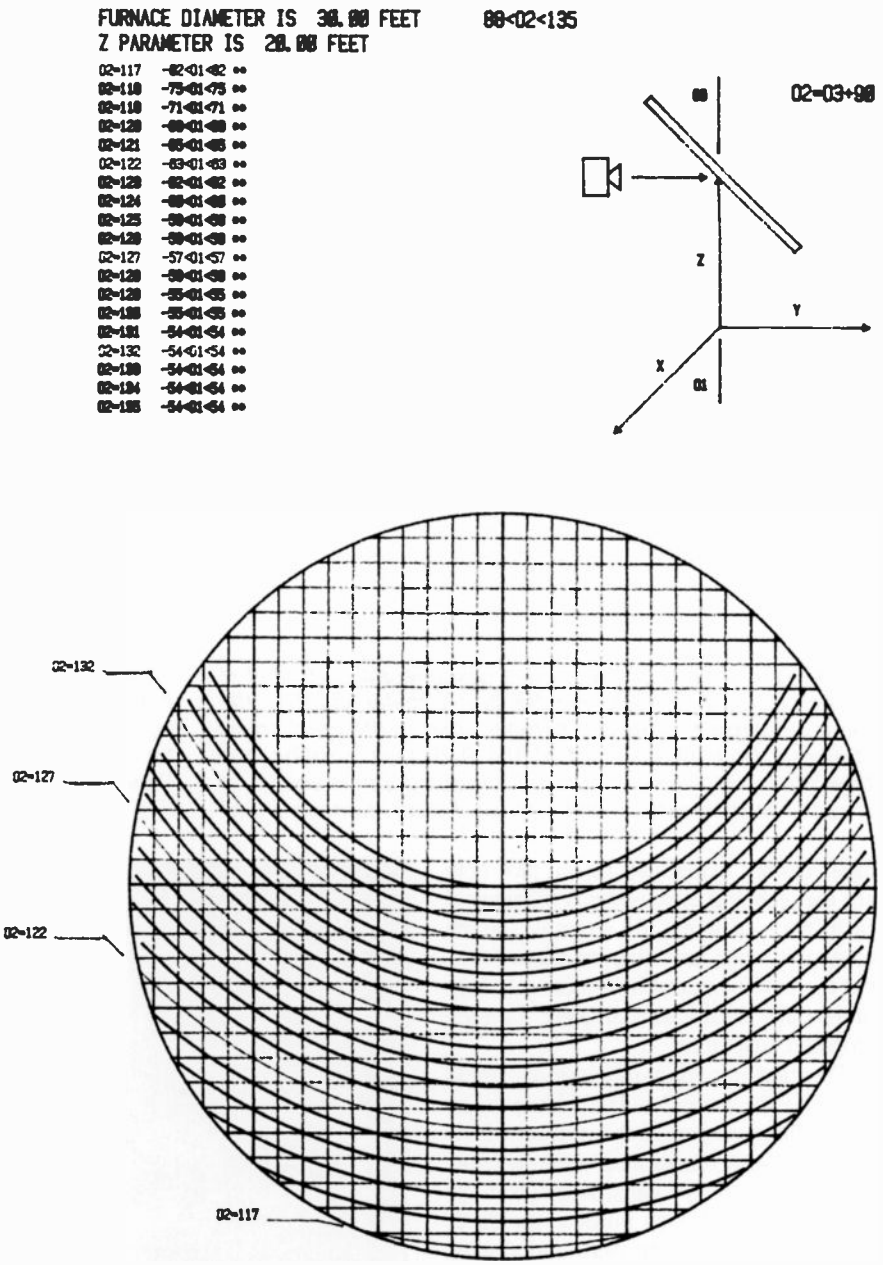

Fig. 5. *Computer simulations showing the scanned position of a radar beam as the reflector is rotated, and the angle of the reflector is varied in one degree increments. θ_2 is the angle of the reflector, and θ_1 is the angle of rotation of the reflector.*

Doppler speed sensor

Originally designed as a simple speed sensor for use first in automobiles,[3] then in locomotives,[4] the RCA Doppler radar saw its most important application as the key element in a much more sophisticated task: that of optimizing locomotive pulling power by accurately controlling wheel slippage. Recent studies apparently show that wheel-to-rail friction is greatest under conditions of slight wheel slippage rather than when slippage is zero. In the attempt to use this effect to dynamically maximize traction—and therefore locomotive pulling power—in their newest diesel-electric locomotives, General Motors/Electromotive Division (GM/EMD) engineers were searching for a ground-speed measuring instrument that is independent of wheel rotation. Our Doppler radar provides such a reference measurement. Its speed measurement is compared with one derived from a more conventional device, in which wheel rotation is translated into speed, and the difference between the two readings is indicative of slip. Then traction motors on the individual driving wheels of the locomotive are automatically adjusted to provide optimum slip, resulting in maximum traction. GM/EMD states that this scheme increases the pulling power by one-third in tonnage—a tremendous increase, considering present emphasis on energy-conservation measures.

The present version of the Doppler speed sensor retains the basic approach of the original prototype, but incorporates a number of mechanical and circuit modifications. The unit, photographs of which are shown in Figs. 7 and 8, is housed in a relatively massive casting, the front compartment of which contains the printed-circuit antenna and microwave components (oscillator, circulator, mixer), with the signal-processing and control circuits placed in the back. Both compartments are sealed against the environment; the rf section is pressurized and protected from rocks and debris by a high-impact plastic window, and the processor board is encapsulated in a resilient elastomer to eliminate false signals caused by microphonics. The unit (several hundred have been manufactured) undergoes elaborate burn-in and acceptance test procedures (including temperature shock), not unlike equipment intended for military use.

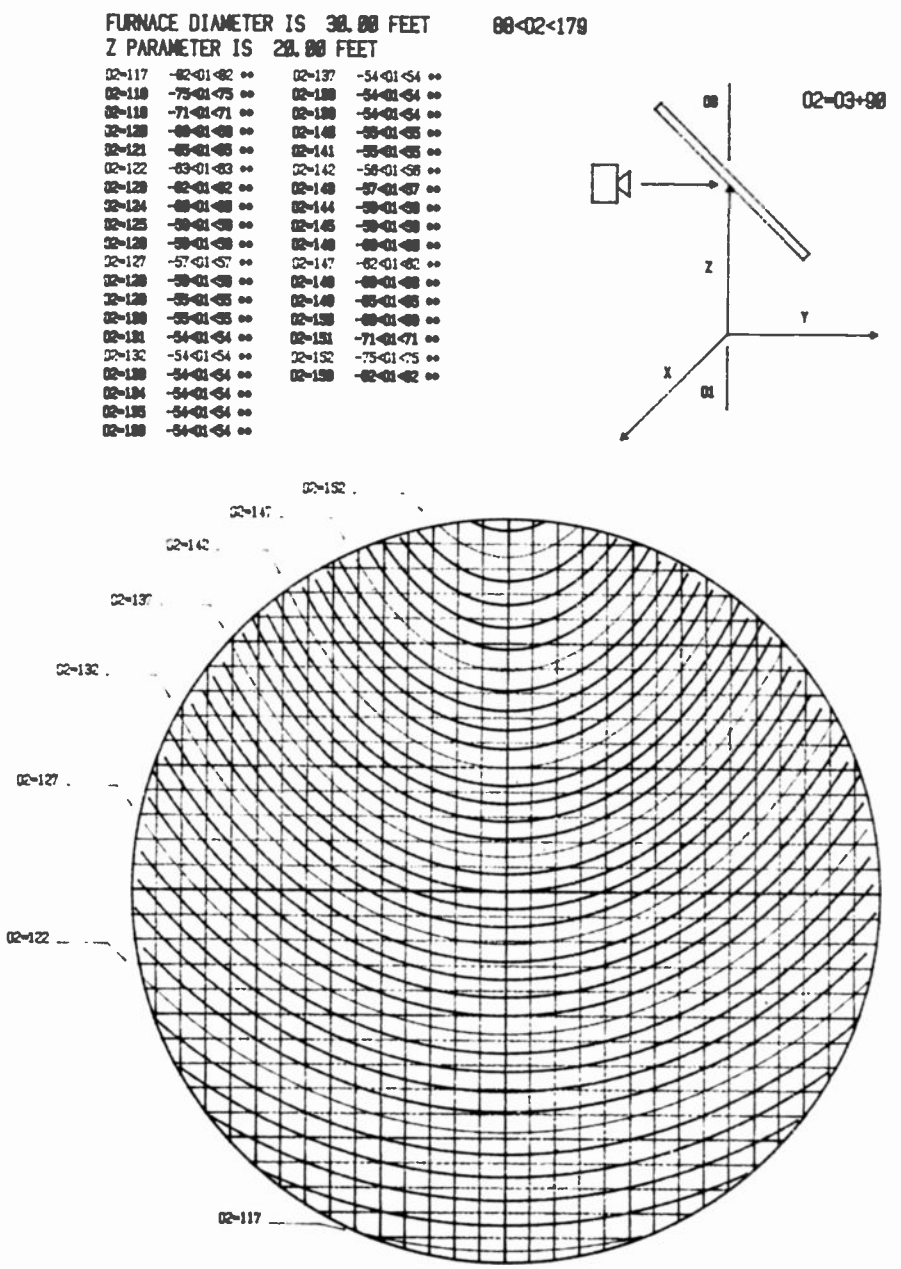

Fig. 6. *Same as Fig. 5, except that the θ_2 angle is increased to 153°. θ_2 is physically limited to 135° by the structure of the blast furnace; therefore, the addition of an 18° wedge would artificially allow the reflector (the back of the chute) to traverse the area that is missed in Fig. 5.*

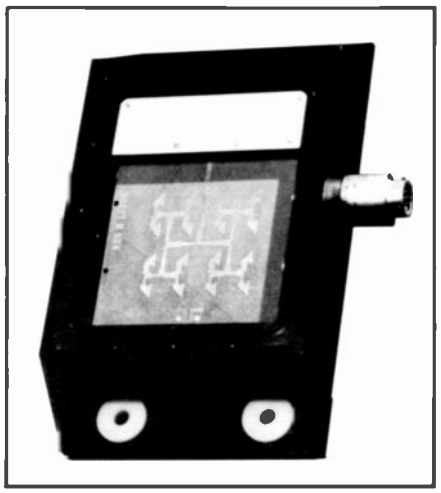

Fig. 7. *The cast-aluminum radar-speed-sensor housing with the protective face-plate removed shows the printed circuit dipole array antenna and the coverplate that shields the microwave oscillator and mixer.*

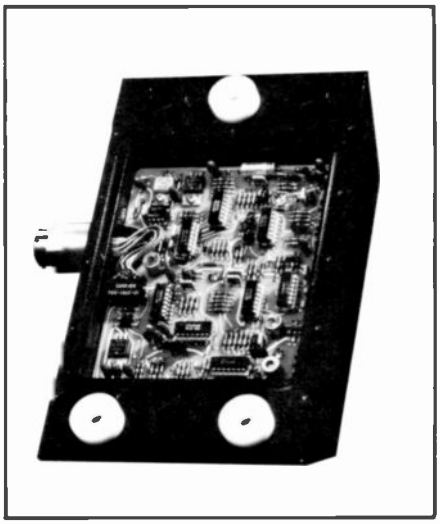

Fig. 8. *The processor's printed-circuit board is mounted in the gasket-sealed back compartment of the housing and is encapsulated in a resilient elastomer for dampening of microphonics and shock.*

Linearity of response

The Doppler frequency shift, which is processed by the radar speed sensor, is a function of observation angle as well as of relative speed. In conventional applications of a Doppler radar, the target is usually far enough from the radar antenna so that it is illuminated by a small sector angle of the transmitted beam pattern, and the Doppler-shifted return signal is essentially a single frequency. In the case of the locomotive application, the antenna is mounted at a 45° angle about 18 inches from the ground, and the return signal produces a Doppler spectrum with frequency components resulting from the various angle components of the antenna pattern.

The more-vertical components of the antenna beam see a better backscatter angle and traverse a shorter path, and the resulting Doppler spectrum is strongly skewed toward the lower frequencies rather than having a distinct peak at the frequency corresponding to the 45° mounting angle. When amplified and processed conventionally, this skewed spectrum causes a nonlinear relation between actual speed and measured Doppler frequency. Linearity could be obtained by shaping the response of a preamplifier stage to have a particular increasing gain vs. frequency characteristic, but the resulting large gain variation would cause either insensitivity at low speeds or instability at high speeds. In the early models, H.C. Johnson solved the problem by switching in or out four shunt capacitors at appropriate approximate speeds to satisfy the accuracy requirements of the customer during the initial stages of his program when a speed range of 3 to 40 mph with an accuracy of ±0.5 mph was acceptable.

As the traction-control-system develop-

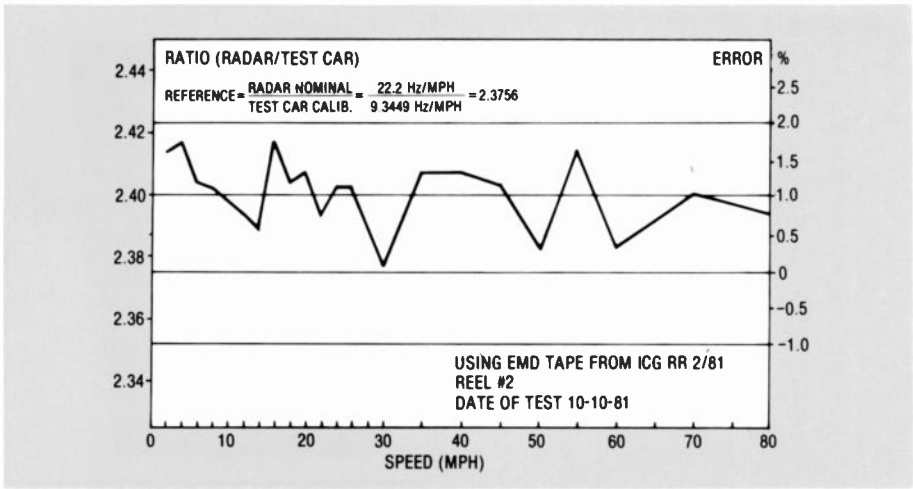

Fig. 9. *Using an instrumentation tape recording made during locomotive operation, comparisons can be made in the laboratory between speed signals from a calibrated non-driven wheel and the processed Doppler signal while circuit variations are evaluated to minimize residual error.*

ment progressed, the scope of applications increased and the objective speed-sensor requirements became more demanding: 1- to 2-percent accuracy from 1 to 120 mph. To meet these requirements, the switched capacitor filter was expanded to six series and five shunt elements, which are adaptively selected as a function of frequency (speed) through the use of a frequency-to-voltage converter and a group of preset comparators. The capacitor values and the specific switching points were empirically selected by means of a multichannel instrumentation recording made by the locomotive manufacturer using a specially instrumented test car during a series of tests on a section of high-speed railroad track. Simultaneous recordings of the unprocessed Doppler signal from the mixer and an accurate digital speed signal from an NBS-calibrated test wheel were made as the train was held at a large number of fixed speeds for several minutes each. The tape was later used in our laboratory to select the optimum values of switched capacitors. The resulting error curve is shown in Fig. 9. Since a low reading from the radar will be interpreted as "slip" by the control system and may cause the locomotive to unload, the error curve was deliberately biased towards high reading errors within the allowed 1- to 2-percent linearity. Figure 10 shows an *x-y* plot of the radar speed output of the newly designed speed-sensor-

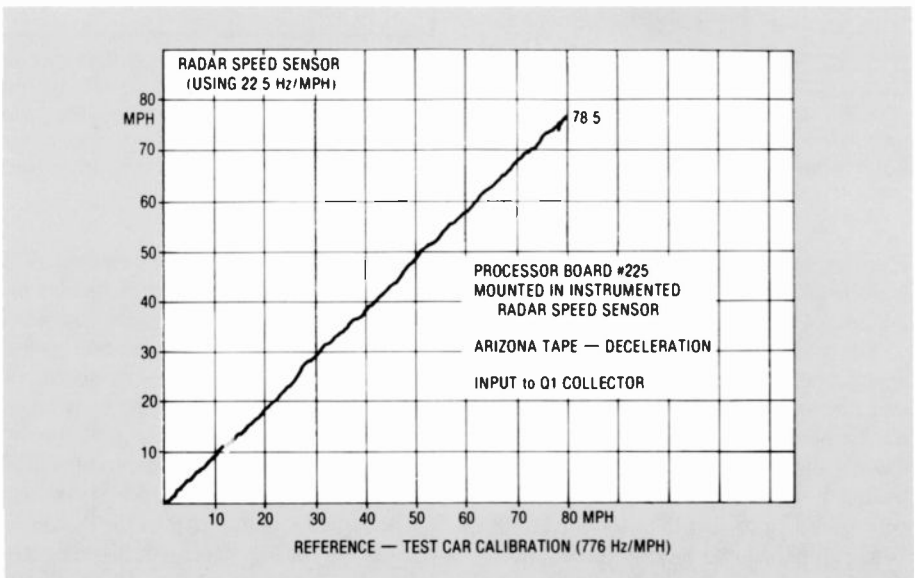

Fig. 10. *Again using the instrumentation tape recording, x-y plots can be made to compare the output speed indicated by the Doppler signal processor with the calibrated wheel speed as a production control.*

Table I. *Locomotive speed sensor (Types S570/S571).*

Range:	1 mph (±0.5 mph) to 120 mph (±2%)
Output:	Square wave, approximately 22.2 Hz/mph
Input:	12-17 V dc (grounded)
Mounting:	45°, facing ground, typically 12" to 18"above ground
Power consumption:	10 W (typical)
Frequency:	10,525 ± 25 MHz
Antenna beamwidth:	20°
Power output (maximum):	15 mW (cw)
Receiver:	Homodyne
Integral calibrator:	1 kHz (approximately 40 mph)
Size:	9" × 5" × 2" (approximate)
Weight:	~3.5 lb

processor circuit using a standard 80 to 0 mph slow deceleration tape made in 1978. Although the general linearity is quite apparent and acceptable, the newer tape with dwells at specific known speeds must be used to determine the accuracy to the extent now required.

Figure 11 shows the block diagram of the instrument, and Table I lists the operating characteristics. The RCA unit is certified by the FCC.

Conclusions

The two cited examples of microwave radars, which are based on essentially established technologies, but are adapted for specific industrial tasks and environments, exemplify the opportunities for microwave equipments to penetrate a new market. The two instruments offer unique, effective, and reliable solutions to industrial control problems, and were enthusiastically received by the customers' industrial engineers. We expect that both instruments will be adapted for new applications. The distance-measurement system could be used for ranging to liquid or solid materials in ladles, storage bins, different types of furnaces, and so on. The Doppler radar could be used for rate-flow measurements of metals and liquids and, possibly, for motion-detection applications.

As automation of industrial processes moves into an even more advanced phase

and the use of robotics increases, the need for industrial sensors is likely to increase as well. Microwave radars may provide relatively simple, cost-effective solutions to sensor problems, particularly in environments hostile to sensors based on different technologies.

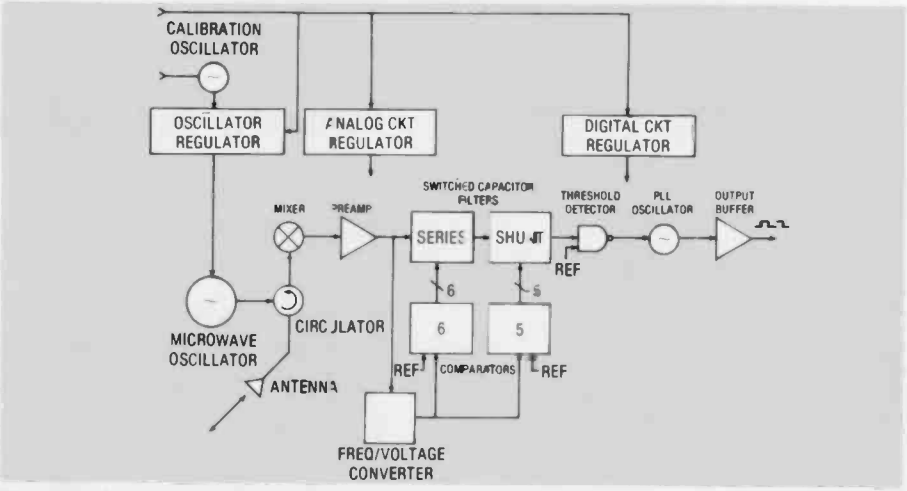

Fig. 11. *The block diagram of the radar-speed sensor highlights the switched capacitor filters necessary to linearize the processor output to compensate for the distorted Doppler spectrum. The phase-lock oscillator provides a flywheel effect to smooth out abrupt signal fluctuations and dropouts.*

References

1. Johnson, H.C., Paglione, R.W., and Hoffman, J.P. (Bethlehem), "A Short-range Radar for Measuring Blast-furnace Burden Height," *RCA Engineer*, Vol. 23, No. 5, p. 66 (Feb./Mar. 1978).
2. Johnson, H.C., "Scanning Radar," U.S. Patent No. 4,219,814.
3. Johnson, H.C. and Presser, A., "Automotive Doppler-radar Speed Sensor," *RCA Engineer*, Vol. 18, No. 6, p. 62 (April/May 1973).
4. Johnson, H.C., "Speed Sensors for Locomotives," *RCA Engineer*, Vol. 22, No. 2, p. 34 (Aug./Sept. 1976).

Markus Nowogrodzki was graduated with the degrees of Bachelor of Electrical Engineering, *cum laude*, in 1948, and Master of Electrical Engineering, in 1951, both from the Polytechnic Institute of Brooklyn. In 1955, he joined RCA and was engaged in the development and manufacture of magentrons, microwave triodes, traveling-wave tubes, and solid-state subsystems. As Manager, Traveling-Wave Tube Operation, he supervised a department comprising design, manufacturing, applications, and program-control activties.

Mr. Nowogrodzki left RCA in 1967, and returned in January 1973, as Manager, Division Liaison, at RCA Laboratories' Microwave Technology Center. He is now in charge of the Center's Subsystems and Special Projects group. Mr. Nowogrodzki has written more than twenty papers on various aspects of microwave component design and applications. He holds six patents.

Contact him at:
RCA Laboratories
Princeton, N.J.
TACNET: 226-2521

Ron Kipp joined the Microwave Technology Center of RCA Laboratories as a technician in 1966. In 1972, he left to join the Institute for Defense Analysis as a computer design engineer. In 1977, he returned to the Microwave Technology Center of the Laboratories as the project engineer for the Blast Furnace Radars. In 1978, he received an RCA Laboratories Outstanding Achievement Award for contributions to the team effort for the development of small cw radars.

Contact him at:
RCA Laboratories
Princeton, N.J.
TACNET: 226-2618

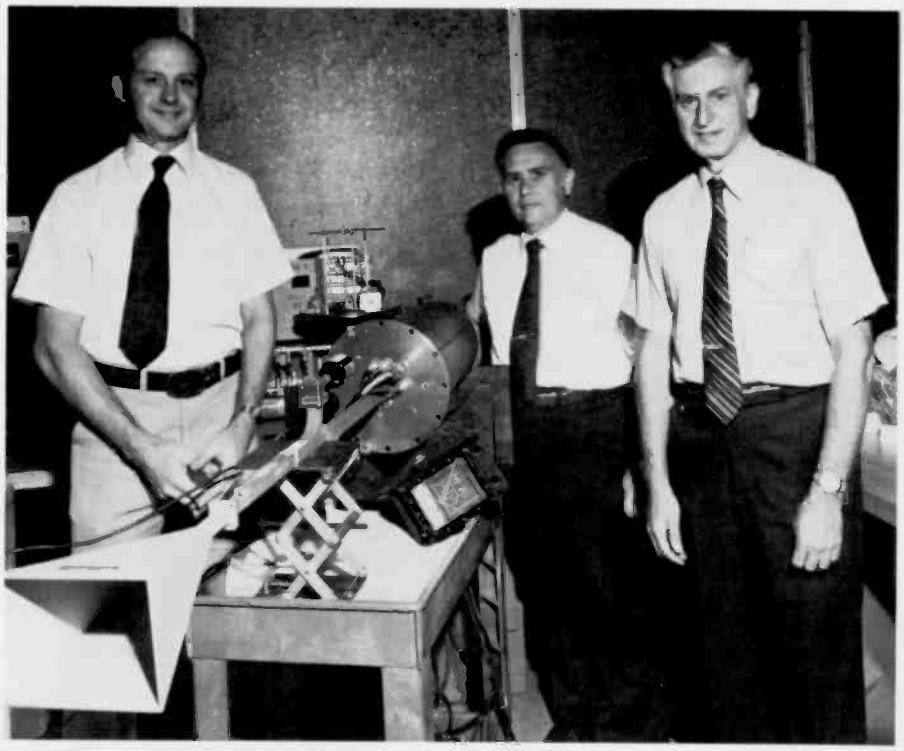

Authors (left to right) Kipp, Mawhinney, Nowogrodzki

Dan Mawhinney joined RCA in 1952 working in the Microwave Equipment Development group in Harrison, N.J. He later became involved with the design and development of various solid-state microwave oscillators and subsystems and served as Engineering Manager of the Microwave Solid State Design group before transferring to RCA Laboratories, Princeton, N.J., in 1975. As a Member of Technical Staff of the Microwave Technology Center, he continues to work primarily on the design, development, and prototype manufacture of small military and commercial microwave subsystems. Mr. Mawhinney received the BEE degree from the Polytechnic Institute of Brooklyn and the MSEE from Newark College of Engineering.

Contact him at:
RCA Laboratories
Princeton, N.J.
TACNET: 226-2802

EDITORIAL INPUT

Two new editorial features

Read more easily, communicate more effectively.

This issue of *RCA Engineer* contains two changes that I want to call to your attention. They are practical things done to make it easier for you to glean information about technologies in RCA.

Read more.

To improve legibility a new typeface has been selected for the main text of articles. Though similar in style to the type used previously, the new design offers three advantages: Contrast between letterforms and background is improved (the type is heavier, blacker, stronger). The lowercase alphabet is larger, more open. And the letters link well together. The resulting "tighter fit" permits the eye to grasp word outlines more easily. For you, with an ever-increasing amount of information to digest, we hope this enhancement has value. Good typography, like good architecture, is made to be enjoyed as it is used.

Write less.

The second change in this issue affects content as well as form. On page 21, you will find a new department called "The Engineer's Notebook." It will permit us to accommodate a variety of brief technical communications in an appropriate manner.

For your reference, here are the specifications.

Subject matter: Anything that ought to be known by your fellow engineers in other disciplines and locations. Consider it a kind of bulletin board. (It is conceivable that for proprietary reasons only a brief description of a new development may be disclosed. This is the place for that note.)

Length: 250 to 1,000 words.

Illustrations: One to three, with descriptive captions.

Contact for further information: Supply name, affiliation and TACNET phone number. No biographical data or author photo.

Method of presentation: Be concise, simple, direct.

Approval cycle: Identical to full-length articles.

How to submit material: Before writing, talk with the Editorial Representative for your business unit. Ed Reps' names are listed on the inside back cover of this issue. Then call Mike Sweeny or me.

Thomas E. King
Editor

W.T. Patton

Low-sidelobe antennas for tactical phased-array radars

Antenna sidelobe-level reduction is a cost-effective approach to improving radar effectiveness in an electronic countermeasures environment.

Abstract: *As the technology of warfare progresses, we find increasingly sophisticated weapon systems beginning to rely almost entirely on radar for targeting and accurate weapon delivery, to the extent that rendering the radar ineffective will disable the weapon it guides. This situation favors the deployment of massive radar countermeasures by a potential enemy and means that tactical radar performance must be optimized for operation in an electronic countermeasures environment. Such optimization can be achieved in large part through careful consideration of the role of antenna-sidelobe levels in determining radar performance.*

Although the U.S. approach to electronic countermeasures may be to make the enemy radar scopes go black (through Stealth technology), it is clear that the Russian approach is to make the radar screens go white (by raising the system noise floor through extensive use of barrage jamming). It is, of course, the goal of electronic countermeasures (ECM) to deny the use of radar to the enemy, a technique whose effectiveness was recently demonstrated in Lebanon. This objective is reinforced by the increasing military reliance on radar data for quick reaction, precision fire control, and general engagement management.

Noise jammers can be separated into two basic categories: high-power units, distributed across the enemy approach corridors, which act to screen incoming flights; and somewhat smaller units carried by individual aircraft used to deny range data on an incoming aircraft. The first category is usually called standoff jamming, and the latter category self-screening jamming. The standoff-jammer threat is the one handled most effectively by reduced sidelobe levels although performance improvements resulting from lower antenna sidelobe levels are also beneficial in combating other ECM techniques.

Another device used to discourage the use of radar is the anti-radiation missile. Since these missiles depend on the nearly continuous radiation from the transmit-antenna sidelobes, they can be economically decoyed when the transmit sidelobes are made sufficiently low. Indeed, deployment of decoys is a principal determinant in establishing transmit-sidelobe-level criteria. (It must be noted, however, that practical decoying can be defeated by more sophisticated anti-radiation missile receivers that can provide guidance with an occasional sample of the main beam.)

In the intense Electronic Warfare environment anticipated in any future hostile engagement between major powers, the performance of a radar system will be improved directly as sidelobe level is reduced. However, the techniques used to reduce sidelobe level must not detract from other techniques used to counter the jamming threat, such as the use of a wide signal spectrum. The performance of other techniques for handling jamming, such as sidelobe blanking, is improved by lowering the antenna sidelobe level. Since a low-gain blanker antenna can be used to cover very low sidelobe levels, the effective system noise or loss in sensitivity due to the blanker is reduced. This overall increase in sensitivity will make more radar resources available to devote to techniques, like burn-through, used to counter self-screening jammers.

An alternative method of achieving such a performance increase might be simply to increase the transmitter power by an order of magnitude. However, this approach would severely strain not only current transmitter technology, but microwave power transmission and antenna component technology as well. On the other hand, the recent explosion of ultra-precision design and fabrication technology due largely to the solid-state industry, and also, to some extent, to the nuclear power industry, makes the design and fabrication of phased-array antennas with ultra-low sidelobe levels economically feasible. In this context, then, antenna sidelobe level reduction is a very cost-effective approach to the ECM threat.

The requirement

Radar-jamming signals may enter the radar through the main beam (self-screening jamming) or through the sidelobes (standoff jamming). A self-screening jammer is in the main beam when the radar is trying to obtain track data on the vehicle carrying it. However, this jammer is also in the sidelobes of the beams illuminating other nearby targets, thereby acting as a standoff jammer with increased effectiveness at reduced ranges.

© 1982 RCA Corporation
Final manuscript received July 22, 1982
Reprint RE-27-5-6

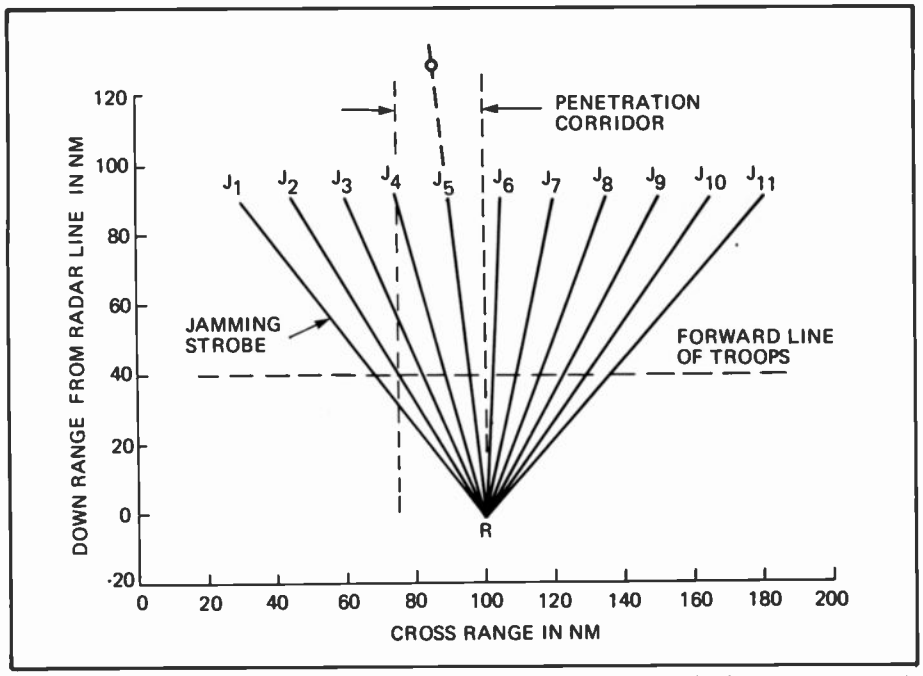

Fig. 1. *Radar, penetrator, standoff-jammer geometry. Typical deployment of standoff jammers by an adversary to defeat radar coverage of a planned penetration corridor.*

Standoff jammers may emit signals based on the radar's emission (deceptive jamming) or random-noise signals (barrage jamming). Deceptive standoff jammers are effectively countered by sidelobe blanking, which inhibits false detections outside the main beam. Sidelobe blanking makes use of an auxiliary antenna whose gain exceeds that of the sidelobes of the main array. The radar will ignore all signals that produce a larger response in the auxiliary (sidelobe-blanking) channel than that produced in the main channel. This effectively prevents the radar from responding to target-like signals entering through the sidelobes. Sidelobe blanking is, of course, made easier as the antenna sidelobe level is reduced, but this aspect of radar performance is not subject to the orders-of-magnitude improvement that can be obtained by sidelobe-level reduction in the case of the standoff-barrage jammer.

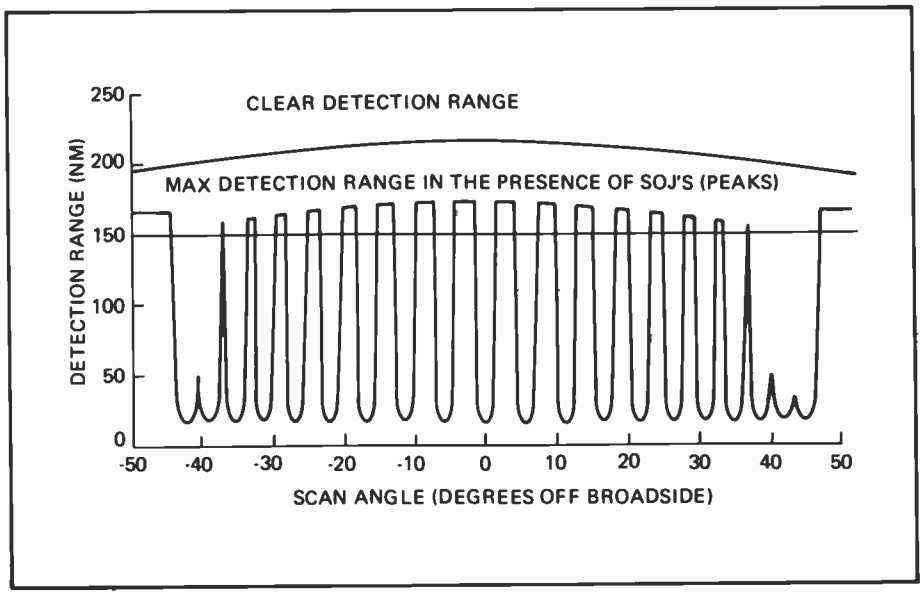

Fig. 2. *Radar detection range at those beam angles that do not contain a jammer is controlled by the antenna sidelobe level. Troughs (very low detection range) indicate jamming in the main beam. Notes: detection probability equals 0.8 for a 3m² target cross section at 200 nm; effective radiated power equals 100 W/MHz; the number of jammers is 25; range to jammers is 100 nm; azimuth beamwidth is 1.3°; and peak azimuth sidelobes are -50 dB.*

The standoff-barrage jammer is a relatively inexpensive radar countermeasure and can be expected to be deployed in large numbers during tactical engagements. One possible deployment, useful for analysis, is shown in Fig. 1. The detection range of a target approaching the radar at various angles through this screen is depicted in Fig. 2. Here we see the severely restricted range when the target is aligned with one of the jammers and the very much larger range when the target is between jammers.

The average detection probability over all angles is displayed as a function of range in Fig. 3. This figure illustrates the dependence of radar performance on antenna beamwidth and sidelobe level in a jamming environment such as that shown in Fig. 1, when the radar is scanning the lower elevation angles in which the jammers are most likely to occur. The antenna bandwidth is seen to set the probability of detection largely independent of range in those cases where beamwidth is narrow enough to resolve the jammers. Where the target is separated from the jammers by at least a beamwidth, however, a dB of reduction in the sidelobe level is equivalent to a dB increase in transmitted power.

This is the target geometry that can be expected to exist almost everywhere above the radar horizon. A dramatic increase in performance over such a large portion of the radar coverage volume will make a great deal more of the radar resource (energy and time) available for the main beam jamming situation.

Array design for low sidelobes

If we are to achieve economical realization of the tremendous potential for radar performance improvement offered by a very low sidelobe antenna design, we must balance the various contributors to the sidelobe structure of the antenna pattern. These can be broadly grouped into three categories: diffraction sidelobes, random-error sidelobes, and quantization sidelobes. The relative cost of controlling each of these will be discussed below.

Diffraction sidelobes

Diffraction sidelobes are those that would be achieved with no errors in the feeding and steering of the array and with no quantization effects. They are controlled

by the illumination function chosen by the designer. However, as the intensity of the illumination at the outer edges of the aperture is lowered to reduce sidelobe level, less-efficient use is made of the available aperture. This less-efficient use is manifest in reduced gain and larger half-power beamwidth for the given aperture. Gain and beamwidth can be recovered by increasing the size of the aperture with a proportional increase in cost and weight of the antenna. The cost for achieving low diffraction sidelobes is rather clearly seen in Fig. 4. Changing the diffraction-sidelobe level from −35 dB to −55 dB results in a beamwidth or array-length increase of 1.2 or about 0.8 dB. This 20 dB of radar performance improvement for 0.8 dB cost increase is very cost effective indeed.

The cost of providing low diffraction sidelobes on transmit can be deduced from Fig. 5. Our primary interest in reducing transmit-sidelobe levels is to make it economically feasible to mask the energy radiated by the radar through its sidelobes by that radiated by a sacrificial decoy remotely located. Since the decoy must radiate over very wide angles with an effective radiated power equal to the peak power in the sidelobes of the transmitter, the power that the decoy must radiate varies directly with the sidelobe level. Reducing the diffraction-sidelobe level from −35 dB to −55 dB is accompanied by a reduction in antenna gain of 0.8 dB. Stated differently, one can achieve a 20-dB reduction in the required decoy power level for a 25-percent cost increase in the array.

Random-error sidelobes

The random-error contribution to sidelobe level is set largely by design, manufacturing, and testing technology. The relative importance of these technologies depends on the required bandwidth and the approach to array control taken by the designer. But to attain the necessary performance (−55 dB rms sidelobe level, with an array whose gain is 40 dB; −15 dBi sidelobe level, relative to an isotropic radiator; or −20 dBe, relative to an element with 5 dB of directive gain), one must reduce phase errors to near the limits of current measurement technology and minimize correlation of errors between elements.

Minimizing correlation of errors suggests measuring the phase errors in the feed network to each element of the array and using the beam-steering phase shifters to compensate for that error. This approach reduces the effective element phase error

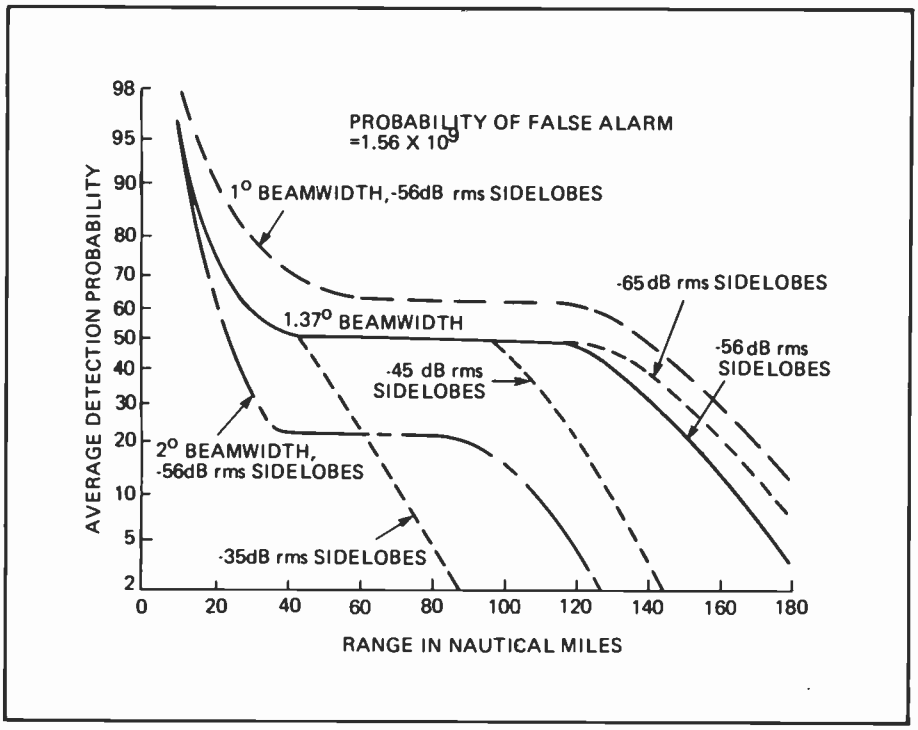

Fig. 3. *Low sidelobe tactical array performance against distributed standoff jamming is controlled by both antenna beamwidth and sidelobe level.*

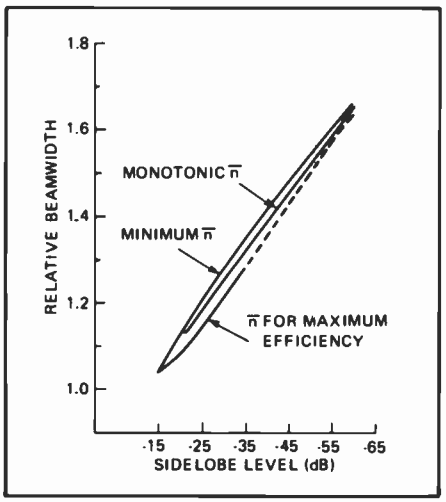

Fig. 4. *Linear Taylor distribution, with the beamwidth relative to uniformly illuminated aperture versus sidelobe level, shows that a modest sacrifice in beamwidth is required to achieve very low sidelobe levels when the aperture dimension is held constant.*

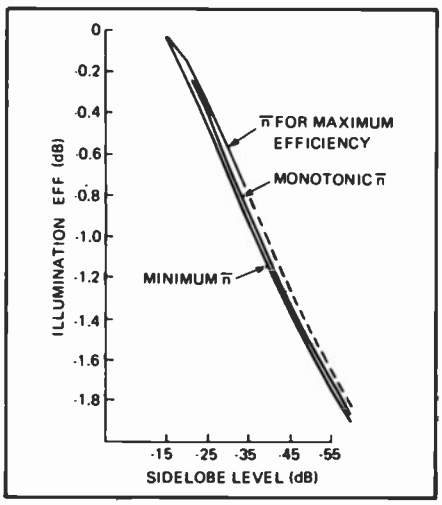

Fig. 5. *Linear Taylor distribution, with the illumination efficiency versus sidelobe level, indicates the small loss in mainbeam gain associated with large reductions in the sidelobe level.*

to that of the phase-shifter-quantization error within our ability to measure the feed error. The residual error after correction will be a function of bandwidth, with additional allowances needed for tracking and alignment between beamformer channels.

The way in which the array error budget is modified by this approach is illustrated in Tables I and II. Table I shows a typical error budget for an array of moderate sidelobe-level design, where some errors were correlated over 64-element subarrays and some errors over entire columns of elements. Correlated errors are multiplied by the number of elements affected by the error.

The elements that share a given error act together as a subarray. In this way, the effect of the error has gain due to the directivity of the concerted action of the elements within the correlation interval. This directivity has an effective beamwidth

proportional to the length of the correlation interval—a beamwidth less than that of a single element but greater than that of the entire array. The energy scattered by correlated errors is distributed over the appropriate beamwidth centered on the beam of the total array.

The rms sidelobe level due to these errors, at about 1 dB below the element gain, can most easily be reduced by reducing the correlation interval. Decorrelating the errors would reduce the rms sidelobe level to 8.6 dB below the element level. This sidelobe level is largely determined by the insertion phase errors in the phase shifters and the distribution paths to the radiating elements. Insertion phase error is most easily reduced by measuring the phase error and using the phase-shifter commands for correction.

Reduction of correlation intervals and correction of phase errors using the beam-steering control system, combined with improved design and manufacturing technology, can lead to the error budget in Table II. The resulting reduction in rms sidelobe level is accomplished without cost from a performance standpoint, but rather with an increase of about 0.5 dB in array gain due to improved accuracy in the aperture distribution function.

The cost of implementation is more difficult to quantify, but is based heavily on the rapidly developing digital technology, including large-scale-integrated circuits, distributed microprocessors, and inexpensive memory elements. Such implementation also requires appropriate use of computer-aided design, manufacturing and testing technologies, with their inherent potential for precision fabrication at low unit cost.

Table I. *Design for moderate sidelobes—random errors.*

	Distribution					
	Element-to-Element		Subarray-to-Subarray		Column-to-Column	
Source	Phase deg rms	Amplitude V/V rms	Phase deg rms	Amplitude V/V rms	Phase deg rms	Amplitude V/V rms
Radome and Radiator	1.0					
Phase Shifter	11.0	0.01				
Differential Phase Setting	12.6	0.02				
Subarray Divider	7.7	0.13	3.0			
Column Beamformer			4.6	0.04		
Horizontal Beamformer					4.0	0.04
$\Sigma()^2$	340.05	0.0174	30.16*	0.0016*	16.00**	0.0016**
Weighted $\Sigma()^2$	340.05	0.0174	1930.24	0.1024	16.00	0.0016
ϵ_ϕ^2 =	340	+	1930	+	16	
ϵ_Λ^2 =		0.0174	+	0.1024	+	0.0016

$\epsilon_\phi^2 = 2286 \text{ deg}^2 = 0.696 \text{ rad}^2$

$\epsilon_\Lambda^2 = 0.1214 \text{ (V/V)}^2$

$\epsilon^2 = \epsilon_\phi^2 + \epsilon_\Lambda^2 = 0.818$

Close-in array-factor sidelobes = 10 log ϵ^2 = −0.9 dBe

Far-out array-factor sidelobes = 10 log 0.1382 = −8.6 dBe

* Impact of correlation is sensitive to the standoff-jammer distribution.

** Unweighted since correlation concentrates sidelobes where main beam jamming outweighs sidelobe jamming.

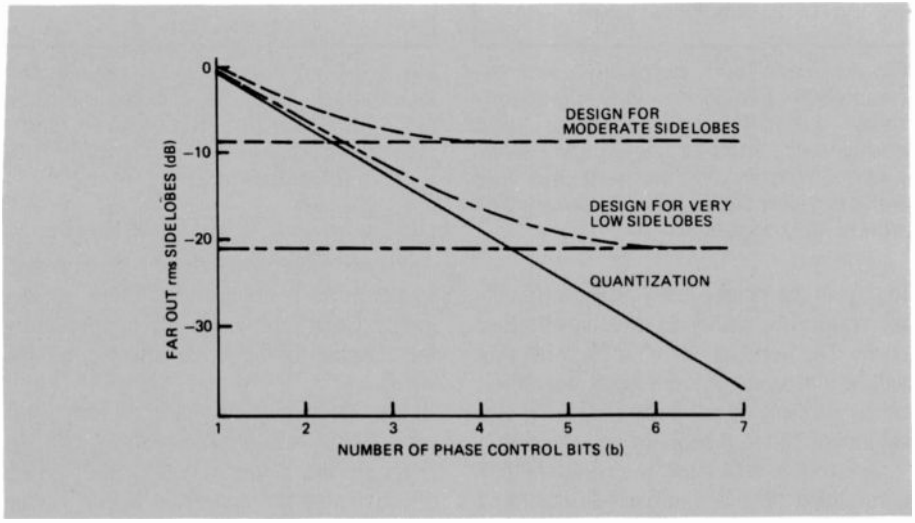

Fig. 6. *Relative impact of phase quantization and random errors on sidelobes indicates the need for more phase-control bits for very low sidelobe arrays.*

Quantization sidelobes

The contribution of amplitude quantization to the sidelobe level decreases by 6 dB for each fourfold reduction in the number of elements in a subarray. Thus, reducing the number of elements in an array from 64 elements to one element should result in an 18-dB reduction in amplitude-quantization sidelobes. However, at the single-element level, in an array with suitable inter-element spacing, there is no amplitude-quantization contribution and for some spacings there may be negligible contribution even at two elements per subarray.

The rms sidelobe level due to phase-shifter control quantization also is reduced by 6 dB for each additional bit of control. This is illustrated in Fig. 6, which also shows the contribution of this factor to the total rms sidelobe structure of the two array examples presented in Tables I and II, indicating a proper choice of 4 or 6 control bits, respectively, for the phase shifters in these two cases.

The cost for implementing a greater number of control bits is nearly linearly dependent on the number of bits for the logic and control distribution. The cost impact on the phase shifter depends on its design, being negligible for digitally controlled ana-

log devices, and varying linearly with the number of bits for discrete-bit phase-control devices.

Low-sidelobe-array cost and weight

A detailed cost study has been performed to determine the impact of sidelobe objectives on array cost. The method used was to develop concept designs for three different arrays, all with about 40-dB directive gain, with sidelobe levels differing by steps of 6 dB. At each sidelobe level a balanced design of diffraction, error, and quantization contributions was effected, with appropriate attention given to the beamformer at each level. The designs were not simply scaled from one level to the next, but rather were independently optimized at each level. Independent cost estimates were obtained for each design, using both standard production cost-estimating techniques and RCA PRICE analysis.

These estimates show the sidelobe-dependent cost sensitivity to be about −0.1 dB/dB for a constant aperture, and about −0.14 dB/dB for constant beamwidth or gain. This means that the cost of building the array increases about 2.3 percent for each dB the sidelobe level is reduced when the size of the array is held constant, and that when the array size is increased to hold the beamwidth of the antenna constant, the cost increases about 3.2 percent for each dB of sidelobe level reduction.

Weight estimates for these arrays designs were also made. The sensitivity of array weight to sidelobe level derived from these estimates is −0.05 dB/dB for fixed aperture designs and −0.09 dB/dB for constant beamwidth. This result is consistent with the cost sensitivity since one would expect the increased complexity of very low sidelobe designs to cause cost to increase at a somewhat faster rate than weight. In either case, the sensitivity to sidelobe reduction is remarkably low.

Reliability

A very low sidelobe array will be of little value in the field unless it can be adequately maintained at that level of performance. Obviously a zero-failure design is impractical because there must be some allowance for event occurrence, detection, and correction. A reasonable design procedure is to make an allowance in the random-error budget for element failures, to provide required redundancy, and to provide for easy maintenance of the critical components.

Table II. *Design for very low sidelobes—uncorrectable random errors.*

	Distribution					
	Element-to-Element		Subarray-to-Subarray		Column-to-Column	
Source	Phase deg rms	Amplitude V/V rms	Phase Tracking (Σ-Δ_β) deg rms	Amplitude V/V rms	Phase Tracking (Σ-Δ_α-Δ_β) deg rms	Amplitude V/V rms
Phase Shifter		0.006				
Differential Phase Setting	3	0.010				
Subarray Divider		0.008				
Column Beamformer			2	0.015		
Horizontal Beamformer					2	0.010
Measurement	2					
$\Sigma(\ )^2$	13	0.000200	4*	0.000225*	4**	0.000100**
Weighted $\Sigma(\ )^2$	13	0.000200	8	0.000450	4	0.0001000
ϵ_ϕ^2 =	13	+	8	+	4	
ϵ_A^2 =		0.000200	+	0.000450	+	0.000100

$\epsilon_\phi^2 = 25\ \text{deg}^2 = 0.0076\ \text{rad}^2$

$\epsilon_A^2 = 0.00075\ (\text{V/V})^2$

$\epsilon^2 = \epsilon_\phi^2 + \epsilon_A^2 = -0.00835$

Far-out array-factor sidelobes = $10 \log \epsilon^2 = -20.8$ dBe

* Weighted by number elements in subarray due to correlation in standoff-jammer threat region.

** Unweighted since correlation concentrates sidelobes where main beam jamming outweighs sidelobe jamming.

Willard Patton has been involved in research and development of phased array antennas since joining RCA in 1962. Dr. Patton is currently Manager, Advanced Antenna and Microwave Technology in MSR's Engineering Department.
Contact him at:
RCA Missile and Surface Radar
Moorestown, N.J.
TACNET: 224-2730

A probability of 0.008 that an element has failed will lead to an rms sidelobe contribution of −21 dB relative to the gain of a single element. This is the same level as the random errors given in Table II. If the array contained 4000 elements, this would allow failure of 32 elements. Assuming an initial balance between diffraction sidelobes, random-error sidelobes, and sidelobes due to failed elements, the act of doubling the number of failed elements would degrade the rms sidelobe level by 1.25 dB.

A detailed analysis of the reliability of a very low sidelobe array depends very much on the technology and the devices used in its construction as well as the built-in maintenance features provided. Such an analysis is beyond our scope here, but it may be helpful to note the sensitivity of the expected period between major overhauls of an array to the choice of phase-shifter technology for a very low sidelobe array. Recently completed reliability studies have shown that an array using ferrite phase shifters with separated drivers will satisfy its performance objectives for more than four years before overhaul.

These results show that, although careful attention must be given to maintenance provisions and component reliability, very low sidelobe array performance can reasonably be expected to be maintainable in service.

Conclusion

This paper has examined the impact of the sidelobe-level objective on the cost and weight of a phased-array antenna for tactical radar. The results indicate that dramatic system-performance improvement in a jamming environment can be obtained with only a moderate increase in antenna cost and weight.

A performance increase in an EW environment of more than 12 dB appears to be quite feasible by means of sidelobe-level reduction. A 12-dB system-performance increase in a jamming environment achieved by other means, such as increasing transmitter power 15 times, is clearly not feasible. This is not a performance increase for peacetime operation in a friendly environment. Rather it is a performance increase for the heat of battle—when it counts.

How many of these *RCA Engineer* issues should you have read?

Order them now.

Back issues and reprints listed here may be ordered from the *RCA Engineer* Editorial Office, 204-2, Cherry Hill.

All back issues are $2.00 except the *Index*, which is free.

Photocopy this form. Include your name, RCA charge number and your internal mailing address.

THEME-RELATED ISSUES

- ☐ Consumer Electronics Manufacturing
  VOL. 24, NO. 4 Dec 78/Jan 1979
- ☐ Microelectronics
  VOL. 24, NO. 6 Apr/May 79
- ☐ Microprocessor Applications
  VOL. 25, NO. 3 Oct/Nov 79
- ☐ Quality (Do it right the first time)
  VOL. 25, NO. 4 Dec 79/Jan 80
- ☐ RCA International
  VOL. 25, NO. 5 Feb/Mar 1980
- ☐ Color TV Receivers
  VOL. 25, NO. 6 Apr/May/Jun 1980
- ☐ 25th Anniversary Issue
  VOL. 26, NO. 1 Jul/Aug 1980
- ☐ Communications Trends
  VOL. 26, NO. 3 Nov/Dec 1980
- ☐ Mechanical Engineering
  VOL. 26, NO. 4 Jan/Feb 1981
- ☐ Increasing Your Effectiveness
  VOL. 26, NO. 5 Mar/Apr 1981
- ☐ "SelectaVision" VideoDisc, Part II
  VOL. 27, NO. 1 Jan/Feb 1982
- ☐ Manufacturing Engineering
  VOL. 27, NO. 2 Mar/Apr 1982
- ☐ Electro-Optics
  VOL. 27, NO. 3 May/Jun 1982

COLLECTIONS OF ARTICLES

- ☐ Consumer Electronics
  PE-515 1971
- ☐ Solid State Technology
  PE-552 1972
- ☐ COS/MOS Technology
  PE-580 1973
- ☐ Automotive Electronics
  PE-681 1976
- ☐ Microprocessor Technology
  PE-702 1976
- ☐ Electro-Optics
  PE-703 1976
- ☐ Picture Tube
  PE-748 1980

CUMULATIVE INDEX

- ☑ 25-Year Index to *RCA Engineer*
  Aug 1980

H. Goldberg

Wideband receivers for communications satellites

RCA Astro-Electronics manufactures a microwave product line of low-noise high-performance receivers, at C-band and Ku-band, for three communications satellite programs.

Abstract: *Astro-Electronics has developed wideband receivers in both C-band and Ku-band for use in communications satellites. These receivers are all solid-state units having a transmission bandwidth of 500 MHz and operating in the 5.9- to 6.4-GHz and 14- to 14.5-GHz bands.*

The C-band receiver was first designed for and flown on RCA Satcom III and is currently in production for two satellite programs requiring seven spacecraft. Improvements in noise figure and third-order intermodulation distortion compared to the original RCA Satcom receivers is achieved by the use of GaAs FET transistors. In addition, the intermodulation performance has been greatly improved, resulting in a third-order intercept point of +28 dBm, which is approximately 10 dB greater than that of previous receivers.

More recently, AE has developed two new Ku-band receivers that operate in the 14- to 14.5-GHz band. These receivers are to be used on the GSTAR and Spacenet satellite programs.

Astro-Electronics has been designing and building communications satellites since the early 1970s, but not until 1978 did AE begin to design the microwave hardware used in the communications-system transponder. One of the first microwave boxes to be designed and put into production is the 6/4-GHz communications receiver. This unit is a wide-bandwidth receiver covering the full communication spectrum assigned to the satellite, and it amplifies all of the signals of a transponder simultaneously. For C-band communications satellites, the receiver-input band (uplink) is 5.925 to 6.425 GHz, and its output band (downlink) is 3.7 to 4.2 GHz.

For the RCA Satcom satellites, all 12 channels of a transponder are amplified and translated to the output frequency by the 6/4-GHz reciever. Two transponders operate without interference, using the same frequency spectrum, by cross polarization of input and output signals, thus requiring two communications receivers operating continuously to provide 24-channel capacity.

Description of 6/4-GHz receiver

The performance summary of the 6/4-GHz receiver is shown in Table I, and a block diagram of the receiver is shown in Fig. 1. Input signals are amplified at 6 GHz by a low-noise FET amplifier and then down-converted to 4 GHz by combining the signals with the 2.225-GHz local oscillator in a diode double-balanced mixer. The resulting 4-GHz signal is then amplified to the required level by a four-stage FET amplifier. The stabilized voltage required by the amplifiers and local oscillator are produced by a power-regulator circuit that operates from the spacecraft's unregulated bus voltage. A photograph of the receiver is shown in Fig. 2.

The 6-GHz amplifier consists of two GaAs FET amplifier modules separated by ferrite isolators. Isolators are also used at the input and output to obtain a low voltage standing-wave ratio (VSWR) for the amplifier. The two-stage amplifier provides 24 dB of gain and a flat response across the 5.925- to 6.425-GHz band.

Down conversion to the 4-GHz band is achieved in the mixer, which has isolators

Table I. *Receiver performance summary.*

Parameter	*6/4-GHz Receiver*	*14/12-GHz Receiver*
Input/Output Frequency	5.9-6.4/3.7-4.2 GHz	14-14.5/11.7-12.2 GHz
L.O. Frequency	2.225 GHz	2.3 GHz
L.O. Stability	±1 ppm	±1 ppm
Noise Figure	3.5 dB, max	5 dB, max
Gain	60 ±1 dB	50 ±1 dB
Gain Slope	0.02 dB/MHz, max	0.02 dB/MHz, max
Group Delay	1 ns/36 MHz, max	2 ns/72 MHz, max
3rd Order IM Intercept	+28 dBm, min	+24 dBm, min
Input/Output VSWR	1.2:1, max	1.15:1, max
DC Power	8 W, max	8.4 W, max
Size	8.7 × 3.3 × 4.5 inches	8.38 × 4.67 × 5.75 inches
Weight	3.25 pounds	3.5 pounds

©1982 RCA Corporation
Final manuscrip: received July 30, 1982
Reprint RE-27-5-7

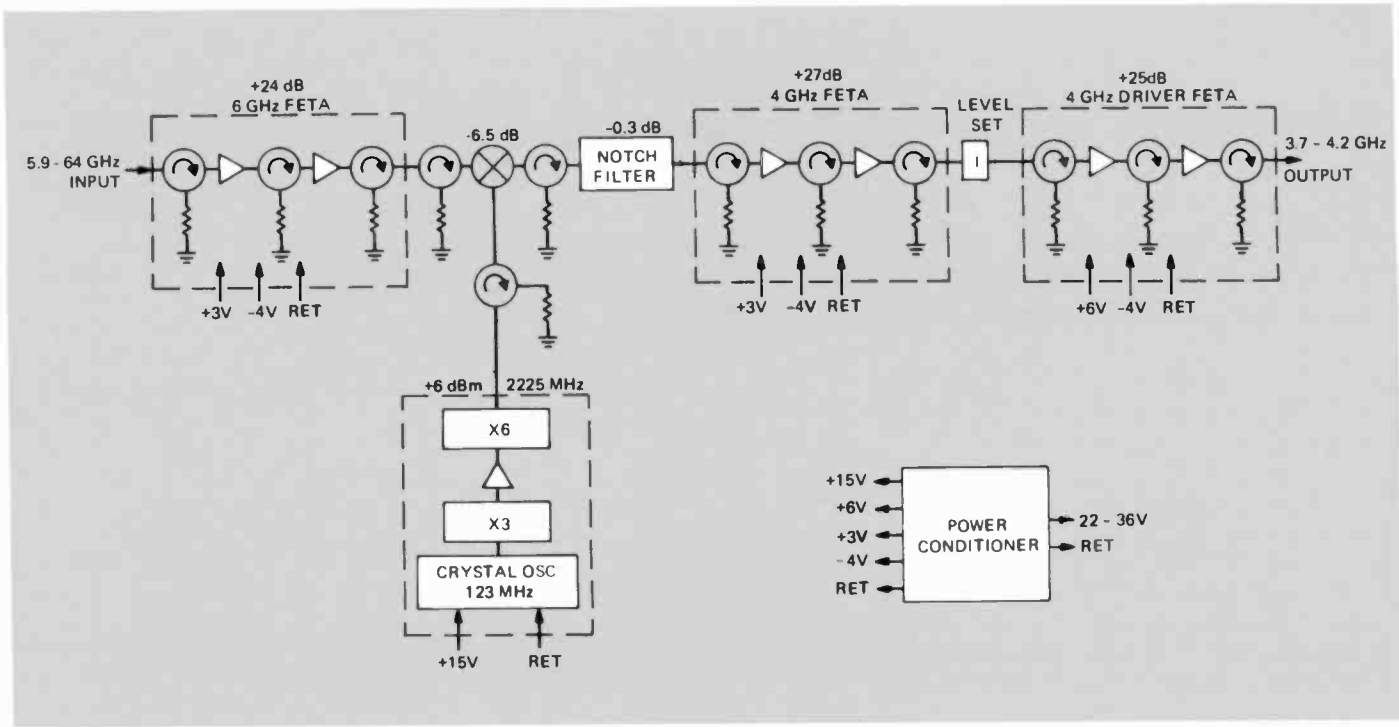

Fig. 1. *The 6/4-GHz receiver. The 6-GHz signals received from the ground are down-converted to 4 GHz for retransmission to the ground.*

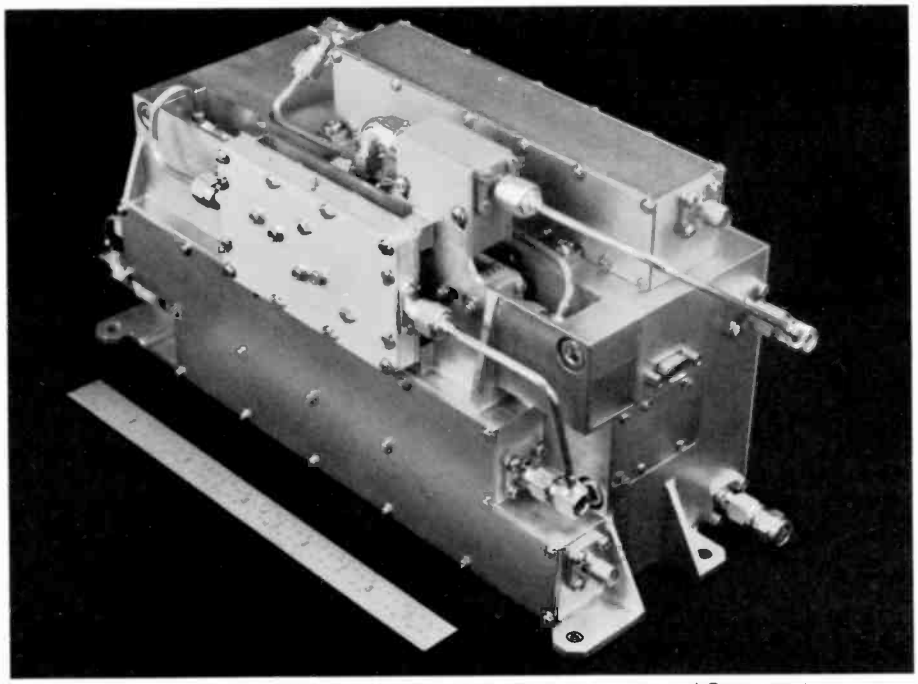

Fig. 2. *Assembled 6/4-GHz receiver used on RCA Satcom and Spacenet.*

incorporated at all ports to minimize reflection on coaxial lines interconnecting modules. A notch filter is provided after the mixer to attenuate the second harmonic of the local oscillator at 4450 MHz, which is generated in the mixer.

The 4-GHz output from the mixer assembly is amplified by two 4-GHz FET amplifiers consisting of two transistors for each amplifier. The first amplifier provides 27 dB of gain over the 3.7- to 4.2-GHz band, while the second unit provides 25 dB of gain. The two amplifiers are similar in design, with isolators at the input and output of each transistor stage; however, the output stage of the second amplifier contains a medium-power FET to provide low intermodulation in output signals.

FET amplifiers

The 6- and 4-GHz FET amplifiers are similar in design. They consist of input and output matching circuits in microstrip on 25-mil alumina to match the low impedance of the GaAs FET to 50 ohms. Matching networks were designed with the aid of COSMIC computer programs using transistor "S" parameters. The matching network employed on both input and output is a two-stage Chebyshev quarter-wave transformer. Selection of transforming line lengths and impedance (width) is made by the computer to provide flat frequency response and the best impedance match across the full frequency band of the amplifier.

Interstage ferrite isolators are used at the input and output of each amplifier to achieve low input and output return loss and to prevent the input of the following stage from affecting the frequency response of each FET amplifier. The isolators are drop-in type, microstrip construction and are connected to the amplifier by welded gold ribbons. Figure 3 shows the 6-GHz FET amplifier. The two FET amplifiers with input and output matching networks are mounted on Kovar carriers and drop into the chassis, while isolators are soldered directly to the chassis.

Assembled amplifiers do not always give the performance they were designed to produce, because of variations in transistor

S-parameters and in assembly techniques. The amplifier must be tuned to the desired performance level after final assembly. This is done by placing tuning tabs on the input and output microstrip lines to tune for a flat frequency response. Gold tuning tabs are secured to the substrate metalization by welds.

FET temperature compensation

The 6/4-GHz receiver operates over a temperature range of −7° to +45°C. The uncompensated FET amplifier will show a drop in gain at high temperature and an increase in gain at cold temperature. To offset this effect, the current in the transistor can be increased at high temperatures and decreased at low temperatures. This is done by varying the gate bias of each FET to hold the gain constant using a simple voltage-divider circuit containing a temperature-sensitive component and resistors. The temperature-sensitive component is a sensistor with a positive temperature coefficient that causes the FET current to increase at high temperature and decrease at low temperature. The other resistors in the circuit set the gate voltage and linearize the temperature-compensating effect of the sensistor. By proper component selection, the uncompensated gain change can be reduced by a factor of three to five depending on transistor type and initial operating current.

Receiver local oscillator

The local oscillator consists of a crystal oscillator at 123.611 MHz, multipliers, amplifiers, and filters to generate a signal at 2.225 GHz. Each module is designed to work into a 50-ohm impedance and is tuned up and tested in test fixtures before assembly in the local oscillator housing as shown in Fig. 4.

The output of the crystal oscillator is multiplied by three in a transistor and then amplified to a power level of +19 dBm at 370 MHz. This signal is then applied to a step recovery diode to generate the sixth harmonic at 2.225 GHz. A microstrip bandpass filter and a lumped-constant low-pass filter are used to produce an output at 2.225 GHz in which spurious signals are down at least 80 dB from the carrier.

The quartz crystal of the oscillator section is placed in a self-contained transistor/thermistor-controlled oven kept at 65° ±2°C. This results in a frequency drift of less than ±1 parts per million over the operating temperature of −5° to +55°C.

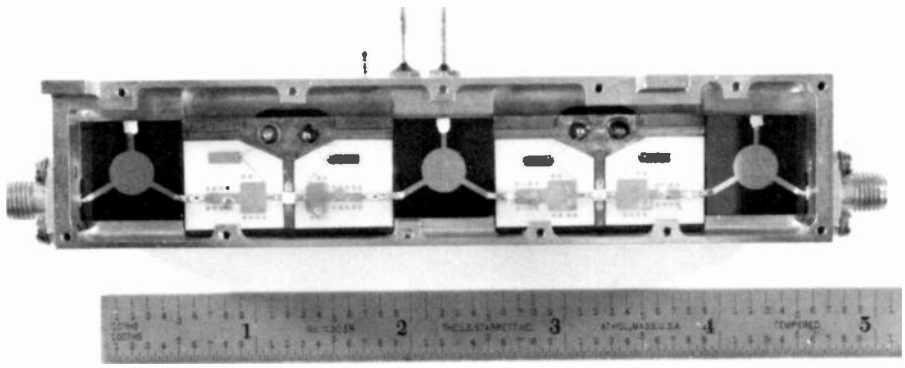

Fig. 3. *The 6-GHz amplifier, showing transistors and microstrip matching circuits and isolators at input and output of each amplifier.*

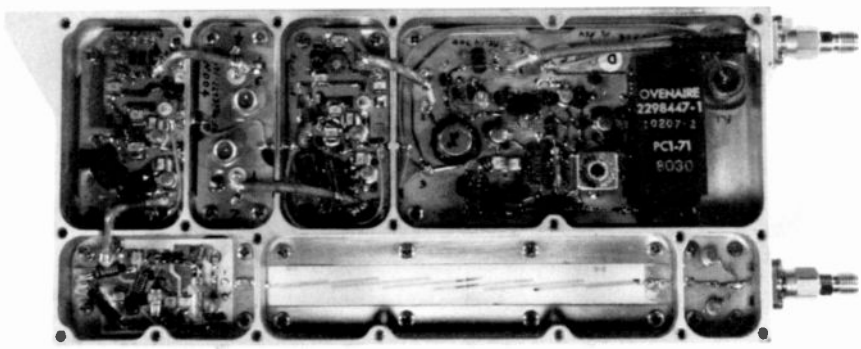

Fig. 4. *The 6/4-GHz receiver local oscillator generates a signal at 2.225 GHz from an oven-controlled crystal oscillator at 123.611 MHz.*

Mixer and notch filter

The mixer is a double-balanced diode design. It is optimized for inputs in the 5.925- to 6.425-GHz range and produces an intermediate frequency (i.f.) output at 3.7 to 4.2 GHz when used with a local oscillator frequency of 2.225 GHz. The mixer is designed to operate with a local oscillator input-power level of +6 dB and can be operated over the input range of +4 to +8 dBm with little change in the conversion loss of 6 dB. Isolators are placed at all three mixer ports to obtain low VSWR and prevent reflections on signal lines that would introduce ripple in the passband of the receiver.

The notch filter is required to reduce the level of the second harmonic (4.45 GHz) of the local oscillator, which is generated by the mixing process. A two-pole filter is required to reduce this signal by at least 30 dB. The filter consists of two quarter-wavelength resonators—short-circuited at one end and open-circuited at the other—that are proximity coupled to the main transmission line.

Filter tuning is accomplished with capacitive-loading tuning screws located on the side covers of the filter. The tuning screws adjust the end-effect loading at the open end of the quarter-wavelength resonant lines and also the capacitive coupling between the resonant lines and the main transmission line. The center frequency of the notch is tuned to 4.448 GHz (1.2 MHz below 4.450 GHz) to account for a frequency shift when operated in a vacuum.

Receiver testing

Extensive testing is performed on each receiver to verify that it meets all performance specifications. Testing starts at the module level, with each FET module being tested to demonstrate gain and flat response across the band and in the temperature range of −7° to 45°C. Modules are then placed in a chassis, and tuned and retested at the subassembly level.

The same testing process is repeated on the local oscillator printed-circuit boards so that each is aligned in a test fixture. After all subassemblies are tested, they are assembled into the receiver chassis, and the completed receiver FET amplifiers are fine tuned with gold tabs on the alumina substrate to equalize the gain so that variations in gain across the 500-MHz band are

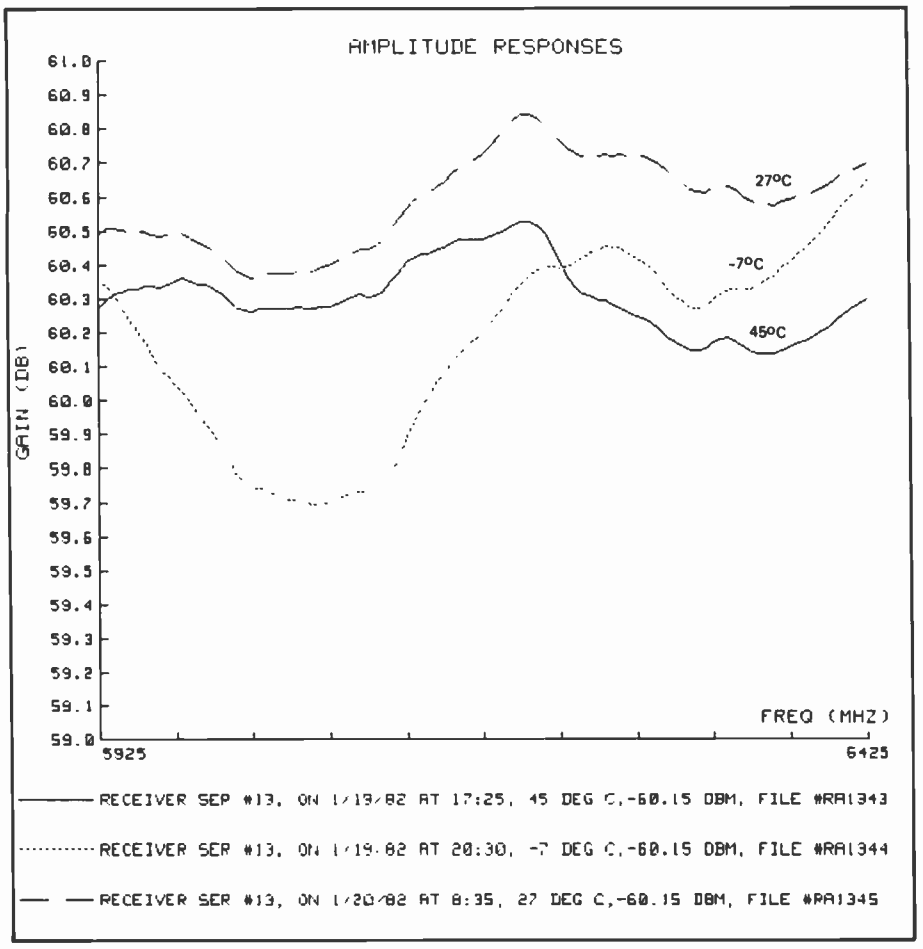

Fig. 5. *Typical gain and frequency response of the 6/4-GHz receiver at three temperatures.*

no more than about 0.5 dB. Receiver gain is set to 60 dB using a fixed attenuator pad in the 4-GHz FET amplifier, and a series of temperature tests are performed to measure gain at hot and cold temperatures. Figure 5 shows the gain of a typical receiver at −7°, +27°, and +45°C in which the gain-adjust attenuator pad had been reselected to put the receiver gain in the range of 59 to 61 dB over the temperature range. A receiver-noise figure of 3.0 dB is typical at ambient temperature across the 500-MHz frequency band. At +45°C an increase of 0.2 dB in the noise figure can be expected.

In addition to the bench and thermal tests, the receiver is subjected to vibration in three planes and several days of operation in a thermal vacuum to verify performance in a simulated space environment.

14/12-GHz receiver

As the communications satellite allocations at C-band are becoming filled, the industry's attention is shifting to Ku-band frequencies (14- to 14.5-GHz uplink and 11.7- to 12.2-GHz downlink). Astro-Electronics has recently developed an all FET Ku-band receiver for use on two Ku-band spacecraft that will be launched in early 1984. A block diagram of this receiver is shown in Fig. 6, and a performance summary is listed in Table I. The receiver is

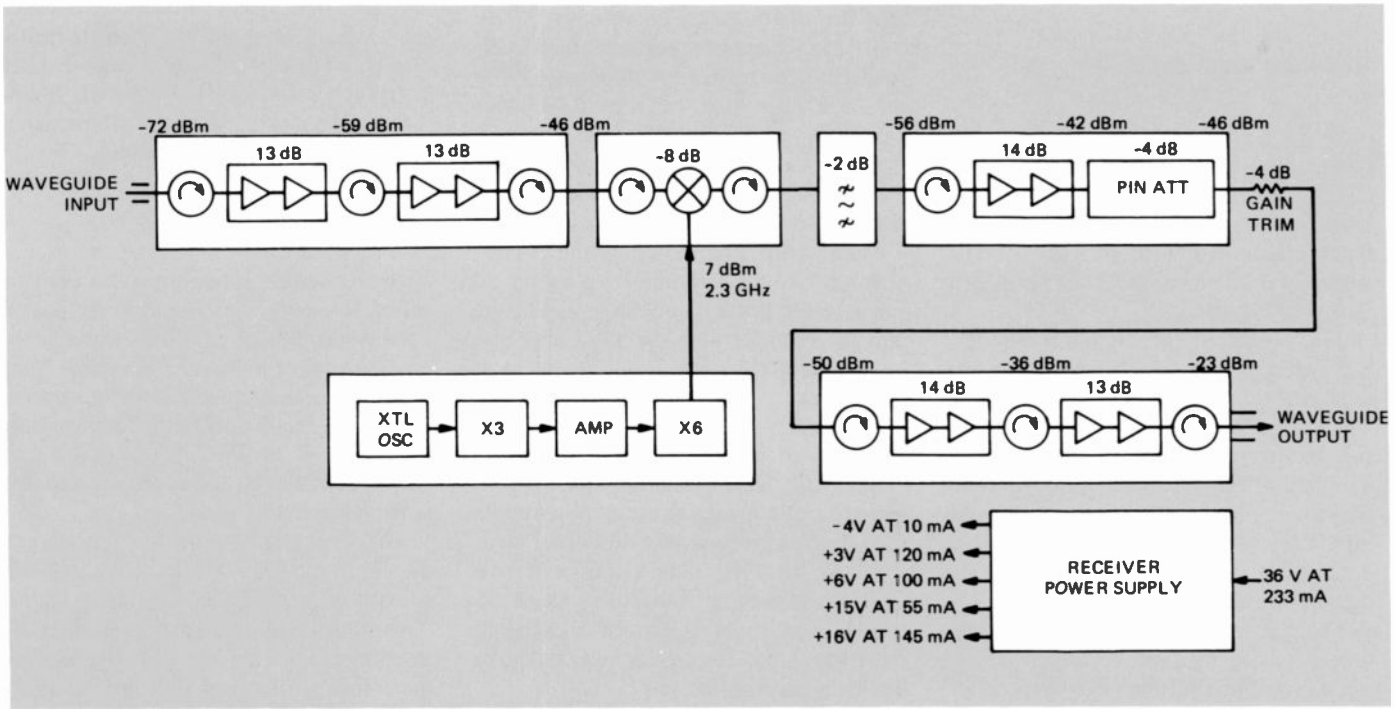

Fig. 6. *The 14/12-GHz receiver. Similar to the 6/4-GHz receiver, the 14/12-GHz receiver down-converts the uplink (14-GHz) signal to 12-GHz for retransmission to the ground.*

similar in design to the C-band unit except that the low-noise FET amplifier is now at 14 GHz and the output is at 12 GHz. A close look at the Ku-band design shows that the FET amplifiers consist of two transistors that form a basic gain block or module. These two transistor modules are then cascaded with isolators at the input and output. This technique reduces the size of a two-transistor amplifier by eliminating the interstage isolator and combining the output matching network with the input network of the next stage.

A typical two-stage amplifier at 14 GHz, using NE13783 transistors, has 14 dB of gain and about a 3-dB noise figure. When two such units are combined in an amplifier chassis (Fig. 7), the resulting amplifier has about 28 dB of gain and less than 0.5-dB gain variation across the 14- to 14.5-GHz band as shown in Fig. 8. A microstrip isolator has not been used at the input to the 14-GHz amplifier because it would contribute to the loss and noise figure. Instead an isoadaptor, a waveguide-to-SMA adaptor with a built-in isolator, is used which only adds 0.25-dB input-insertion loss and maintains input VSWR of 1.15:1.

Design of the 12-GHz FET amplifiers are similar to the 14-GHz unit except that the transistors are HFET 2201 for small-signal stages, and a medium-power FLX03 is used in the output stage to provide low intermodulation distortion. The HFET 2201 does not provide as low a noise figure as the NE13783, but it does have S-parameters that can be easily matched to 50 ohms.

The 12-GHz FET amplifier is shown in Fig. 9. A *pin*-diode attenuator is included in this design after the first transistor pair so that the receiver gain can be adjusted to correct for decreases in gain from aging of the transistors. This *pin* attenuator provides 3.5 dB of gain adjustment in 0.5-dB steps. An additional fixed attenuator pad is used to set the total receiver gain during alignment.

The mixer is a double-balanced microstrip design and is followed by a waveguide bandpass filter that attenuates the fifth and sixth harmonics of the local oscillator at 11.5 and 13.6 GHz. The local oscillator at 2.3 GHz is similar to that of the 6/4-GHz receiver except that the circuits are shifted from 2.225 to 2.3 GHz. This 3.4-percent shift in frequency is accommodated by the variable adjustments of the local oscillator circuits without design modification.

Receiver frequency response is shown in Fig. 10. Slight retuning of the FET

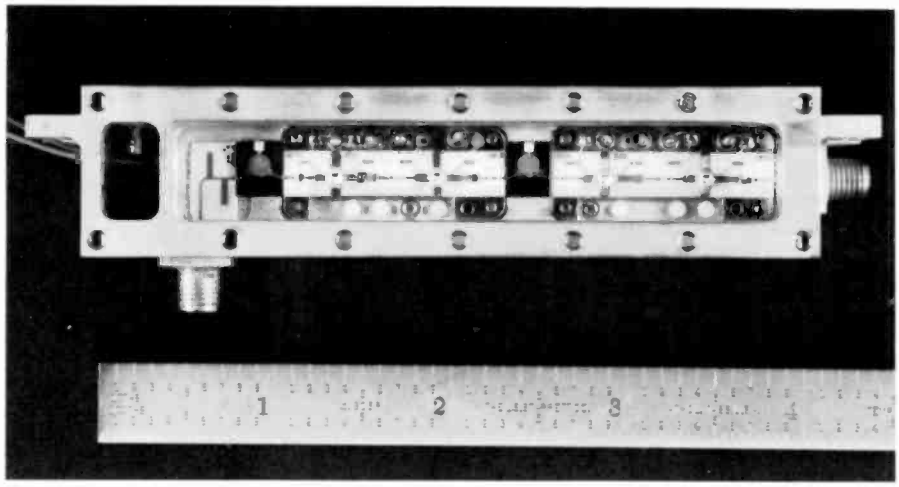

Fig. 7. *Two-stage 14-GHz low-noise FET amplifier. Each stage consists of a two-transistor amplifier on a drop-in carrier.*

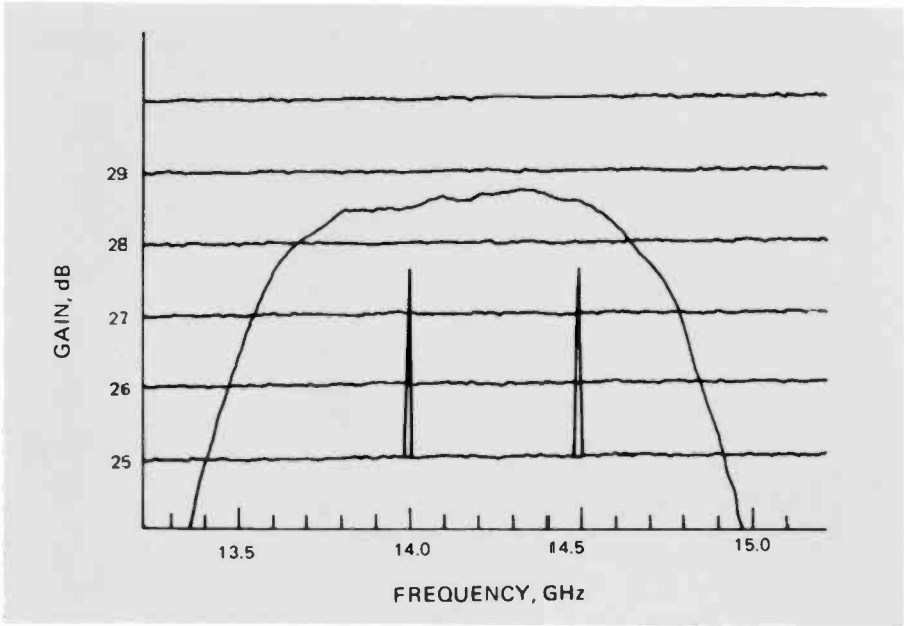

Fig. 8. *Frequency response of the 14-GHz FET amplifier over frequency range of 13.2 to 15.2 GHz. Note flat response over communication band of 14 to 14.5 GHz.*

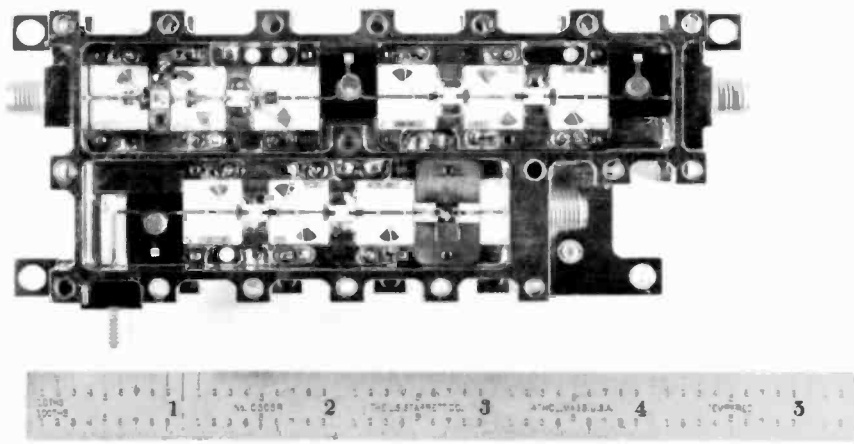

Fig. 9. *The 12-GHz FET amplifier used in Spacenet and Gstar receivers.*

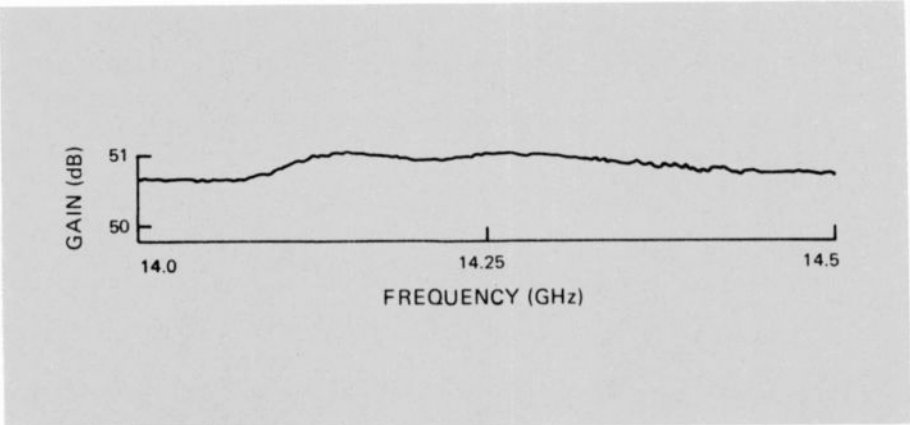

Fig. 10. *Gain and frequency response of the 14/12-GHz receiver. Gain variation across the 500-Hz communication band are about 0.5 dB.*

amplifiers was necessary to keep receiver-gain variations to less than ±0.5 dB over the full 500-MHz band.

In the past four years, Astro-Electronics has developed a microwave product line that is supplying low-noise high-performance receivers at C-band and Ku-band for three communications satellite programs. The C-band receivers have proven their performance by reliable operation in space on the RCA Satcom IIIR since November 1981. These receivers are currently in production for the Spacenet and advanced RCA Satcom spacecraft. The Ku-band receivers are in production for the Spacenet and GSTAR spacecraft, which are scheduled for launch in early 1984.

Harold Goldberg, Manager of Receiver Design, began working at Astro-Electronics in 1977 and was responsible for the design of the wideband communication receiver currently used on RCA Satcom satellites. Mr. Goldberg holds a BSEE degree from Lafayette College and an MSEE from Cornell University.

Contact him at:
RCA Astro-Electronics
Princeton, N.J.
TACNET: 229-3284

C.E. Profera | G.L. Rosol
H.H. Soule | J. Kara

Shaped-beam reflector antennas for communications satellites

Antenna performance is a key element in satellite communications. Increased flexibility, directivity and system optimization are in the shape of things to come.

Abstract: *Engineers are improving antenna performance. At RCA, the offset paraboloid reflector shaped-beam antenna has been adapted to the linear-polarization frequency-reuse requirements of the Satcom satellites. The advanced dual-reflector assembly is first completely designed by RCA Astro-Electronics, and its design is reviewed. The antenna-coupling network, and the testing procedures and results, are other topics handled by the authors.*

The geostationary communications satellite is popularly referred to as a "microwave relay in the sky." The major elements of the communications payload of this satellite are the transponders and the antenna subsystem. The transponder amplifies the received (uplink) signals from earth, down converts their carrier frequencies to the transmit (downlink) band, and amplifies the down-converted carrier for relay back to earth. The antenna subsystem contains a receive antenna that couples the uplink signals to the transponder's receiver, and a transmit antenna that radiates the down-converted signals back to earth. A simplified block diagram of a typical frequency-division multiple-access (FDMA) satellite-communications system is shown in Fig. 1, wherein a common transmit/receive antenna is employed.

The overall quality of the satellite-communications subsystem is defined by the system's G/T (gain divided by temperature, in dB/K) and EIRP (effective isotropically radiated power, in dBW), which are wholly dependent on the performance characteristics of the two principal subsystems. The system's G/T is a measure of the sensitivity of the system to discern the uplink signals from system-generated and external noise. The G/T characterizing the system is the ratio of receive antenna gain at the uplink frequencies, referenced to the input port of the low-noise amplifier (LNA), and the effective system-noise temperature, referenced to that same port. EIRP is the ratio of the available radiated downlink power from the satellite-antenna system to the radiated power that would be supplied by an omnidirectional (unity gain) antenna fed from the same source.

Antenna performance factors

Two major factors that influence the EIRP and G/T are related to antenna performance. These are antenna gain and antenna-system loss, as achieved in both the downlink and uplink frequency bands. The "shaped-beam" communications-satellite antenna permits the optimization of EIRP and G/T by providing an antenna pattern with its beam shape "tailored" to produce a "footprint" on earth that follows the boundaries of a geographical land mass to be serviced. A shaped-beam antenna pattern may be generated by superposition of a number of more directive, symmetrical antenna beams, commonly referred to as component beams. A typical shaped-beam antenna system composed of a multiple-beam antenna providing the component beams and a power-dividing (transmit) or combining (receive) shaped-beam-forming network for superposition of beams, is illustrated in Fig. 2.

The multiple-beam antenna most commonly used on today's communications satellites is the paraboloid reflector with a multiple-horn feed array, wherein a single component beam is associated with each

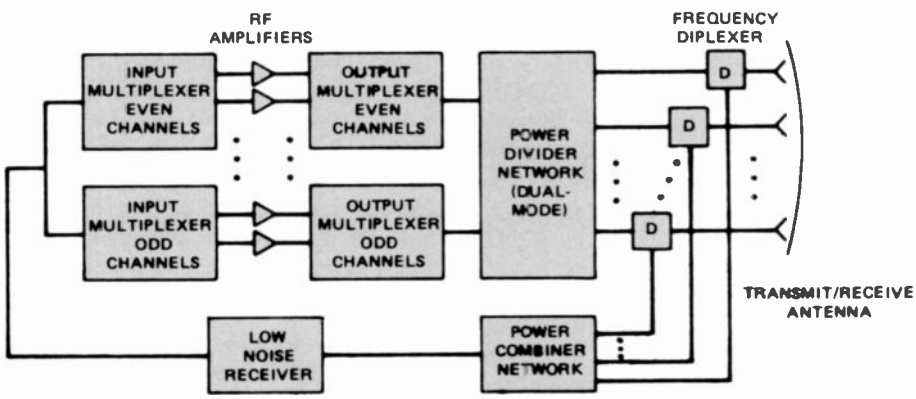

Fig. 1. *A simplified block diagram of an FDMA satellite-communications system with dual-mode transmit network and a common transmit/receive antenna.*

© 1982 RCA Corporation
Final manuscript received August 23, 1982
Reprint RE-27-5-8

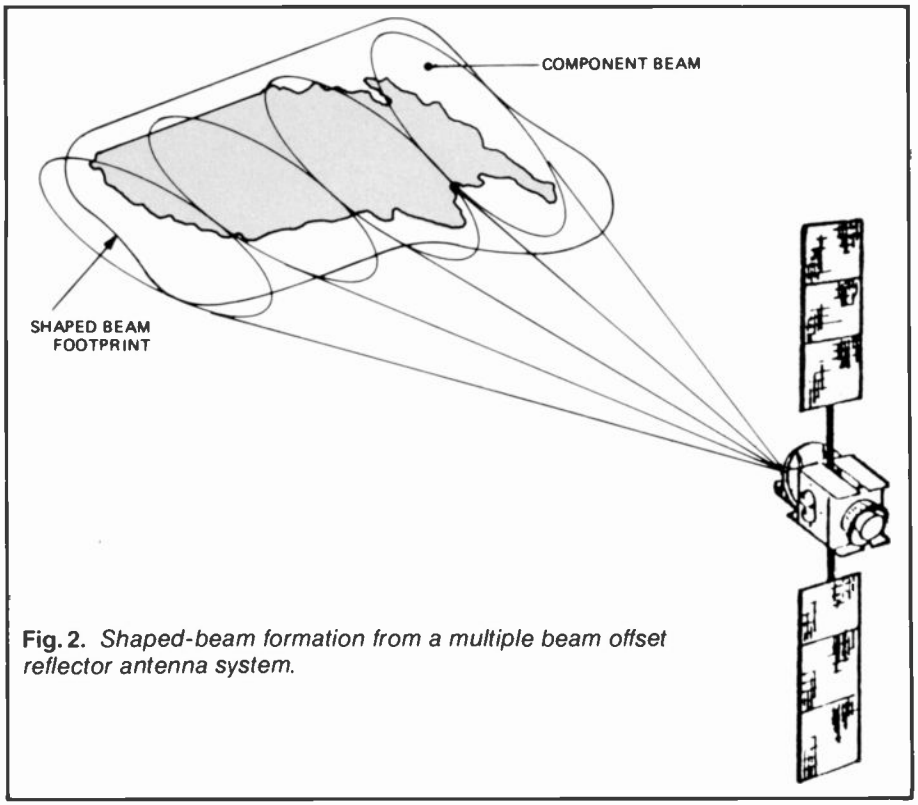

Fig. 2. *Shaped-beam formation from a multiple beam offset reflector antenna system.*

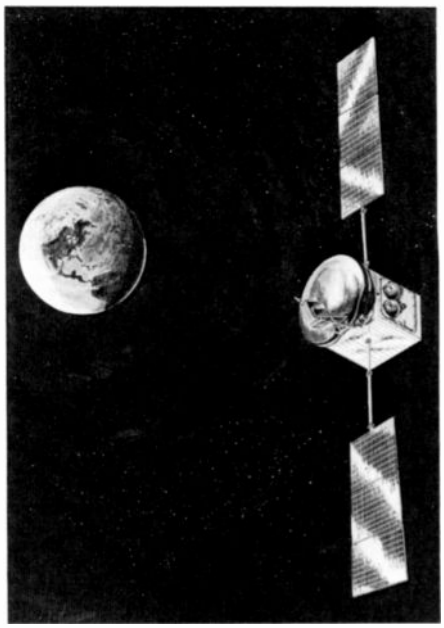

Fig. 3. *An artist's concept of the Satcom F satellite and frequency reuse antenna system with overlapped, gridded reflectors and multiple-horn, vertically and horizontally polarized feed array.*

horn element of the array. An offset section of the paraboloid reflector is most often used to avoid aperture blockage by the feed array and its mechanical supporting structure.

The shaped beam-forming networks may take several forms, dependent upon the operating frequency and the size and weight requirements imposed by the satellite system. For C-band communications-satellite applications (3.7- to 4.2-GHz downlink-frequency band, 5.9- to 6.4-GHz uplink-frequency band) both waveguide and coaxial networks have been and are being used. Waveguide networks are typically minimum loss, but of greater size and weight. Coaxial beam-forming networks offer attractive size, weight, and packaging alternatives at the cost of an added insertion loss and, thus, reduced EIRP and G/T. K-band applications (11.7- to 12.2-GHz downlink-frequency band, 14.0- to 14.5-GHz uplink-frequency band) require all-waveguide networks, as the increased coaxial-network losses encountered at these frequencies are prohibitive.

Frequency reuse

The offset paraboloid reflector shaped-beam antenna can be readily adapted to a linear-polarization frequency-reuse requirement such as that of the RCA Satcom series of satellites. The communications-satellite frequency bands may be used twice, within the same communications subsystem, if the antenna-system design has a dual-polarization capability.

For such a frequency reuse to be effective, the dual-polarized antenna system must provide an isolation between corresponding points in orthogonally polarized beams of typically 33 dB. The polarization-isolation requirement precludes the use of a single, solid paraboloid reflector with a dual-polarized feed array. Instead, independent orthogonal linearly polarized antenna systems are realized by using a pair of linearly gridded reflectors, which may be completely overlapped, resulting in a shared-aperture antenna system. Each reflector is illuminated by its own, linearly co-polarized feed array such that two virtually independent orthogonally polarized antenna systems occupy the space normally required for a single antenna system. This results in a very effective use of valuable satellite real estate and an antenna system with adequate polarization isolation suitable for frequency reuse. The Satcom F satellite with its dual, linearly polarized shaped-beam antenna system, illustrated in Fig. 3, is a prime example of this type of design.

Dual-mode network

The design of a shaped-beam satellite-communications antenna is often influenced by the requirements imposed on the transponder multiplexing filter assembly. To avoid the insertion loss of contiguous channel multiplexing, alternate channel multiplexing is adopted. The antenna beam-forming network is then required to produce a pair of beams from a single antenna structure, into which alternately multiplexed channels are transmitted. This type of beam-forming network is commonly referred to as a dual-mode network. Figure 1 includes a dual-mode network.

The dual-mode network is a dual-beam network that, from either of two signal input drives, produces two equal sets of amplitude coefficients for equivalent illumination of the feed array. The associated phases are constrained to particular sets of conjugate values. This results in an antenna gain, for either shaped beam, that is typically 0.5 dB less than optimum. Where this antenna-gain penalty (hence, EIRP) is less than the cost of contiguous channel multiplexing, dual-mode antenna designs are imposed.

Shaped-beam design

Design of a shaped-beam antenna begins by considering the land area to be covered by the beam. For the offset paraboloid antenna design, the reflector diameter establishes the component beamwidths and the number of beams required to form the shaped beam. Large reflectors produce sharp-

er component beams. Large numbers of these beams may then be employed to more closely match the shaped-beam footprint to the land area.

For most communications-satellite applications, the launch-vehicle configuration limits the reflector diameter that may be employed. The Satcom F antenna dimensions, for example, were established by the 85-inch Delta-launch-vehicle shroud limit.

Shaped-beam antenna gain increases slowly as the reflector diameter is increased; however, implementation complexities and increased beam-network losses associated with larger feed arrays may eventually nullify the increased gain. Some of the operational advantages of large-diameter antennas which, for particular applications, offset the complexity and added loss are:

- Improved efficiency of beam shaping;
- Sharper component beams to accommodate additional frequency reuses; and
- Shaped-beam reconfigurability for changes in communication traffic density or satellite orbit.

The angular location of a component beam is established by the location of its associated feed in the focal plane of the reflector. Additional component beams are formed by placing feed horns at points removed from the focus. As feed horns are translated from the focal point, loss of component beam gain and beam distortion occur. These effects may be reduced by selection of a longer focal length. However, the focal length, as well as the reflector diameter, is usually limited by launch-vehicle dimensions.

The shaped-beam antenna design proceeds by modeling aperture shapes, sizes, and horn arrangements with a reflector-antenna computer program. When the reflector and feed-array designs are established, a shaped-beam optimization computer program is used to establish feed-horn amplitude and phase excitations for desired gain and sidelobe characteristics. The antenna design having been finalized, the antenna and system performance parameters are identified by graphically displaying communications-system performance (G/T and EIRP) on global map projections. Figure 4 illustrates typical EIRP performance from a domestic communications satellite at a longitude of 135°W.

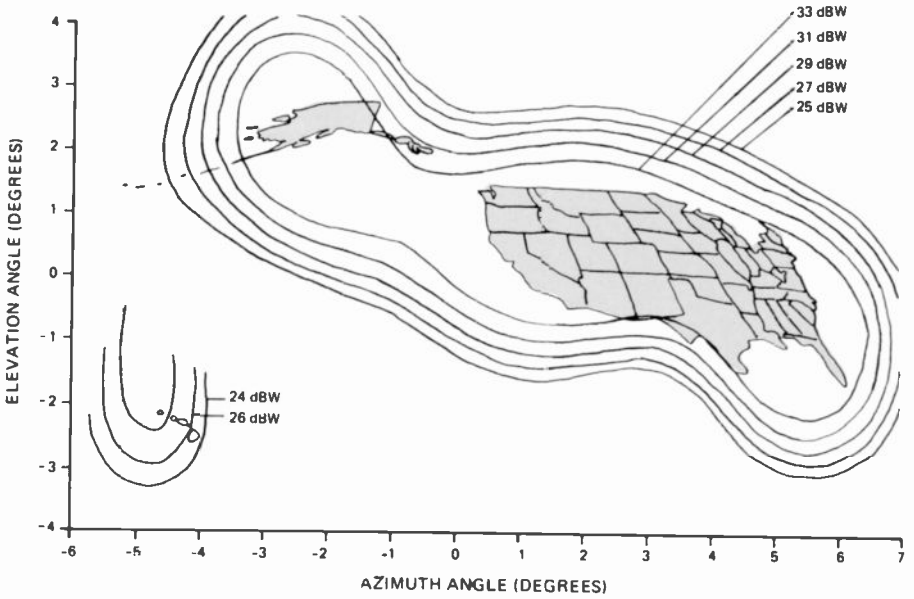

Fig. 4. *A computed shaped-beam antenna pattern footprint illustrating CONUS, Alaska, and Hawaii EIRP coverage from a geosynchronous satellite located in the 135° W longitude orbital slot.*

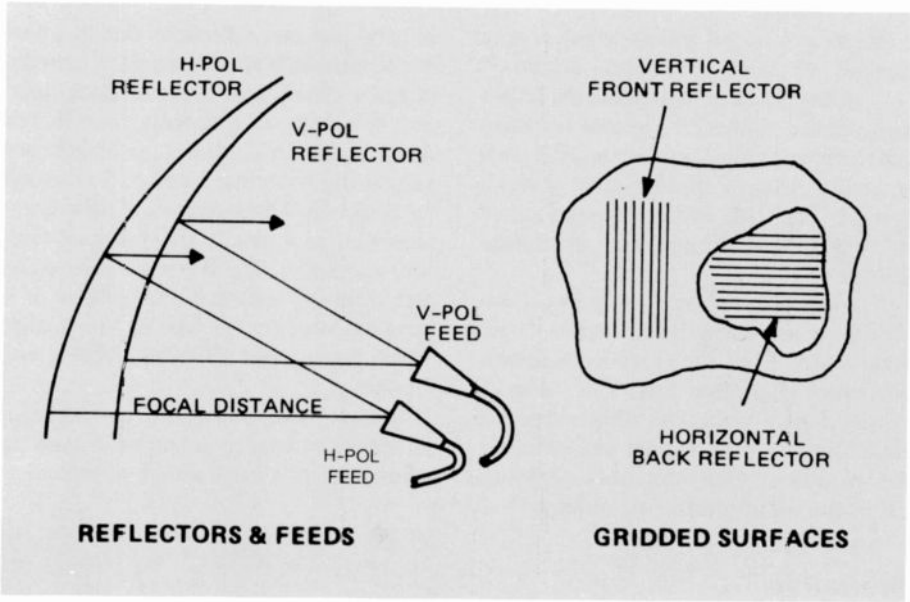

Fig. 5. *The shared-aperture, offset reflector concept for frequency reuse via orthogonal polarization.*

Reflector assembly

The Satcom F dual-reflector assembly is the first completely designed by RCA Astro-Electronics and is an excellent example of an advanced offset-reflector design. Thirteen feed horns, in independent 6- and 7-element arrays, illuminate it to provide 24-channel dual-polarized shaped-beam coverage in the 6/4-GHz frequency range. Frequency reuse is made possible with vertical and horizontal polarization operation, as previously described.

Two large-diameter offset reflectors are fully overlapped (Fig. 5) and the forward surfaces of each are made reflective to vertical and horizontal polarization by the use of printed copper grids. Closely spaced, narrow-gridded surfaces become excellent reflectors when the strips lie parallel with the incident polarization. Transmission occurs through grids placed orthogonal to the sense of the incident polarization; hence, cross-polarization radiation is supressed. The forward-reflector grids further attenuate the cross-polarized components of the inner reflector, thus improving polarization purity and co-frequency channel isolation.

The parabolic surface of a typical gridded communications-satellite antenna is fabricated using Kevlar/epoxy laminate and honeycomb core in a sandwich construction. The reflecting surface is provided by

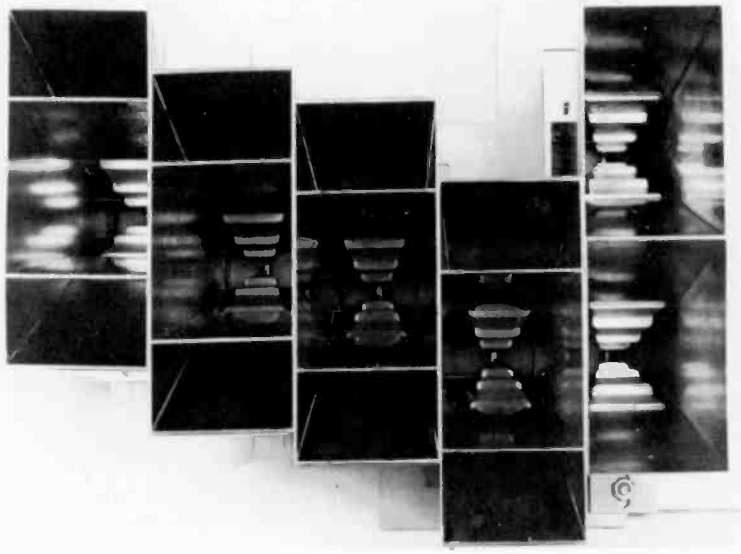

Fig. 6a. *The 6-element, breadboard, vertically polarized Satcom F feed array using ridge loaded, trifurcated rectangular horns with dominant E-plane flare. The inverted pictures (Figs. 6a and 6b) illustrate the horn coverage corresponding to the shaped-beam pattern of Fig. 4.*

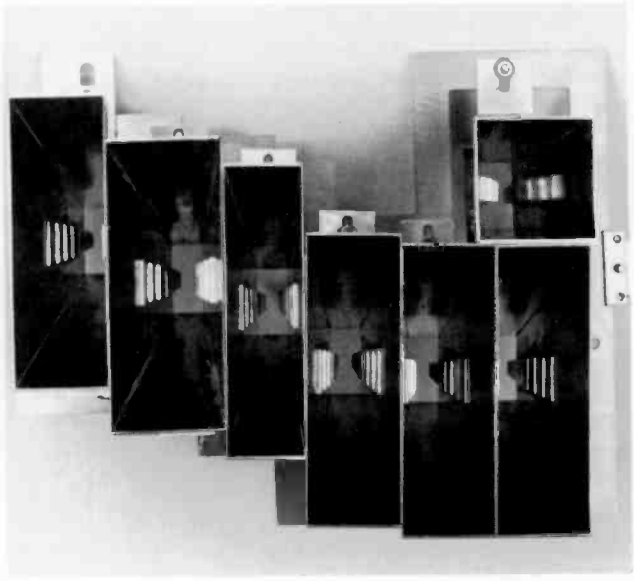

Fig. 6b. *The 7-element, breadboard, horizontally polarized Satcom F feed array using ridge-loaded rectangular horns with dominant H-plane flare.*

conducting grids of photo-etched copper bonded to 0.001-inch-thick Kapton™ (Dupont) film strips applied to the reflector surfaces. A typical C-band reflecting surface is controlled to within 0.015 inch rms, thus ensuring that no more than 1.0 percent (0.05 dB) of the energy incident on the surface is lost due to surface distortion.

The gridded reflector assembly is designed for strength with low weight. Outer and inner reflectors are joined by a crossed-rib structure of low loss. This forms a "super-sandwich" that can withstand severe launch stresses and thermal distortion forces encountered in orbit, with negligible deformation of the reflecting surfaces.

Feed array

Horn elements for C-band communications satellite applications operate over the 3.7- to 6.4-GHz frequency range because they are used for both downlink and uplink operation. Double-ridged waveguide transmission line is used to transmit and receive because it has a wide bandwidth. This loading technique eliminates the need for separate waveguide runs for uplink and downlink. The horns, therefore, are designed to interface with ridged-waveguide lines. A stepped or tapered ridge transformer is designed to go from a loaded, reduced dimension of waveguide to an expanded dimension, as found in a tapered rectangular waveguide horn. The ridge width, height, and number and size of steps combine to provide minimal reflections due to impedance mismatch at the boundary between ridged and unridged sections. Each aperture size requires a separate transformer design. Figure 6 illustrates the breadboard vertical and horizontal polarized horn arrays for Satcom F. Flight versions of these horns are investment cast, in one piece, of thin-wall aluminum. The horns are oriented as seen from the surface of the reflector. It is possible from this viewpoint to visualize which horns cover CONUS, Alaska, and Hawaii.

Because ridge loading of a horn changes its electrical length, attention is paid to adjustment of a ridge design to match, as closely as possible, the electrical length of horns of differing aperture and flare dimensions in the same array. This is essential because of the need to maintain phase-matched paths to each horn of the array.

The antenna-coupling network

The antenna-coupling network (ACN) is the remaining portion of the antenna subsystem and, as shown in Fig. 7, is an assembly of microwave components coupling the transponder to the antenna-feed array. For frequency reuse, ACNs are required for each polarization for the following:

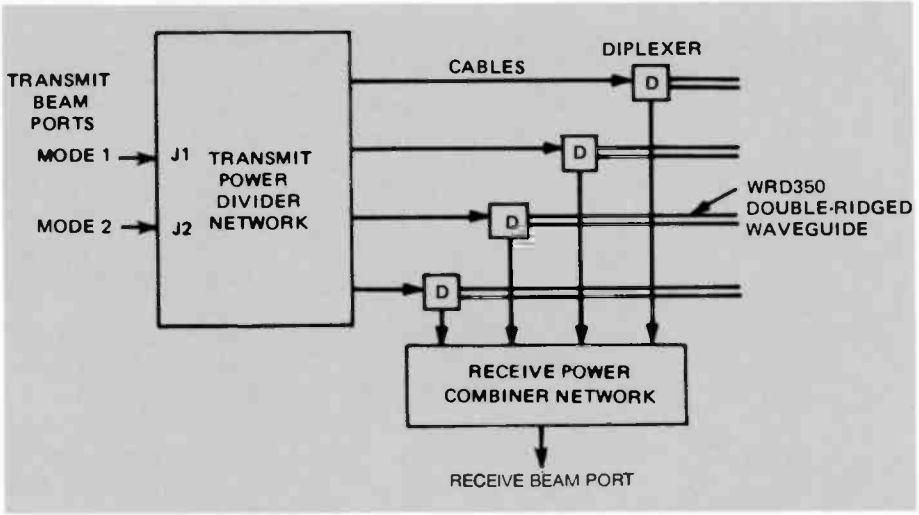

Fig. 7. *The antenna coupling network of a transmit/receive antenna system showing diplexers, dual-mode transmit and single-mode receive networks.*

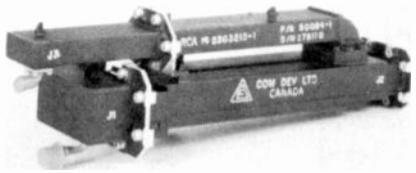

Fig. 8. *The Satcom F flight diplexer with waveguide antenna port and coaxial transmit and receive ports.*

- To couple transmit and receive channels to feed arrays of both polarizations;
- To generate the required transmit/receive amplitude and phase distributions at both feed arrays;
- To allow phase correction to maintain equal delay to each feed aperture;
- To provide dual-mode operation for transmit channels when required; and
- To isolate transmit and receive portions of the transponder.

Components used in the typical communications satellite ACN configuration include diplexers for transmit/receive isolation, a power-divider network (PDN) for transmit channels, a power-combiner network (PCN) for receive channels, and transmission lines that may be waveguide or coax for interconnection of subassemblies.

Design of the ACN is a trade-off between weight, size, and insertion loss. In a typical C-band ACN design, the divider and combiner networks may be waveguide or coax, so the trade-off must consider the reduced size and weight of coax versus the reduced insertion loss of waveguide. RCA Astro C-band designs have employed hybrid-transmission-line coupling networks, wherein the complex divider and combiner are built in TEM (transverse electromagnetic) rectangular coax, while the other components are of waveguide construction. For typical K-band ACN designs, waveguide weight and size are not prohibitive, and waveguide construction is favored for minimum loss.

The typical diplexer for a communications satellite must be a low-loss three-port unit providing a common transmit/receive port to the feed horn and isolated ports for transmit and receive sections of the ACN. Figure 8 shows the Satcom F flight diplexer consisting of a three-port waveguide junction, a band-reject filter (BRF) in the transmit arm, and a high-pass filter (HPF) in the receive arm. The BRF isolates the receiver from spurious transmit components in the receive band. The HPF protects the receiver from high transmit power. Salient characteristics of the diplexer are listed in Table I.

Table I. *Diplexer characteristics.*

Parameter	Value (dB)	
	Transmit	*Receive*
Insertion loss	0.10	0.12
Isolation	85	45

The PDN and PCN establish required amplitude and phase distributions at the feed array and may be single- or dual-mode networks, as dictated by multiplexer filter and transponder requirements. A schematic of a typical dual-mode PDN is shown in Fig. 9. For C-band application, this component must maintain amplitude and phase distribution over a 12-percent bandwidth and over temperature ranges as wide as −40°C to +50°C. Besides the low loss and weight requirements, the unit must typically be able to handle 50 watts into each input simultaneously.

C-band PDNs developed for RCA communications satellites use TEM rectangular coaxial airline. The PDNs are composed of quadrature-phase branchline couplers, fixed transmission-line phasing sections, and phase compensators. Branchline couplers are used because of bandwidth and high-power considerations. Phase compensation, via line lengths and fixed phase shifters, is necessary to achieve dual-mode illumination characteristics over the full bandwidths of the networks. The dual-mode relative power and phase distributions generated by the PDN illustrated in Fig. 9 are shown in Table II. Other typical PDN performance characteristics are listed in Table III.

Uplink signals are combined by the PCN and coupled to the receiver. The PCN is a single-beam network that establishes the array-amplitude distribution with co-phased horns. A typical PCN network that uses cascaded backward-wave couplers, which are ideal for low-power, wideband applications, is shown in Fig. 10. Salient characteristics of a C-band PCN are listed in Table IV.

Shaped-beam antenna testing

The performance of a communications-satellite antenna system is evaluated by comprehensive testing conducted on an antenna-pattern test range. Astro-Electronics currently has two such ranges. The source antenna is mounted atop a 200-foot tower. Distance to the satellite reflector, situated inside an rf anechoic chamber, is 400 feet.

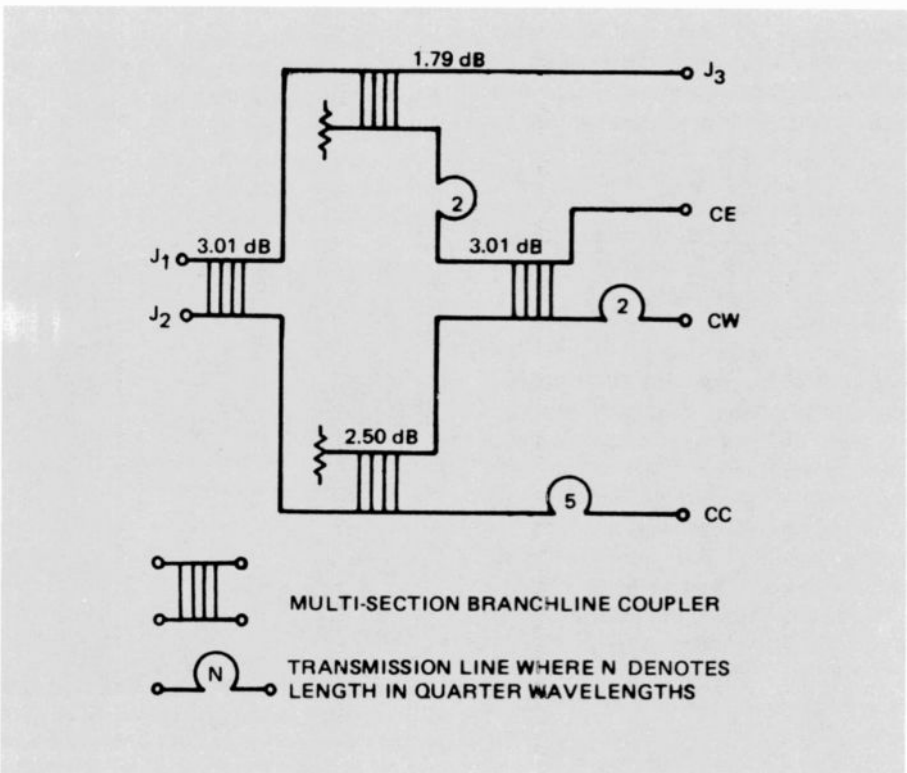

Fig. 9. *A schematic of a 2:4 dual-mode transmit network employing branch-line directional couplers and phase compensation for 3.7- to 4.2-GHz operation.*

Table II. *Dual-mode power and phase distributions.*

Antenna port	Relative power	Relative dual-mode phases	
		J1	J2
1	0.306	+69.8	-69.8
2	0.219	+22.5	-22.4
3	0.306	-24.8	+24.8
4	0.169	-67.5	+67.5

Table III. *PDN performance characteristics.*

Parameter	Value
Coupling tolerance	±0.25 dB
Insertion loss	0.20 dB
Isolation between ports	25 dB
Phase error	±3.0°

Table IV. *PCN performance characteristics.*

Parameter	Value
Coupling tolerance	±0.20 dB
Insertion loss	0.20 dB
Phase error	±2.0°

The RCA anechoic chambers viewed from the outside are shown in Fig. 11. Integration radiation tests in progress on Satcom E are shown on the left, and development tests underway on a breadboard Satcom F antenna are shown on the right. Both antennas are in a clean environment protected by an rf transparent film of 0.002-inch-thick Mylar. Absorbent material, seen on the ground area near the window, is used to suppress ground reflections. The reflector shown between the chambers is used as a reference source to monitor phase and amplitude changes in the received signal that may occur during test.

Measurements made on the antenna ranges are computer-assisted. An HP1000 computer with a dual-disk drive controls antenna positioning, frequency selection, and phase and amplitude data acquisition. Software within the system operates on stored data to produce radiation patterns in several display formats, including the contour representation most commonly used to show satellite-antenna coverage.

Typical test-measurement results are shown in Fig. 12. These patterns are in the contour format wherein lines of constant gain are seen to diminish in level as they spread outward from the coverage area. The map of the United States is shown as viewed from a satellite located over the equator at longitude −143.0 degrees. Antenna boresight is directed at longitude −127.7 degrees and latitude 37.3 degrees.

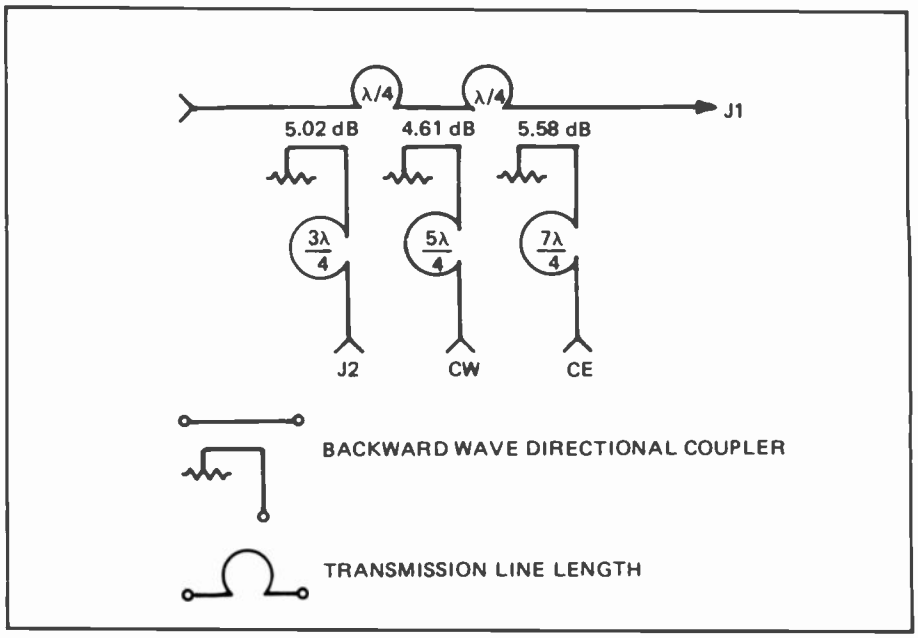

Fig. 10. *A schematic of a 4:1 single-mode receive network employing backward-wave directional couplers and phase compensation for 5.9- to 6.4-GHz operation.*

Customer acceptance of a satellite-antenna system is often based on absolute gain values measured at specified city locations. These are obtained by an interpolation technique that computes gain at any specified angular coordinates within the measured gain data matrix. Other radiation measurements performed to characterize the antenna system are cross-polarization isolation, gain slope, and the level and location of sidelobes.

Conclusion

The multiple-beam offset reflector is the baseline design for the majority of current and proposed satellite-communications-system, shaped-beam antennas. In future applications that use higher frequency bands and larger launch vehicles (that is, space Shuttle, Ariane), larger antenna apertures will be accommodated, and antenna-system requirements will be expanded to incorporate many new features. Reconfigurable shaped-beam antennas are already

Fig. 11. *An internal view of the RCA Astro-Electronics 400-foot range, dual anechoic chambers, showing the Satcom E spacecraft (on the left) and the developmental model Satcom F antenna (on the right) undergoing rf testing. The room, located between the chambers, houses the automatic antenna analyzer and other ancilliary test equipment.*

on the drawing boards. Variable power divider/combiner networks that permit feed-array distributions to be selected or altered in orbit will enable a single antenna design to function over a wide orbital range, eliminating the current approach of multiple antenna designs customized for orbital location.

To avoid prohibitive network losses as feed arrays increase in size and complexity, particularly at higher frequencies, some antennas will be designed with active feed-array elements. These elements will be integrated with solid-state rf amplifiers and employ pre-amplifier variable beam-forming networks, making the antenna system much more tolerant of network losses. Increased antenna directivity at higher frequencies makes multiple, low-sidelobe spot beams available for multiple-frequency reuse through the high beam-to-beam isolation that can be obtained. Sharper component beams also permit smaller, more highly shaped beams to be formed for such usage as time-zone coverage.

The antenna system will continue to be a key element of communications-satellite designs, by providing an ever-increasing number of operational options. The field of communications-satellite antenna design is expanding and presents many technically challenging and interesting problems for antenna design engineers.

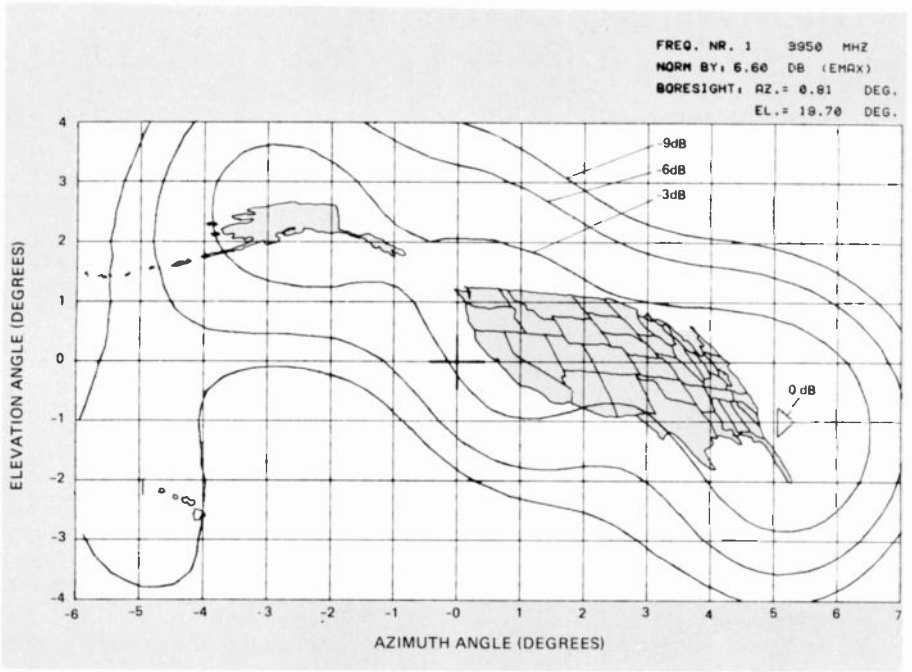

Fig. 12. *An experimentally obtained shaped-beam pattern from the Satcom F breadboard antenna showing relative gain levels. This pattern is similar to that shown in Fig. 4.*

Chuck Profera is the Manager, Antenna Technology, at RCA Astro-Electronics. He is currently supervising the design efforts for the Satcom and Spacenet communications-antenna systems. His group is also undertaking an IR&D project that addresses several configurations of communications antennas. Prior to joining Astro in 1979, he was a Member of Government Systems Division Engineering Staff, which was preceded by 19 years of antenna/microwave design work at RCA Missile and Surface Radar. Dr. Profera received his BS, MS, and PhD from Drexel University.
Contact him at:
RCA Astro-Electronics
Princeton, N.J.
TACNET: 229-3224

Hendrick Soule, Principal Member Technical Staff, received a BS degree from Syracuse University in 1969. He was involved in microwave receiver and signal-processing advanced development before joining RCA Astro-Electronics in 1979. As a member of Astro's Communications Satellite System Group, Mr. Soule has contributed to design and computer modeling of antennas for the Satcom F/G/H series satellites. Recent work includes the study of reconfigurable antenna systems employing active feed elements in offset parabolic and dual-reflector antenna configurations.
Contact him at:
RCA Astro-Electronics
Princeton, N.J.
TACNET: 229-3120

George Rosol, Principal Member Technical Staff, joined the Antenna Technology group of RCA in 1978. His extensive experience in microwave antennas for aerospace applications is being applied to development of communications-satellite antennas at Astro. Mr. Rosol received a BSEE degree from Tri-State University and did graduate work at Ohio State University.
Contact him at:
RCA Astro-Electronics
Princeton, N.J.
TACNET: 229-3228

John Kara, Principal Member Technical Staff, received his BSEE from the University of Pennsylvania. He has been with Astro-Electronics since 1959 and has worked in project engineering, rf system engineering, and antenna-design capacities. In recent years, his responsibilities have included the design and implementation of C-band antenna coupling networks for communications satellites
Contact him at:
RCA Astro-Electronics
Princeton, N.J.
TACNET: 229-3103

Authors (left to right) Soule, Profera, Rosol, and Kara.

E.J. Denlinger

Active and passive microwave components

The development of state-of-the-art active and passive microwave components is essential for RCA's growth in electronics.

Abstract: *The author summarizes recent work at RCA on active and passive microwave components. In the active device area, GaAs FETs and their applications are emphasized. Passive components discussed include power combiners/dividers,* pin *diode switches, phase shifters, mixers, and filters. The author predicts that in coming years, new device and circuit technology for millimeter-wavelength frequencies will be emphasized.*

A state-of-the-art review for microwave active and passive components is a broad subject indeed. Emphasis, here, has been placed on describing briefly the work that has recently been done within RCA. The purpose is to make the RCA engineer fully aware of the extensive microwave capability that exists within this company.

Active devices

Bipolar transistors

The basic principles of operation of bipolar microwave transistors are the same as those of low-frequency bipolar transistors. However, the requirements on dimensions, process control, packaging, heat sinking, and rf circuitry are much more severe. The bipolar transistor competes well against the gallium arsenide field-effect transistor (GaAs FET) only at frequencies below about 5 gigahertz (GHz). Figure 1 lists the typical continuous wave (cw) and pulse performance of these devices.

As oscillators, bipolar transistors have been reported to have lower FM noise than GaAs FETs at low microwave frequencies. Within RCA, they have been used for fast-tuning voltage-controlled oscillators in various microwave systems. Bipolar transistors have been tuned with a hyperabrupt varactor over an octave in the S-band frequency range.

GaAs FETs

A GaAs FET is a majority-carrier device that is finding many system applications because of its superior frequency response and versatility. The cross section of a typical GaAs FET is shown in Fig. 2. An epitaxial *n*-layer is deposited on a semi-insulating GaAs substrate. Ohmic source and drain contacts and a Schottky-barrier gate contact are formed on the *n*-layer. In operation, the gate is biased negative and the drain, positive, with respect to the source. The microwave input signal is applied between gate and source, and modulates the depth of the depletion layer underneath the gate. This modulates the current flowing from source to drain. The amplified signal is taken from a load resistor in the source-drain circuit.

Applications for single-gate GaAs FETs include low-noise and medium-power amplifiers as well as oscillators. The versatile dual-gate FET is being used for mixers, switches, automatic gain control (AGC) amplifiers, limiting amplifiers, phase shifters, and frequency discriminators. In addition, FETs are key elements in miniature monolithic and hybrid circuits and also multigigabit-rate digital integrated circuits. The frequency range of FETs is rapidly expanding into the millimeter-wave region.

Power FETs. The state of the art for commercial and laboratory power FETs is

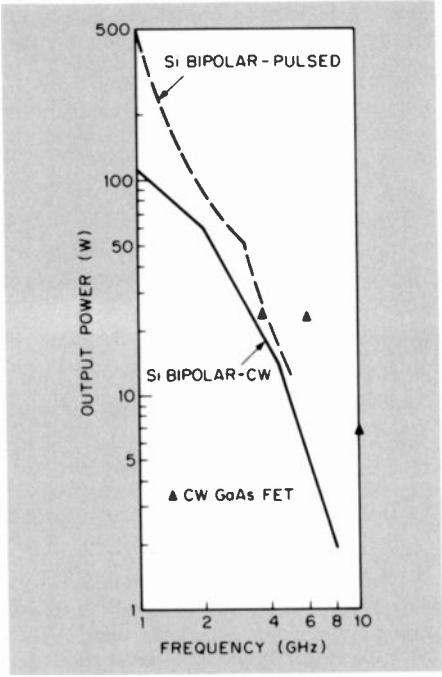

Fig. 1. *CW and pulsed output power versus frequency for bipolar microwave transistors. Some additional data points for GaAs FETs show that the bipolar transistor is a good competitor only at frequencies below about 5 GHz. (Courtesy of S.Y. Narayan).*

© 1982 RCA Corporation
Final manuscript received August 5, 1982
Reprint RE-27-5-9

shown in Fig. 3. FETs that have been demonstrated range from multichip devices that generate 20 to 30 watts (W) at C-band to single chips that generate 100 mW at 26 GHz. RCA has recently made power FETs, with ion-implanted active and contact layers, which produced 100 mW with 3-dB gain at 26 GHz.[1] Efforts have been made to lower the gate resistance by plating the gate metal into a thick T-shaped geometry that also allows gate lengths to be reduced below one micrometer.

Work at RCA[2] has shown that GaAs FETs operate with efficiencies as high as 72 percent at 2.45 GHz with the power output of 1.2 W. Proper shaping of voltage and current waveforms in the device was necessary to achieve these results.

Very small lumped-element amplifiers that use a flip-chip-mounted FET have been demonstrated.[3] This type of lumped-element amplifier has exhibited very broad bandwidth performance. A minimum output power of 0.6 W has been achieved over the 6- to 12-GHz band. Multistage amplifiers giving 1 W over 7- to 12-GHz have been developed using these units. A new miniature circuit using thin-film distributed and lumped circuit elements defined on beryllium oxide (BeO) is presently being developed.[4] Initial results of a 12-GHz lumped-element amplifier, shown in Fig. 4, gave a power-added efficiency of 38 percent at a power output of 135 mW and a gain of 5 dB. Amplifiers designed to provide as much as 1 W at 16 GHz are also being developed using this BeO circuit technology.

By combining multiple FETs in an amplifier circuit chain, RCA has developed and space-qualified an 8.5-W, 55-dB gain amplifier with 33-percent overall efficiency for Satcom application in the 3.7- to 4.2-GHz band.[5]

Besides their use in amplifiers, FETs have also been used for oscillators, frequency discriminators, and active, high-Q tunable filters. FET oscillators can provide higher efficiency than is possible with the normally used transferred-electron oscillators (TEOs). For example, Camisa and Sechi at RCA have demonstrated oscillators with output powers of 390 mW at 8.5 GHz with 22-percent efficiency, and 290 mW at 11.7 GHz with 26-percent efficiency.[6] In addition, varactor-tuned oscillators have been electronically tuned over a 35-percent bandwidth at X-band with efficiencies of about 5 percent. An FET oscillator developed by Sechi for operation at 16 to 16.5 GHz produced 105 mW with an efficiency of 19 percent.[7]

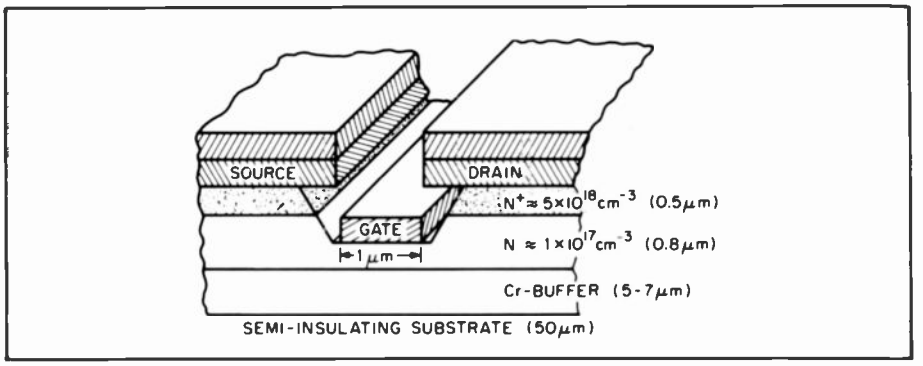

Fig. 2. *A cross section of a power GaAs FET developed at RCA Laboratories. The FET operates by controlling the current flow through a conducting n-doped channel by means of a Schottky-barrier control gate.*

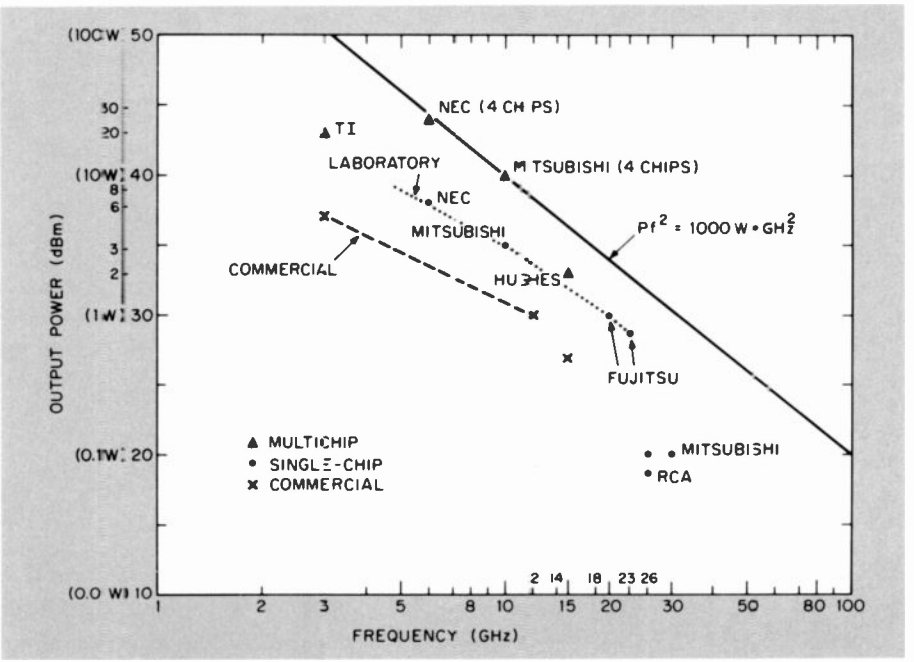

Fig. 3. *Output power versus frequency data for both laboratory and commercial GaAs power FETs. Commercial devices with 0.75 W at 15 GHz are available and experimental devices operating up to 30 GHz have been reported. (Courtesy of S.Y. Narayan)*

Efficiencies of TEOs are typically 1 percent to 2 percent. Furthermore, FET oscillators have been demonstrated by Sechi to have noise outputs that are comparable with typical TEOs.[8] Excess noise in FET oscillators was found to be caused by rf-induced voltage breakdown in the Schottky-barrier gates of the FETs. If the circuit is adjusted to reduce the breakdown gate current to a low value ($\approx$ 90 μA), the AM and FM noise are reduced significantly with only a small sacrifice in power output.

Frequency discriminators consisting of a GaAs FET and a silicon (Si) beam-lead Schottky diode have been demonstrated at RCA for use in an X-band Smart Noise Generator for electronic warfare. The discriminator can cover the range from 7 to 11 GHz, producing dc-output voltages for an rf input of 0.2 mW that range from −200 mV at 7 GHz to +300 mV at 11 GHz.[9] Compared to interferometer-type discriminators, the FET units have much smaller fine-grain variation in their output and provide a significantly larger output-voltage range. High-Q varactor-tuned filters using FETs have been demonstrated at X-band.[10] The negative resistance of an FET is used to compensate for the circuit and varactor losses. This technique results in a filter that is tunable in frequency and whose Q can be adjusted independently. Such a filter is not only extremely small, but offers orders-of-magnitude faster tuning speeds than do comparable yttrium iron garnet (YIG) filters. A tuning range of 2.5 GHz at X-band with a 3-dB bandwidth of 20

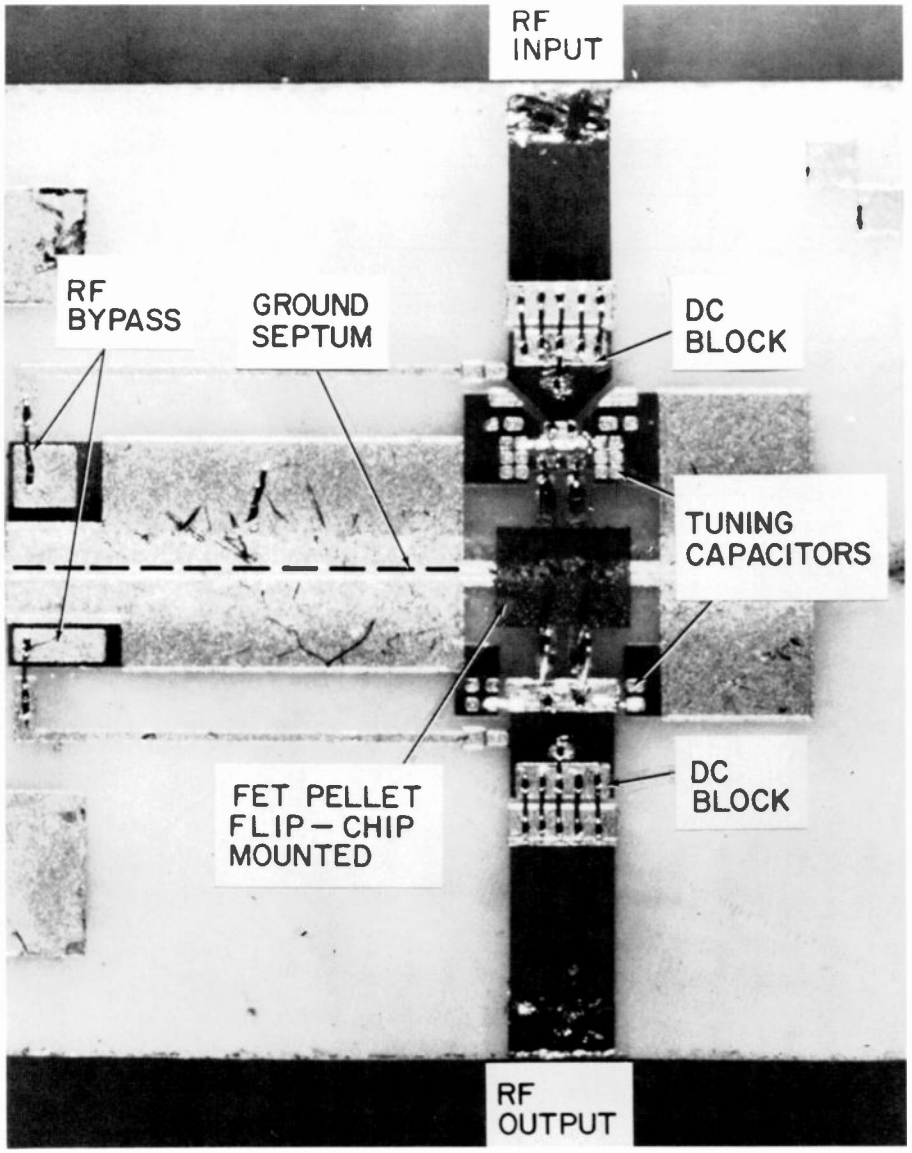

Fig. 4. *Photograph of a lumped-element GaAs FET amplifier operating at 12 GHz. This is a new miniature beryllia circuit (MBC) that uses thin-film distributed and lumped-circuit elements defined on a beryllium oxide substrate. (Courtesy of H. C. Johnson).*

to 40 MHz was achieved with a single-section filter. Two-section and three-section filters have also been built with much sharper skirt selectivity and with mid-band losses of about 0 dB.

Dual-gate FET. By adding a gate to the structure shown in Fig. 2, one can form a new device called a dual-gate FET. These versatile devices are used in a great variety of ways, including mixers, switches, AGC amplifiers, limiters, and discriminators. As variable-gain amplifiers, the rf input is applied to the first gate, and the dc control voltage to the second gate. Figure 5 shows gain versus frequency as a function of dc-bias voltage on the second gate of a two-stage dual-gate FET amplifier. Note that the gain can be continuously varied from +20 dBm to −40 dBm by varying the voltage on the second gate from +1 V to −2 V. Dual-gate FET amplifiers saturate "hard" and are, therefore, useful as limiting amplifiers.[11] Another application lies in the use of dual-gate FET amplifiers to form wide-band continuous phase shifters. A 4- to 8-GHz 360° phase shifter[12] and a Ku-band unit using a different design[13] have been developed. Both designs offer continuous phase/amplitude control and would be suitable for a variety of adaptive phased-array applications, where the presently used hand-trimming to obtain given gain and phase shift can be replaced with computer-controlled adjustments of phase shifters using dual-gate FETs.

Low-noise FET. To obtain an FET with a low-noise figure, the gate length, the source-parasitic resistance, and the gate-metal resistance must be reduced. The best published data are shown in Fig. 6. The noise figure of Si bipolar transistors is also shown to illustrate the superior performance of GaAs FETs at high frequencies. Various low-noise FET amplifiers have been built within RCA for radars and satellite communications. One example is a two-stage amplifier operating over the 7.25- to 7.75-GHz band that showed a noise figure of 2.1 dB with a gain of 16.5 dB. When the amplifier was Peltier-cooled to a temperature of −23°C, the noise figure was reduced to 1.8 dB.[14]

Other FET devices. Current research at RCA and other laboratories includes investigation of other III-V compounds, such as $Ga_{0.47}In_{0.53}As$, that have electrical properties superior to those of GaAs; also, new devices such as metal-insulator semiconductor FETs (MISFETs) and permeable-based transistors are being investigated. The $Ga_{0.47}In_{0.53}As$ crystal lattice, matched to an InP substrate, has the potential advantages of higher low-field electron mobility and peak electron-drift velocity over GaAs. With this material, RCA is developing MISFETs.[15] Potential advantages are: operation at zero gate bias, simplifying the bias circuitry and leading to improved linearity; lower noise figures because of the higher electron mobility; and the possibility of inversion-mode, enhancement devices that may provide simpler, lower-power gigabit-rate logic circuits. Ternary MISFET devices with gate lengths of 3 μm have been fabricated and have demonstrated 4 dB of gain at 6 GHz with power-added efficiency of 20 percent at 50 mW power output. A cross section of the device is shown in Fig. 7.

Transferred-electron devices

Transferred-electron devices (TEDs) are two-terminal devices that exhibit a negative resistance (and negative differential mobility) caused by the transfer of electrons from high- to low-mobility energy bands. They are easier to use for an oscillator rather than for an amplifier. For the latter, a circulator or quadrature 3-dB hybrid must be used to separate input and output signals. TEDs are structurally simple semiconductor devices made of either GaAs or InP. They consist of a bar of transferred electron material with ohmic contacts to form the anode and cathode. The anode is biased positive with respect to the cathode

at a magnitude larger than a threshold voltage where the differential mobility becomes negative.

The cw power outputs that can be obtained from TEDs range from 600 mW at 10 GHz to 20 mW at 100 GHz. Conversion efficiencies are only a few percent. The AM noise from transferred-electron oscillators (TEOs) is significantly lower than that from impact-avalanche and transit-time (IMPATT) diodes and, therefore, TEOs are very useful for receiver local oscillator applications. Noise figures of transferred-electron amplifiers range from 10 to 20 dB. Pulsed power outputs range from 50 W at 10 GHz to about 5 W at 40 GHz.

Within RCA, TEOs have been used for many system applications—mostly for receiver local oscillators and highly stable power sources for radars operating in the 8- to 18-GHz frequency range. Power outputs from both mechanically-tuned and varactor-tuned waveguide-cavity oscillators are typically 20 to 100 mW with efficiencies of about 1 percent to 2 percent. Included among the systems built at RCA that incorporated TEDs are a 9.4-GHz solid-state weather radar, a 17.5-GHz radar-controlled collision mitigation system for a research safety vehicle, an oscillator for a satellite ground terminal, a locomotive-speed sensor, and a microwave stockline-measuring system for a steel company's blast furnace.

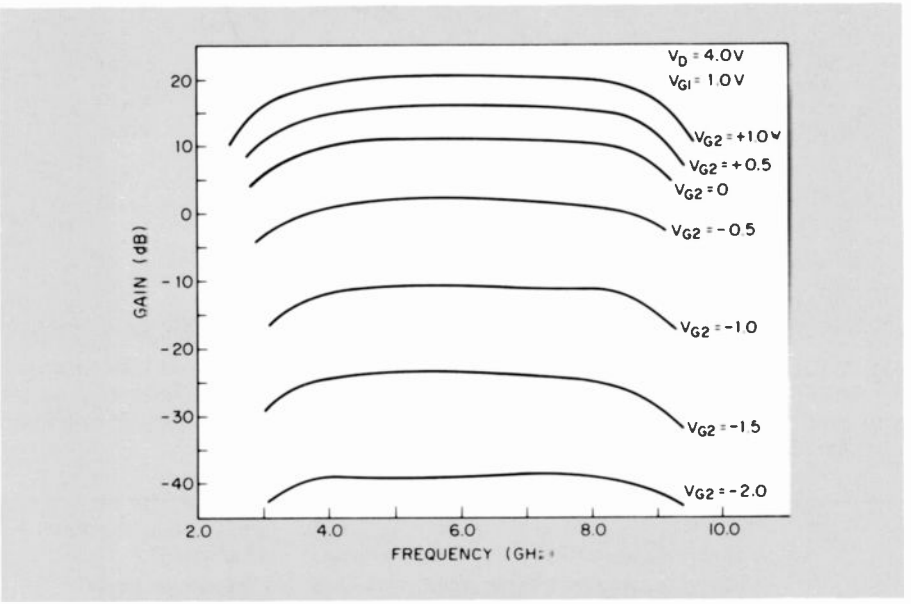

Fig. 5. *Gain versus second gate bias voltage of a 4- to 8-GHz, dual-gate GaAs FET amplifier. Note that the gain can be continually varied over a 60-dB dynamic range by varying the second gate voltage from +1 to -2V.*

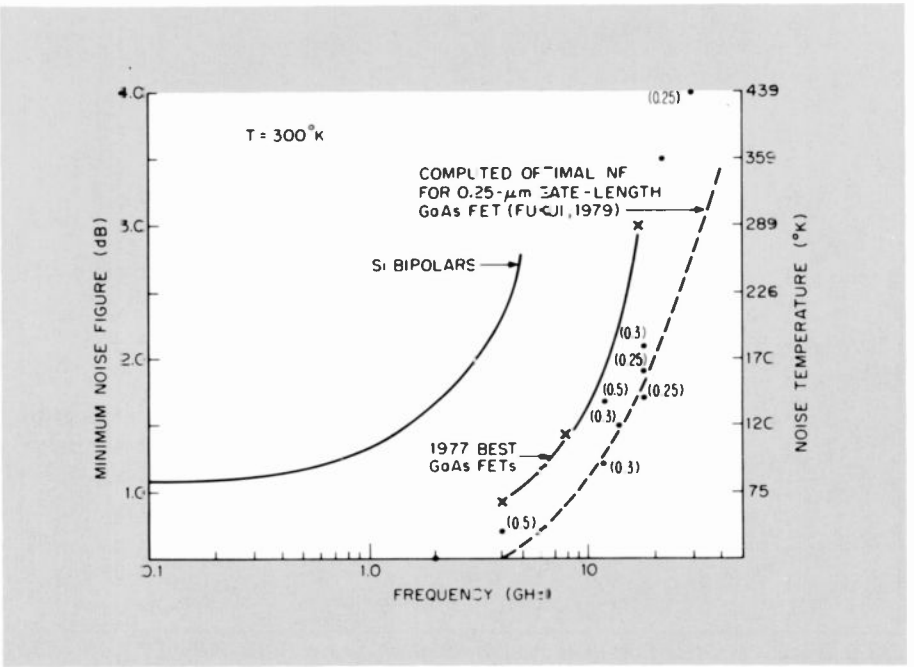

Fig. 6. *State-of-the-art noise-figure versus frequency of GaAs FET. The noise figure of Si bipolar transistors is also shown to illustrate the significantly superior performance of GaAs FETs. Up to 18 GHz, the experimental GaAs FET data falls close to a theoretical curve computed by Fukui in 1979. (Courtesy of S.Y. Narayan).*

Avalanche diode

Avalanche diodes are two-terminal, junction devices that produce a negative resistance by appropriately combining impact-avalanche-breakdown and charge-carrier transit-time effects. Avalanche breakdown occurs in the most comonly used materials of silicon and gallium arsenide when the electric field becomes high enough to cause the charge carriers to create electron-hole pairs by impact ionization. Transit-time effects occur if the time the charge carriers spend traversing the diode becomes an appreciable fraction of an rf period. Two important classes of avalanche diodes are IMPATT diodes and trapped-plasma avalanche-triggered-transit diodes (TRAPATT). For IMPATTS, the transit angle of the carriers traversing the diode is approximately 180°, whereas, for the TRAPATT, this angle is much smaller than 180°.

Like the TED, the avalanche diode can be used as an oscillator or, in combination with a circulator or a 3 dB quadrature hybrid, as an amplifier or injection-locked oscillator. CW power levels range from about 10 W at 10 GHz to 70 mW at 200 GHz. The pulsed devices produce power levels ranging from 50 W at 10 GHz to 1.5 W at 200 GHz. In the past, RCA has spent a considerable effort in research and development on millimeter-wave IMPATTS operating from 26 to 60 GHz, X-band GaAs Read IMPATTS, and TRAPATT diodes operating from L-band to X-band. The powers and efficiencies achieved with the complementary, *p*-type, single-drift IMPATTs having all-epitaxial layers of silicon are still state-of-the-art performances in the millimeter-wave band. For example, at 26 to 40 GHz, power levels of 500 to 700 mW with efficiencies of nearly 10 percent were achieved in waveguide radial-disc-cavity circuits.[16] At 50 to 60 GHz, double-drift IMPATTS produced 400 mW

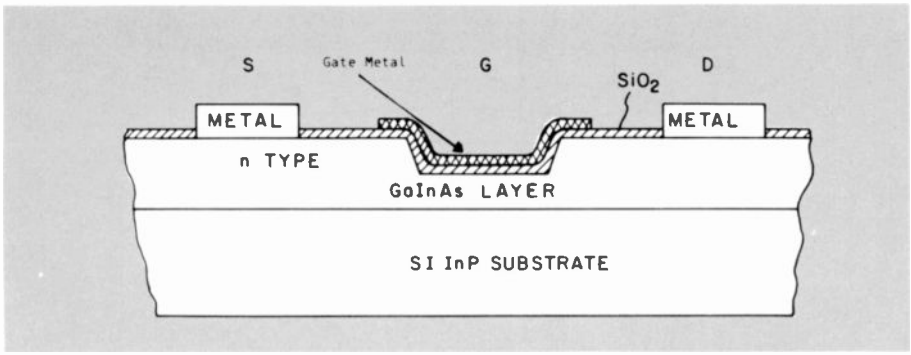

Fig. 7. *Cross section of a ternary metal-insulator-semiconductor field-effect-transistor (MISFET) device. The potential advantages over conventional GaAs devices are improved linearity, lower noise figure, and simpler, lower-power gigabit-rate logic circuits. (Courtesy of P.D. Gardner).*

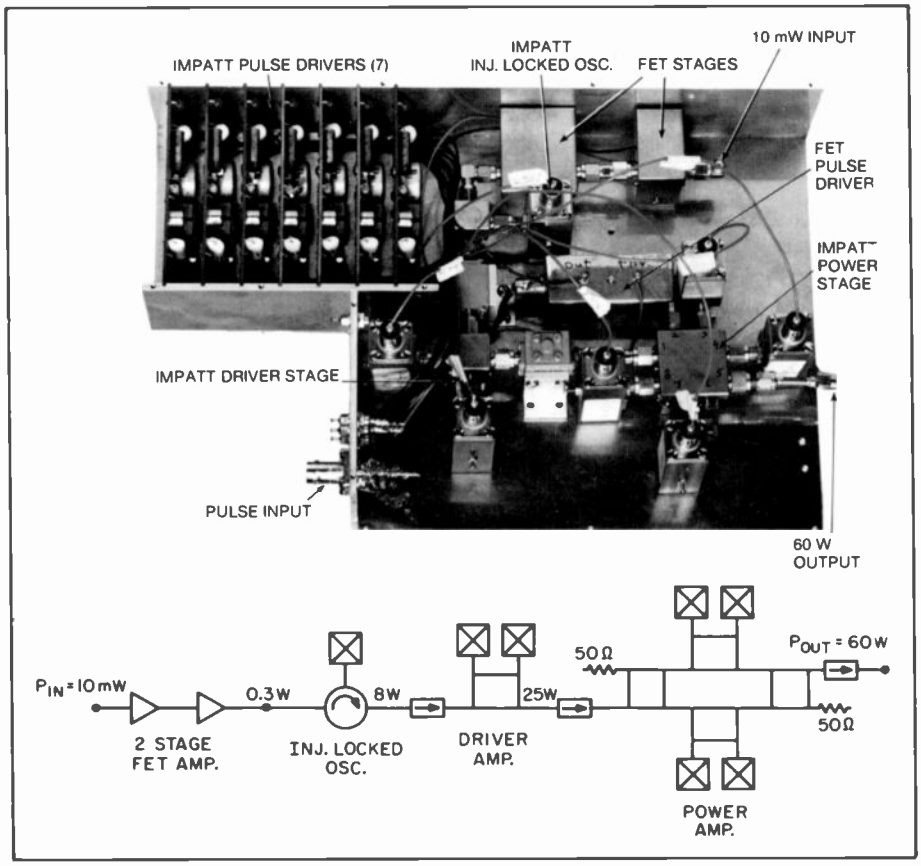

Fig. 8. *A 60-W, 9.4-GHz pulsed power amplifier using GaAs IMPATT diodes. This amplifier was developed at RCA Laboratories for a solid-state, airborne weather radar that equalled the performance of standard kilowatt-level magnetron radars.*

with an 8-percent efficiency.[17] With the TRAPATT diodes, harmonic extraction was commonly used and made possible peak power levels ranging from a few hundred watts at L-band (1 to 2 GHz) to a few tens of watts at X-band (8 to 12 GHz). More recently, pulsed GaAs IMPATT diodes made by Varian Associates were used in a 60-W amplifier chain for a 9.4-GHz solid-state transmit-receive module. This module was developed for the first solid-state airborne weather radar that equalled the performance of standard magnetron-powered radars. A picture of the amplifier is shown in Fig. 8.

Passive components

Pin *diodes*

Junction diodes in which a heavily doped p^+ layer and a heavily-doped n^+ layer are separated by a high-resistivity intrinsic *(i)* layer are called *pin* diodes. These diodes are widely used in microwave switches, phase shifters, electronically variable attenuators, and limiters. When the diode is reverse-biased, the intrinsic region is depleted of mobile charge, so that the diode approximates a low-loss capacitor. Under forward bias, the p^+ and n^+ regions inject holes and electrons into the intrinsic region, thereby forming highly conductive plasma so that the diode then becomes a small series resistor. The intrinsic region's thickness strongly influences the diode's forward resistance, the diode Q, the diode's thermal properties, and the breakdown voltage.

Pin diodes have been developed within RCA for both low-power switching applications and for high-power switches and phase shifters. All-epitaxially-grown structures were developed for low-power switches operating at UHF and at X-band.[18] With 1-pF diodes at UHF frequencies, an rf-measured series resistance of less than 0.2 Ω was achieved at 10-mA forward-bias current. At 8 GHz, a single-pole, double-throw (SPDT) switch with an insertion loss of about 0.2 dB and an isolation of 53 dB was developed with these all-epitaxial diodes. The key factors to the diode's excellent performance are the extremely thin, highly doped contact layers and the Au-Cr-Pd_2Si metal contact layers that gave a very low contact resistance.

High-power *pin* diodes have been developed for antenna-interface switching at very low frequencies (2 to 30 MHz) and for phase shifters at S-band frequencies.[19] The low-frequency application requires thick intrinsic-layer diodes having very long lifetimes (20 to 30 μs) in order to meet severe distortion specifications (harmonics −60 dB below fundamental). Stacks of diodes were formed in a batch-fabrication procedure to achieve breakdown voltages of several thousand volts. For S-band phase-shifter applications, diodes have been demonstrated to operate at pulse peak-power levels as high as 7 kW and at pulse widths of 50 μs. Breakdown voltages exceeded 1700 V and the forward resistance at 50 mA was 0.3 Ω.

An example of a *pin*-diode phase-shifter circuit developed at RCA Moorestown that used the diodes described above is shown in Fig. 9. It contains three hybrid-coupled bits, each of which uses a diode pair to terminate a branch-line quadrature hybrid junction. Impedance transformers between the diode and the hybrid junction help produce the correct differential phase shift for each bit. The circuit pattern and blocking capacitors are formed on the 40-mil-thick alumina substrate by the use of thick-film screening methods. The phase-shifter circuit handles 3.5 kW of peak power, has

an insertion loss of 1.25 dB, and has a 12° rms differential phase-shift error over the 12-percent operating bandwidth. In comparison, a 4-bit ferrite phase shifter has a loss of 0.7 dB and handles about 5 kW of peak power but has greater size and weight than has the diode phase shifter.

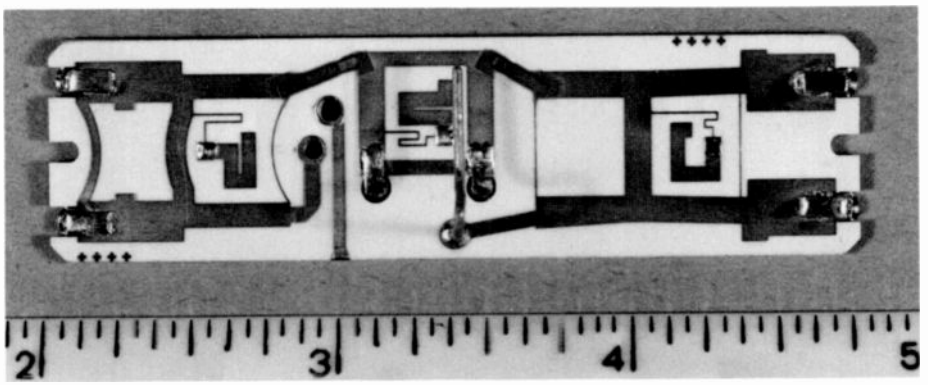

Fig. 9. *A three-bit* pin *diode phase shifter for a phased-array radar. The S-band unit handles 3.5 kW of peak power, has an insertion loss of 1.25 dB, and has a 12° rms differential phase-shift error over the 12-percent operating bandwidth. (Courtesy of M.E. Breese).*

Varactor diodes

A varactor diode is a *p-n* junction diode that is specifically designed for applications that make use of the voltage dependence of the diode depletion-layer capacitance. The voltage-dependent junction capacitance C_j is given by

$$C_j = K(\phi - V_j)^{-n}$$

where K is a constant, ϕ is the contact potential, V_j is the voltage across the junction, and n is a coefficient whose value depends on the doping profile ($n = 1/3$ for a graded junction, $n = 1/2$ for an abrupt junction, and $n = 1$ for a hyperabrupt junction).

Varactors are usually fabricated from either silicon or gallium arsenide. They are widely used as tuning elements in voltage-controlled filters and oscillators, in harmonic generators, and in parametric amplifiers and frequency converters. The performance of a varactor is characterized by the Q factor, the usable capacitance tuning ratio, and the maximum rf handling capability. An important figure of merit is the cutoff frequency, which is defined by

$$f_c = \frac{1}{2\pi R_s C_j}$$

where R_s is the series resistance of the diode. Diodes with cutoff frequencies of many hundreds of GHz are commercially available.

At RCA, development work has been done on both GaAs hyperabrupt varactors and high-Q silicon varactors. The GaAs devices were developed for TV-tuner applications and for voltage-controlled oscillators operating up to 18 GHz. Recently, a new method of fabricating high-Q and high-voltage silicon diodes was developed.[20] The process uses ion implantation and laser annealing for forming heavily-doped p^{++} and n^{++} layers and epitaxial growth for the low impurity concentrations. The techique provides good yield and repeatability, and it has allowed fabrication of diodes that have breakdown voltages of 120 V and a Q of 600 at −8 V bias and 50-MHz frequency.

Schottky-barrier diodes

Schottky-barrier diodes are majority-carrier rectifiers that are used as the nonlinear element in frequency converters and detectors. The rectifying junction is formed at the interface or slope of a deposited metal layer and a semiconductor crystal, usually silicon or gallium arsenide. Important figures of merit for a diode are the *n*-factor in the *I-V* forward-bias characteristic and the cutoff frequency taken at zero bias.

Several years ago, high-performance GaAs mixer diodes having an excellent diode *n*-factor (<1.1) and a zero bias cutoff frequency of >700 GHz were developed at RCA.[21] These diodes had large plated-gold bumps supported by polyimide to make contact to a small cross-shaped Schottky-junction area with extremely low parasitic capacitance and inductance. The diode was used in a single-ended image and sum-enhanced microstrip mixer operating with an rf of 12 GHz and an intermediate frequency (IF) of 500 MHz. The conversion loss of the mixer was only 2.4 dB with 4 mW of local oscillator (LO) power applied to the diode.

Another example of mixer work at RCA was an image-reject mixer operating with an rf of 9.35 GHz and an IF of 3 MHz.[22] The microstrip mixer consisted of two balanced mixers, a quadrature hybrid to introduce a 90° phase shift between the LO ports, a Wilkinson hybrid to apply the signal equally (in-phase) to the two mixers, and an IF quadrature hybrid for combining the mixer outputs. Beam-lead diodes were mounted on a thin-film microstrip circuit on a 15-mil-thick alumina substrate. The final performance characteristics were: a conversion loss of 7 dB, rf-LO isolation of 22 dB, VSWR < 2:1, an image rejection of 22 dB, and LO power of 13 mW.

Ferrite phase shifters

An alternative to the diode phase shifter discussed previously is the ferrite phase shifter, which has been widely used for large, high-power phased-array radars. Its operation is based on the nonreciprocal properties of a garnet material that is in the form of a toroid and magnetized by drive current in a latch wire through its center. The toroid is loaded with high-dielectric-constant inserts and housed in a waveguide. A picture of a 7-bit garnet phase shifter developed at RCA Moorestown is shown in Fig. 10. It has a coaxial input consisting of an electric probe inserted through a slot in the garnet toroid wall. At the waveguide output, spring fingers contact the inside surfaces of an open-ended waveguide radiator. The unit handles 5 kW of peak power, has an insertion loss of 1.1 dB, and the differential phase shift is accurate to within 3° rms over a 12-percent bandwidth at S-band.

Circulators

Like ferrite phase shifters, circulators also depend on the nonreciprocal properties of magnetized ferrite material. The most common Y-junction circulators allow signals to rotate clockwise (or counterclockwise depending on the dc magnetic-field polarity) to an adjacent port with the third port, which is isolated. In the stripline or the microstrip version, the junction of the three lines consists of a metallized ferrite disk that is magnetized perpendicular to the broad face. The spacing between the center strip and the ground plane as well as the internal properties of the ferrite material (saturation magnetization, linewidth) are major factors affecting the insertion loss and power-handling capability of the device. For many microstrip circuit applications within RCA, drop-in types of microstrip circulators and isolators (one-port terminated in 50 Ω) are commercially available

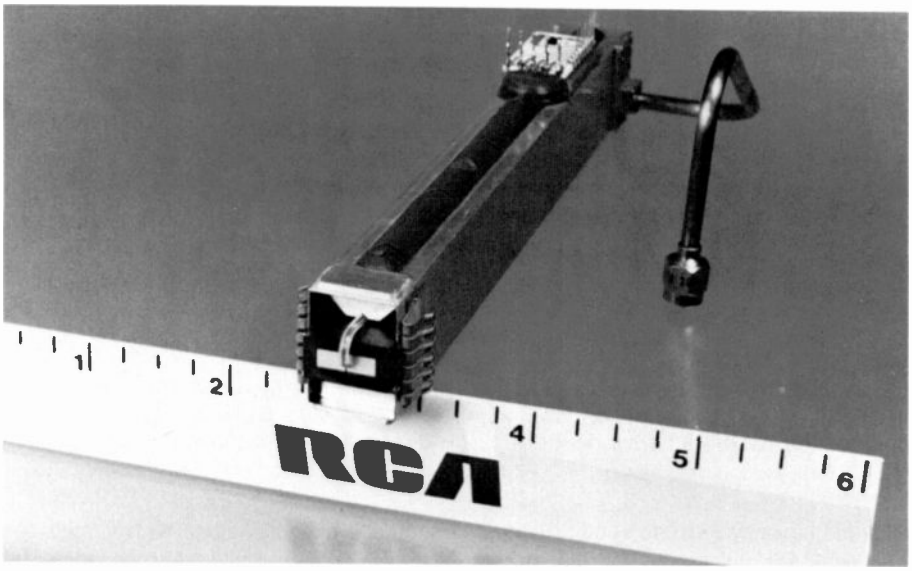

Fig. 10. *A seven-bit garnet phase shifter for a phased-array radar. The unit handles 5 kW of peak power, has an insertion loss of 1.1 dB, and has a 3° rms differential phase shift error over a 12-percent bandwidth at S-band. (Courtesy of M.E. Breese).*

for operation to frequencies as high as 18 GHz with typical insertion losses of 0.5 dB, isolation of 20 dB, and voltage standing-wave ratios (VSWRs) of <1.3.

The waveguide version has a vertically magnetized ferrite rod at the junction of three waveguides. A design procedure, for millimeter-wave circulators consisting of a partial-height ferrite post, was developed at RCA.[23] Circulators at 38 GHz with 16 percent, 20-dB isolation bandwidth and 0.25-dB insertion loss were demonstrated by use of this design technique. Also, circulators at 60 GHz with 5-percent bandwidth and 0.3-dB loss were built.

Filters

Bandpass, bandstop, low-pass, and high-pass filters can be realized in many forms, including lumped element, distributed-transmission line, and waveguide. Within RCA, the most common forms are lumped-element and distributed-line (usually microstrip or stripline) filters. The latter uses open and/or short-circuited stubs, straight-line or ring resonators, parallel-coupled lines, high-impedance/low-impedance combinations of transmission line, and so on. Recent additions to the microwave filter family are surface acoustical wave (SAW) filters and dielectric resonator filters. SAW filters have excellent skirt selectivity but are useful only below about 1 GHz. They are widely used today in the IF section of TV receivers and are starting to be used for oscillators, frequency synthesizers, and channelized receivers. Dielectric resonator filters are becoming widely used at frequencies ranging from 1 GHz to the millimeter-wave bands. Recently, high-dielectric-constant material with unloaded Qs of 6000 and frequency-temperature coefficients near 0 parts per million (ppm) per degree Celsius have become available from commercial sources. These dielectric resonators, which are either cylindrical or rectangular, can be placed near microstrip transmission lines to frequency-stabilize solid-state sources or to make extremely narrow bandstop or bandpass filters.

Power combiners/dividers

The most popular combiners/dividers formed on microstrip or stripline include the branch-line hybrid, rat-race hybrid, Wilkinson hybrid, broadside coupler, and interdigitated coupler. An example of using the first three forms all in one microstrip circuit is the image-reject mixer that was discussed in the section on Schottky-barrier diodes. The branch-line hybrid, the broadside coupler, and the interdigitated coupler produce a 90° phase shift between the coupled ports, while the Wilkinson hybrid's coupled ports are in-phase and the rat-race hybrid's coupled ports are 180° out of phase. As mentioned previously in the section on IMPATT diodes, branch-line hybrids have been used for combining high-power two-terminal solid-state devices for radar applications at RCA. For combining the power from multiple FETs, the most popular combiner is the interdigitated coupler. With this coupler at frequencies less than 4 GHz, Presser[24] has shown they can be reproducibly fabricated (to within ±0.2 dB) with coupling between 2 and 7 dB. Isolation greater than 25 dB over an octave bandwidth with insertion losses of <0.35 dB could be obtained. Coupling split can be ±0.3 dB over one octave. At higher frequencies (13 to 17 GHz), Klatskin [25] built four-line and six-line couplers on quartz that had losses at the two coupled ports of 3.5 dB and isolation at the fourth port of >15 dB. Monolithic GaAs interdigitated couplers with impedances of 50 and 25 ohms have been developed for the 4- to 8-GHz frequency band.[26] Losses for the four-line, 50-ohm coupler were 0.5 dB with isolation greater than 18 dB. A six-line, 25-ohm coupler produced losses of only 0.3 dB with isolation better than 17 dB over the 4- to 8-GHz band.

Conclusions

The advance in the state of the art of microwave components within RCA is extremely important for effective support of key RCA electronic divisions. During the next few years, new device and circuit technology for frequencies approaching the millimeter-wave region will be emphasized. Monolithic and miniature hybrid technology will have a great impact on the design options available to system engineers.

References

1. Taylor, G.C., Yun, Y.H., Liu, S.G., Jolly, S.T., and Bechtle, D., "GaAs Power Field-Effect Transistors for K-Band Operation," *RCA Review*, Vol. 42, No. 4, pp. 508-521 (December 1981).
2. Sechi, F.N., "High Efficiency Microwave FET Power Amplifiers," *Microwave Journal*, pp. 59-64 (November 1981).
3. Camisa, R.L., Klatskin, J.B., and Mickelsons, A., "Lumped-Element GaAs FET Power Amplifiers," *RCA Review*, Vol. 42, No. 4, pp. 557-575 (December 1981).
4. Sechi, F.N., Brown, R., Johnson, H., Belohoubek, E., Mykietyn, E., and Oz, M., "Miniature Beryllia Circuits—A New Technology for Microwave Power Amplifiers," *RCA Review*, Vol. 43, No. 2, pp. 363-374 (June 1981).
5. Dornan, B., Slusark, W., Wu, Y.S., Pelka, P., Barton, R., Wolkstein, H., and Huang, H., "A 4 GHz GaAs FET Power Amplifier: An Advanced Transmitter for Satellite Down-Link Communication Systems," *RCA Review*, Vol. 41, No. 3, pp. 472-503 (September 1980).
6. Camisa, R. and Sechi, F.N., "Common-Drain Flip-Chip GaAs FET Oscillators," *IEEE Trans. on Microwave Theory and Techniques*, Vol. MTT-27, No. 5, pp. 391-394 (May 1979).
7. Sechi, F.N. and Brown, J.E., "Ku-Band FET Oscillator," *IEEE ISSCC Digest*, pp. 124-125 (February 1980).
8. Sechi, F.N., Johnson H., Brown, J., and Marx, R., "Solid-State Ku-Band Radar," *RCA Review*, Vol. 42, No. 4, pp. 672-690 (December 1981).

9. Rosen, A., Mawhinney, D., and Napoli, L.S., "A Novel FET Frequency Discriminator, *RCA Review*, Vol. 38, No. 2, pp. 238-252 (June 1977).

10. Presser, A., "Varactor-Tunable, High-Q Microwave Filter," *RCA Review*, Vol. 42, No. 4, pp. 691-705 (December 1981).

11. Rosen, A., Wolkstein, H.J., Goel, J., and Matarese, R.J., "A Dual-Gate GaAs FET RF Power Limiter," *RCA Review*, Vol. 38, No. 2, pp. 253-256 (June 1977).

12. Kumar, M., "Dual-Gate FET Phase Shifter," *RCA Review*, Vol. 42, No. 4, pp. 596-616 (December 1981).

13. Johnson, H. and Gazit, Y., "A Ku-Band Continuously Variable Phase/Amplitude Control Module," *RCA Review*, Vol. 42, No. 4, pp. 617-632 (December 1981).

14. Askew, R. and Wolkstein, H.J., "A Low-Noise, Peltier-Cooled FET Amplifier," *RCA Review*, Vol. 42, No. 4, pp. 661-671 (December 1981).

15. Gardner, P.D., Narayan, S.Y., Colvin, S., and Yun, Y., "$Ga_{0.47}In_{0.53}As$ Metal Insulator Field-Effect Transistors (MISFETs) for Microwave Frequency Applications," *RCA Review*, Vol. 42, No. 4, pp. 541-556 (December 1981).

16. Swartz, G.A., Chiang, Y.S., Wen, C.P., and Gonzalez, A., "Performance of P-Type Epitaxial Silicon Millimeter-Wave IMPATT Diodes," *IEEE Trans. Electron Devices*, Vol. ED-21, pp. 165-171 (February 1974).

17. Wen, C.P., Chiang, Y.S., and Denlinger, E.J., "Multi-Layer Epitaxial Grown Silicon IMPATT Diodes at Millimeter-Wave Frequencies," *Journal of Electronic Materials*, Vol. 4, pp. 119-129 (February 1975).

18. Chiang, Y.S. and Denlinger, E.J., "Low-Resistance All-Epitaxial *Pin* Diodes for Ultra-High-Frequency Applications," *RCA Review*, Vol. 38, No. 3, pp. 390-405 (September 1977).

19. Rosen, A., Martinelli, R., Schwarzmann, A., Brucker, G., and Swartz, G.A., "High-Power Low-Loss *Pin* Diodes for Phased-Array Radar," *RCA Review*, Vol. 40, No. 1, pp. 22-58 (March 1979).

20. Rosen, A., Wu, C.P., Caulton, M., Gombar, A., and Stabile, P., "Method of Fabricating High-Q Silicon Varactor Diodes," *Electronics Letters*, Vol. 17, No. 19, pp. 706-708 (September 17, 1981).

21. Denlinger, E.J., Liu, S.G., Veloric, H., Duigon, F., and Lawson, V., "High Performance Mixer Diode," *Int'l Electron Device Meeting Digest*, pp. 87-89 (1976).

22. Communication with J. Rosen, RCA Laboratories.

23. Denlinger, E.J., "Design of Partial Height Ferrite Waveguide Circulators," *IEEE Trans. on Microwave Theory and Techniques*, pp. 810-813 (August 1974).

24. Presser, A., "Interdigitated Microstrip Coupler Design," *IEEE Trans. on Microwave Theory and Techniques*, Vol. MTT-26, No. 10, pp. 801-805 (October 1978).

25. Communication with J. Klatskin, RCA Laboratories.

26. Kumar, M., Subbarao, S., Menna, R., and Huang, H., "Monolithic GaAs Interdigitated 90° Hybrids with 50- and 25-ohm Impedances," 1982 IEEE Microwave and Millimeter-Wave Monolithic Circuits Symposium, Dallas, Texas.

Edgar Denlinger received the B.S. in Engineering Science from Penn State University in 1961, and the M.S. and Ph.D. degrees in Electrical Engineering from the University of Pennsylvania in 1964 and 1969, respectively. He joined RCA Applied Research in Camden, New Jersey, in 1961 and researched solid-state masers, superconducting magnets, and transistors. From 1965 to 1967, he had a research assistantship at the University of Pennsylvania where he did research on bulk-effect oscillators. In 1967, he joined MIT Lincoln Laboratory and worked on microwave integrated circuits for phased-array radars and air-traffic-control systems.

Since joining RCA Laboratories in 1973 as a Member of Technical Staff, he has been engaged in research on various microwave solid-state devices, microwave integrated circuits, low-noise receivers, and IMPATT amplifiers. In 1979, he received an RCA Laboratory Achievement Award for development of a solid-state airborne weather radar. He holds five patents and has authored 30 technical publications.

Contact him at:
RCA Laboratories
Princeton, N.J.
TACNET: 226-2481

H.C. Huang | L.C. Upadhyayula | M. Kumar

A review of GaAs microwave monolithic integrated circuits

GaAs MMICs could be making and receiving the waves of the future in high-volume applications. Direct Broadcast Satellite markets may be the key.

Abstract: *Development of GaAs microwave monolithic integrated circuits is moving forward. Both enhancement- and depletion-mode devices are considered and compared for GaAs MESFET logic circuits. The advantages and disadvantages of these two logic families are described. Applications in analog and digital circuits are given. RCA's and the industry's results are reported.*

Since the first report of the GaAs microwave monolithic integrated circuit (MMIC), almost all the major microwave companies have been carrying out development efforts in MMICs. There are two major categories of MMIC—the digital MMICs and the analog MMICs. The digital MMICs are aimed at signal-processing functions in devices such as the static binary divider, A/D converter and multiplexer. The analog or linear MMICs are used for transmitter or receiver applications. Although most of the technology is the same for the analog and digital circuits, the material requirements are similar but not the same for both. Device geometries, packing densities and thermal considerations are also different. This paper will review the state-of-the-art performance of both the digital and the analog MMICs.

Why GaAs for MMICs?

Analog circuits

Although two-terminal devices such as IMPATT diodes and mixer diodes have demonstrated high-frequency operation up to 200 gigahertz (GHz), a three-terminal device is in general preferable for amplifier applications.

Silicon bipolar devices are available for the lower spectrum of the microwave frequencies. The cutoff frequency of microwave semiconductor devices is inversely proportional to the product of the electron and hole mobilities. The carrier mobilities in silicon (Si), however, limit the three-terminal bipolar transistor performance to about 10 GHz. Other materials with higher carrier mobilities are more suitable for microwave devices for higher frequency operation. The electron mobilities in GaAs are five to six times higher than in Si. However, the hole mobilities in GaAs are very low. Therefore, only unipolar device operation is feasible with GaAs for higher frequencies. GaAs MESFETs (metal-semiconductor field-effect transistors) exhibited gain at microwave frequencies as high as 40 GHz. Low-noise figures were achieved using GaAs FETs. It has also been established that semi-insulating substrates are suitable for microwave integrated circuits up to 60 GHz. Therefore, GaAs FETs are almost universally used as the active elements in today's MMICs. They are versatile devices that can provide excellent performance in a variety of microwave analog systems.

Digital circuits

During the past two decades, silicon devices (TTL, ECL, MOS, and so on) have been the mainstay of digital integrated circuits. For most of the commercial applications, circuit speed is not a major consideration. But some communications and military systems require very-high-speed devices. Recently, a very-high-speed integrated-circuit (VHSIC) program was initiated in Si for military applications. The speed improvement is expected to result from the submicron geometries for the devices. Fabrication of submicron geometry devices requires sophisticated and expensive technology (X-ray or electron-beam lithography). Consequently, the argument that Si ICs are cheap may not be valid in this case. In view of this, other semiconductor materials with superior electronic properties should also be considered to achieve the high-speed performance of the digital ICs. Because of the advances made in materials as well as device technology, GaAs FETs are ideal for such applications. GaAs is superior to Si because of the following electronic properties: its high electron mobility at low electric fields results in small series resistances and a high average carrier velocity; velocity saturation occurs at relatively small electric fields and results in lower operating biases; the excellent semi-insulating property of the substrate results in low interconnect line losses; and the short lifetimes of excited carriers results in better radiation hardness.

During the past ten years, remarkable progress has been made in GaAs device technology. The GaAs MESFET emerged as a work horse. Digital MSI/LSI logic circuits with GaAs MESFETs

©1982 RCA Corporation
Final manuscript received August 18, 1982.
Reprint RE-27-5-10

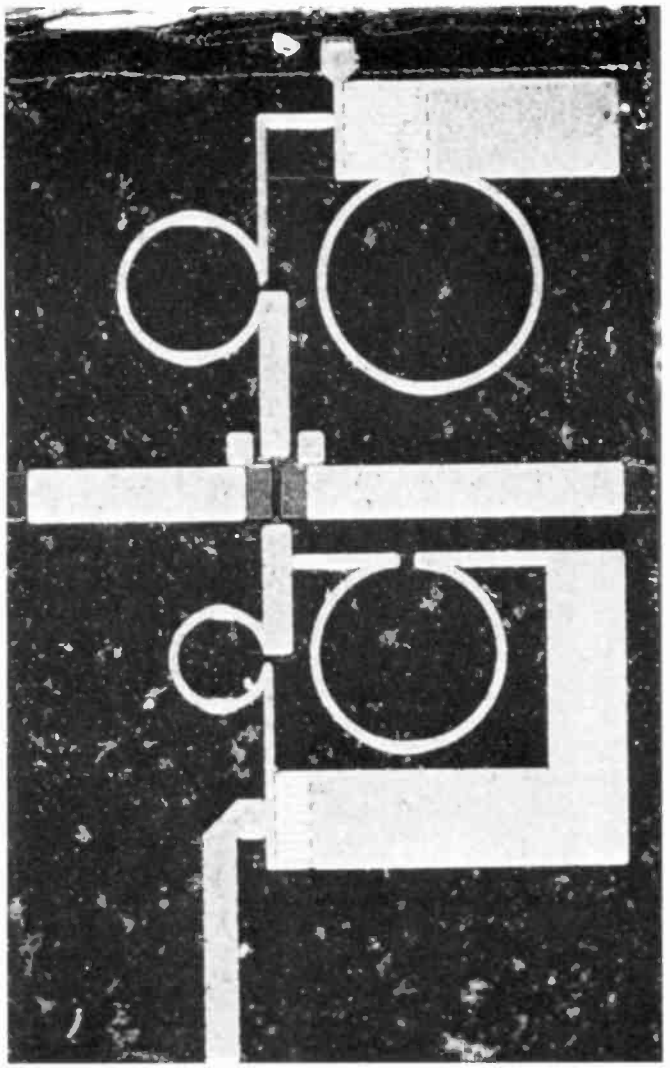

Fig. 1. *The monolithic dual-gate FET amplifier.*

have been developed. Propagation delays as small as 30 ps, static binary dividers operating at 4 to 5 GHz, and analog-to-digital circuits working at a 1.0-GHz sampling rate have been reported in the literature using 1.0-μm gate technology. Improved performance is possible with submicrometer gate-length devices.

Both the enhancement- and depletion-type devices will be considered for GaAs MESFET logic circuits. The advantages, and disadvantages of these two types of logic families will be described. State-of-the-art results demonstrate the capability of GaAs MESFETs in digital microwave monolithic integrated circuits (DMMICs).

Analog monolithic microwave integrated circuits

The most promising technology for fabricating monolithic microwave integrated circuits involves the integration on semi-insulating GaAs substrates of passive lumped/distributed circuit components with field-effect transistors and diodes. With the development of MMIC technology, certain microwave applications, such as direct satellite-to-TV-receiver communication and phased-array systems based on a large number of identical elements requiring small physical volume and/or light weight, may finally become cost effective.

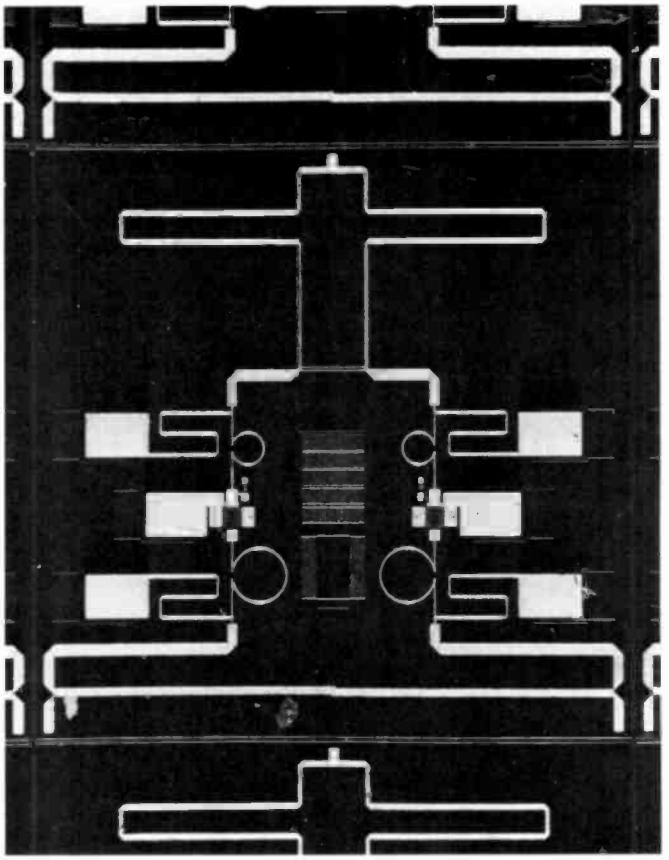

Fig. 2. *The monolithic dual-gate FET phase shifter.*

A major impetus for development of GaAs MMIC technology is the cost savings that can be realized by producing microwave circuits monolithically. Complete circuits deposited on a GaAs chip need no tuning. Hence, microwave circuits could be mass-produced monolithically without the time-consuming and costly tweaking that is required now. Also, subsystems defined on a chip could open up new block-diagram approaches for system designers who need to make equipment that ranges from test and measurement hardware to space-based radar. The reduced size and power consumption of monolithic GaAs circuits is particularly beneficial for space applications.

At the Microwave Technology Center, RCA Laboratories, we are developing the technology base for GaAs monolithic microwave integrated circuits. We are developing a monolithic GaAs dual-gate FET phase shifter.[1] The goal of this program is to achieve a continuous 360° phase shift over the 4- to 8-GHz range on a GaAs monolithic chip. This phase shifter consists of interdigitated couplers, dual-gate FET amplifiers, and an in-phase combiner. We have developed these components individually in monolithic form, and now we are developing the phase shifter.

Figure 1 is a photograph of the monolithic GaAs dual-gate FET amplifier.[2] The thickness of the GaAs wafer is 0.1 mm and its size is 4 mm × 2 mm. This amplifier exhibited a gain of 3 to 5 dB over the 4- to 8-GHz frequency band. The GaAs monolithic 90° phase shifter, which consists of a 90° interdigitated coupler, two dual-gate FET amplifiers, and an in-phase combiner, is shown in Fig. 2. The size of the phase-shifter chip is 4.5 mm × 4.5 mm × 0.1 mm. In this circuit, air-bridges are used for connecting the interdigitated conductors of the coupler as well as the two second-gate pads of the dual-gate FET. Silicon

GaAs MESFETs for logic applications

Normally-on, depletion-mode MESFETs (d-MESFETs) and normally-off enhancement-mode MESFETs (e-MESFETs) are shown in the Fig. 3a. In the e-MESFET, the active channel (t_e) under the gate is chosen such that the built-in Schottky barrier voltage (V_B) depletes all the mobile carriers. The device current is zero when the external bias on the gate is 0 V and it increases with increasing positive voltage on the gate. In the d-MESFET, the active channel (t_d) is only partially depleted by Schottky-gate, built-in voltage. The device draws current with 0 V on the gate. A negative voltage applied to the gate turns it off.

For depletion-mode circuits, the popular forms are buffered-FET logic (BFL) and Schottky-diode FET logic (SDFL). BFL and SDFL circuits both require negative as well as positive power-supply voltages. Four input NAND/NOR gates of BFL and SDFL circuits are shown in Fig. 3b. Both of these circuits use FETs and Schottky diodes. In BFL circuits, the logic function is realized in FETs and diodes are used for level shifting the output so that the input and output are compatible. In the SDFL circuits, the logic function is realized in Schottky diodes and FETs are used for restoring the logic levels and providing the load currents. BFL circuits are operated at the highest clock rates. They also consume more dc power than SDFL circuits. The low power dissipation for SDFL circuits arises from smaller voltage swings for the logic (1 V for SDFL and 2 V for BFL).

Two-input NOR-gate implementation with e-MESFETs is shown in Fig. 3c. Logic functions are realized in MESFETs. No Schottky diodes are used in these circuits. A resistor, an ungated FET, or a d-FET is used for the load. The circuit is simple and operates with a single bias supply. The logic swing is about 0.6 V. The smaller logic swing results in smaller propagation delay and very low power dissipation. The noise margins are small (0.1 V for e-FET logic and 0.5 V for d-FET logic). Technologically, d-FET logic circuits are much easier to fabricate than e-FET circuits.

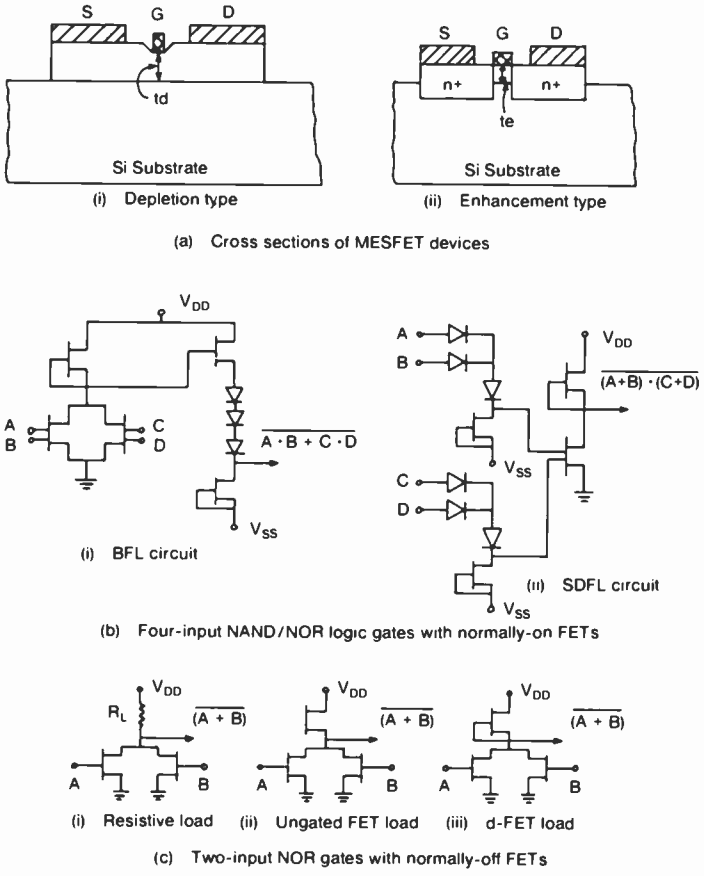

Fig. 3. *MESFET logic devices and circuits.*

nitride metal-oxide-metal (Si_3N_4 MOM) rf bypass capacitors are fabricated on the same chip. VIA holes, plated through the hole connecting the circuit pattern on the top side of the substrate to the ground plane on the bottom side of the substrate, are used to ground the source pads of the FET and the bottom plates of the capacitors. This chip is in the process of being fabricated.

So far, we have discussed the work being carried out at the Microwave Technology Center; now we will briefly describe some of the efforts, as of this writing, in the development of MMICs being carried out at other institutions and laboratories around the world.

The first monolithic GaAs FET power amplifier using VIA holes for grounding the source pads was designed by Pucel, *et al.*[3] Significant progress has been made in the development of monolithic GaAs power amplifiers with improved performance in power and frequency of operation. A maximum power level of 2.1 watts (W) has been achieved with 3-dB gain at 10.5 GHz.[3] The size of this amplifier chip is 4.8 mm × 6.3 mm × 0.1 mm.

The first monolithic low-noise amplifier was reported by Higashisaka.[4] A noise figure of 6.2 dB with 7.5-dB gain on a 2.75 mm × 1.95 mm × 0.15 mm monolithic FET amplifier chip has been reported at 20.5 to 22.5 GHz.[4] A low-noise figure of 3 dB has been obtained at 9.5 GHz with 17-dB gain (two-stage-amplifier). Also, power levels of 200 mW at 12 GHz, and 17 mW at 17 GHz, have been achieved with monolithic GaAs FET oscillators.[5]

Until now, we have described very briefly the circuits which are of low-level complexity. The most complex chip reported so far is an integrated receiver front end on a GaAs chip, intended for use in Direct Broadcast Satellite ground-terminal applications, operating at 12 GHz.[6] This chip is 10 mm × 10 mm and

contains two FET amplifiers, an 11-GHz FET oscillator and a dual-gate FET mixer.

Digital microwave monolithic integrated circuits (DMMICs)

The key word in GaAs digital IC technology is "high speed." It is difficult to develop a logic technology that simultaneously meets the requirements of maximum speed, minimum dissipation, and ease of implementation. Thus, it is necessary to consider carefully the complex trade-offs between the various logic approaches and then determine the optimum compromise.

Depletion-mode (d-mode) MESFET logic families are normally-on, and enhancement-mode (e-mode) MESFETs are normally-off. These two MESFET logic families have received the most attention in recent years. The basic logic gates of these two types and their operation are shown in Fig. 3 (see sidebar, page 60). The propagation delay, power dissipation and versatility of these logic types are compared in Table I. In this comparison, we kept the currents the same for both types of devices because the device currents determine the propagation-delay, the rise and the fall times. To determine the best performance possible from each of these devices, the effects due to parasitics (for example, series resistances, stray capacitances, and so on) were not included. In actual devices, such effects cannot be separated and hence the performance will be below these expectations.

For several years, the Microwave Technology Center at RCA Laboratories has been involved in the development of GaAs monolithic MESFET logic circuits for operation at gigahertz clock rates.[7,8] Because of the large noise margins and less-stringent requirements for material and process variables, we, at RCA, have selected depletion mode (d-mode) buffered FET logic (BFL) for our implementation. To demonstrate the technology development, the following test vehicles were chosen: ring oscillators for evaluating speed and power dissipation; type-D flip-flops for frequency dividers; analog-to-digital converters (A/Ds) for radar-signal processing; pseudorandom-code generators; and programmable dividers for synthesizer applications. RCA technology has been developed for fabricating ICs with 1.0-μm gate-length MESFETs. Figure 4 shows a fabricated IC. The chip size is 3.0 mm $\times$ 2.23 mm and the chip contains 334 FETs and 168 diodes. Ring-oscillator results yielded a 125-ps propagation delay for a fan-out of 2 at 13.5-mW power dissipation. Divider circuits have been operated at gigahertz clock rates. The 2- and 3-bit A/Ds have been operated satisfactorily at a 1.0-GHz sampling rate.[9] This sampling rate is the highest rate reported for any A/D operating at room temperature. Programmable dividers and PRN (pseudorandom noise) circuits are currently being evaluated.

Ring oscillator circuits were used to determine the propagation delay and power dissipation per logic gate. Ring oscillator results do not provide any insight into noise margins, tolerances and signal levels. Often, the loading (i.e., fan-in and fan-out) varies from 1 to 3. Therefore, ring oscillator results cannot be used to predict the system performance. However, ring oscillator results can be used to test the device models and compare various technologies. Vantuyl, *et al.* [10] reported 90-ps propagation delay for a fan-out of 2 with 10-mW power dissipation in buffered FET-logic (BFL) gates using 1.0-μm gate-length devices. At RCA, we achieved 125-ps propagation delay at 13.5-mW power dissipation for a fan-out of 2. Our results are in good agreement with other published data. Substantial improvements in logic gate performance can be obtained with submicrometer gate-length devices and these are not included in our study.

Table I. *Device and circuit parameters for d- and e-mode MESFET logic.*

Parameter	*d-Mode Logic*	*e-Mode logic*
Pinch-off voltage	$\simeq 4\ V_B$	$\simeq V_B$
Active layer thickness	1800 - 2000 Å	900 - 1000 Å
Pinch-off voltage	~ 0.5 V	~ 0.1 V
Propagation delay	3 tr	$\sqrt{3}$ tr
Load	FET with $V_{GS} = 0$ I_L/I_S well defined.	Ungated FET or resistive load used. I_L/I_S not well defined.
Noise margins	~ 0.5 V	~ 0.1 to 0.2 V
Fan-in and fan-out	Limited only by the desired response time.	Severely limited by leakage currents and load resistances.
Bias	Requires both positive and negative biases.	Requires only one bias.
Power dissipation	Rather high	Very low

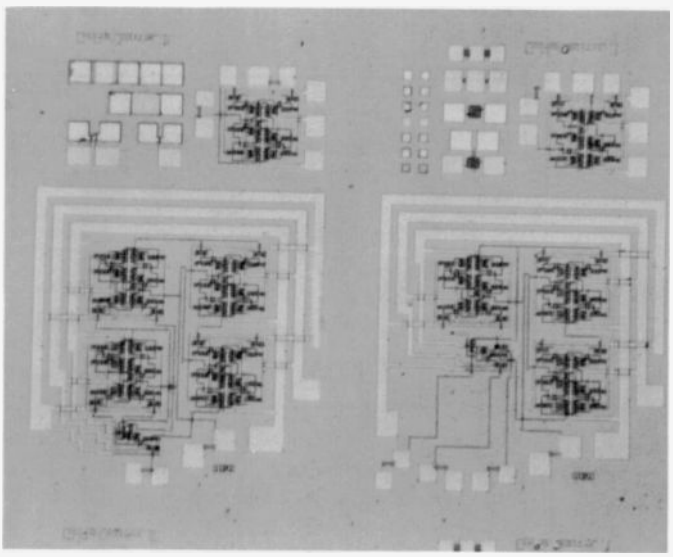

Fig. 4. *GaAs digital IC fabricated at our laboratory. It contains 334 FETs and 168 diodes. The IC is 3.0 mm $\times$ 2.25 mm. FETs with 1.0-μm gate lengths are used for operation at above 1- to 2-GHz clock rates.*

Extremely thin active layers required for enhancement-mode operation of FETs and the presence of surface depletion in GaAs devices make it very difficult to realize e-mode logic circuits. However, propagation delay of 39.5 ps with 4.0-mW dissipation was recently reported[11] in e-mode logic. It is evident that the e-mode logic gates are as fast as, if not faster than, depletion-mode logic gates. Also, the power dissipation per gate is at least lower by a factor of two for e-mode logic.

Static divide-by-two circuits have been fabricated to demonstrate the capabilities of d-mode FET logic gates. Division was

observed at as high as 2.2 GHz with single-clock input-type dividers. At RCA, we realized divide-by-two operation at 1.0 GHz with single-clock input. The circuits are being evaluated for higher-frequency operation. Using circuit techniques and complementary clock inputs, frequency division was achieved up to 5.0 GHz.[12]

Liechti, *et al.*,[12] reported on the largest IC fabricated with BFL technology. The IC consisted of 600 active devices and operated as a word generator at a 5-Gbits/s data rate. Long, *et al.*,[13] reported on the biggest IC fabricated with Schottky-diode FET logic (SDFL) gates. The IC consisted of 6,048 active devices (1,008 gates).

Most of the work on enhancement-mode FET logic is directed toward the development of static RAMs. Fujitsu,[14] Nippon Telegraph & Telephone,[15] Thomson-CSF[16] and Lockheed are all working on 1K RAMs with 1- to 2-ns access times. Preliminary results may be available before the end of this year.

Conclusions

We have presented a general survey of both the analog and the digital microwave monolithic integrated circuits. These circuits represent a worldwide cross section of the efforts in the field, which has emerged within the last three to four years. We have also described a variety of circuit applications amenable to the monolithic approach. The promising attributes of the monolithic technology are the potential reduction of fabrication costs, the improved reliability and reproducibility, and reduced size and weight. Those attributes will overcome many of the shortcomings of the hybrid-circuit approach. MMICs have, however, certain disadvantages, which include the relatively low Q of the passive reactive elements, and the poor use of the GaAs substrate real estates.

Based on the cost considerations, the potential markets for the analog MMIC will be in the systems that require large quantities of circuits of the same type and, therefore, can take full advantage of batch processing. Those systems are, to name a few, phased-array radars, airborne active-radar antennas, and electronic countermeasure systems. The promise of direct satellite-to-the-home broadcasting would also require tens of millions of GaAs receiver downconverters for use in the home-television systems.

On the other hand, GaAs digital technologies have been developed for both d-mode and e-mode MESFET logic. Ring-oscillator results indicate that the propagation delays are somewhat smaller and power dissipation is a lot less for e-mode logic gates. E-mode FETs require extremely thin GaAs layers that can be completely depleted (shut off) with no gate bias, and this translates into less than 100-mV tolerance in pinch-off voltage. Also, the noise margins are much better for d-mode FET logic.

MSI circuits using d-mode FETs operated at the highest data rates. However, work is now underway to develop 1K static RAMs with e-mode FETs. At RCA, we demonstrated the technology to fabricate depletion-type MSI circuits. We still have to improve the uniformity before we can embark on LSI circuits.

Authors (left to right) Upadhyayula, Huang and Kumar.

Ho-Chung Huang is Head of Microwave Processing Technology in the Microwave Technology Center of RCA Laboratories. He has responsibility for the modeling and fabrication of microwave devices, including GaAs power FETs, dual-gate FETs, transferred-electron oscillators, silicon millimeter-wave IMPATT diodes, and *pin* diodes. He is also responsible for the development of space-qualified GaAs FET amplifiers for satellite-communication applications, microwave switches, limiters, phase shifters, as well as pilot-line production of custom microstrip integrated circuits. Dr. Huang is a senior member of the IEEE. He has published and presented numerous technical papers and has been granted six U.S. patents. He is a recipient of the 1980 RCA Laboratories' Outstanding Achievement Award for the development of the space-qualified, solid-state GaAs FET power amplifiers for use in RCA Satcom satellites.
Contact him at:
RCA Laboratories
Princeton, N.J.
TACNET: 226-2447

L. Chainulu Upadhyayula is a Member of Technical Staff, Microwave Technology Center, RCA Laboratories, Princeton, N.J. He joined RCA in 1969 and engaged in solid-state research, including the design and development of microwave amplifiers and oscillators and high-speed digital devices and circuits. He is presently involved with the development of GaAs MESFET technology for MSI/LSI logic circuits operating above 1.0-GHz clock rates. Dr. Upadhyayula has published over 25 technical papers, was issued ten U.S. patents, and is a senior member of the IEEE. He received RCA Laboratories' Outstanding Achievement Award in 1970 for a team effort in the development of GaAs transferred electron amplifiers.
Contact him at:
RCA Laboratories
Princeton, N.J.
TACNET: 226-2048

Mahesh Kumar received his Ph.D. degree in Electrical Engineering from the Indian Institute of Technology, India, in 1977. From 1976 to 1978 he was a lecturer with the Radar and Communication Center, Indian Institute of Technology. There he was engaged in research and development of the feed for phased-array radar. In 1978, Dr. Kumar joined RCA Laboratories, Princeton, N.J., as a Member of Technical Staff. Since then, he has been involved in research and development of dual-gate FET amplifiers, phase shifters, and monolithic microwave integrated circuits.
Contact him at:
RCA Laboratories
Princeton, N.J.
TACNET: 226-3136

References

1. Kumar, M., "Dual-Gate FET Phase Shifter," *RCA Review*, Vol. 42, No. 4, pp. 596-616 (December 1981).
2. Kumar, M., Taylor, G.C., and Huang, H.C., "Monolithic Dual-Gate FET Amplifier," *IEEE Trans. Electron Devices*, Vol. ED-28, pp. 197-198 (February 1981).
3. Pucel, R.A., *et al.*, "A Monolithic GaAs X-Band Power Amplifier," *EIDM Tech. Digest*, pp. 266-268 (1979).
4. Higashisaka, A., IEEE MTT-S Workshop on Monolithic Microwave Analog ICs (1980).
5. Tserng, H.Q., and Macksey, H.M., "Performance of Monolithic GaAs FET Oscillators at J-Band," *IEEE Trans. Electron Devices*, Vol. ED-28, pp. 163-165 (February 1981).
6. Harrop, P., *et al.*, "GaAs Integrated All-Front End at 12 GHz," *GaAs IC Symposium Res. Abstract*, Paper No. 28, Las Vegas, Nevada (November 4-6, 1980).
7. Upadhyayula, L.C., Matarese, R.J., and Smith, R., "Technology Development for Gigabit-Rate GaAs Integrated Circuits," *RCA Engineer*, Vol. 26, No. 9, pp 86-91 (November/December 1982).
8. Upadhyayula, L.C., Smith, R., and Matarese, R., "GaAs Integrated Circuit Development for Gigabit-rate Signal Processing," *RCA Review*, Vol. 42, No. 4, p. 522 (December 1981).
9. Upadhyayula, L.C., Curtice, W.R., and Smith R., "Design Fabrication and Evaluation of 2- and 3-Bit GaAs MESFET Analog-to-Digital Converter ICs," to be published in *IEEE Trans. on MTT* (January 1983).
10. Vantuyl, R.L., and Liechti, C., "High-Speed GaAs MSI," *ISSCC Digest of Technical Papers*, pp. 20-21 (February 1976).
11. Yamasaki, R., *et al.*, "Self-align Implantation for n+-Layer Technology (SAINT) for High-Speed GaAs ICs," *Elec. Letters*, Vol. 18, No. 3, pp. 119-121 (February 1982).
12. Liechti, C.A., Baldwin, G.L., Gowen, E., Jolly, R., Namjoo, M., and Podell, A.F., "A GaAs MSI Word Generator Operting at 5 Gbits/S Data Rate," *IEEE Trans. MTT* (July 1982).
13. Long, S.I., Welch, B.M., Asbeck, P., Lee, C.P., Kirkpatrick, C., Lee, F., Kalin, G., and Eden, R.C., "High-Speed GaAs Integrated Circuits," *Proc. IEEE*, Vol. 70, No. 1, pp. 35-45 (January 1982).
14. Yokoyama, N., *et al.*, "TiW Silicide-Gate Self-alignment Technology for Ultra-high-speed GaAs MESFET LSI/VLSIs," to be published in *IEEE Trans. Elec. Dev.*
15. Ino, M., Hirayama, M., Ohwada, K., and Kurumada, K., "GaAs 1Kb Static RAM with E/D MESFET DCFL," to be presented at the GaAs IC Symposium, New Orleans, Louisiana (November 1982).
16. Nuzillat, G., Perea, E.H., Bert, G., Damay-Davala, F., Gloanec, M., Peltier, M., Ngu, T.P., and Arnodo, C., "GaAs MESFET ICs for Gigabit Logic Applications," *IEEE Tr. of Solid-State Circuits*, Vol. SC-17, No. 3, p. 568 (June 1982).

J.B. Klatskin | D. Haggis
R.L. Camisa | B.T. Joyce

Automated assembly of lumped-element GaAs MESFET power amplifiers

Wire bonds, to be used as inductor elements, are automatically placed in a lumped-element, microwave power-amplifier configuration.

Abstract: *Automatic assembly techniques for fabrication of lumped-element microwave power amplifiers are described. Small power amplifiers are constructed within the GaAs MESFET package. The amplifiers were designed for wideband (6-to 11-GHz) operation with a minimum power out of 27.8 dBm and 3-dB gain. Discussion areas include wire bonding, wire-bonder operation, inductors, and capacitors as related to lumped-element automated construction, amplifier optimization using computers, and inspection procedures.*

During the course of the program, twenty amplifiers were constructed. Prototypes were fabricated at RCA Laboratories to evaluate the circuit. Improvements were implemented, where feasible, after which the manufacturing techniques were introduced by RCA Automated Systems, Burlington, Massachusetts. Typical performance across the frequency band was 3.5- to 4.5-dB power gain with power-added efficiencies of 12 to 20 percent at 24-dBm input power.

Military electronic warfare (EW) systems often require the packaging of large amounts of microwave power into small, lightweight units. In addition, these systems must display high reliability and, in many cases, wide-bandwidth operation. EW system development also requires large production runs in which tight operating specifications must be maintained.

An improved method for meeting the demand for EW microwave amplifiers is to use lumped-element components. Research at RCA Laboratories, Princeton, N.J., has shown that wideband (6- to 11-GHz) operation and significant size reduction can be achieved using lumped-element matching techniques for GaAs MESFET amplifiers.[1] Lumped-element circuits show two immediate improvements over distributed circuits: easier fabrication and small size. Additionally, lumped-element fabrication lends itself nicely to automated assembly. Amplifiers based on this concept have demonstrated output power of 5 W from 9.5 to 10.5 GHz, and 1.5 W from 6.0 to 12.0 GHz.

This paper describes a joint effort undertaken by RCA Laboratories and RCA Automated Systems, Burlington, Mass., to develop techniques for automated fabrication of wideband lumped-element matched GaAs MESFET power amplifiers.

The lumped-element approach

Lumped-element fabrication can be realized within the transistor package by use of the periphery of the MESFET carrier as a platform for mounting capacitors. The inductor elements are

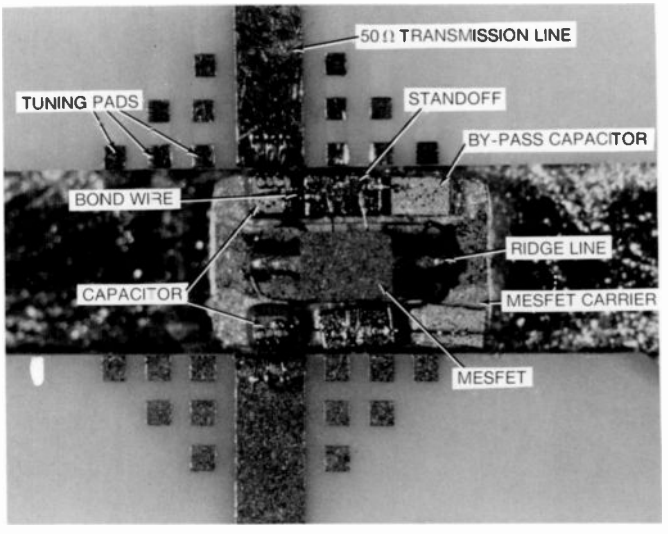

Fig. 1. *Lumped-element amplifier. Wire-bond inductors are automatically placed within the transistor package. The MESFET amplifier is now called an amplifier module.*

© 1982 RCA Corporation
Final manuscript received June 18, 1982
Reprint RE-27-5-11

realized by the self-inductance of a straight wire. The small size of the lumped elements, in fact, is why the circuits usually possess wide-bandwidth properties (Fig. 1). Parasitic inductances are greatly reduced or are incorporated into the design in a useful manner. The technique also contributes to greater efficiency at operating power levels.

The intent is to fabricate individual amplifier modules that can act as "drop-in" units for larger power-combined amplifier assemblies. The feasibility of this approach has been demonstrated in prototypes produced on both RCA- and Government-sponsored programs. Figure 2 shows a 1.5-W power amplifier made with this technology. Amplifier modules are identically constructed and similar in performance. The modules are combined through quadrature interdigitated couplers that provide a minimum of 20-dB isolation among the four output units, while providing the required 50-ohm system match to all six amplifier modules. The input and output ports use an equal-phase "split-tee" combiner for rf transfer to and from the outside world. All six modules operate at a common voltage, further simplifying amplifier production.

Automated construction

Automating the fabrication of microwave power amplifiers requires that the design and assembly be addressed in terms of what kind of equipment is available. Fortunately, at microwave frequencies, an inductor can be realized by a straight wire, which in turn makes the wire bonder a desirable tool for fabricating inductor elements.

Wire bonding. In ultrasonic wire-bonding, the bond is formed by the transmission of ultrasonic energy under pressure to the bond interface. Thermocompression bonding, in contrast, is a process using heat, pressure, and time to join the wire and workpiece. The introduction of ultrasonic energy allows us to reduce the temperature to 150°C from a pure thermocompression temperature of 350°C. The combination is called thermosonic bonding.

The GCA automatic wire bonder employed on this program uses the thermosonic bonding process. A 25-μm gold wire is fed through a capillary bore. A hydrogen-fueled flame-off torch is used to melt the wire and cause a ball to be formed at the wire end. Figure 3 illustrates the process in detail. Initially, a ball bond is formed at the first programmed wire position,with an optional fine-position adjustment by the operator. The second programmed connection is a wedge bond. The wire is "cut" at the weakened section of the wedge by the machine as it pulls on the wire, creating a so-called tail-less bond.

Inductors. The self-inductance of a round straight wire is readily determined from well-known equations found in the literature.[2] There are three methods for adjusting the inductor value: changing the wire length; varying the height above ground plane; and using parallel wires. Two methods usable in the amplifiers described here are to change the wire length and to use parallel wires. Increasing wire length will increase inductance in a nearly linear manner; however, adding a parallel wire will not decrease the single-wire inductance by one-half as one would expect. Instead, the total inductance is a function of the spacing between wires. The inductance decreases from 85 percent of a single wire value at 0.001-inch spacing to 50 percent at 0.0040-inch spacing between wires. The simplicity of the wire inductor makes it the best method for adjusting the circuit for optimal operation.

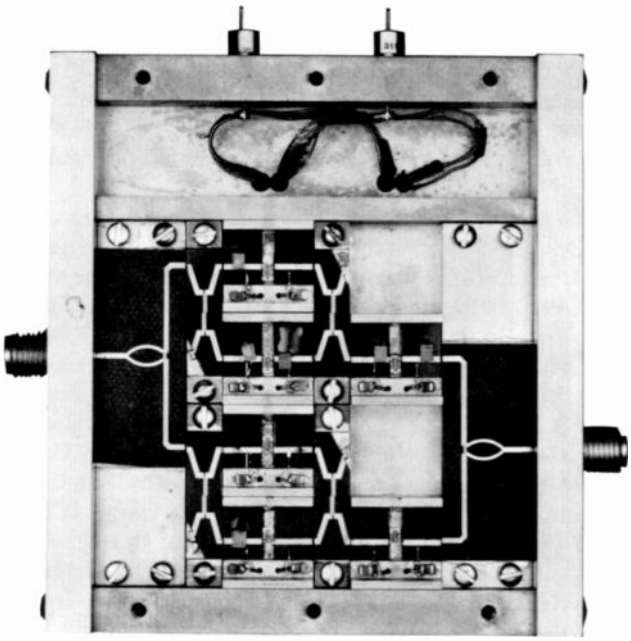

Fig. 2. *Power amplifier (1.5 W). Individual modules are combined into higher-power units.*

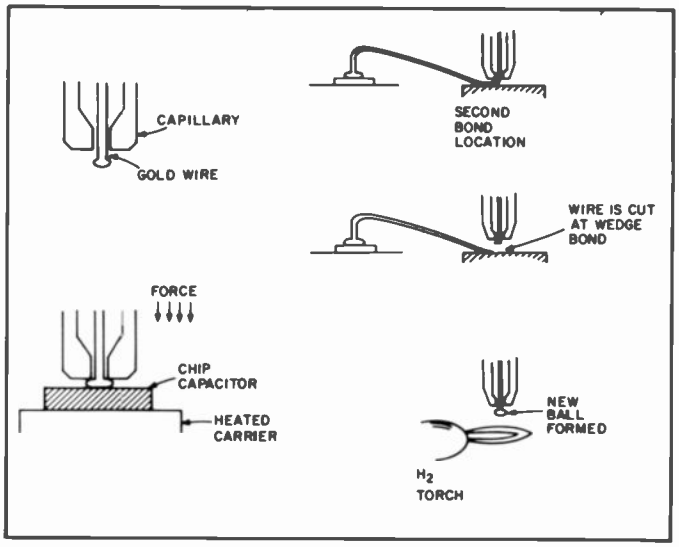

Fig. 3. *Wire-bonding sequence. Rapid wire-bond formation can be realized when all bonding functions are under computer control.*

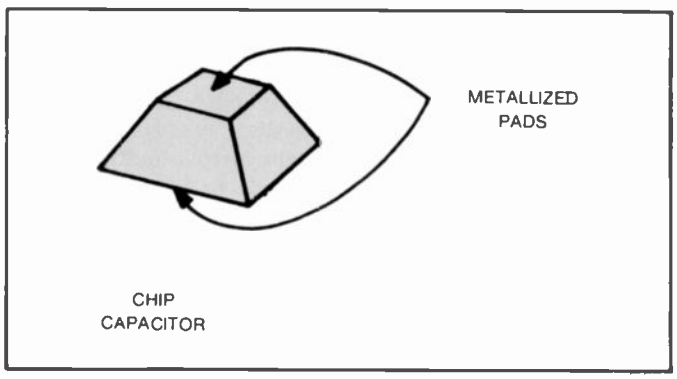

Fig. 4. *Chip capacitor. The capacitors are laser-trimmed to the desired value.*

Capacitors. Chip capacitors (Fig. 4) are realized by forming two parallel metal plates sandwiching a dielectric material. In the applications described here, small capacitance values (0.1 to 1.0 pF) and small size are necessary to realize the circuit within the transistor package. Porcelain dielectric capacitors provide the low-dissipation and small-size requirements of this program.

Transistors. GaAs has relatively poor thermal conductivity. Provisions must be incorporated into the transistor package design for removing heat generated during operation. One method used in low- and some high-power devices is to thin the device to an extremely small value before attachment to the heat sink. The fragility of the thinned wafer hinders large production runs. A more efficient packaging design is the "flip-chip" mounting technique developed at RCA Laboratories. In this technique, the device is bonded source-side-down onto a copper ridge. Copper, with excellent heat-conducting properties, serves as the heat sink. The technique is far more efficient because, in a GaAs MESFET, heat is generated at the source interface. A greatly reduced source inductance is an additional benefit of this procedure.

The RCA and Microwave Semiconductor Corp. microwave power devices are the only transistors available in the open-package flip-chip configuration. The cell electrical specifications for both types are similar, with differences in the way cells are combined. Shown in Table I are the MESFET specifications for the MSC 88104 used on this program. The flip-chip device can be seen in the center of Fig. 1.

Table I. *DC specifications of the MSC 88104.*

I_{DSS}	500 to 900 mA at 5 V
g_m	140 mS
Reverse V_{GS}	-8 V at 160μA
RF specifications	
Output power	29 to 30 dBm at 12 GHz
Gain at 1-dB compression	5 dB at 12 GHz

Circuit

Power MESFET devices operating in our frequency band generally exhibit gate-to-source impedances of 5 to 10 ohms and only slightly higher drain-to-source impedance. The circuit transformation network must be able to match the upper band-edge frequency to the 50-ohm system impedance. Secondly, provisions for introducing bias voltages must be addressed. A number of circuit configurations are suitable for this task; however, the realization will be difficult for some. We used the low-pass circuit shown in Fig. 5 because it meets the following requirements for our program: bias can be applied through circuit elements; wire bonds make up the tuning elements; a wire bonder can be programmed to fabricate the inductor elements; and the circuit will match the upper band-edge frequencies to 50 ohms.

High-frequency rf-power generation requires that circuit operation be efficient. To achieve efficient operation, the designer must be involved in the implementation of the design down to the smallest detail. At submicrowave frequencies, one could allow the technician freedom in selecting component vendors, but at microwave frequencies, the seemingly most insignificant component could ruin a project. An example would be the resistor used on the split-tee directional coupler. The circuit divides rf

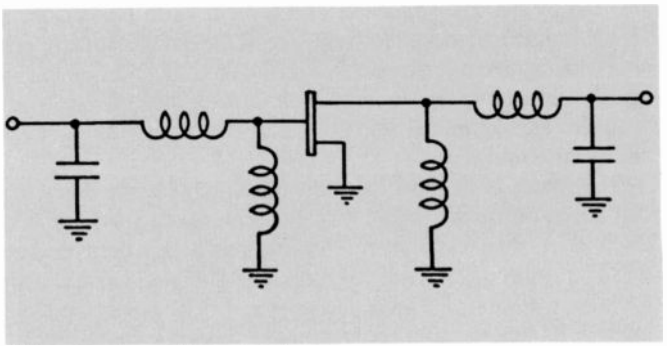

Fig. 5. *Circuit diagram of lumped-element amplifier. The low-pass configuration allows device bias to be applied through the inductor elements.*

power into two arms, each 3-dB down from the original signal level. A large physical size will cause reflections back to the input, thereby setting up a high VSWR and limiting an already tight bandwidth. The coupler can be seen at the input and output ports of Fig. 2.

Amplifier optimization

Large-quantity production of microwave power amplifiers should include provisions for optimizing performance at the point of manufacture. Tuning amplifiers at microwave frequencies requires that a highly skilled, experienced technician make the necessary adjustments to bring the unit into operating limits. The process is time consuming and costly. It would be more desirable to have people not trained in microwave participate in the task and thus allow more efficient management of resources.

We plan to use computers in as many tasks as possible. Computers, with proper programming, can measure amplifier performance by direct operation of test equipment. Computers can make the correct decisions to adjust circuit elements, and computers will be necessary for data collecting to reduce the enormous amount of paper generated during performance testing.

To learn more about the problems of computer optimization, we developed a simple computer program to analyze our circuit and to suggest corrective measures to restore performance. The operator enters either S_{11} or S_{22} (S-parameters relate current and voltage in two-port networks) into the computer where the program will, by de-embedding sections of the circuit, recompute the design. A comparison is made of the measured capacitance and inductance to the design values using the original device S-parameters. From this information, a course of action is chosen that will improve the module performance. Three options are available. First, should a wire be greatly oversized, replacement is the only alternative; second, within the range of inductance that can be adjusted by a parallel wire, this will be printed out; and third, if the capacitor is at fault because of too low a value, the connection of tuning pads on the 50-ohm line will be suggested. The amplifier module is measured again after the changes have been made and the program is again used to evaluate performance. When further improvement is no longer feasible, "No Tuning Needed" is printed out.

Inspections

As in any good manufacturing process, tight assembly schedules must be maintained. Inspections are a part of the quality-control

process in the assembly schedule. The two most important inspections are of incoming devices and capacitors. The GaAs MESFETs undergo the most intense acceptance testing because of the many parameters inherent in their design. First, a visual inspection is used to confirm both proper chip placement on the carrier ridge line and correct alignment of the gate and drain standoffs. Second, dc characterization is performed with special emphasis on gate reverse-breakdown and voltage I_{DSS}, the zero bias drain current. The two parameters must be within certain limits to be of use in our application. Third, small-signal rf testing is performed on every FET used on the program. This information is used in amplifier optimization and in the initial construction of the amplifiers where we try to correct for differences among devices.

The capacitors are visually inspected for proper size and the quality of the thin-film metallization. Poor metallization will cause weak wire bonds. Improper size could cause a poor fit of the device carrier to the module carrier.

In Fig. 6, we show the amplifier construction schedule. The section "circuit design" refers to the adjustment of circuit values for different MESFET units as determined from the S-parameter measurements made during the incoming inspection. As an example, if device 1 requires an inductor of length x and device 2 requires an inductor of length y, we try to accommodate each by small adjustments of wire length and capacitor placement.

Amplifier performance

The power-gain plot of Fig. 7 is for two amplifiers. The different gain figures can be traced to differences in drain current. This is an ongoing problem with power devices and must be corrected for in-assembly procedures. In our inspection procedures, we single out drain current for close scrutiny. In addition, we adjust element values during construction for best performance.

Automatic bonder programming

Programming the GCA automatic wire bonder involves two steps. First, an accurate representation, including dimensions, is drawn up. The drawing serves to locate bond positions, and to identify dangerous areas. The danger areas are near the MESFET chip. The chip is located about 0.050-inch above where the bonds are placed on the standoffs and capacitors. The wire-bonder capillary is tapered and, therefore, must not be allowed to travel within one-half the shank diameter to the FET chip. The problem is compounded by variations in chip placement by the vendor.

The bonder must be programmed for capacitor-placement variations. Since the bonder can move in 12-μm steps, we can be somewhat peremptory in our demands. Our measurements of incoming devices have shown that tight component values must be maintained to achieve acceptable performance. While fabricating the amplifier modules, we vary the location of the capacitor elements as needed to realize the design.

The accuracy and speed of the bonding system is in the controller instructions that tell the controller how far the tool should be moved and in what direction to go from one bonding position to another. The second step then is to program the controller. Originally, this was a tedious task because bonding positions had to be specified by their Cartesian coordinates. The coordinates then had to be transferred to truth tables and converted into a special binary-coded-decimal (BCD) format before being entered into the controller.

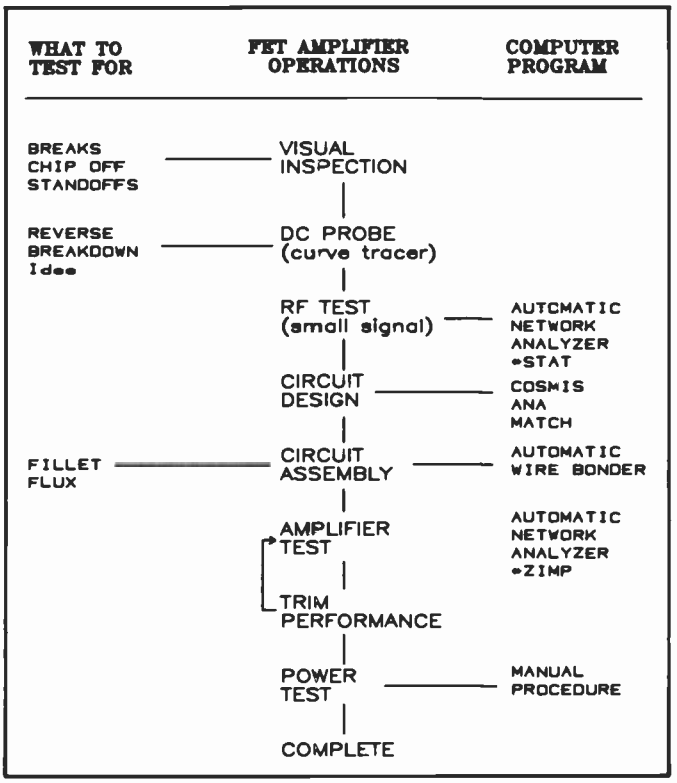

Fig. 6. *Schedule of manufacturing operations. Device and amplifier performance is monitored through careful inspection and measurement.*

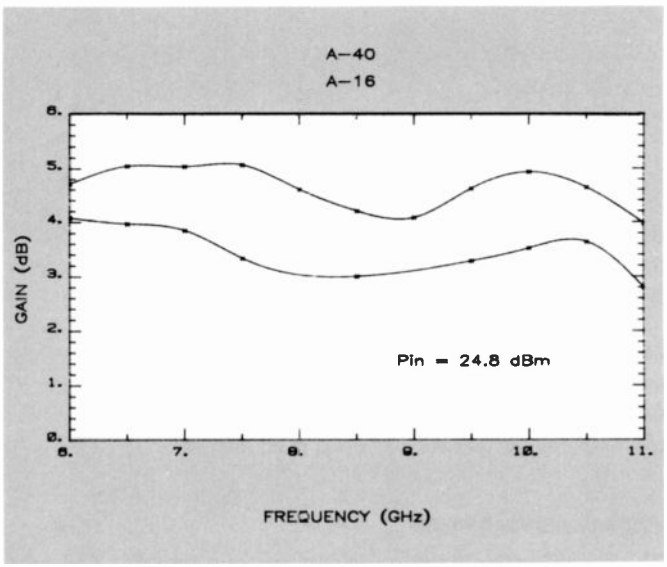

Fig. 7. *Power-gain performance. Device drain-current capability results in different power-gain performance.*

A computer is now used to perform the coordinate conversion to BCD directly and, at the same time, generate paper tape for transfer to the controller. Depicted in Figs. 8 and 9 is a typical computer-session printout used in programming for the lumped-element amplifiers. The controller only responds to figures between the explanation marks. The first number is the memory address and storage location. The second and third numbers are the coordinates in 0.0005-inch steps for the positions of the bond. The "P" and "L" indicate Pad or Lead. This

```
FNTTBL  22-JAN-82  11:57


CIRCUIT NAME? MICROWAVE FET
ASSEMBLY NO.? 1
FILE NAME (6 CHAR MAX)? MW1

SUBSTRATE SIZE (INCHES):
X? .465
Y? .600

FIRST MOVE ADJUSTMENT (YES/NO)? YES
NEG. NOS. AWAY FROM HOME;POS. NOS. TOWARD HOME:
X CHANGE (MILS)? -236
Y CHANGE (MILS)?  114

THETA CORRECTION (YES/NO)? NO

HOW MANY CHIPS?
6
DOES CHIP-COORDINATE FILE EXIST? YES

DO YOU LIKE TO CHECK THE DATA ? NO

FRONT TABLE PROGRAM FOR AUTOMATIC WIRE BONDING OF
MICROWAVE FET
ASSEMBLY NO. 1


TO RECORD FRONT TABLE PROGRAM,
TURN PUNCH ON NOW, TURN OFF AT THE END OF 25TH SPACE

OUTPUT     '4000 -1209 -391 3'
INPUT      '4001 -0054 -004 4'
SHUNT L O '4002 +0052 -029 5'
SHUNT L I '4003 -0053 +001 6'
SERIES L O'4004 +0052 +032 7'
SERIES L I'4005 -0049 -005 8'
HOME'4006 +1161 +296 E'

IS PUNCH OFF?


ANY CORRECTIONS TO INPUT DATA? NO
```

Fig. 8. *Computer printout of controller instructions. If a wire bond requires rework, numbers for recall are assigned.*

tells the controller what is to be moved. Head movement is used to form the bond, while table movement is used to locate each new wire-bond position. The wire bonds are assigned numbers for recall, should a particular bond need rework.

Alignment mechanism

The alignment mechanism includes the two movable tables on which are mounted the X-Y manipulator, the vacuum cups, and the heater. These tables are linked mechanically to the X-Y manipulator and theta wheel. They can move independently to correct for X-Y and theta errors in chip placement (Fig. 10).

Head-positioning mechanism. The head-positioning mechanism moves the bonding head to the correct position for each bond. This mechanism can be moved in both the X and Y directions. The theta stage on which the head is mounted, is rotated to provide theta motion. The correction is provided by two sensors at the front of the main bearing. When theta correction is made during the alignment procedure, a plate moves with

```
BNDNOR  22-JAN-82  10:48


CIRCUIT NAME? MICROWAVE FET
ASSEMBLY NO.? 1
FILE NAME (6 CHAR. MAX) ? MW!\1
HOW MANY CHIPS & ALIGNMENT POSITIONS? 4
PRINTOUT WB PROGRAM? YES

NORMAL MODE BOND PROGRAM FOR CHIPS OF
MICROWAVE FET
ASSEMBLY NO. 1
TO RECORD BOND PROGRAM ON PAPER TAPE,
TURN PUNCH ON NOW

OUTPUT  '1100 -108 -306 P '   '1101 +030 +004 L '
OUTPUT  '1102 -030 +006 P '   '1103 +030 +001 L '
OUTPUT  '1104 -030 +009 P '   '1105 +030 -004 LL'

INPUT   '1200 -048 -306 P '   '1201 -030 +004 L '
INPUT   '1202 +030 +006 P '   '1203 -030 +001 L '
INPUT   '1204 +030 +009 P '   '1205 -030 -004 LL'

SHUNT L '1300 -078 -356 P '   '1301 +001 +060 LL'

SHUNT L '1400 -078 -320 P '   '1401 +001 +024 L '
SHUNT L '1402 -013 -024 P '   '1403 +001 +024 LL'


TURN PUNCH OFF
END OF BOND PROGRAM.
```

Fig. 9. *Computer printout of controller instructions. Pad and lead instructions enable head and table motors.*

the theta table. A second plate attached to the main bearing remains stationary. The relative positions of the two plates represent the angular misplacement of the work.

Head mechanism. The head mechanism consists of the capillary or bonding tool, the support arm, head motor and cams. Working together, these items place the wire on the chip-bond position, make the bond, pull the wire to the lead position, make the second bond and separate (cut) the wire from the lead bond.

Torch system. The torch burns off the wire just below the tip of the capillary after the second bond has been made. The torch is fueled by hydrogen and oxygen, and it burns continuously until power is removed from the bonder.

Electronic systems. The function of the electronics is to control the mechanical functions involved in the bonding process. This control allows the entire bonding process to be automated and, if need be, stopped at any point for the purpose of examination. The controller is a small computer. The controller outputs are machine-instruction words that enable machine-control circuits. The controller inputs use sensor feedback from these circuits.

Amplifier production

Following prototype development at RCA Laboratories, the amplifier-fabrication effort was transferred to Automated Systems. Small modifications were incorporated into the amplifiers to account for differences in wire-bonding systems. At the Labo-

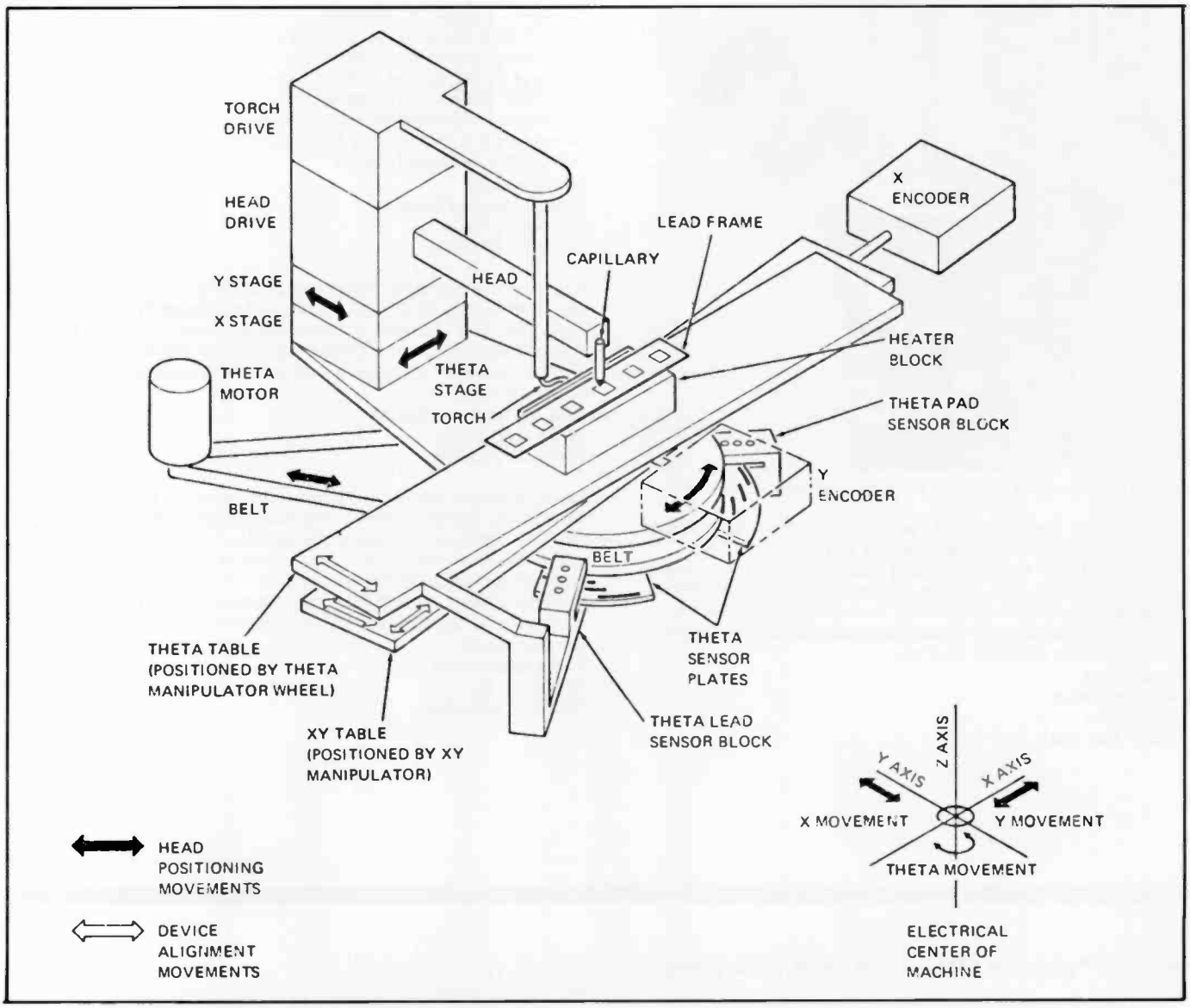

Fig. 10. *Alignment mechanism. The relationship of various wire-bonder components is shown. All operations are under computer control.*

ratories we used an ultrasonic, manual wire-bonding system that creates straight point-to-point wire bonds, while the automatic bonder at Burlington forms looped bonds. We knew about these differences from the beginning of the program; therefore, during modeling of the inductors, we observed the behavior of the two bonds. Our tests showed virtually no operational differences between parallel straight and looped wires. The inductance of the pair behaves in the manner described earlier. Single-wire inductance of straight or looped wire is still a function of length. The only problem was in determining the actual wire length. The automatic bonder forms bonds looped differently for different spacing between pads. The empirical data from the first few amplifiers made at Burlington gave us the necessary information to adjust for these anomalies.

Twenty amplifiers were fabricated during the course of this program and each module performed above our minimum of 3-dB power gain at 25-dBm input. Future plans call for combining the amplifiers into higher-power units with hermetically-enclosed housings.

Conclusion

We have shown the feasibility of using automatically placed wire bonds as inductor elements in a lumped-element microwave-power-amplifier configuration. Fabrication techniques were described along with procedures for optimizing performance by the use of computers as the analysis medium. Wire bonding and wire-bonder operation were described in detail.

With automatic assembly, operational variations can be traced and corrected in a systematic manner. The procedures and techniques developed during this program should enable personnel without the special skills of a microwave design group to fabricate microwave amplifiers.

References

1. Klatskin, J.B., *et al.*, "Fabrication of Lumped-Element Broadband GaAs MESFET Microwave Power Amplifiers," *RCA Review*, No. 42, p. 576 (December 1981).
2. Terman, F.E., *Radio Engineers' Handbook*, McGraw-Hill Book Co., Inc., New York, N.Y. (1943).

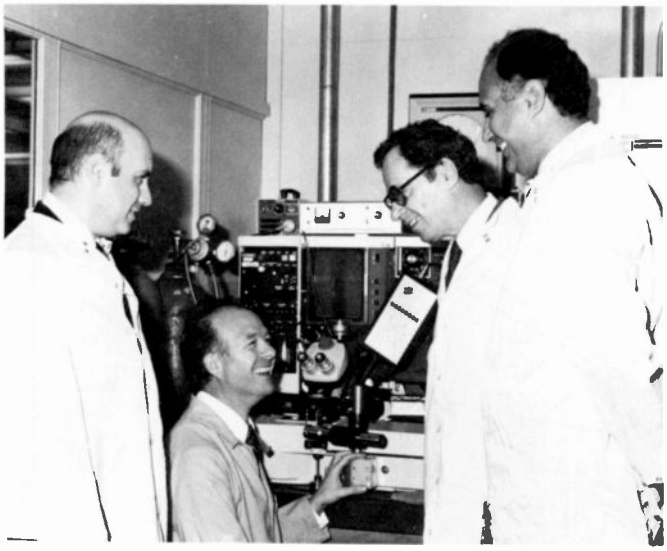

Authors (left to right) Klatskin, Haggis, Joyce, and Camisa.

Jerome Klatskin is a Member of Technical Staff in the Microwave Technology Center at RCA Laboratories, Princeton, N.J. Mr. Klatskin joined RCA in 1962, working initially on traveling-wave tubes. From 1970 to 1975, he was involved in IMPATT and TRAPATT device fabrication. Since 1975, he has done amplifier circuit design and is currently investigating lumped-element matching techniques for MESFET devices.
Contact him at:
RCA Laboratories
Princeton, N.J.
TACNET: 226-2691

Demetrios Haggis, is a Senior Member of the Production Engineering Staff. He joined Automated Systems, Burlington, in 1979 after having previously worked for Datel Systems, Inc. He holds M.S. and Ph.D. degrees in Solid State Physics from Northeastern University. His current responsibility is to transfer the technology of building broadband power microwave amplifiers from RCA Laboratories in Princeton to Automated Systems, Burlington, using computer-aided design.
Contact him at:
RCA Automated Systems
Burlington, Mass.
TACNET: 326-3982

Brad Joyce is Manager, Techniques, for the product and process engineering for hybrid microcircuits at Automated Systems, Burlington, and has been active in this field since 1971. He has previous experience as a design manager for signal-processing electronics, digital computers, and automatic test equipment.
Contact him at:
RCA Automated Systems
Burlington, Mass.
TACNET: 326-2226

Ray Camisa is a Member of Technical Staff in the Microwave Technology Center at RCA Laboratories, Princeton, N.J. Since 1974, he has been involved in the development of GaAs FET devices and circuits. In 1974, Dr. Camisa was a member of the research team that developed the first 1-W GaAs FET. In 1979, he received a David Sarnoff Award for the development of microwave lumped-element GaAs FET amplifiers.
Contact him at:
RCA Laboratories
Princeton, N.J.
TACNET: 226-2510

Have you "given a stroke" to your TEC lately?

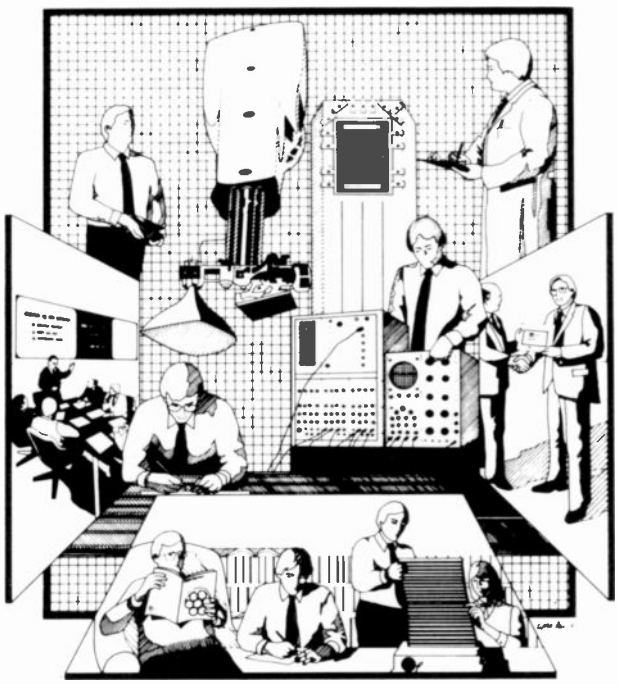

Do you know that engineers at RCA are devoting time and effort to help you in establishing and maintaining a satisfying career? They are your Technical Excellence Committee and they attempt to contribute to a stimulating working environment by determining your needs in the areas of technical education, technical information, professional activities and recognition. Once the need is established, they move on to develop and execute supportive activities.

Most of you are somewhat aware of and use the technical excellence activities. But have you paid your dues by expressing your appreciation to your TEC representative? Or even better, do you tell him your views on today's engineering climate and the career needs you perceive?

Engineers are highly skilled professionals, but all too often they keep their thoughts and needs to themselves, perhaps because they are busily engaged solving their problems. Technologies, techniques, and engineering tools—the entire supporting environment is constantly changing and better ways to do engineering work are evolving. Do you take the time to discover and master them? This is where the TEC is attempting to support you—you can help the TEC help you, by sharing your thoughts with the TEC members. Then give them credit for their efforts, every once in a while.

M.E. Breese | R.J. Mason

Computer-aided manufacture of precision microwave components for phased-array radar

Numerically controlled machining has been exploited to achieve the close mechanical tolerances required of phased-array radar components.

Abstract: *To perform effectively in severe electronic countermeasures environments, tactical radar systems must have very low antenna sidelobes. To achieve these sidelobe levels, manufacturers must fabricate microwave components to extreme accuracies—a function ideally suited to computer-aided design and manufacturing techniques. This paper describes the successful application of these techniques to the fabrication of precision components for an advanced tactical phased-array radar.*

Combat systems need multifunction radars wth sharply reduced susceptibility to enemy countermeasures. This need translates, in part, to requirements for planar phased-array antennas with much lower sidelobe levels.

One measure that is essential in achieving significant reductions in sidelobes involves imposition of very close mechanical tolerances on the fabrication of components to control impedances and transfer-phase functions. However, achieving these tolerances by standard, operator-controlled machining processes proves to be extremely difficult because of uncertainties caused by backlash, possible measurement inaccuracies, variations in tool and table speeds, and so on.

In modern metalworking facilities, numerically controlled and/or computer-controlled machining are widely used for repetitive operations, to substantially reduce labor costs and raise yields. The machine characteristics that provide these advantages also make it possible to produce parts that are accurately replicated and free of the uncertainties that characterize operator-controlled machining. This precision-control feature can be exploited to provide the close mechanical tolerances needed for precision phased-array radar components. The following paragraphs describe a number of these components, which were fabricated successfully through application of computer-aided manufacturing techniques as an integral part of the microwave design and development process.

© 1982 RCA Corporation
Final manuscript received July 20, 1982
Reprint RE-27-5-12

This paper is based on the authors' presentation at the 1982 International IEEE Antennas and Propagation Society Symposium held in Albuquerque, New Mexico, in May 1982. The paper was selected by the AP Society Awards Committee for the Best Hardware Paper Award.

Linear array

A 12-foot 80-element linear array was designed for −35 dB peak-sidelobe levels over a 12-percent operating range at S-band. Extensive use was made of numerically controlled (NC) machining in the beamformer that provides both sum (Σ) and difference (Δ) monopulse pattern beams. The beamformer collects the signals from the elements in pairs, the paired elements being equidistant but on opposite sides of the array center line as illustrated in Fig. 1. The sum and the difference of each pair of signals are formed by using a hybrid junction. These results are then weighted in amplitude to achieve a smoothly varying aperture illumination for each of the two patterns. For the sum pattern, a Taylor weighting function was selected with a −53 dB design sidelobe level and $\bar{n}$ of 10 (that is, nine lobes on each side of the main beam at the design level). The difference pattern was weighted with a Bayliss function for a −50 dB design sidelobe level and $\bar{n}$ of 12. The weighting was accomplished in the combiner networks, shown in Fig. 1. This method of achieving independent control of the sum and difference patterns is known as a multiple-interferometer phase-monopulse network. It can readily be extended to planar arrays using such networks for each of two orthogonal coordinates, for example, columns and rows of the two-dimensional array.

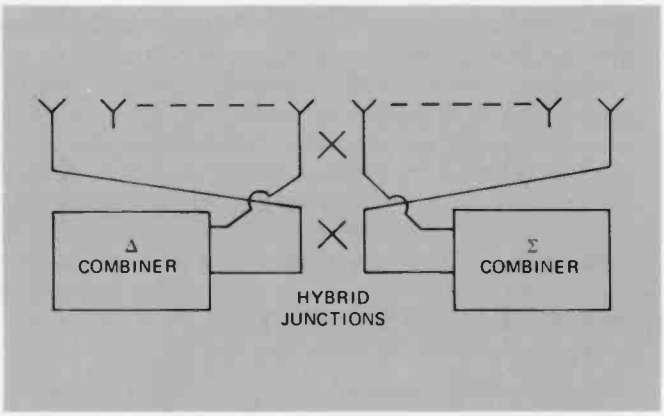

Fig. 1. *Schematic diagram of a linear array shows how signals from pairs of elements are combined in an interferometer arrangement, allowing independent optimization of Σ and Δ weighting.*

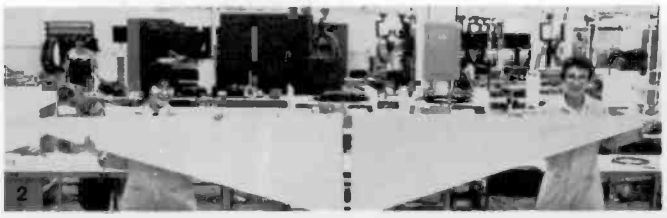

Fig. 2 *shows the two identical housings for right and left distribution networks, fabricated as part of an IR&D effort. The NC-milled grooves forming the outer conductors for the coaxial lines are visible on the right. Installation of tubular center conductors supported by Teflon beads is shown in* **Fig. 3.**

Distribution networks

To minimize phase errors due to the voltage standing-wave ratio (VSWR) and/or tolerances of dielectric material properties, distribution networks to connect the radiating elements to the centrally located hybrid junctions were designed as bead-supported, air-filled coaxial lines with square outer conductors milled into aluminum plates, as shown in Fig. 2. The 40 center conductors of each network consist of lightweight tubing and NC-milled angled sections, as shown in Fig. 3. These 6-foot assemblies mate directly to the three-branch coaxial hybrid junctions (Fig. 4) used to form sum and difference signals from oppositely disposed pairs of elements.

Differencing hybrids

The hybrid junctions are three-branch coaxial branchline couplers that have been designed for NC-milling of both inner and outer conductors to maximize the unit-to-unit uniformity; the cross sections of both conductors are square. Figure 5 shows the features incorporated into the design to facilitate milling of these parts. The direct mating, without coaxial connectors, of the distribution networks with the hybrid junctions is shown in Fig. 6. As shown, signals from oppositely disposed elements are delivered to the two terminals of one hybrid function. The vector sum of these signals appears at one of the output terminals, and the vector difference at the fourth port.

Power combiner networks

The most complex parts of the beamformer are the power combiner networks, which provide the weighted illumination for low sidelobes. These networks (one for the Σ and one for the Δ pattern) were designed in two sections—one is a brazed waveguide network, and the other is an NC-milled coaxial network (Fig. 7). Wilkinson-type split-tee-junctions were used throughout the latter. The 32 junctions for each of these networks were designed using a computer-aided design program, with a rectangular cross section so that both inner and outer conductors can be fabricated on a computer-controlled milling machine. The power-division ratios varied from 3.0 to 7.0 dB. A breadboard 4.5-dB junction is shown in Fig. 8. The resistor to terminate the fourth port, mounted on a beryllium oxide (BeO) heat sink, is soldered to the center conductor via metal ribbons.

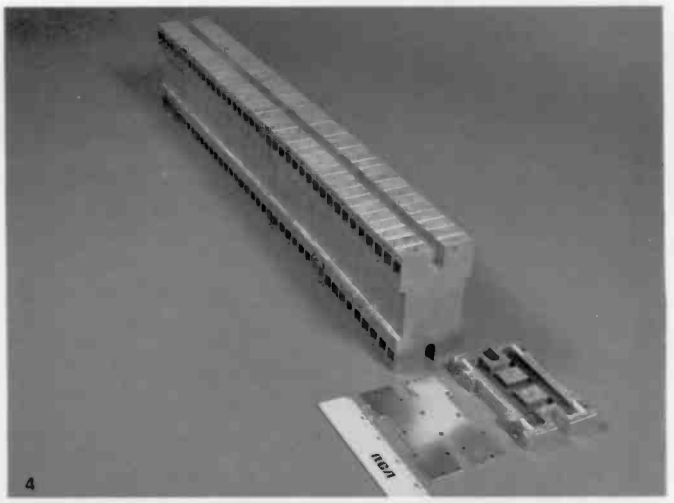

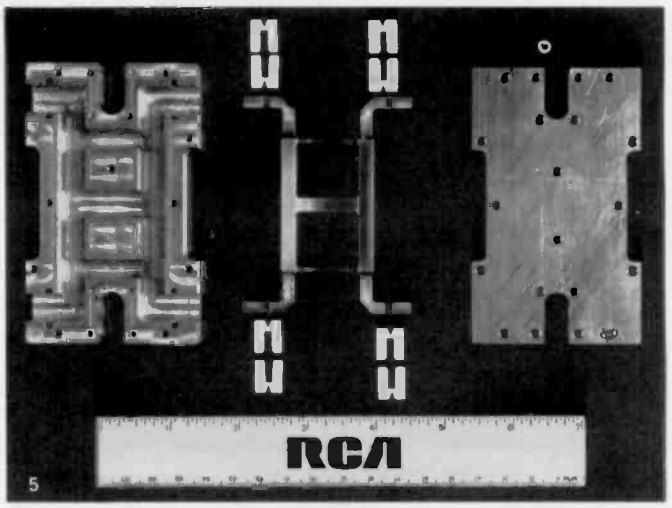

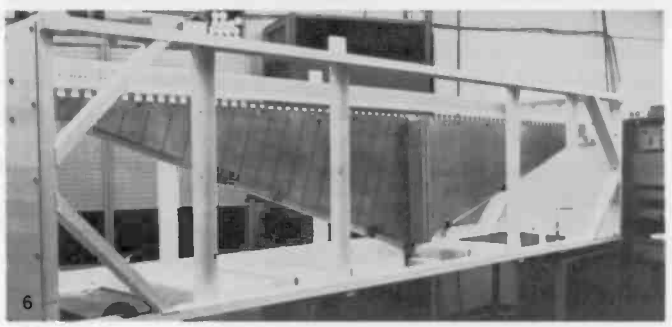

The 40 three-branch coaxial hybrid junctions used to combine the signal pairs are shown in **Fig. 4,** *arranged for installation between the distribution networks. Details of the parts,* **Fig. 5,** *show the radii included in the design to be compatible with NC milling. The combined assembly of IR&D hybrid junctions and distribution networks is shown in* **Fig. 6.**

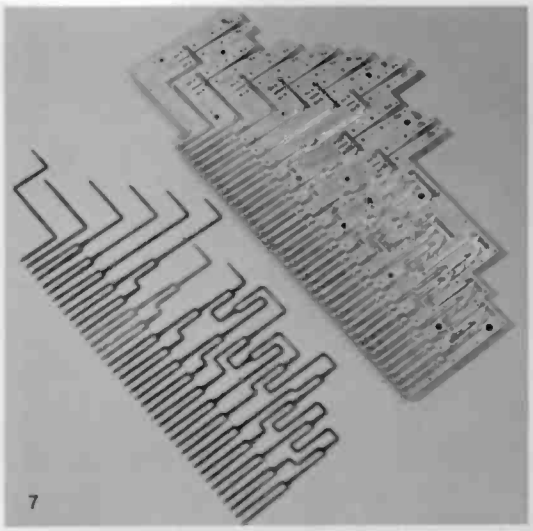

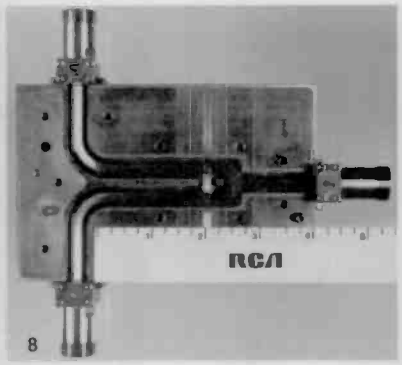

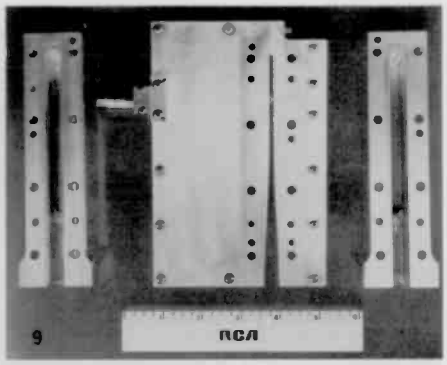

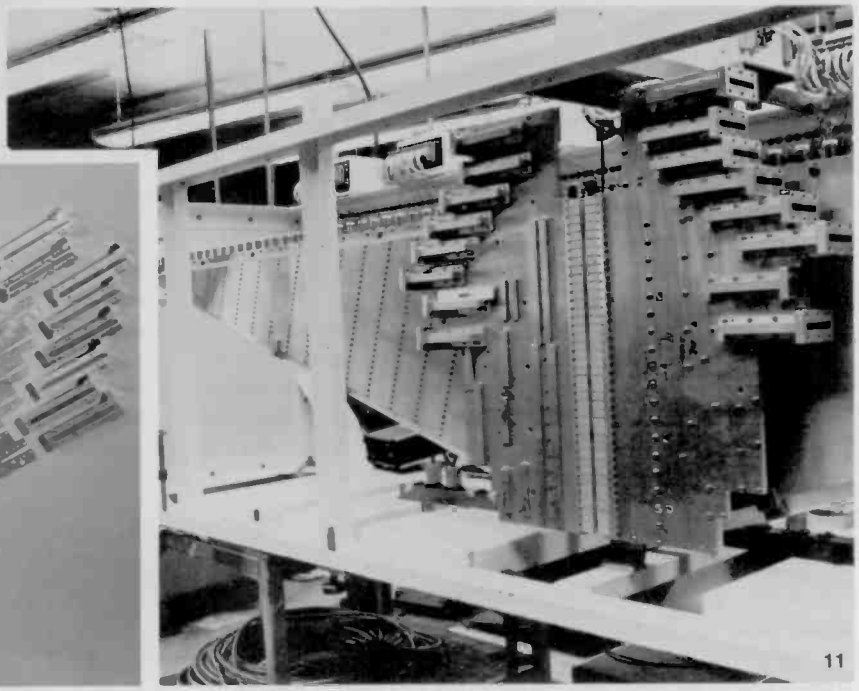

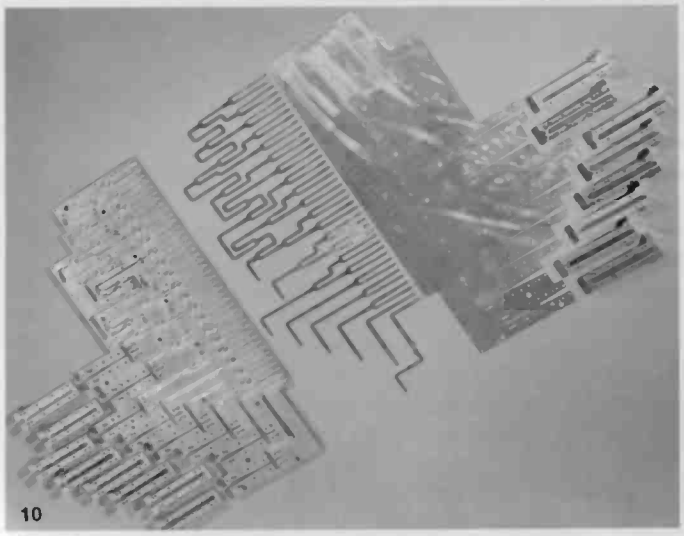

Fig. 7 *shows the NC-milled inner conductors (left) and outer conductors (grooves in aluminum plate) for a 40-port to 8-port IR&D power combiner network. One of the Wilkinson-type split-tee divider junctions is shown in* **Fig. 8**; *the network includes 32 such junctions of varying designs.* **Fig. 9** *is a photograph of the test fixture for the transition from the network to waveguide. Tapered grooves for eight of these are milled into the housing shown in* **Fig. 7.** *All the parts of a single combiner network are displayed in* **Fig. 10,** *and* **Fig. 11** *shows both networks installed, with hybrid junctions and distribution networks.*

The interface between the combiners and the hybrid junctions is by direct mating in the same manner as used for the distribution networks. The interface to the waveguide networks is via tapered ridged-waveguide transitions. A breadboard transition is shown in Fig. 9. In the network of Fig. 7, the tapered ridges for eight such transitions are milled into the outer conductor housing, and the transitions are then completed by adding two "half" waveguide sections (also fabricated by NC-milling), as shown in the exploded view of Fig. 10. In Fig. 11, the two 6-foot distribution networks and the two combiner networks are interconnected through the 40 hybrid junctions. All the sum signals are fed to the Σ combiner, while the difference signals enter the other, Δ, combiner.

Cross-section dimensional tolerances for all these components were specified to be ± 0.001 or ± 0.002 inch. Positional tolerances were specified to be ± 0.002 to ± 0.005 inch. The first NC-machined combiner inner conductor was generally 0.002 inch over tolerance, but this was caused by the omission of a final "spring" cut, that is, a repetition of the same tool path in case the work forced the tool to bend (or spring) away slightly. The second inner conductor was within tolerance. These close tolerances were held in a part that meanders over an area of 11×14 inches even though cross sections were as small as 0.040×0.161 inch.

The cross-sectional dimensions of the channels that form the outer conductor of the combiners were within tolerance. The difficult machining on the housing was in the 0.400-inch-thick curved and tapered ridges where a small-diameter cutter was required because the distance between tapered surfaces reduces to 0.094 inch. Multiple passes using light cuts produced a smooth and accurate surface.

Radiating elements

Radiating elements for the linear array are flared horns, as shown in Fig. 12. These were designed for NC milling, with the bottom of each horn serving as cover for the one below when installed in the array, as shown in Fig. 13 The array was

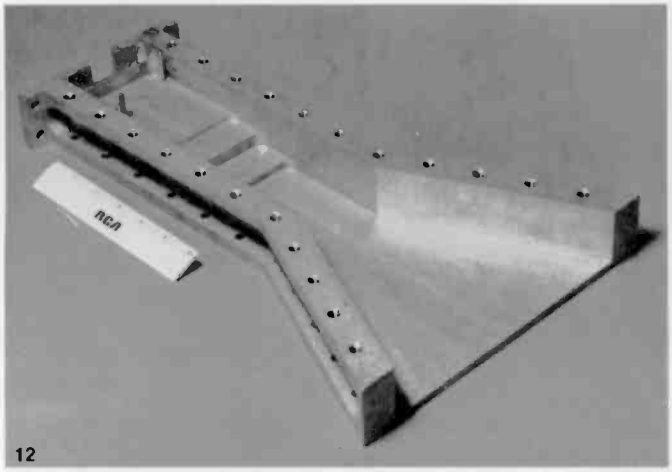

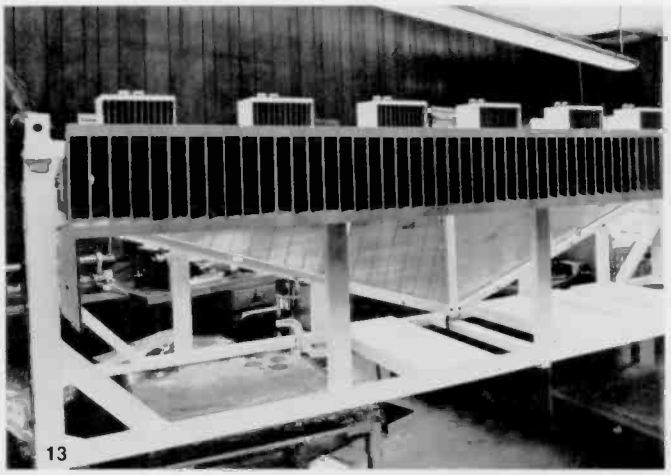

Fig. 12 *shows a flared horn designed as a radiating element for an IR&D phased array, with quarter-wave impedance transformers machined as steps, and inductive posts pressed into precision holes. The linear array of 80 horns is shown in* **Fig. 13,** *with the beamformer of* **Fig. 11** *feeding the array.*

equipped with waveguide networks and ferrite phase shifters, and evaluated on RCA's near-field antenna test range. After alignment, the patterns exhibited −36 dB peak and −44 dB rms sidelobe levels. In NC machining, any small discrepancy in a machined part is likely to appear in all other parts. This was vividly demonstrated when the 80 radiating elements were stacked together. A small difference in height of one side wall with respect to the other wall on all the elements caused a noticeable curve in the array—fortunately not affecting performance.

Planar arrays

The technology employed in the linear array beamformer is also directly applicable to precision planar arrays. An interesting example is shown in Fig. 14, a photograph of a portion of a milled aluminum plate designed to serve as both the front structural member and the radiating elements of a large S-band planar array. The elements are open-ended waveguides. This method of fabrication can yield the small errors necessary for low-sidelobe-level arrays. In an array 12 feet in diameter, one can expect each radiating element to be positioned within ±0.006 inch of its true position with respect to the center of the array; radiating elements themselves can be machined to a tolerance of ±0.002 inch.

Stripline circuits

Computer-aided design and computer-aided manufacturing are also applicable to stripline microwave circuits suitable for phased arrays. For low-power applications, sum and difference combiner networks similar to those described above have been designed and constructed in stripline, with both sum and difference combiner networks, as well as 3-dB hybrid junction couplers to form sums and differences from pairs of signals, all on one etched circuit. An 880 Applicon system was programmed to generate the various Wilkinson split-tee power dividers from the required coupling ratios. An eight-character input is sufficient to generate a junction having a specific coupling, phase compensation, and matching and interface geometry. The same entry is used to generate the aperture paths for a Gerber photoplotter, which is used to make a glass photomask.

The 880 Applicon/Gerber combination has several characteristics that are well suited to the fabrication of precision microwave circuits: (1) it is easy to generate Wilkinson junctions in an interconnecting circuit to obtain a desired rf energy distribution; (2) after the artwork has been generated in the Applicon, it is easily scaled linearly in size to compensate for any predictable material dimensional change that results from etching; (3) circuit linewidth can be changed by simply changing the aperture size in the Gerber plotter; (4) mirror-image circuits can be obtained at the push of a button; and (5) accuracy and precision, the most important of all factors, are obtainable. Tolerances within the Applicon are ±0.0001 inch on linewidth and ±0.00005 inch on position over the full size of the circuit. (The etched circuit is less accurate, but the inaccuracies are not the fault of the database.)

The Applicon database is also used to make drawings of the ground planes and other parts. A punched paper tape is also obtained from this database to drive a numerically controlled Wiedemann punch to manufacture the ground planes; this assures proper alignment between the combiner circuit and the ground planes without additional tooling.

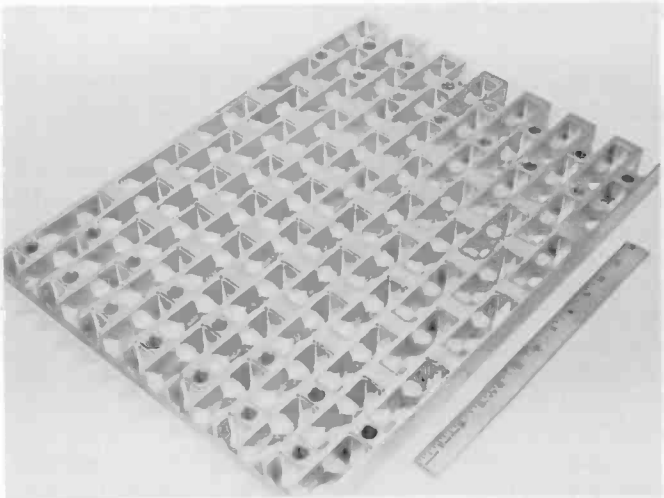

Fig. 14 *is a segment of a planar-array aperture, fabricated as part of an IR&D project on a numerically controlled milling machine. The radiating elements are waveguide horns formed into the front structural plate.*

Conclusion

The fabrication of microwave components has taken a step forward since the introduction of modern numerically controlled (NC) machine tools. Starting at the breadboard stage, where controlled changes in configuration are essential to obtaining precise design data, and continuing through production, where exact replication is so important to modern phased-array performance, the use of NC machine tools must be included in the design approach.

Bob Mason has been engaged in the mechanical design and packaging of microwave and antenna components and systems since joining RCA in 1950. He is presently involved in the design of large precision phased arrays for radar applications.
Contact him at:
RCA Missile and Surface Radar
Moorestown, N.J.
TACNET: 224-2377

Maurice Breese has worked on phased array development since joining RCA in 1965. He is presently guiding the development of arrays for future tactical radars.
Contact him at:
RCA Missile and Surface Radar
Moorestown, N.J.
TACNET: 224-2417

Authors (left) Mason and Breese (right).

RCA Corporate Engineering Education Course Catalog Released

Eleven new video course packages and other educational services for RCA's technical staff are announced in the 1982-83 RCA Corporate Engineering Education Course Catalog. The catalog is mailed yearly to RCA engineers on the *RCA Engineer* mailing list. Additional copies are available on request, from Margaret Gilfillan, TACNET 222-5255.

Three courses have been added to the already extensive CEE computer curriculum. The effort to provide courses for manufacturing personnel has been accelerated and a "Manufacturing" category has been added to this catalog's contents section. Expansion of the range of programs in the CEE Videotape Library has enhanced its value.

Here's a quick preview of the contents of this year's catalog.

What's New?—*A brief summary of the new courses in this catalog.*

What's Coming?—*A look at CEE plans for the year ahead.*

CEE Video Courses—*Eighty-three video course packages now available.*

Computer Curriculum Flowcharts—*Help in selecting the course that's right for you.*

CEE Resource Guide—*Answers to all your questions about CEE services.*

CEE Videotape Library—*What's available and how to obtain it.*

CEE Short Courses—*Information about Fall, 1982 offerings.*

CEE Staff—*A look at some new and some familiar faces on the CEE staff.*

CEE Video Course enrollments passed the 2000 mark for the first time in 1981. You could be a part of record enrollments this year, too, after you look through CEE's new catalog and decide on the technical course for you.

B.S. Perlman | D.L. Rhodes | J.L. Schepps

Computer-aided design and testing of microwave circuits

Dedicated computers simplify the tasks of designing and characterizing microwave circuits.

Abstract: *Computer-aided design and testing has greatly affected the state-of-the-art of microwave circuit design. Increasing demands on circuit performance have led to more complexity. This circuit complexity takes on two forms: elaborate topology, and detailed element models. The result has been an ever-increasing use of computers to analyze and optimize these circuits. Computer-aided testing provides measurement capabilities that could not be achieved manually. This paper describes RCA's current capabilities in computer-aided design (CAD) and computer-aided testing (CAT) for microwave and rf applications.*

Presently, we at RCA's Microwave Technology Center (MTC) in Princeton use a number of dedicated minicomputers to perform automatic measurement, data collection and computer analysis, and optimization of microwave and high-frequency circuits. Each computer is capable of multitasking, permitting several programs to run simultaneously.

Overall, the objective of an automated design and measurement facility is to improve the productivity of available human resources. Facilities, such as those developed at MTC, can effectively handle complex tasks that might otherwise be impossible or certainly more difficult and less cost effective. A complete facility would include capabilities for circuit synthesis, analysis and optimization, layout and fabrication, measurement and testing, and tuning. Such computer aids are helping produce superior products with greater reliability and yield. The next section describes some of the resources available in microwave computer-aided design (CAD) at MTC for circuit analysis and optimization at microwave frequencies. Following that, computer-aided testing (CAT) is described as it relates to microwave measurement and testing.

©1982 RCA Corporation
Final manuscript received August 18, 1982
Reprint RE-27-5-13

Microwave CAD

During the initial phases of design, the ability to predict the performance of a circuit is crucial; this enables the engineer to re-evaluate the circuit and make changes required to obtain the design goals more closely. Because physical construction of the proposed circuit, followed by testing to determine whether it meets the requirements, is costly, circuit analysis is the alternative.

Circuit analysis requires that some mathematical approximations of the physical properties of the circuit components be made. Generally, the intent of the modeling is to generate electrical properties from the given physical ones (sizes, lengths, and so on). The computer provides high-speed mathematical computation that is well suited to the analysis of microwave circuits. This has resulted in more accurate component models and more elaborate circuit topologies than those obtained manually.

Microwave CAD takes place at various levels in the design process. Programs can provide electrical properties of simple devices (for example, the transmission-line impedance value) based on physical measurements of the component. The electrical properties estimated with programs of this fundamental type can then be used as data for higher-level programs that compute overall circuit performance. A circuit-level program can analyze circuit topologies that are combinations of components specified by the user. In addition to circuit analysis, some programs provide a method of altering element values to achieve a user-defined performance goal (optimization).

Element modeling

The basic building blocks for constructing a circuit topology are the individual circuit elements (for example, resistors, capacitors, transmission lines, and so on). A CAD program requires mathematical models or tabulated values that approximate these elements. The accuracy of the overall CAD process is limited by the accuracy of these models.

After a physical process is mathematically modeled, the values for the element models can be determined either analytically or empirically. In its simplest form, the empirical method uses experimental (measured) data to represent an element. Here the measured data is generally a tabulated set of S-parameters (or any other completely descriptive parameters) versus frequency. This simple empirical method is often used for empirical modeling of transistors. The more general empirical approach requires building a series of elements, which are identical except for variation in a single parameter. This series of measurements can then be "curve fit" to approximate data at points that were not ever measured. An example of this technique might be the modeling of a transmission line. Measurements can be made for a transmission line on a particular sub-

strate for various line widths, within a useful range. The resulting S-parameters can be curve fit, for interpolated points and in some cases for extrapolated points, to show dependence on line width (and frequency).

In contrast, the analytic approach uses fundamental laws or theoretical models about the element to arrive at some method to describe the electrical properties. The analytic approach has a great advantage over the empirical method in that it avoids the expensive construction and testing of microwave circuits. Also, the range of validity of the analytic equations is usually well known due to the known approximations that are part of the method. Some specific examples of computer programs based on the analytic method are given below.

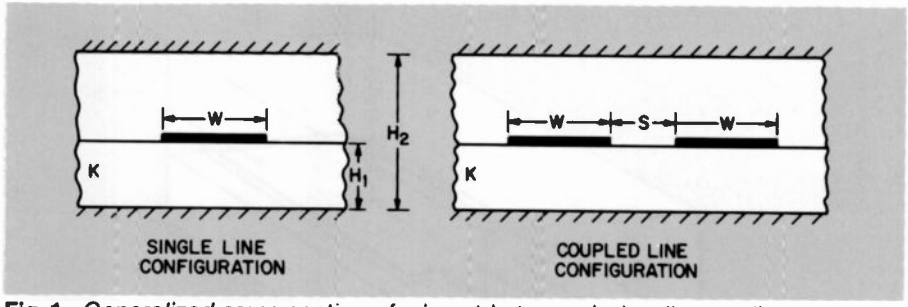

Fig. 1. *Generalized cross section of microstrip transmission-line media.*

Computer programs based on analytic methods

MSTRIP. Figure 1 shows a generalized cross section of a model of microstrip transmission media, looking in the direction of wave propagation. The program, MSTRIP,[1] analyzes this configuration for both the single-line and coupled-line systems, although the single-line case can be handled much easier by other methods. As input, the dimensional ratios of S/H_1, W/H_1, H_2/H_1 and the dielectric constant K are given. The program computes the quasi-static even- and odd-mode impedances and effective dielectric constant as well as the phase velocity. By taking advantage of the symmetry of the system, a static solution reduces to the determination of even- and odd-mode potentials; that is, the even mode with +V, +V and the odd mode with −V, +V on each of the strips. A static solution involves splitting the strips into N substrips (each of width W/N) and iteratively solving for the potential distribution. As is the case for all iterative methods, an initial starting point is required. A potential distribution can be computed in closed form by assuming that the dielectric is not present. This distribution was used as the initial distribution in the original method.

A later refinement of this initialization incorporated the dielectric Green's function directly as a Fourier integral to account for the presence of the dielectric. Now that a good starting point is known, the solution involves field "relaxation" of the current potential distribution to the final distribution to satisfy Laplace's equation. Field relaxation involves the iterative application of difference equations. The convergence of this method to the exact solution is well behaved as the number of substrips (N) is increased, and the iterative convergence is also quite good. The only drawback of the method is that the results are only correct for the quasi-static case, (when the dielectric thickness is less than about 3 percent of the wavelength) although various dispersion relations can be used to approximate results for higher frequencies

IMP. The program IMP[2] is a collection of computational aides in both the analysis and synthesis of microstrip transmission lines. The program allows analysis and synthesis of both single and coupled symmetric microstrip-transmission lines. The effects of metallization thickness and of frequency are accounted for, but proximity effects of metallic enclosures are not.

In the analysis mode, the input consists of the various dimensional ratios, substrate dielectric constant and thickness, as required; and as output the program generates the impedance(s), phase velocities, line losses, and coupling value. In the synthesis mode, input consists of the dielectric constant and thickness of the substrate and generates the required line width(s) for specified impedance(s).

The program also allows for the analysis and synthesis of Lange couplers that consist of n identical interdigitated lines (for n even). Closed-form expressions derived from conformal mapping techniques,[3] together with empirical approximations, are used to compute analyzed and synthesized properties of single lines. Line losses are evaluated with the aid of the "incremental-inductance rule."[4] The frequency dependency of the line properties are computed with approximate dispersion formulas[5] derived by conformal mapping methods. Coupled lines are analyzed and synthesized using the results of an approximate procedure derived from conformal mapping.[6] The analysis and synthesis of the Lange coupler uses published equations[7] combined with the coupled-line analysis.

ELOP. The program ELOP[8] was written to solve general electro-optic problems in two dimensions. The algorithm solves a finite-difference matrix on a x-y grid of points and allows for more general configurations than MSTRIP. Notice that MSTRIP calculations for coupled lines are restricted to symmetric lines.

ELOP performs a finite-difference solution on a generalized x-y cross section, which includes strip metalization, electron beams, and so on. Accuracy is only limited by the grid spacing, which can be different in the x and y directions. Although the program was originally written to solve general electro-optic problems, the microwave applications include the computation of coupling between microstrip transmission lines. The configurations are similar to those in Fig. 1, but with asymmetric line widths as well as symmetric. The method solves for the potential distribution through the use of a successive over-relaxation of the difference equations determined through Laplace's equation. The over-relaxation method attempts to improve the algorithmic convergence over the relaxation method. A poor choice of the relaxation factor can produce oscillations which actually degrade the performance, thus great care is used in calculating the relaxation factor. The computational costs of this program are greater than for MSTRIP since symmetry cannot be used to advantage.

TLM. A three-dimensional version of finite-difference techniques is applicable whenever variation in all three dimensions occurs. This is the case for computing discontinuity parameters for such topologies as steps or bends in microstrip transmission lines. A Transmission-Line Method (TLM)[9] has been developed for these cases. Current versions of the method require that equal spacing in all three dimensions be used to determine the grid points. The input must specify the conductivity and dielectric and magnetic properties at the grid points in three dimensions.

The grid points are bounded in an imaginary box by electric or magnetic walls (an

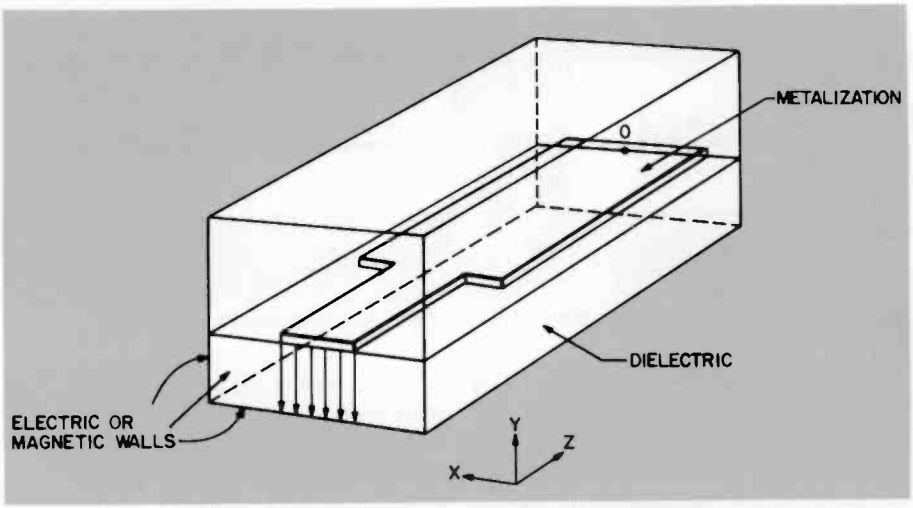

Fig. 2. *Configuration for using the TLM method in computing the discontinuity parameters of a step in microstrip media.*

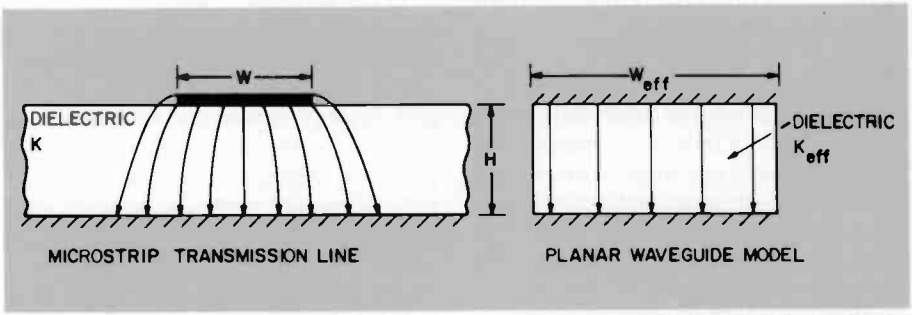

Fig. 3. *Cross sections of transmission-line configurations used by the Planar Waveguide Model.*

electric wall has infinite conductivity in the plane of the wall, forcing any electric field contingent on it to be perpendicular, similarly for magnetic walls). An initial field distribution (electric or magnetic) must also be specified. The solution involves the field relaxation of an input excitation and gives the time-domain output at any desired point in the grid.

Here, the difference equations required to perform the field relaxation are based on the more general Maxwell's equations (instead of Laplace's). The configuration pictured in Fig. 2 shows how this can be useful for microstrip steps. Here, the initial field configuration is shown by the arrows, and the output can be sampled at the point marked "O." This initial field configuration approximates a TEM (transverse electromagnetic) step input. The electric field normal to the conductor at the output point is stored for increasing values of time. This is the approximate step response of the system. The only theoretical accuracy limitation lies in the finite number of points in the grid, and unfortunately the computational problem grows extremely rapidly, limiting the practical usefulness of this method.

MSTRIP, ELOP, and TLM all employ the fundamental laws of physics (Laplace's or Maxwell's equations) directly in a finite-difference solution. These solutions all have the disadvantage of requiring that convergence be reached, after perhaps many iterations on either a two- or three-dimensional grid of points. The program IMP uses explicit equations derived from physical considerations, avoiding the computational problems of field relaxation. Thus far, the only method mentioned for computing transmission-line parameters is TLM, which is, unfortunately, also the method that requires the most computation. This method can be made very accurate by allowing the grid spacing to be very small, but, of course, doing this rapidly increases the time and memory requirement.

PWM. A simplification of the discontinuity environment can be made with the Planar Waveguide Model (PWM).[10-13] This model can be used as an approximation to the microstrip media, as shown in Fig. 3. The model assumes magnetic walls, and also assumes that the electric field between the two conducting surfaces is a superposition of up to ten TE_{no} modes. To account for the fringing field in the physical structure, the effective width of the model, W_{eff}, is greater than the physical line width, W. The dielectric constant of the model, K_{eff}, is lower than that of the physical structure, to account for the fact that the fringing field exists partly in air. Simple closed-form expressions exist for computing the model parameters from the physical ones.

Once this model is accepted, an alternate approach to the computation of the discontinuity parameters for microstrip transmission lines is possible with a mode-matching technique. In the case of a microstrip bend, the method matches the magnetic field for a specified number of modes, up to ten, in the area between the two lines. By superposition of the electric fields in this area, the scattering matrix of the bend can be computed. The speed with which a scattering matrix for a particular geometry at a specified frequency can be computed depends on the number of modes that must be matched. The only drawback to this method lies in the simplicity of the underlying model; once this is assumed, the mode-matching technique supplies good results.

The circuit level

All of the above programs represent an attempt to achieve accurate results for a specific physical domain. Emphasis was given to microstrip transmission lines and discontinuities. Generally, these results are either used as input or, if simple to compute, are internal to a circuit-level program. A circuit-level program allows the analysis of circuit topologies which, in general, contain both passive elements (transmission lines, lumped elements, and so on) and active elements (transistors). Descriptions of several circuit-level programs that are currently in use throughout RCA follow.

SUPER-COMPACT is a large program, requiring 2 megabytes of virtual storage. In its present form, its use is restricted to the larger class of computers, with the associated costs. On the other hand, both of the programs COSMIC-S and ANA are segmented to allow them to execute on more memory limited, non-virtual machines, such as those used for measurement automation.

COSMIC-S. The program COSMIC-S[14] has circuit analysis and optimization capability, although it restricts the topology to one that can be expressed in terms of ABCD matrices. The analysis capability

includes lumped elements (resistors, capacitors, inductors, transformers), and transmission lines, as well as tabulated S-parameters representative of an element (very useful for transistors). The full input description, including the circuit, frequency range, type of output, and optimization parameters and goal, can reside in memory or on disc. All input is in the form of numeric codes that represent the circuit. The program supports many types of output including S-parameters, Z- or Y-parameters, various gain parameters, group delay, and so on, that may be freely specified in any combination. The objective function to be optimized can include any combination of the output parameters.

The optimization method that COSMIC-S employs is a version of a randomized pattern search rather than one that uses partial derivatives. This implies that computation of the gradients (or sensitivity) of the objective function, with respect to each variable element, is not required in finding search directions.

ANA. For circuit topologies that can be represented in terms of ABCD chains, the program COSMIC-S provides fast analysis and optimization. But many circuits cannot be represented with this restriction and require a general *nodal* analysis. The program called ANA[15] performs general nodal analysis of microwave circuits. This program allows for both memory- and disc-resident circuit descriptions with output capabilities similar to COSMIC-S. Coding of the circuit topology with mnemonics (alphanumeric strings) facilitates the input.

The program also allows for the analysis of coupled lines, including interdigitated couplers and comb-line filters. Another feature of the program is the use of graphics output, such as shown by the example in Fig. 4. The present version of ANA does not include provision for computerized optimization; however, a tuning mode is provided to iteratively increment or decrement any element value by a previously defined step.

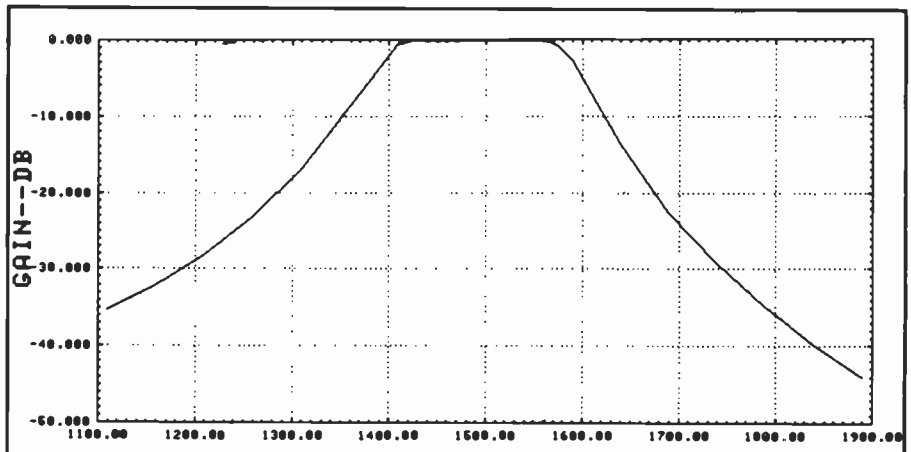


```
ANALYZE?,CHANGES?,WRITE?ANALYZE
8:29 AM  THU., 29  APR., 1982
TITLE: COMB LINE FILTER

 FREQ        GAIN          GA1           GA2           VSWR
  MHZ     DB     DEG     MAG    DEG    MAG    DEG     IN     OUT
1110.0 -35.34 4.307 .99982 94.23 .99982 94.39 10950. 10979
1160.0 -31.97 -2.27 .99964 87.62 .99964 87.84 5543.3 5550.
1210.0 -28.00 -10.2 .99915 79.61 .99915 79.94 2360.6 2362.
1260.0 -23.14 -20.6 .99750 69.09 .99750 69.65 798.75 799.2
1310.0 -16.93 -36.1 .98970 53.26 .98971 54.37 193.22 193.3
1360.0 -8.582 -66.2 .92783 22.32 .92785 25.28 26.712 26.71
1410.0 -.5365 -141. .33928 -61.2 .33940 -41.2 2.0270 2.028
1425.0 -.0396 -168. .09000 -121. .09030 -35.3 1.1978 1.199
1840.0 -39.69 -173. .99989 96.62 .99989 96.51 17659. 17696
1890.0 -43.97 -179. .99993 90.34 .99993 90.26 26799. 26972

ANALYZE?,CHANGES?,WRITE?
```

Fig. 4. *Examples of ANA output capabilities.*

SUPER-COMPACT. Some of the limitations of COSMIC-S and ANA are overcome in the program SUPER-COMPACT.[16] This program supports both ABCD-chain and nodal-analysis capabilities with provision to optimize specified performance objectives. Data input is facilitated using alphanumeric strings. Circuit-element statements are contained in a file, where one specifies type, connection, and value of each component within a circuit. Lumped, coaxial, microstrip, stripline, coplanar waveguide and suspended substrate elements can be analyzed. Topologies are organized by using node numbers in the statement for the element specification, with provision for mixed forms of cascade and nodal interconnections. Additionally, special instructions and specifications may be entered for optimization, tolerance analysis, and network synthesis.

Circuit optimization is available using either a gradient or randomized pattern-search procedure. These methods may be combined by the user for maximum efficiency and probability in finding the global minimum. Multiport optimization is available for circuits requiring different characteristics at various input/output ports. Additionally, a device-modeling extension allows automatic input/output impedances to be generated for any active two-port and provides terminations that can be used directly for synthesis. Tolerance effects may also be included. Performance spreads are predicted using Monte-Carlo analysis.

The program includes an on-line database of product information and measured characteristics for a variety of commercially available transistors and dielectric materials. Output data may be plotted on polar or rectangular charts with the frequency response of any of the available two-, three-, or four-port parameters. In addition, constant noise, constant gain and stability circles may also be plotted on the Smith Chart for any two-port. A typical example of the input and output of COMPACT can be seen in Fig. 5 (taken from reference 17).

Computer-automated microwave measurements

Measurement automation provides considerably more benefits than simply reducing the time and effort needed to obtain accurate manual microwave measurements. Such benefits include increased accuracy, ease of data manipulation and processing, as well as higher productivity.

Accuracy enhancement is provided in a number of ways, depending on the specific measurement system. For example, a system's hardware limitations may require that a set of preliminary calibration measurements be performed, the number of which is determined by the complexity of the model used to represent the system's error sources. Once these sources are quantified, say as a function of frequency, their effects can be removed mathematically from all

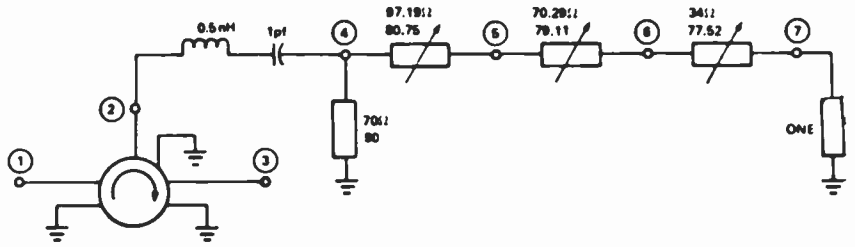


```
$ RND SCOMPACT

SUPER COMPACT  Version 1.5+1  9/10/81      27-OCT-81  18:10:14

CMD > EX13
CMD > LIS
* [COMPACT.TEST]EX13.DAT
*
F1: 8500MHZ
BLK
 THR 1 2 3 Q1
 SLC 2 4 L=.5NH C=1PF
 SST 4    Z0 70       ELEN 90       F F1
 TRL 4 5 Z0 ?97.19? ELEN ?80.75? F F1
 TRL 5 6 Z0 ?70.29? ELEN ?79.11? F F1
 TRL 6 7 Z0 ?34?    ELEN ?77.52? F F1
 ONE 7   Q2
A:2POR 1 3
END
OUT
 PRI A S
END
FREQ
 STEP 7GHZ 10GHZ 1GHZ
END
OPT
 A MS21 7.5DB
 TERM .01
END
DATA
Q1:S
* Data for 'THR' -- 3x3 s-matrix in polar form
* 7GHZ
 .026 55 .018 17 .967  93
 .963 72 .014 16 .046  14
 .056 25 .961 91 .034 125
* 8GHZ
 .031  172 .040 -119 .962  -14
 .959  -36 .039 -175 .040 -115
 .051 -118 .958  -16 .024 -159
* 9GHZ
 .034   30 .047  -48 .979 -118
 .976 -142 .014   27 .053  -59
 .045  -42 .977 -120 .043   47
* 10GHZ
 .059 -89 .092  146 .957 140
 .957 137 .063 -125 .095 137
 .078 157 .956  137 .051 -62
Q2:S
* Data for 'ONE' -- reflection coefficient in polar form
 1.34 -161
 1.8   175
 2.82  136
 2.29   74
END


CMD > ANA

CIRCUIT:  A
S-MATRIX, ZS =   50.0+J   0.0  ZL =   50.0+J   0.0

  FREQ          S11          S21          S12          S22        |S21|  STAB SGN
   GHz        MAG   ANG    MAG   ANG    MAG   ANG    MAG   ANG     db     K  B1
   7.00000  0.060   14   2.378   64   0.965   93   0.100   24   7.53   1.37 -
   8.00000  0.105 -134   2.140  -17   0.958  -13   0.103 -107   6.61   1.27 -
   9.00000  0.120  111   2.480   54   0.985 -117   0.141  120   7.89   1.41 -
  10.00000  0.190   99   2.613   90   0.975  139   0.214   81   8.34   1.43 -

PLOT, PRINT OR QUIT? (PL/PR/<Q>): Q
```

Fig. 5. *Examples of SUPER-COMPACT input and output.*

subsequent measurements. As more error sources are accounted for, the more accurate the corrected data are likely to be. However, the complexity of the mathematics required to perform the error correction increases. A point is quickly reached where adequate error correction could not practically be done without the use of the computer. This is especially true in cases requiring iterative correction algorithms where closed-form solutions are not available.

The accuracy enhancement provided by error correction not only compensates for hardware limitations but also allows measurements to be performed on circuits in the presence of other networks whose contributions are not desired. On the basis of additional calibration measurements (or previously measured data), the desired circuit parameters can be removed from the measured data by appropriate algorithms. Useful applications of such de-embedment procedures are the removal of contributions from a device's matching circuits or the effects of connectors from the measured data. Such techniques have been applied to our network-analyzer system described below.

The improved accuracy afforded by measurement automation can also be obtained by ensuring measurement repeatability. Computer-controlled swept-frequency or swept-power measurements can ensure that the frequency and/or power will be accurate and identical on all successive sweeps. Additional parameters such as signal modulation, device biases, and temperature can be held to precise specifications as well.

Once data has been acquired by the measurement system, the computer can process, display, and store it. The data presentation can range from simple listings to full-color graphic displays, permitting the user to see the end results of the measurements right at the test site. The ability to conveniently store this data is one of the most important aspects of automation. This allows other programs (for example, CAD programs) to access the data for further processing.

From a productivity standpoint, computer-automated measurement and testing provides other benefits as well. Proper software design allows the less-skilled operators to perform these complex measurement tasks. For example, in a manufacturing environment, assembly-line testing systems could enable one to perform a series of measurements, process the data, perform tolerance checking based on predetermined criteria, display the results in an appropriate format, and catalog the entire sequence, all via a few simple menu-driven commands. In a research environment, the measurement system is made more flexible, allowing the user to have more control over the measurement sequence and over how the data is to be processed and displayed. In this case, it is desired to provide the more skilled user with as much information as possible, upon which further design efforts can be based.

Automated measurement systems

A variety of automated microwave-measurement systems have been developed at RCA. These include a highly interactive network-analyzer system,[18,19] a high-power network analyzer,[20] a microwave waveform-measurement system,[21] and a load-pull measurement system.[22,23] In each of these systems, the computer plays the following roles in the measurement process:

- Prompts the operator for the appropriate actions or input required during the measurement procedure;
- Provides control over the test instrumentation;
- Acquires measurement data from the instrumentation;
- Corrects the data based on calibration information and computes the desired output parameters;
- Presents the processed data to the operator; and
- Stores the data for future use.

Although the above discussion is applicable to all the automated systems, the network analyzer is the most heavily used measurement system in the microwave circuit-design process. We will, therefore, describe this system in some detail.

Automated network analyzer system: PLANA/1000. The automated network analyzer system is shown in Fig. 6. This instrumentation configuration is similar to the Hewlett-Packard 8409B system,[24] but with the addition of an S-parameter test set, programmable power supplies for device biasing, and programmable power meters. The main difference, however, is the use of an HP-1000F minicomputer as the system controller in place of an HP-9845T desk-top calculator (normally provided with the standard system), and the development of an extensive controlling software package called PLANA/1000 (Phase-Locked Automatic Network Analyzer/HP-1000).[18,19] In addition, a color-graphics-display system has been added to provide real-time interactive color graphics. A complete system is shown in Fig. 7.

The use of the HP-1000 minicomputer as the system controller and the color-graphics-display system provide capabilities that surpass those of the commercially available HP-8409 system. Supported by a user-configured operating system, the HP-1000 supports high-level-language program development, multiple terminals, and multi-user capabilities. The multi-programming feature means that the computer can control several automated systems concurrently, as well as support other users while measurements are taking place. As mentioned above, perhaps the most significant advantage in using the HP-1000 is the ease of establishing a database of corrected measurement data and the ability to access that data from other programs and terminals, for use in either CAD or production environments.

PLANA is a highly interactive, user-oriented measurement system. The PLANA/1000 software provides for hardware calibration and device measurement, device de-embedment algorithms, extensive listing and plotting routines (including color graphics), complete operator control over all the instruments controlled via the HP-IB (IEEE-488) bus, and data-file management. A mnemonic interpreter allows simple English command strings to be entered at the terminal. Commands can also be entered via a digitizing tablet. A large percentage of the commands are interactive with the color-graphics system, allowing for various types of real-time user interaction.

PLANA/1000 offers five modes of system calibration, the choice of which depends on the type of measurement (reflection, transmission, or both) and the desired degree of error correction (ranging from simple one-term transmission normalization to a complete twelve-term system error model). The standard calibration procedures use short circuits, a choice of opens or offset shorts, and fixed or sliding loads

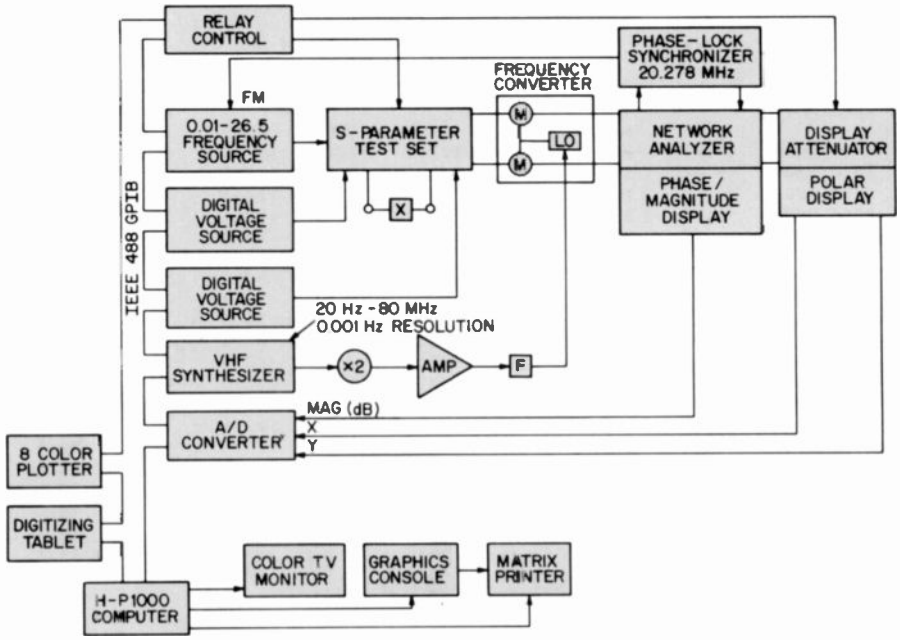

Fig. 6. *The PLANA system hardware configuration.*

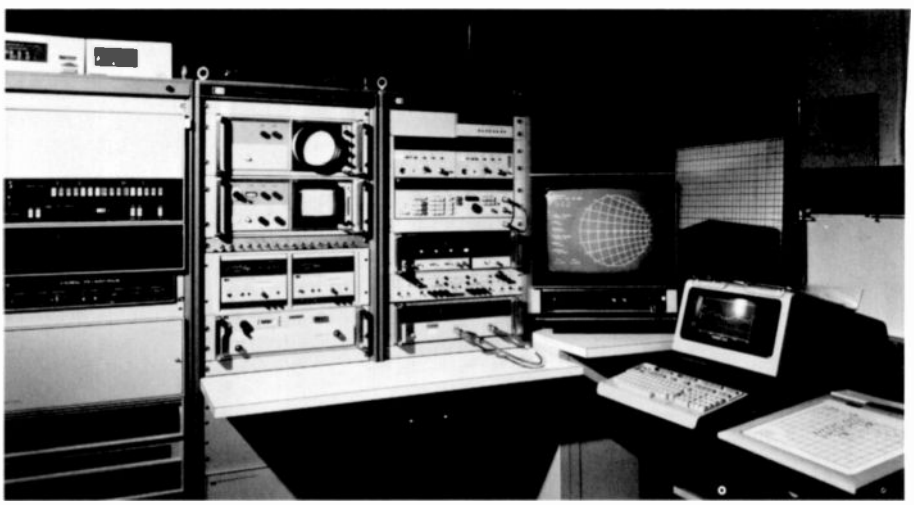

Fig. 7. *The PLANA/1000 measurement system, showing the HP-8409 instrumentation the HP-1000F computer, and the color-graphics subsystem.*

TWO-SECTION FILTER #2 12:37 PM THU., 17 DEC., 1981
100UW INPUT

FREQ(MHz)	S11		S21		S12		S22	
	DB	ANG	DB	ANG	DB	ANG	DB	ANG
9450.0000	-.67	19.1	-46.93	127.5	-41.15	107.1	-.10	28.0
9470.0000	-.58	16.4	-46.26	141.4	-41.06	112.6	-.10	25.4
9490.0000	-.63	13.3	-46.67	125.5	-41.29	124.1	.03	21.7
9510.0000	-.59	10.3	-41.88	105.9	-39.55	113.4	.10	18.1
9530.0000	-.67	6.2	-35.08	105.0	-36.28	98.9	.26	15.2
9550.0000	-.75	1.8	-32.27	105.3	-32.19	100.3	.39	11.7
9570.0000	-.86	-3.8	-29.28	100.2	-28.53	99.4	.51	8.0
9590.0000	-1.09	-11.0	-24.75	92.2	-23.94	91.0	.64	2.3
9610.0000	-1.29	-22.8	-18.52	81.1	-18.02	77.9	.66	-7.4
9630.0000	-3.49	-55.7	-9.72	47.1	-9.66	47.5	.17	-28.8
9650.0000	-14.81	90.4	-2.10	-37.3	-2.85	-40.5	-7.54	-77.1
9670.0000	-10.19	69.9	-2.94	-139.3	-3.80	-132.9	-6.77	120.4
9690.0000	-2.24	51.4	-11.48	156.1	-10.73	160.0	-.15	62.3
9710.0000	-1.01	34.4	-19.30	135.8	-17.70	137.8	.20	41.0
9730.0000	-.70	24.7	-24.84	122.0	-22.90	128.6	.22	31.5
9750.0000	-.76	18.5	-29.28	117.1	-26.51	120.8	.25	26.1
9770.0000	-.84	13.9	-33.74	124.9	-30.00	118.8	.21	22.6
9790.0000	-.88	10.2	-37.44	111.3	-34.79	115.8	.27	19.2
9810.0000	-.91	6.9	-37.05	78.6	-38.11	116.4	.34	16.4
9830.0000	-.88	3.3	-39.22	66.2	-35.53	134.2	.44	14.4
9850.0000	-.84	.1	-40.18	45.8	-36.71	140.6	.55	11.6

Reference Planes: RP1= 0.000cm, RP2= 0.000cm

Fig. 8. *Sample listing of PLANA measurement data.*

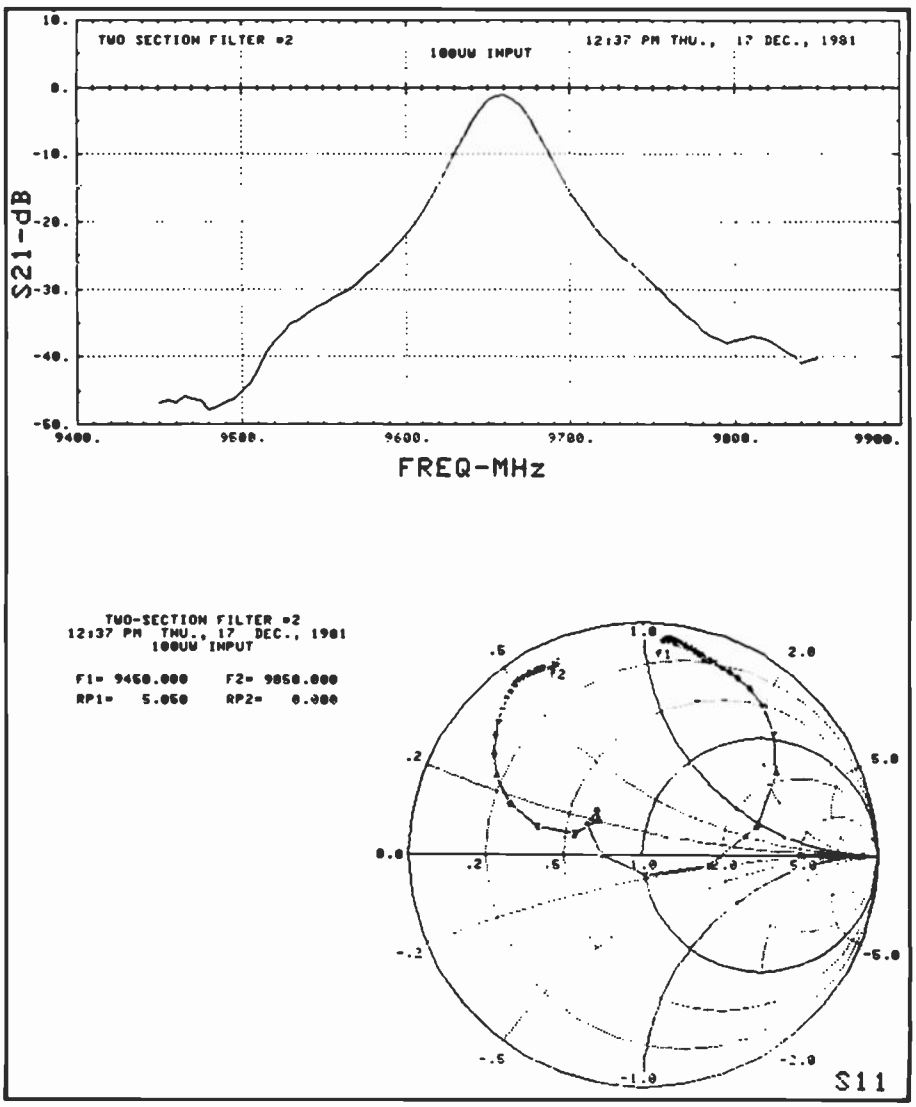

Fig. 9. *Examples of PLANA video graphics on the HP-2648 terminal.*

as the calibration standards.[25,26] TSD, a new procedure that uses only a Thru, Short, and a Delay (a longer thru) as the calibration standards, is also being implemented.[27]

Device measurements can be performed in three modes. Normally, measurements are made at all test frequencies, corrected for system errors, and made ready for listing or plotting. The continuous mode performs the device-measurement loop repetitively, updating the listed or plotted results automatically after each loop. The real-time mode is a special case of the continuous mode using the color display. In this mode, a reflection or transmission measurement is performed, corrected, and displayed on the color monitor (in rectangular, polar, or Smith-chart format) as the data are being acquired. The result is a real-time display of corrected S-parameter data (S_{11} or S_{21}) dynamically updated at a rate of about seven points per second. This allows the user to perform operations such as device tuning while measurements are taking place, and to see the effects in real-time.

PLANA/1000 offers a wide variety of listing formats and video graphics using the HP-2648 terminal. Output options include S-parameters, impedance, admittance, group delay, gain, and stability factor. Any data that can be listed can also be plotted at the terminal. The graphics include rectangular and polar displays (with automatic scaling) and Smith-chart formats. Some examples are shown in Figs. 8 and 9.

The color-graphics system and digitizing tablet, shown in Fig. 10, further enhance the capabilities of the PLANA system. By switching the input commands over to the tablet, using the digitizing pen, the operator can get a variety of displays by simply touching the appropriate boxes on the tablet. But the use of the tablet does more than just eliminate typing. It allows the user to perform interactive commands that cannot be done via the keyboard. For example, using the rotate commands, the measurement-reference planes can be moved in either direction, while the data on the display is instantly updated. Similarly, using the marker commands, the user can "slide" markers across the displayed data and get a readout of the magnitude and phase at any desired position. Figure 11 shows some of the output-format capabilities of the color display.

The present system is very flexible and expandable. Work is continuing in an effort to develop new features, including a time-domain analysis segment,[28] a macro-command processor, and increased use of the

digitizing tablet and color graphics.

Whereas the automated network-analyzer system is an extremely versatile system for characterizing microwave circuits and devices, its operation is limited to small-signal measurements. To perform measurements under large-signal conditions, three systems have been devised. The first is an extension of the standard network analyzer system, the second uses a unique technique to measure voltage and current waveforms in the circuit, and the third uses a programmable impedance tuner.

Automated high-power network-analyzer system. The network-analyzer system described above is normally operated at low power levels (typically less than zero dBm at the input of the device under test) due to limitations imposed by the reflectometer and detector circuitry. To perform large-signal, swept-power measurements with such a system, the incident power level must be controlled and the output power from the circuit under test must be attenuated to be within the operating range of the network analyzer. This can be accomplished by providing a source capable of the maximum power level required, a programmable input attenuator, and a pair of programmable attenuators to maintain appropriate power levels with respect to the network-analyzer detectors.

Figure 12 shows a block diagram of the modified network analyzer used to make high-power reflection or transmission measurements.[20] The system is first calibrated with respect to the power at a particular frequency by measuring the power available at port 1 as a function of the input-attenuator setting, and then characterizing either the reflection or transmission path (amplitude and phase response without device) as a function of the same attenuator settings. For reflection, the device under test is replaced by a short; for transmission, port 1 is connected through to port

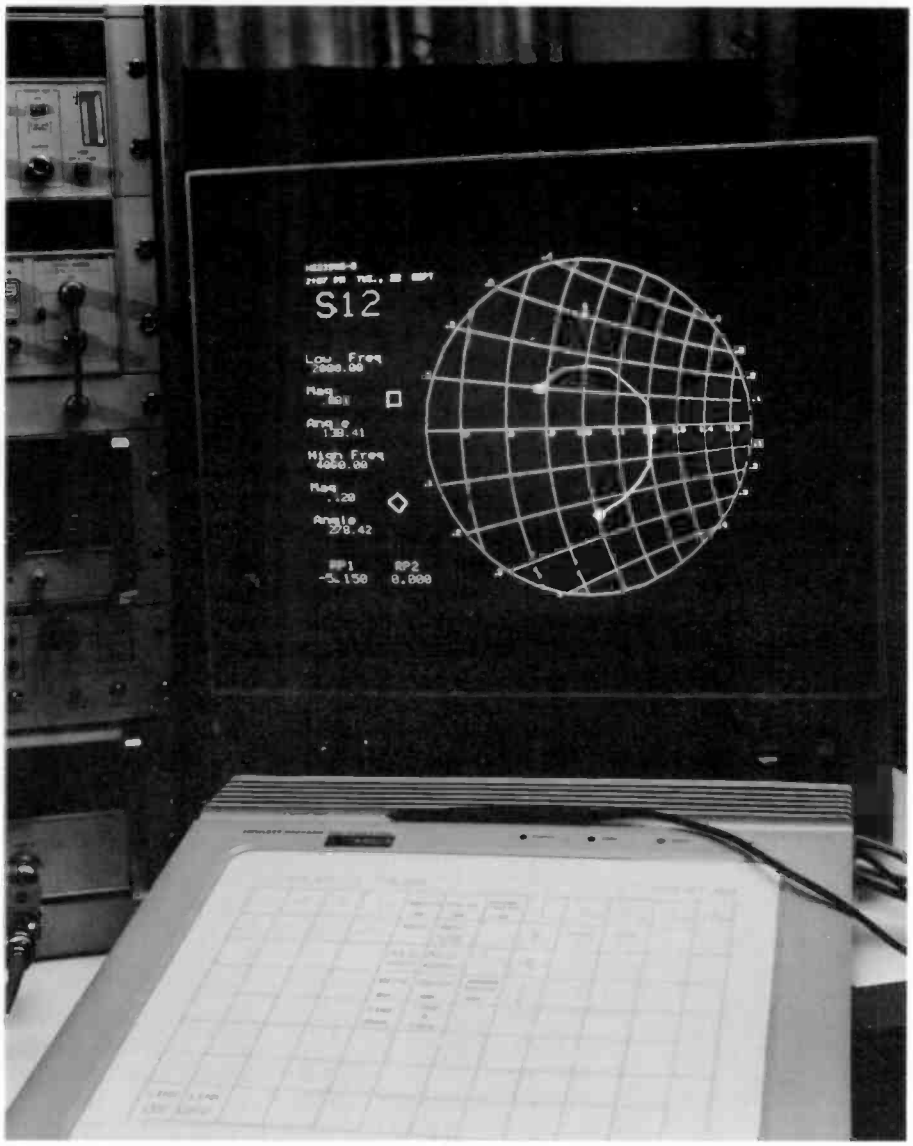

Fig. 10. *Digitizing tablet and color monitor used with PLANA.*

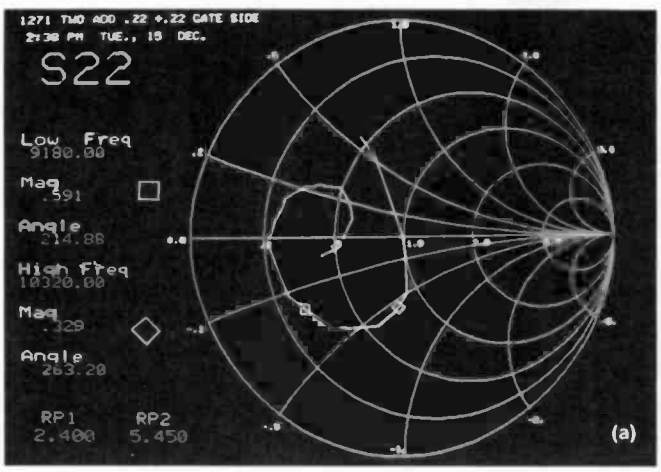

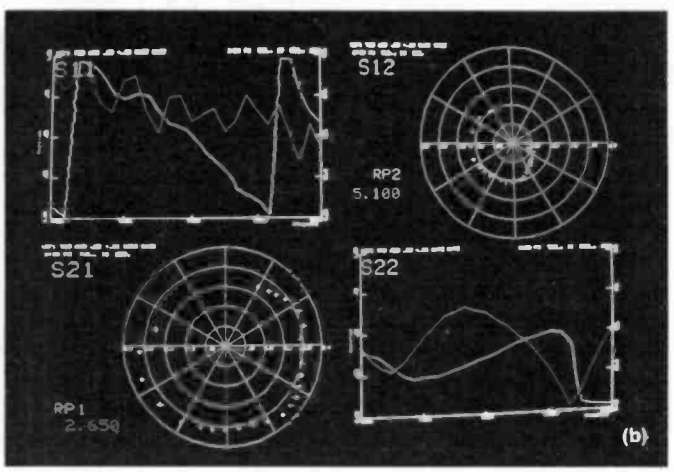

Fig. 11. *Examples of color-graphics displays.* ***(a)*** *Smith-chart overlay.* ***(b)*** *Simultaneous display of all four S-parameters.*

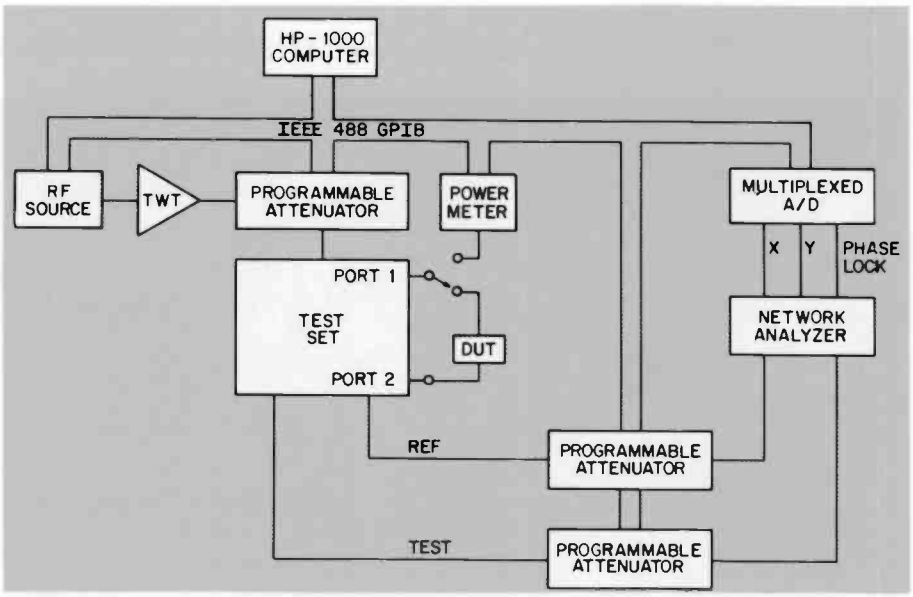

Fig. 12. *The high-power network analyzer system.*

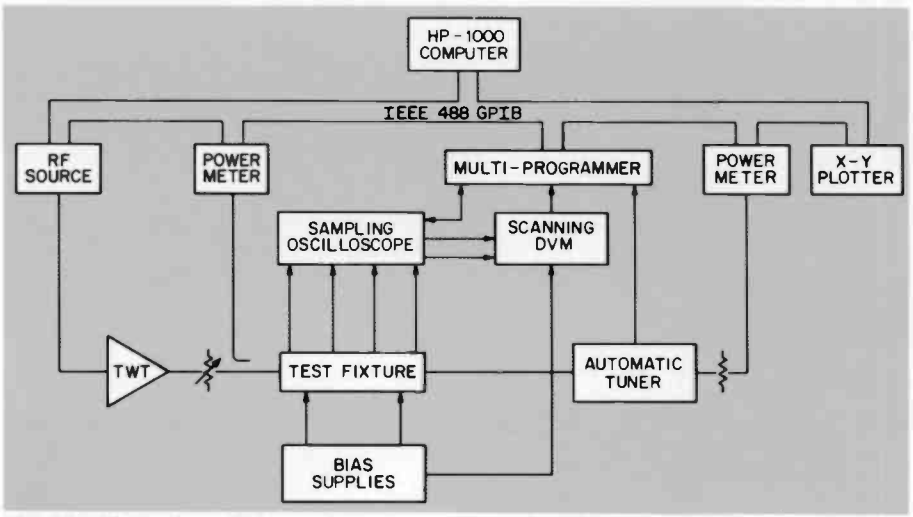

Fig. 13. *The automated waveform-measurement system.*

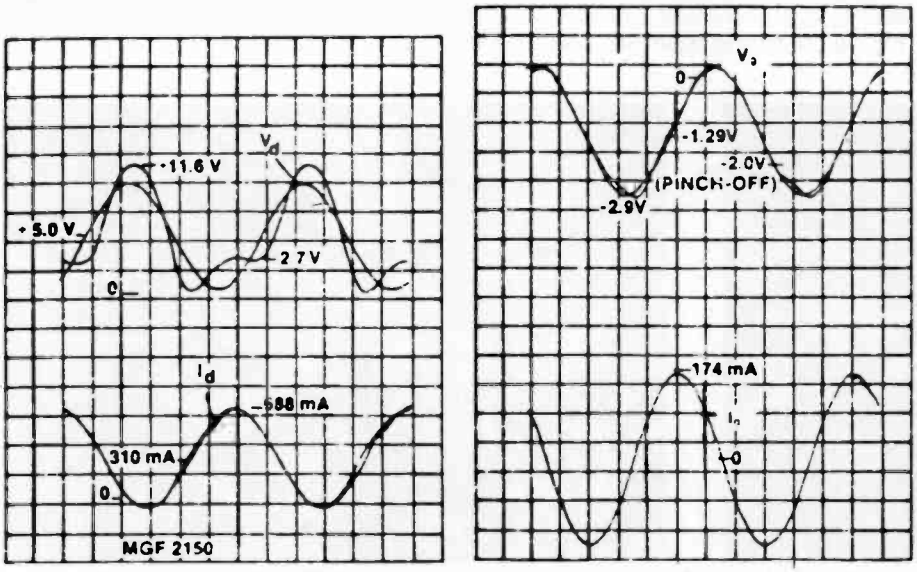

Fig. 14. *Sample plot of an FET gate voltage and current waveforms produced from the automated waveform measurements.*

2. This procedure is then repeated for each frequency. The large signal amplitude and phase response for the device under test is then obtained by inserting the device, repeating the attenuator sequence, and correcting the measured data for the appropriate path errors. This technique is especially useful in obtaining the static amplitude-modulation-to-phase-modulation characteristic of amplifiers.

Automated waveform measurement system. To perform nonlinear waveform measurements at the device level under large-signal operating conditions, a system to measure the voltage and current waveforms of active devices (for example, FETs) has been developed.[21] Waveform measurements yield important information regarding transistor saturation, breakdown voltage, cutoff frequency, and other factors affecting the efficiency of amplifier performance. With detailed knowledge of such nonlinear characteristics, transistor amplifiers can be better designed for optimum power and/or efficiency.

A block diagram of the waveform measurement system is shown in Fig. 13. The FET under test is mounted in a test fixture containing input and output matching circuits and four tuned resistive probes to sample the voltage at different points in the circuit. Power in and out of the test circuit is monitored by programmable power meters. By the use of computer-controlled rf switches, signals from the probes are multiplexed to the vertical inputs of a dual-channel sampling oscilloscope. The horizontal (time) axis of the oscilloscope is controlled via a D/A converter. This enables the computer to step across the horizontal axis and sample the waveform at 256 points. At each point the vertical outputs of the oscilloscope are read via an A/D converter and stored. The result is a digitized representation of the voltage waveforms present at each probe.

Data processing consists of first transforming the voltage data into the frequency domain using the fast Fourier transform. This data is then corrected for the frequency response of the voltage probes, using previous calibration data stored in disc files. Then, using transfer matrices for the appropriate circuit sections, the current spectra are calculated from the corrected voltage spectra. Finally, the current spectra are reverse transformed back to the time domain. Plots of the voltage and current waveforms are then generated by the computer on an X-Y plotter. A typical waveform-measurement plot is shown in Fig. 14.

Automated load-pull measurement system. In the design of microwave circuits, it is often desirable to determine the circuit performance as a function of the input or output impedance. Such information enables one to design circuits that give optimum performance (for example, maximum output power, highest efficiency). Unfortunately, the use of calibrated tuners to provide a desired impedance level cannot always provide the required accuracy and repeatability. Additionally, the use of manual tuners to search for impedance loci that result in constant circuit performance with respect to some desired parameter (such as gain or efficiency), would be prohibitively time consuming. Consequently, an automated tuning (load-pull) system has been developed.[22,23]

The system, shown in Fig. 15, uses a double-ended coaxial slotted-line section as the tuning assembly. Two dielectrically insulated metal slugs ride on the inner conductor, driven by stepper motors under computer control. The use of a computer to control the position of the tuning elements allows the designer to either determine the impedance corresponding to the present position of the tuner or to automatically set the tuner to a desired impedance level. More important, under computer control the system can perform several automatic search routines. These include mapping of impedance contours for constant power gain, output power, or efficiency; searching for specific target values of power or efficiency; and searching for the maximum power or efficiency point. Automatic plotting of the impedance contours (or specific points) is performed on a Smith chart by an X-Y plotter (Fig. 16).

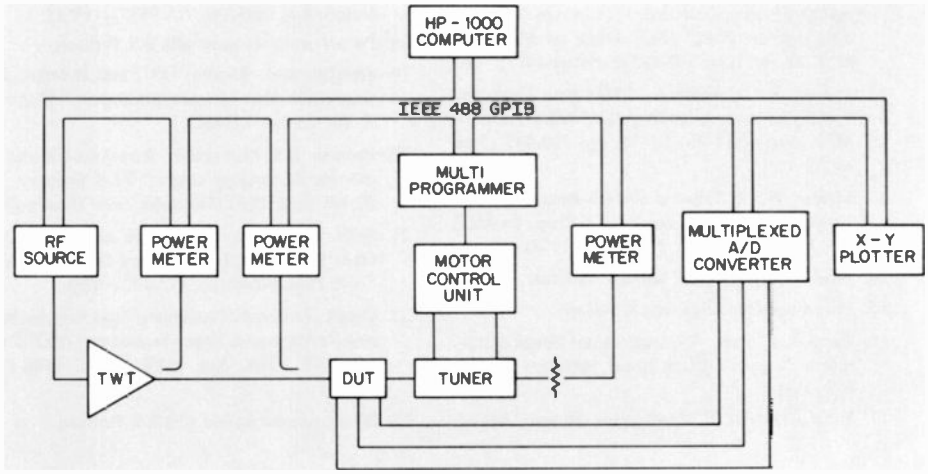

Fig. 15. *The automated load-pull measurement system.*

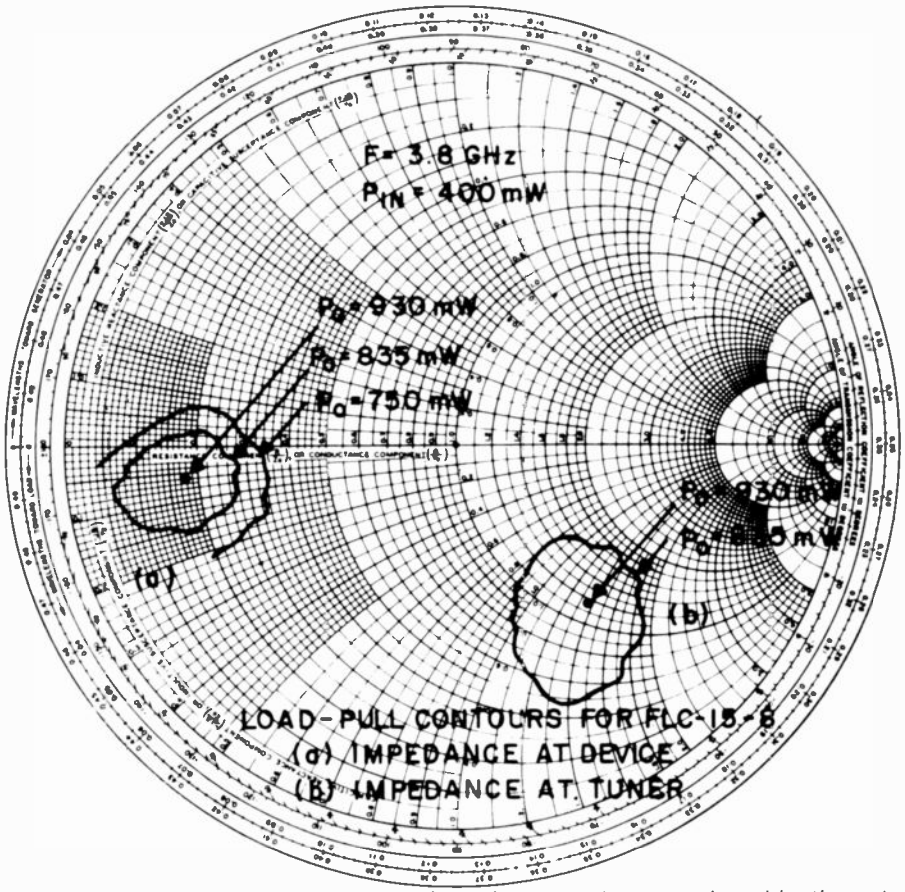

Fig. 16. *Examples of constant-power impedance contours produced by the automated load-pull system.*

Summary

The overall process of microwave circuit development is greatly improved by the use of CAD and CAT. These tools help the engineer produce results faster, more accurately, and repeatably. The computer allows circuit designers to spend more time interpreting data and designing. In the future, computer-aided design should produce friendlier user interfaces, increasingly accurate models, on-line database capabilities, and more.

References

1. Weiss, J.A., "Microwave Propagation on Coupled Pairs of Transmission Lines," *Advances in Microwaves*, ed. L. Young and H. Sobol, Vol 7, Academic Press (1974).
2. Private communication with A. Presser, RCA Laboratories.
3. Wheeler, H.A., "Transmission Line Properties of a Strip on a Dielectric Sheet on a Plane," *IEEE Trans. on MTT*, Vol. MTT-25, No. 8 (August 1977).
4. *ibid.*, "Formulas for the Skin Effect," *Proc. IRE*, Vol. 30 (September 1942).
5. Yamashita, E., *et al.*, "Microstrip Dispersion in a Wide Frequency Range," *IEEE Trans. on MTT*, Vol. MTT-29, No. 6 (June 1981).
6. Akhtarzad, S., *et al.*, "The Design of Coupled Microstrip Lines," *IEEE Trans. on MTT*, Vol. MTT-23, No. 6 (June 1975).
7. Oe, W.P., "Design Equations for an Interdigitated Directional Coupler," *IEEE Trans. on MTT*, Vol. MTT-23, No. 2 (February 1975).
8. Private communication with F.J. Campbell.
9. Akhtarzad, S., and Johns, P.J., "Three-Dimensional Transmission-Line Matrix Computer Analysis of Microstrip Resonators," *IEEE Trans. on MTT*, Vol. MTT-23, No. 12, pp. 990-996 (December 1975).
10. Kompa, G., and Mehran, R., "Planar Waveguide Model for Calculating Microstrip Components," *Electr. Lett.*, Vol. 11, pp. 459-460 (1975).

11. Menzel, W., and Wolff, I., "A Method for Calculating the Frequency Dependent Properties of Microstrip Discontinuities," *IEEE Trans. on MTT*, Vol. MTT-25, No. 2, pp. 107-112 (February 1977).

12. Mehran, R., "Calculation of Microstrip Bends and Y-Junctions with Arbitrary Angle," *IEEE Trans. on MTT*, Vol. MTT-26, No. 6, pp. 400-405 (June 1978).

13. Menzel, W., "Calculation of the S-Parameters of an Unsymmetrical T-Junction," *IEEE Trans. on MTT*, Vol. MTT-26, No. 3, p. 217 (March 1978).

14. Private communication with B.S. Perlman.

15. Private communcation with S. Perlow.

16. Gupta, K.C., *et al.*, *"Computer-Aided Design of Microwave Circuits,"* Artech House, publisher, pp. 632-637 (1981).

17. *Super-COMPACT, Applications Manual*, Vol. 1, (available through Compact Engineering, 1131 San Antonio Rd., Palo Alto, CA 94303) (1981).

18. Private communication with B.S. Perlman.

19. Perlman, B.S., Rhodes, D.I., and Schepps, J.L., "Interactive ANA Measurement System," *Microwave J.*, Vol. 25, No. 4 (1982).

20. Perlman, B.S., "Laboratory Automation in the Microwave Technology Center," *RCA Engineer*, Vol. 20, No. 4, pp. 75-81 (December 1974/January 1975).

21. Sechi, F.N., *et al.*, "Waveforms and Saturation in GaAs Power MESFETs," *Digest 8th Europ. Micro. Conf.*, Paris, France, pp. 473-477 (1978).

22. Cusack, J.M., *et al.*, "Automatic Load Contour Mapping for Microwave Power Transistors," *IEEE Trans. Micr. Th. Tech.*, Vol. MTT-12, pp. 1146-1152 (1974).

23. Private communication with B.S. Perlman.

24. "8409B Automatic Network Analyzer," *Hewlett-Packard Operating and Service Manual*, Hewlett-Packard Co., Santa Rosa, CA (1980).

25. Fitzpatrick, J.K., "Automatic Network Analyzer Accuracy: How To Get It, Lose It, Then Regain It," *Micr. Sys. News*, Vol. 10, pp. 77-93 (1980).

26. Rytting, D., "An Analysis of Vector Measurement Accuracy Enhancement Techniques," Hewlett-Packard Network Measurements Div., Santa Rosa, CA (1981).

27. Franzen, N.R., and Speciale, R., "A New Procedure for System Calibration and Error Removal in Automated S-Parameter Measurements," *Proc. 5th Europ. Micr. Conf.*, Hamburg, Germany, pp. 69-73 (1975).

28. Hines, M.E., and Stinehelfer, H.E., Sr., "Time Domain Oscillographic Microwave Analysis Using Frequency Domain Data," *IEEE Trans. on Micr. Th. Tech.*, Vol. MTT-22, pp. 276-282 (1974).

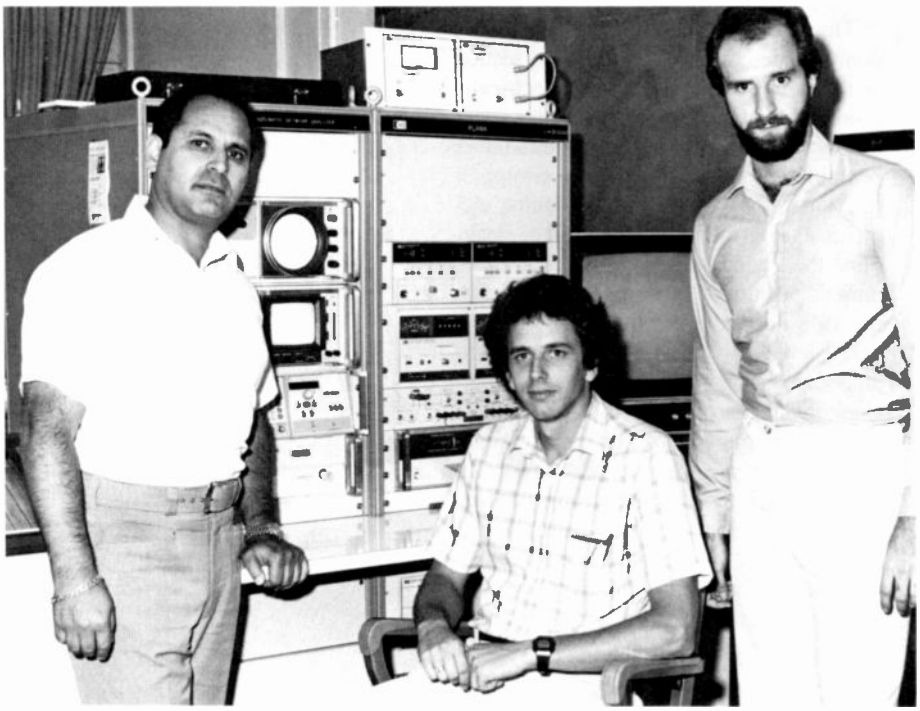

Authors (left to right) Perlman, Schepps, Rhodes

Jonathan Schepps received the BA degree in Biology from Hofstra University in 1976, and the MSE and PhD degrees in Bioengineering from the University of Pennsylvania in 1978 and 1981, respectively. His graduate work involved the use of the microwave network analyzer for accurate dielectric measurements on biological materials and an analysis of the biophysical mechanisms responsible for the mesured properties. Since July 1981, he has been working for the Microwave Technology Center at the RCA David Sarnoff Research Center, Princeton, N.J., in the area of microwave design and measurement automation. He is a Member of Technical Staff.
Contact him at:
RCA Laboratories
Princeton, N.J.
TACNET 226-2185

David Rhodes received the BSEE degree from Rutgers University in 1980 and the MSE degree in electrical engineering from Princeton University in 1982, under the RCA Graduate Study Program. As a Member of Technical Staff, he is currently working in the areas of Computer-Aided Design (CAD) and Testing (CAT) for microwave applications at the RCA David Sarnoff Research Center, Princeton, N.J.
Contact him at:
RCA Laboratories
Princeton, N.J.
TACNET: 226-3165

Barry Perlman received the BEE degree from the City College of New York in 1961, and the MSEE and PhD Degrees in Electrophysics from Brooklyn Polytechnic Institute in 1964 and 1973, respectively. He is presently Manager of CAD and Testing in the Microwave Technology Center at the RCA David Sarnoff Research Center, Princeton, N.J. His group is responsible for the development of computer-aided design, advanced automated measurement techniques and other computer aids to engineering. He has published more than 30 technical papers in the fields of solid-state devices, microwave networks and CAD, and he has received four patents. In 1969, he received an engineering achievement award for advanced device development, and in 1970, he shared an RCA Laboratories Outstanding Achievement Award for his part of a team effort in the development of wideband transferred-electron amplifiers. In 1975, he received an individual RCA Laboratories achievement award for his contribution to computer-aided design and laboratory automation. He is founding member and current President of the HP-1000 Computer International Users Group.
Contact him at:
RCA Laboratories
Princeton, N.J.
TACNET: 226-2661

G.P. Bolger | V.D. Holaday

Computer design and testing of a microwave antenna-feed manifold

Complex equations that define critical microwave parameters are solved by computer at RCA Automated Systems.

Abstract: *A computer program was developed for the design of a microwave stripline antenna-feed manifold. The program outputs dimensioned drawings that can be interfaced with the Applicon for photomask generation. A program was also developed for automatic measurement and optimization of the manifold. Several manifolds have been built in microwave bands and qualified to full environmental requirements for an airborne antenna application. These manifolds achieved a phase tracking of ±2 degrees and an amplitude tracking within 5 percent of designed value over nearly an octave bandwidth (in H-I-J bands).*

Computer design of microwave devices has replaced the traditional practice of interpolating values from standard design curves. Microwave parameters are derived from complex equations that before the use of computers were subject to time-consuming calculations, that due to their complexity, were subject to error. Each time new designs were required, the time-consuming process was repeated. A computer program was written that performs all the calculations and then outputs dimensioned drawings.

Test programs have been developed to control all performance measurements using the HP8409 automatic network analyzer and to output results in such a manner that minimum operator interpretation is required. In addition, test measurements for all manifolds are stored in a data bank for future reference.

©1982 RCA Corporation
Final manuscript received July 30, 1982
Reprint RE-27-5-14

Antenna-manifold requirements

A very-low-level sidelobe (>30 dB down) Chebyshev array has been developed at Automated Systems for operation over an octave bandwidth in the H-I-J band region. The array has six elements, is flush mounted, and conforms to the mounting surface. The antenna-feed manifold then must be a group of unequal split power dividers that will give the desired amplitude taper with in-phase characteristics at the output ports. The phase variation requirement of the manifold has been found to be ±2 degrees at the low-frequency end of the band, while amplitude tracking must be within 5 percent of the desired value across the band. These characteristics must be obtained while maintaining high isolation between the output ports.

Design considerations

The main considerations in the design of the manifold were to keep size and weight minimal since the antenna is designed for airborne use. The two main candidates for manifold construction were stripline and microstrip.

Microstrip/stripline difference

Microstrip consists of a conductor above a ground plane, separated by an insulating medium. Stripline differs from microstrip in that the conductor is sandwiched between two ground planes, each separated by an insulating medium. Power dividers were built and tested using both types of construction. Stripline has a better-controlled dielectric material (especially with the possible bonding of the ground plane) than microstrip, which has a partial air dielectric. This is advantageous under high-humidity conditions. The stripline allows a low-profile package when completed. These reasons, coupled with the slightly lower cost per unit, led to the choice of stripline over microstrip for this application. To keep production costs low, the manifold had to be easily produced and assembled, but just as important the testing and trimming process had to be simple yet effective.

Power dividers—design detail

The power dividers chosen were described by Wilkinson[1] for the case of an equal division of power. This was later modified by Parad and Moynihan[2] for the special case of an unequal power split. The basic power divider is a series-terminated, three-port, in-line circuit. It consists of a pair of quarterwave sections with an impedance of 59.4 ohms, which are series terminated at the output into a 100-ohm resistor. A quarterwave transformer was added in front of the power-division junction to transform from the 50-ohm input to the 35-ohm impedance seen at the junction. In the case of the unequal split, output quarterwave impedance transformers were added to the normal three-port circuit. The design equations for the impedances of the quar-

Table I. *A summary of the design equations for unequal split power dividers. Pa and Pb are the relative power levels at the two output ports. The ratio of these, represented by K, is the defining parameter for the impedance of all quarterwave impedance transformers, Z_1, Z_2, Z_3, Z_4 and Z_5 as well as the input and output characteristics impedance, Z_0, shown in Fig. 1. R is the isolation resistor which is connected between the junction of Z_2 with Z_4 and the junction of Z_3 with Z_5.*

$$K^2 = P_b / P_a$$

$$Z_1 = Z_o \left[\frac{K}{1 + K^2} \right]^{1/4}$$

$$Z_2 = Z_o \left[K^{3/4} (1 + K^2) \right]^{1/4}$$

$$Z_3 = Z_o \left[\frac{(1 + K^2)}{K^{5/4}} \right]^{1/4}$$

$$Z_4 = Z_o \sqrt{K}$$

$$Z_5 = Z_o / \sqrt{K}$$

$$R = Z_o \left[\frac{(1 + K^2)}{K} \right]$$

terwave sections of the power dividers are shown in Table I. In this case Z_0 equals 50 ohms. P_a and P_b are the desired output powers.

R is the isolation resistor, which is different from 100 ohms for the case of unequal power division. Figure 1 shows a schematic layout of the power divider.

A set of in-house computer programs aided in the design, dimensioning and final layout of the individual power dividers, as well as the complete manifold. The HP9845 computer is used as a design tool in conjunction with the 9872A plotter to pro-

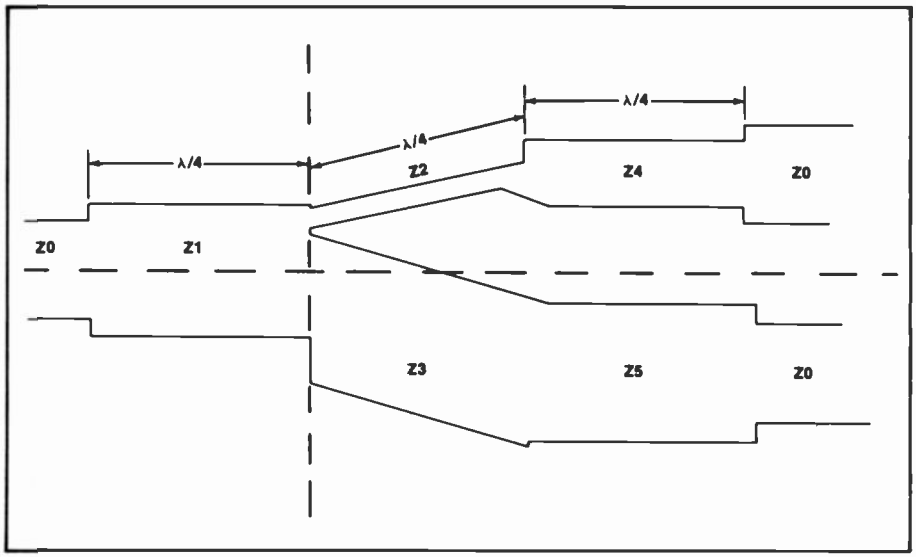

Fig. 1. *Typical center conductor pattern for an unequal split power divider fabricated in stripline. This is a scaled drawing indicating the physical relationship between the various quarter-wave impedance transformers.*

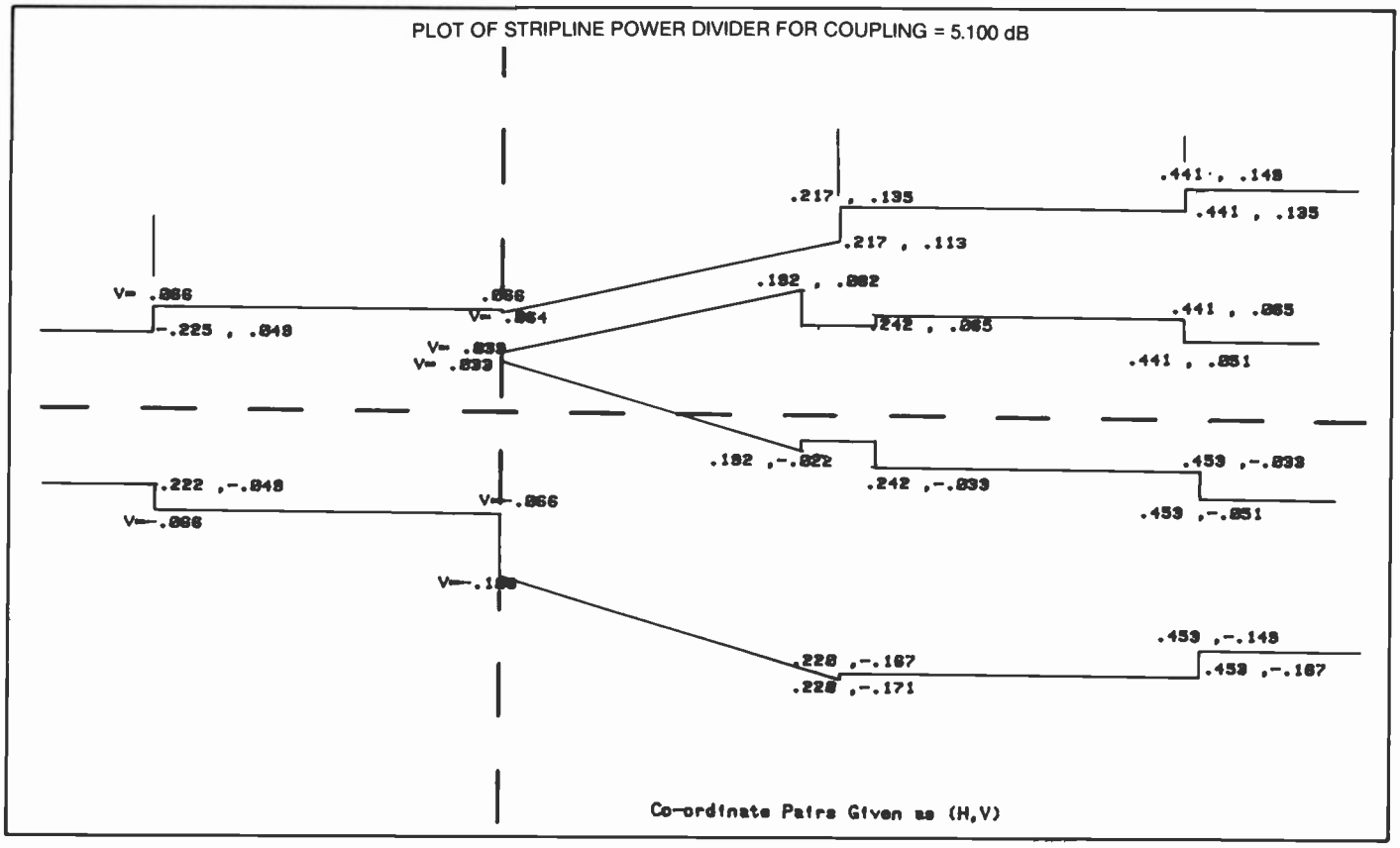

Fig. 2. *A representative output of the power divider design program giving the end point coordinates of all straight-line sections. All coordinates are referenced to the respective horizontal and vertical dashed lines.*

duce scaled drawings of the devices.

Figure 2 shows a drawing of a power divider with dimensions, produced by the 9872 plotter. The drawings of the individual power dividers were then assembled together and interfaced with the Applicon system for photomask generation. Figure 3 shows a negative of the combined manifold produced by Applicon.

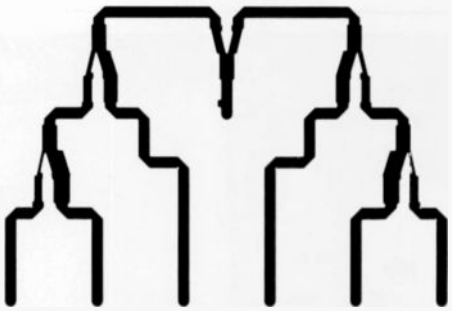

Fig. 3. *Computer developed photo mask used for etching center conductor pattern for complete manifold. Three different ratio power dividers are combined to form the required six-element array feed manifold.*

Hardware description

The entire manifold is etched on 0.062-inch-thick RT/duroid (manufactured by Rogers Corporation) material. The etched board is installed in a channelized housing as shown in Fig. 4. After the mating unpatterned board is installed, a gasketed cover is attached using seal screws. Since all output connections are via hermetically sealed pins, the completed package is unaffected by humidity. The completed manifold package, after testing and trimming, is installed onto the back of the array to make-up the antenna assembly as shown in Fig. 5. The array shown with integral

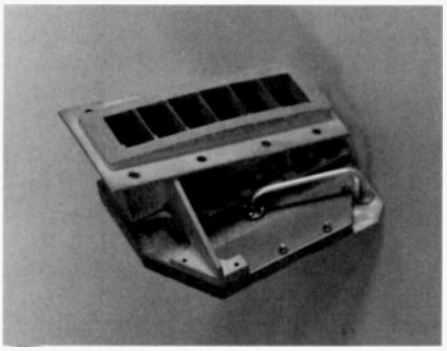

Fig. 5. *Sealed manifold attached to rear of antenna array after testing and trimming. The conformal array is shown with integral radome removed to show details of waveguide radiators.*

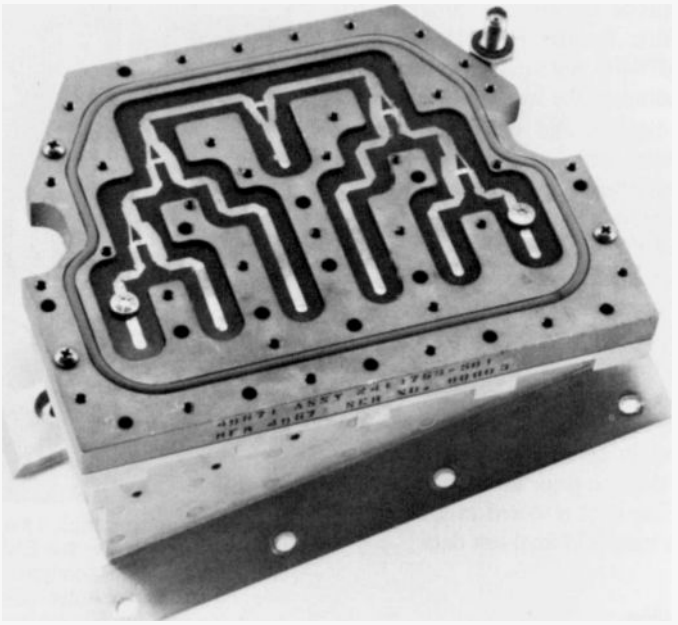

Fig. 4. *The complete manifold etched on glass microfibers reinforced PTFE board installed in channelized manifold housing. The microwave input and six outputs are via hermetically sealed pins on the back side of the housing. A mating unpatterned board and cover are installed prior to mating with antenna array.*

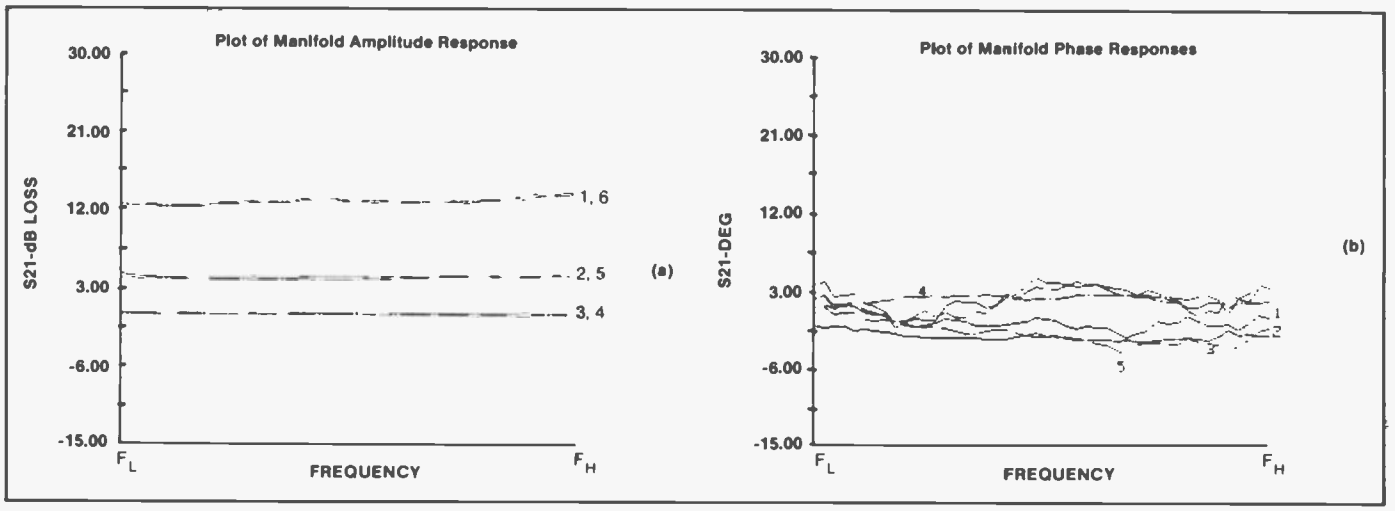

Fig. 6. *Outputs of the program developed for manifold testing and trimming using a controlled network analyzer. The magnitude plot shows the relative amplitude of each of the six outputs in dB, with the average of port 3 and port 4 as the reference. The phase plot shows the relative phase of each of the six outputs with respect to the average of port 3 and port 4.*

radome removed, is a six-element arrangement that uses open-ended waveguide radiators. The face of the array is contoured to conform to the air-vehicle mounting surface.

Computer testing

Performance trimming of the manifold is required to achieve precise phase and amplitude tracking. The trimming process involves a preliminary test of the assembled manifold with an adapter in place of the array. The manifold is then tested for phase and amplitude tracking. A program has been written for the HP9845 computer with the HP8409 Automatic Network Analyzer to compare the measurements of the manifold outputs and determine the required phase and amplitude corrections based upon a set of previously established criteria. Figure 6(a) shows a plot of phase tracking of the six manifold ports. Figure 6(b) shows the amplitude tracking of the manifold outputs. Notches are printed in the stripline corners. Tabs are positioned over the corners to decrease phase delay, and corners are uncovered to increase phase delay. After the trim has been completed, a final test is performed on the unit to measure response prior to mating with the antenna. The data is stored in a file along with other manifold final-test data.

Conclusion

The described design programs have proven to be an accurate and efficient aid in the design of a microwave antenna-feed manifold with stringent performance requirements. Additionally, the test program has permitted performance evaluation and optimization with minimum operator involvement. These programs have contributed significantly to the realization of the feed manifold and consequently the very low sidelobe-level array.

Acknowledgments

The authors would like to thank Gerard DesAutels for his work in the development of the test and design programs.

References

1. Wilkinson, E., "An N-Way Hybrid Power Divider," MTT-8, No. 1, pp. 116-118 (Jan. 69).
2. Parad, L. I. and Moynihan, R. L., "Split Tee Power Divider," MTT-13, No. 1, p. 91-95 (Jan. 1965).

Garrett Bolger graduated from Villanova University in 1980 with a BSEE degree. Since joining the Radiation Systems Engineering section of Automated Systems, he has been responsible for the application of the computer to solve various component and subsystem design problems.
Contact him at:
Automated Systems
Burlington, Mass.
TACNET: 326-2051

Veldon Holaday, Senior Engineering Scientist, is a member of the Radiation Systems Engineering section at Automated Systems. Mr. Holaday originally joined RCA in June 1958 and was involved in the development of parametric amplifiers as well as other microwave devices at Airborne Systems Division in Camden. He transferred to Burlington in 1962 and has been involved in the development of microwave systems and devices for automatic test equipment and airborne electronic systems. He has had hardware design responsibliity for FET amplifiers and the microwave portion of airborne ECM systems. Mr. Holaday received his BSEE from the University of Missouri in 1958 and completed the course work for a MSEE at the University of Pennsylvania in 1960.
Contact him at:
Automated Systems
Burlington, Mass.
TACNET: 326-2336

Patents

Automated Systems

Armstrong, L.R.
Testing the condition of a turbocharger—4334427

Commercial Communcations Systems Division

Abt, R.F. | Behrend, W.L.
Linear loading for PWM filter—4336615

Dennison, R.C. | Walter, J.M.
Synchronizing system with chroma parity detection—4339770

Dischert, W.A.
Length counter for web transport system—4335411

Zorbalas, G.S.
Rapid correlation of recorded information—4335401

Consumer Electronics

Harlan, W.E.
Composite timing signal generator with predictable output level—4337478

Marsh, J.C., Jr. | Snell, M.L., Jr.
Audio de-emphasis circuit—4335470

O'Leary, D.B.
Video disc player—254712

O'Leary, D.B.
Video disc player—264713

Torres, R. | Henderson, J.G.
Automatic tuning circuit arrangement with switched impedances—4339827

Willis, D.H.
Television receiver high voltage protection circuit—4335335

Government Communications Systems

Coyle, P.J.
Method for interconnecting solar cells—4340803

McGuire, K.E. | Brokl, S.S.
Jam-resistant TV system

Packer, M. | Black, D.D.
Coated printed circuit wiring board and method of soldering—4340157

Government Systems Division

Hillenbrand, L.J. | Preston, J.R. | Berry, D.A.
High density information disc—4340629

Laboratories

Alig, R.C. | Barkow, W.H. | Gross, J.
Color television display system having improved convergence—4335366

Aschwanden, F.
Triax safety circuit—4335412

Berkman, S. | Metzl, R.
Method of and apparatus for growing crystal ribbon—4334948

Carlson, D.E.
Fabricating amorphous silicon solar cells by varying the temperature of the substrate during deposition of the amorphous silicon layer—4339470

Credelle, T.L.
Focus mesh structure and biasing technique for flat panel display devices—4335332

Dinter, K.M.
Digital tracking system—4335408

Goldman, A.
Etching method using a hardened PVA stencil—4339528

Goldman, A.
Etching method using a PVA stencil containing n-methydl acrylamide—4339529

Goldsmith, N. | Hsu, S.T.
Method of forming an improved gate member for a gate injected floating gate memory device—4334347

Goodman, A.M.
Method and apparatus for determining minority carrier diffusion length in semiconductors—4333051

Gopog, I. | Leedom, M.A. | Wittke, J.P.
Method and apparatus for positioning a tapered body—4341472

Haferl, P.E.
Vertical deflection circuit—4338549

Holmes, D.D.
Information transmission during first-equalizing pulse interval in television—4335402

Hsu, S.T.
Method of making electrically programmable control gate injected floating gate solid state memory transistor—4332077

Kaganowicz, G. | Robinson, J.W.
Method of coating substrates with an abrasive layer—4339471

Levin, L.J.
Optical recording medium with a thick overcoat—4340959

Marder, W.Z.
Apparatus for handling deformable components supported in a matrix—4333592

Mawhinney, D.C.
Vehicle identification system—4339753

Medwin, L.B.
CMOS device with silicided sources and drains and method—4336550

Miko, S.
Free-running push-pull inverter—4334267

Miller, E.A.
RF heating coil construction for stack of susceptors—4339645

Pampalone, T.R.
Aqueous developable poly(olefin sulfone) terpolymers—4341861

Pankove, J.I.
Method for fabricating adjacent conducting and insulating regions in a film by laser irradiation—4339285

Presser, A.
Electronically tunable resonator circuit—4338582

Reitmeier, G.A. | Dischert, R.A.
Adaptive amplitude averaging for weighting quantizing noise—4334237

Sauer, D.J.
Differential amplifier having a low-pass characteristic—4342001

Tamutus, D.J.
Method of fabricating a color-selection structure for a CRT—4341591

Tanguay, D.J. | Weitzel, C.E.
Use of silicide to bridge unwanted polycrystalline silicon *p-n* junction—4333099

Toda, M. | Osaka, S.
Rotative motor using a piezoelectric element—4339682

VanRaalte, J.A. | Fairbanks, D.W.
Stylus tip positioning technique—4341437

Warren, H.R.
Crosstalk filtering arrangement with variable frequency filtering TC remove effects of FM carrier—4335394

Williams, J.J., Jr. | Dischert, R.A.
Hardware reduction by truncation of selected number of most significant bits for digital video system using subsampling and adaptive reconstruction—4340940

Wine, C.M.
Video accessory having channel identifier—4336555

Wittke, J.P.
Method for machining a workpiece with a beam of radiant energy assisted by a chemically-reactive gas—4332999

Wolkstein, H.J.
Optimization circuit for a serrodyne frequency translator—4338520

Missile & Surface Radar

Goodwin, W.V. | Williams, J.S.
Radar system—4336540

Landry, N.R.
Short horn radiator assembly—4338609

Patent Operations

Christensen, R.M.
Sound field transmission system surrounding a listener—4316058

Picture Tube Division

Griesemer, C.E.
Method for vaporizing getter material in a succession of cathode-ray tubes—4335926

Hale, J.R.
Beading apparatus for making an electron gun assembly having self-indexing insulating support rods—4341545

Handel, R.R.
CRT with arc suppression means therein—4338543

Howard, J.V.
Television deflection yoke mount—4338584

Raush, R.G.
Method and device for separating parts from a strip of material—4334945

RCA Staff

Mackey, D. | Fox, E.D.
Color kinescope convergence measuring system—4316211

RCA "SelectaVision" VideoDisc Operations

Amery, J.G.
Chrominance transcoder—4314273

Bock, M.D.
Apparatus for molding a recorded disc—4334349

Castle, R.M.
Speed deviation detector for servo controlled disc mastering turntable—4316143

Castle, R.M.
Head suspension velocity control apparatus for electromechanical recorder—4317192

Chio, S.
Diamond cleaning—4339281

Chio, S. | Kim, G.A.
Stylus tip fabrication from a synthetic diamond stone—4340954

Christopher, T.J.
Video disc stylus position sensor system—4327434

Elliott, C.A.
Video disc player having turntable assist apparatus—4326284

Elliott, C.A.
Disc player having turntable height varying apparatus—4328575

Hughes, L.M.
Carriage reset apparatus for disc record player—4321702

John, G. | Heyman, P.M. | Bortfeld, D.P.
Variable pitch grooved label for video disc—4341952

Kelleher, K.C.
Processor controlled video disc servo system—4340949

Langley, H.M. | Stephens, J.W.
Video disc defect detector—4325134

McNeely, M.L.
Method for producing disc records having molded-in center holes—4327047

Manson, E.T.
Stone-positioning apparatus and method—4335544

Miller, M.E.
Minimum tracking force stylus—4340956

Nyman, F.R. | Stevens, B.N.
Calamari, Jr. J.A.
High density information disc processing—4327048

O'Connell, P.E. | Hughes, L.M. | Fletcher, J.D.
Video disc player having carriage drive apparatus—4325136

Patel, B.P. | Prusak, J.J.
Record stamper protector—4327830

Price, P.F.
Mold preparation method—4332841

Prusak, J.J. | Whitehurst, M.L.
Apparatus for electroforming—4341613

Prusak, J.J.
Spacer for stacked recorded discs—4316281

Riddle, G.H. | Taylor, B.K.
Video disc cartridge having a self retaining electrode—4320490

Rustman, J.C.
Apparatus for video disc stylus electrode reconditioning—4320491

Shearer, J.D.
Solder draw pad—4339784

Smith, T.E.
Video disc molding process—4318877

Stewart, M.C.
Transducer displacement apparatus for video disc player—4333174

Stewart, M.C.
Carriage alignment apparatus for video disc player—4342109

Taylor, B.K.
Flylead for a video disc stylus cartridge—4337536

Torrington, L.A.
Video disc caddy—4316539

Wharton, J.H.
Video signal processing apparatus—4316210

Wharton, J.H. | James, J.E.
Video processor employing variable amplitude compression of the chrominance component—4316213

Whitehurst, M.L.
Method for the manufacture of recording substrates for capacitance electronic discs—4316778

Ziegel, D.H.
Levelable lapping machine—4321772

Solid State Division

Atherton, J.H. | Dreisbach, W.C.
Level shift circuit—4321491

Benner, T.E. | Month, A.
Mesh assembly having reduced microphonics for a pick-up tube—4323814

Bismarck, O.H.
Fast level shift circuits—4314166

Butterwick, G.N.
Photomultiplier tube having directional

alkali metal vapor evaporation means—4333031

Cardinal, R.E.
Apparatus for resistance welding of an electo-optic device housing—4322599

Giordano, R.L.
Dual output switching circuit—4337423

Gubitose, N.F.
Apparatus for transferring pure abrasive material from one hopper to another—4325419

Hall, W.B.
Megasonic jet cleaner apparatus—4326553

Harbaugh, W.E.
Sputter-ion pump for use with electron tubes having thoriated tungsten cathodes—4334829

Harford, J.R.
Television intermediate frequency and amplifier with feedback stabilization—4342005

Harford, J.R.
Television automatic gain control system—4329713

Hoover, M.V.
Differential-input complementary field-effect transistor amplifier—4333057

Hoover, M.V.
Operational amplifier employing complementary field-effect transistors—4333058

Hoover, M.V.
Complementary symmetry FET frequency converter circuits—4334324

Hoover, M.V.
Class AB push-pull amplifiers—4335360

Kaplan, L.A.
Over-current protection circuits for power transistors—4321648

Kessler, Jr., S.W.
Resilient contact ring for providing a low impedance connection to the base region of a semiconductor device—4327370

Limm, A.C. | O'Brien, J.T.
Colgrove, T.V. | Nyul, P.
Injection laser diode array having high conductivity regions in the substrate—4331938

Malchow, M.E.
Circuit arrangement useful in developing decoupled operating voltages for IF amplifier stages of an integrated circuit—4327332

Malchow, M.E.
Arrangement for selectively routing a signal indicative of received signal strength to different portions of a radio receiver in response to different levels of a control signal—4330866

Malchow, M.E.
Circuitry for generating electric signals with proportional opposite-sense rates of change—4322691

Malchow, M.E.
Biasing of transistor amplifier cascades—4334198

Martin, J.G.
Susceptor for heating semiconductor substrates—4322592

Mayer, A.
Wettable carrier in gas drying system for wafers—4318749

McDonie, A.F.
Rubidium-cesium-antimony photocathode—4331701

McDonie, A.F. | Miller, W.K.
Method of making potassium, cesium, rubidium, antimony photocathode—4339469

Preslar, D.R.
Digital phase comparator with improved sensitivity for small phase differences—4322643

Pudiosky, J.P.
Chuck for use in testing of semiconductor pellets—4327325

Schade, Jr., O.H.
Dynamic current supply—30948

Schade, Jr., O.H.
Temperature-correction network for extrapolated band-gap voltage reference circuit—4325017

Schade, Jr., O.H.
Temperature-correction network with multiple corrections as for extrapolated band-gap voltage reference circuits—4325018

Schade, Jr., O.H.
Level shift circuit—4318015

Schade, Jr., O.H.
Amplifier using lateral and vertical transistors—4334196

Stewart, R.G.
Memory circuit with means for compensating for inversion of stored data—4337522

Stewart, R.G.
Noise protection circuits—4339809

Stewart, R.G.
Overload protection circuit for output driver—4329600

Tomasetti, C.M. | Harsh, M.D. | McDonie, A.F.
Method for stabilizing the anode sensitivity of a photomultiplier tube—4341427

Wallace, L.F.
Low cost reduced blooming device and method for making the same—4329702

Wheatley, Jr., C.F.
Method of fabricating a Schottky barrier contact—4313971

Wilson, R.E.
Switch closure sensing circuit—4318087

Witte, W.R.
Power transformer with high coupling coefficient—4320373

Wu, C.T.
Hardware interpretive mode microprocessor—4323963

Pen and Podium

Recent RCA technical papers and presentations

To obtain copies of papers, check your library or contact the author or his divisional Technical Publications Administrator (listed on back cover) for a reprint.

Advanced Technology Laboratories

W.R. Lile | J.W. Betz (AS)
J.J. Wolcin (NUSC)
Real-Time Maximum A Posteriori-Line Extraction—Naval Postgraduate School, Monterey, Calif. (7/20/82)

Automated Systems

J.W. Betz | W.R. Lile (ATL)
J.J. Wolcin (NUSC)
Real-Time Maximum A Posteriori-Line Extraction—Naval Postgraduate School, Monterey, Calif. (7/20/82)

M.J. Cantella
Schottky Barrier FPA Performance Criteria and Applications—Materials Research Council Advisory Group to DOD/DARPA, La Jolla, Calif. (7/19/82)

Laboratories

M.S. Abrahams
Defects in Heteroepitaxial Silicon on Sapphire—*40th Ann. Proc. Electron Microscopy Soc. Amer.*, Washington, D.C. (1982)

R. Amantea
Interpreting the Beta Versus Collector Current and Temperature Characteristics of a Transistor—*RCA Review*, Vol. 43, No. 2 (6/82)

I. Balberg | P.J. Zanzucchi
Polarized Infrared Transmittance of Carbon Black-Polyvinylchloride—*App. Phys. Lett*, Vol. 40, No. 12 (6/15/81)

R.A. Bartolini
Optical Recording: High-Density Information Storage and Retrieval—*Proc. of the IEEE*, Vol. 70, No. 6 (6/82)

J.A. Bauer
Chip Carrier State of the Art—Panel Member and Presentation: International Electronic Packaging Society (IEPS), Workshop on Chip Carriers, New York, N.Y. (6/21/82)

D.W. Bechtle | A. Siegel
An Optical Communications Link in the 2.0-6.0 GHz Band—*RCA Review*, Vol. 43, No. 2 (6/82)

A.E. Bell
Recording Mechanisms in Antireflection Trilayer Structures—J. Appl. Phys., Vol. 53, No. 5 (5/82)

E. Belohoubek
Radar Control for Automotive Collision Mitigation and Headway Spacing—*IEEE Transactions on Vehicular Technology*, Vol. VT-31, No. 2 (5/82)

D. Botez
Effective Refractive Index and First-Order-Mode Cutoff Conditions in InGaAsP/InP DH Laser Structures (λ = 1.2-1.6 μm)—*IEEE Journal of Quantum Electronics*, Vol. QE-18, No. 5 (5/82)

D. Botez
High-Power Single-Mode Semiconductor Diode Lasers—International Electron Devices Meeting (12/81)

J.K. Butler | D. Botez
Mode Characteristics of Nonplanar Double-Heterojunction and Large-Optical-Cavity Laser Structures—*IEEE Journal of Quantum Electronics*, Vol. QE-18, No. 6 (6/82)

M. Caulton | A. Rosen
P.J. Stabile | A. Gombar
***p-i-n* Diodes for Low-Frequency High-Power Switching Applications**—*IEEE Transactions on Microwave Theory and Techniques*, Vol. MTT-30, No. 6 (6/82)

H.P. Chang, (Univ. Missouri)
J.H. Thomas, III
An XPS Study of X-ray-Induced Dehydrochlorination of Oxygen-free PVC—*Journal of Electron Spectroscopy*, Vol. 26, pp. 203-212, Elsevier Scientific Publishing Co., Amsterdam (1982)

R.S. Crandall
Deep Electron Traps in Hydrogenated Amorphous Silicon—*Physical Review B*, Vol. 24, No. 12 (12/15/81)

M.T. Duffy | J.F. Corboy | G. W. Cullen
R.T. Smith | R.A. Soltis | G. Harbeke
J.R. Sandercock
Measurement of the Near-Surface Crystallinity of Silicon on Sapphire by UV Reflectance—*Journal of Crystal Growth*, Vol. 58, pp. 10-18, North-Holland Publishing Company (1982)

M.T. Duffy | P.J. Zanzucchi | W.E. Ham
J.F. Corboy | G.W. Cullen | R.T. Smith
Optical Characterization of Silicon and Sapphire Surfaces as Related to SOS Discrete Device Performance—*Journal of Crystal Growth*, Vol. 58, pp. 19-36, North-Holland Publishing Company (1982)

M. Ettenberg | D. Botez
High-Power Diode Lasers for Optical Recording with Operating Lifetimes in Excess of 10,000 h.—*Electronics Letters*, Vol. 18, No. 4 (2/18/82)

M. Inoue
Quantum Yield of Electron-Hole Pairs in Semiconductors—*Physical Review B*, Vol. 25, No. 6 (3/15/82)

A.C. Ipri | L.B. Medwin
N. Goldsmith | F.W. Brehm
Two-Dimensional Dynamic Analysis of Short-Channel Thin-Film MOS Transistors Using a Minicomputer—*IEEE Transactions on Electron Devices*, Vol. ED-29, No. 4 (4/82)

L. Jastrzebski (MIT) | J. Lagowski
G.W. Cullen | J.I. Pankove
Hydrogenation Induced Improvement in Electronic Properties of Heteroepitaxial Silicon-on-Sapphire—*Appl. Phys. Lett.*, Vol. 40, No. 8 (4/15/82)

L. Jastrzebski | M.T. Duffy
J.F. Corboy | G.W. Cullen
Relationship Between Crystallinity and Electronic Properties of Silicon-on-Sapphire—*Journal of Crystal Growth*, Vol. 58, North-Holland Publishing Company (1982)

W. Kern | R.B. Comizzoli (Bell Labs)
G.J. Schnable
Fluorescent Tracers—Powerful Tools for Studying Corrosion Phenomena and Defects in Dielectrics—*RCA Review*, Vol. 43, No. 2 (6/82)

S.G. Liu | S.Y. Narayan
C.W. Magee | C.P. Wu
^{29}Si Implantation into ^{40}Ar Implant-Pretreated Semi-insulating GaAs Substrates—Mobility and Activation Efficiency Enhancement—*Appl. Phys. Lett.*, Vol. 41, No. 1 (7/1/82)

P. Schnitzler
A Day in the Life of an IES*
***Information Efficient Scientist**—*IEEE Communications Magazine*, Vol. 20, No. 3 (5/82)

F.N. Sechi | R. Brown | H. Johnson
E. Belohoubek | E. Mykletyn | M. Oz
Miniature Beryllia Circuits—A New Technology for Microwave Power—*RCA Review*, Vol. 43, No. 2 (6/82)

R. Shahbender |K.S. Vanguri |B.T. Khuri-Yakub (with KYS, Inc., Palo, Alto, Calif.)
Approximate Resonance Spectrum of a VideoDisc Cutter—*RCA Review*, Vol. 43, No. 1 (3/82)

E.K. Sichel (now with GTE)
J.I. Gittelman
The Hall Effect in Granular Metal Films Near the Percolation Threshold—*Solid State Communications*, Vol. 42, No. 2 (1982)

E.K. Sichel (now with GTE)
J.I. Gittelman |P. Sheng (Exxon Research & Engineering)
Electrical Properties of Carbon-Polymer Composites—*Journal of Electronic Materials*, Vol. II, No. 4 (1982)

R.T. Smith |C.E. Weitzel (now with Motorola)
Influence of Sapphire Substrate Orientation on SOS Crystalline Quality and SOS/MOS Transistor Mobility—*Journal of Crystal Growth*, Vol. 58, North-Holland Publishing Company (1982)

E. Towe (now at MIT)
Photoluminescence of Undoped $In_{0.53}Ga_{0.47}As/InP$ Grown by the Vapor Phase Epitaxy Technique—*J. Appl. Phys.*, Vol. 53, No 7 (7/82)

J.L. Vossen
Bibliography on Metallization Materials and Techniques for Silicon Devices: VIII—*American Vacuum Society Monograph* (7/82)

J.L. Vossen
Advanced Metallization Materials and Processes for LSI and VLSI—Ninth Annual Symposium on the Physics and Technology of Integrated Circuit Fabrication, American Vacuum Society, Detroit, Mich. (5/25/82)

J.L. Vossen
The Future of VLSI Metallization—Pacific Northwest Chapter, American Vacuum Society Annual Symposium, Portland, Oregon (5/5/82)

L.K. White
Positive and Negative Tone Near-Contact Printing of Contact Hole Maskings—*RCA Review*, Vol 43, No. 2 (6/82)

Missile & Surface Radar

F.J. Buckley
ANSI/IEEE Standard 730—A Standard for Software Quality Assurance Plans—Approved by ANSI (6/21/82)

F.J. Buckley
Software Quality Assurance—EIA G33 Committee, Washington, D.C. (7/20/82)

F.J. Buckley
Software Quality Assurance—Society of Reliability Engineers, Portland, Oregon (6/22/82)

W.C. Grubb, Jr.
Solid State Electronics for Non-Electrical Engineers—Drexel Univ., Philadelphia, Pa. (4/16/82)
George Washington Univ., presented at Naval Air Station, Lakehurst, N.J. (6/4/82)
Naval Air Test Center, Patuxent, Md. (7/30/82)

W.C. Grubb, Jr.
Minicomputers and Microcomputers for Non-Electrical Engineers—George Washington Univ., Washington, D.C. (3/26/82)
Drexel Univ., Philadelphia, Pa. (5/13/82)

D.R. Higgs
Reports and Proposals—Planning, Organizing, and Doing—Technical Writers Institute, Rensselaer Polytechnic Institute, Troy, N.Y. (6/15/82)

L.W. Martinson
Trends in Signal Processing—*TREND* (6/82)

R.J. Mason
Stripline Transmission Line Isolation—Technical Note published 1/28/82

S.A. Steele
System Software Design Trade-offs for Real-Time Measurement and Control Systems—Fourth ISMM International Symposium Mini & Microcomputers in Control and Measurement, Cambridge, Mass. (7/7/82)

Engineering News and Highlights

Jon Shroyer named RCA Solid State Division IC Vice-President

Appointment of **Jon A. Shroyer** as Division Vice-President, Integrated Circuits, for RCA Solid State Division was announced recently by **Dr. Robert S. Pepper,** Vice-President and General Manager.

In this position, Mr. Shroyer reports to Dr. Pepper and will be responsible for all engineering, manufacturing and product-marketing functions for LSI, Bipolar and MOS Integrated Circuits, with operations located in Somerville, New Jersey; Findlay, Ohio; Palm Beach Gardens, Florida; and the Far East.

Before joining RCA, Mr. Shroyer was General Manager of the Semiconductor Division of Data General, Inc. where he was responsible for the design and manufacture of custom and second-source MOS and bipolar products. Before going to Data General, he was Assistant Vice-President for Wafer Fabrication at Mostek. He has also held various operations and technical positions at Texas Instruments and Motorola. Mr. Shroyer received a BSEE from the University of Illinois and attended graduate school at Arizona State University.

Griffin is Broadcast Video Systems Chief Engineer

James S. Griffin has been appointed Chief Engineer for the Broadcast Video Systems function of RCA's Commercial Communications Systems Division. Mr. Griffin is responsible for all engineering activities in

the design and manufacturing of RCA television cameras and video tape recorders.

Prior to his recent appointment, Mr. Griffin had been program manager for the digital optical disc system being developed by RCA's Government Communications Systems business unit, also in Camden. Mr. Griffin joined RCA in 1960 and has held numerous positions in engineering and engineering management.

After serving four years in the U.S. Navy, including duty as a sonarman and electronics instructor, Mr. Griffin received his bachelor's degree in electrical engineering from the University of Florida. He also has taken postgraduate courses at the University of Pennsylvania.

Staff announcements

Jack K. Sauter, Group Vice-President, announces his organization as follows: **Edward A. Boschetti,** Division Vice-President and General Manager, Distributor and Special Products Division; **D. Joseph Donahue,** Vice-President and General Manager, Consumer Electronics Division; **William L. Firestone,** Division Vice-President and General Manager, Cablevision Systems; and **John D. Rittenhouse,** Division Vice-President and General Manager, Picture Tube Division.

Commercial Communications Systems Division

Dennis J. Woywood, Division Vice-President, Broadcast Video Systems announces the appointment of **Carleton H. Musson** as Director, Video Systems Product Management, for RCA Commercial Communications Systems Division.

Consumer Electronics

D. Joseph Donahue, Vice-President and General Manager, Consumer Electronics Division, announces the appointment of **Charles A. Quinn** as Division Vice-President, Operations.

Charles A. Quinn, Division Vice-President, Operations, announces his organization as follows: **James E. Carnes,** Division Vice-President, Engineering; **Dennis L. Dwyer,** Director, Production Planning, Distribution and Transportation; **J. Patrick Keating,** Director, Purchasing; **Leonard J. Schneider,** Division Vice-President, Manufacturing; and **James R. Smith,** Division Vice-President, Product Assurance.

Leonard J. Schneider, Division Vice-President, Manufacturing, announces that **Kenneth D. Lawson,** Director, Facilities Management, will report to the Division Vice-President, Manufacturing.

Globcom

Joe Terry Swaim, Vice-President, Switched Services Engineering and Operations, announces his organization as follows: **William A. Klatt,** Director, Network Operations; **Russell E. Blackwell,** Director, Safetran Operations; **John P. Shields,** Manager, Network Engineering; **Leo A. Tita,** Manager, Administration & Traffic; **Vernon E. Wellington,** Manager, Telex and Data Operations; **Richard L. Chory,** Manager, Software Engineering; **Rudolph K. Lang,** Program Manager, Telex Systems; and **Kenneth H. Wendt,** Program Manager, Message Switching Systems.

Picture Tube Division

John D. Rittenhouse, Division Vice-President and General Manager, Picture Tube Division, announces his organization as follows: **Mahlon B. Fisher,** Division Vice-President, Engineering; **Kenneth R. Greene,** Division Vice-President, Industrial Relations; **Gerald E. LaRochelle,** Division Vice-President, Technical Contracts and VideoColor Support; **Robert K. Lorch,** Division Vice-President, Market Planning, Services and Strategic Planning; **Donald E. Marquart,** Division Vice-President, Latin America Operations; **Robert B. Means,** Division Vice-President, Sales and Market Research; **John A. Neville,** Division Vice-President, Finance; **Stanley S. Stefanski,** Division Vice-President, Manufacturing; and **Charles W. Thierfelder,** Division Vice-President, Product Safety, Quality and Reliability.

Solid State Division

John M. Herman III, Director, Integrated Circuits Design and Process Development, Solid State Technology Center, announces his organization as follows: **Andrew G. Dingwall,** Fellow Technical Staff; **Edward C. Douglas,** Manager, Advanced Process Technology; **John M. Herman III,** Acting Manager, Large Scale Integration Design; and **Roger E. Stricker,** Manager, Process Development and Technology Transfer.

John M. Herman III, Acting Manager, Large Scale Integration Design, Solid State Technology Center, announces the appointment of **Roger G. Stewart** as Leader Technical Staff, Memory Design Engineering.

Edward C. Douglas, Manager, Advanced Process Technology, Solid State Technology Center, announces his organization as follows: **Wolfram A. Bosenberg,** Leader Technical Staff, Device Analysis; **Edward C. Douglas,** Acting Leader Technical Staff, Process Technology; **Bernard C. Leung,** Leader Technical Staff, Silicon-on-Sapphire Very Large Scale Integration; and **Thomas E. Sullivan,** Leader Technical Staff, Bulk Very Large Scale Integration.

Professional activities

Magee wins award

The American Vacuum Society announced that **Dr. Charles W. Magee,** Materials Characterization, RCA Laboratories is the recipient of the 1982 Peter Mark Memorial Award. The citation reads: "for imaginative developments of secondary ion mass spectrometry as a quantitative tool for the solution of materials problems." The Peter Mark Memorial Award is given annually for outstanding technical achievement to a scientist 35 years of age or under. The award was established in 1979 by the Society in memory of Professor Peter Mark, who was the editor of the *Journal of Vacuum Science and Technology* until his untimely death. Before his appointment as Professor of Electrical Engineering at Princeton Unversity, Dr. Mark was a Member of the Technical Staff at RCA Laboratories.

Vossen names chairman

John L. Vossen, Head, Thin Film Technology, RCA Laboratories has been appointed Chairman of Publications Committee of the International Union of Vacuum Sciences, Techniques and Applications (IUVSTA). The IUVSTA is an international umbrella organization for 26 national vacuum societies.

SSD engineers help define QMOS

Dick Funk and **Bryan Petryna** attended a JEDEC meeting in Washington, D.C. to define industry standards for a high-speed CMOS logic family called QMOS.

RCA researcher chairs workshop

The 1982 SOS/SOI Technology Workshop, sponsored by the IEEE Electron Devices Society, was held at Provincetown, Mass., Tuesday, October 5 through Thursday, October 7, 1982. **Achilles Kokkas,** RCA Laboratories, was the General Chairman. The purpose of this Conference is to provide a forum of open discussion for all areas of silicon-on-insulator technologies and their application to VLSI and VHSIC. In addition to the more conventional SOS structures, interest is growing in novel materials growth

techniques and device structures and papers in these areas are encouraged.

In this issue, too

Ho-Chung Huang, Microwave Technology Center, has coauthored a chapter entitled "Thermal Design of Power GaAs FETs," which appears in a current publication, *GaAs FET Principles and Technology.* Huang has also coauthored an article for this issue of the *RCA Engineer,* as has **Herbert J. Wolkstein,** Microwave Technology Center, who received a Gold Certificate of Merit from the National Association of Old Crows (AOC). The AOC is a group devoted to exchanging information on electronic warfare problems.

Honig and Magee elected to Bohmische Physical Society

Richard E. Honig and **Charles W. Magee,** Materials Characterization Research, have been elected Scientific Members in the Bohmische Physical Society. Scientific Members are chosen for their contributions to the field of particle-solid interactions by independent, original research. Dr. Honig was cited for "contributions to the understanding of low energy ion-solid interactions" and Dr. Magee for "contributions to the fields of secondary ion mass spectroscopy and ion implantation." Membership in the Society is international and includes scientific members in Japan, Sweden, Denmark, Germany, Italy, United States and other countries.

Gounder wins speaker's award

Raj N. Gounder, Manager, Advanced Structures, at Astro-Electronics, was awarded the SAMPE Speakers Award at the N.J. Chapter SAMPE Annual Meeting held at Clinton, N.J., on June 11, 1982. Dr. Gounder was the speaker at the March 1982 meeting of the N.J. Chapter of SAMPE. The topic was: "Advanced Composite Applications in RCA Satellites."

Greenstein is society president

Bernie Greenstein, Consumer Electronics Division, Indianapolis, Ind., is President of the International Society for Hybrid Microelectronics (ISHM) Indiana Chapter. He has formerly been Program Chairman and Vice-President.

Former RCA engineer elected to Plastics Hall of Fame

Dr. Otis D. Black, a retired RCA engineer, has been elected to the Plastics Hall of Fame. He was inducted June 22, 1982, at ceremonies in Chicago for his pioneering work on printed wiring and circuits. These components revolutionized electronics by using copper foil, bonded to a thin "board" of plastic, to conduct electricity. Eventually, they replaced hand-wiring.

As a member of the Plastics Hall of Fame, Dr. Black joins notables such as George Eastman, who developed celluloid (a form of plastic) film for photography and motion pictures; Leo H. Baekeland, who developed Bakelite, one of the first widely used plastics of the industrial age; and Willard H. Dow, former head of Dow Chemical, which developed several types of improved synthetic rubber.

Dr. Black was elected for his work in developing materials and processes that led to the first commercial production of printed wiring in the United States. Today, printed wiring and circuits are in most electronic devices, and the raw plastic materials used to make them account for a $2 billion annual segment of the industry. Printed wiring boards also made transistors easier to mount and connect, and contributed directly to the spectacular growth of the transistor industry, Dr. Black's nomination notes.

Dr. Black, 69, worked for RCA, Camden, N.J., from 1942 until his retirement in 1978. As a member of a chemical laboratory team in 1947, he was assigned to develop materials and processes that would improve on a crude printed wiring design that had been developed several years before in England.

Dr. Black guided companies from several different industries, and secured the plastic, copper foil, and adhesive necessary to make the printed wiring. He then set up the first photoengraving operation using production personnel who had no photoengraving training. By 1950, RCA had manufactured printed components for the Hallicrafter company, which used them in a television tuner.

Dr. Black later designed and installed an automatic, conveyorized system for etching circuit patterns into the components. He was also the first to develop and write specifications for certain of the raw plastics materials used in components.

Dr. Black was first nominated to the Plastics Hall of Fame in 1976 by J. Harry DuBois, Chairman of the Board of Governors. The living members of the Hall of Fame and the heads of three industry associations (approximately 20 men) vote every three years on new members. Mr. DuBois said most members were nominated twice before being elected. Mr. Dubois learned of Dr. Black's contributions while researching a book on the history of plastics. Dr. Black received bachelor's, master's and doctor's degrees in physical chemistry from Ohio State University.

Retired RCA scientists honored

Three RCA retired scientists, **Albert Rose, Charles J. Young,** and **Harold G. Greig,** were honored by the Society of Photographic Scientists and Engineers at the Society's 35th annual meeting on May 12, in Rochester, New York.

Dr. Albert Rose was awarded an Honorary Membership in the Society, the highest honor that the group can bestow. Honorary Membership is awarded yearly to a scientist or engineer who has made outstanding contributions to the advancement of photographic science or engineering. Dr. Rose, who retired from RCA Laboratories as a Fellow of the Technical Staff in 1975, is internationally known for his work in the fields of photoconductivity, human vision and solar energy, including his basic contributions to the Orthicon, Image Orthicon and Vidicon TV camera tubes. For the first quarter century of television, the Image Orthicon was the principal camera tube for TV broadcasts throughout the world.

Charles J. Young was Associate Director of the Acoustical and Electromechanical Research Laboratory when he retired from RCA Laboratories in 1965. Mr. Young began work on facsimile systems in the 1930s. In 1954, Mr. Young led a group, including Harold G. Greig, which developed an electro-photographical system known as "Electrofax," which employed a special coated paper as part of its facsimile process. The system was subsequently licensed by RCA to several photocopier manufacturers.

Harold G. Greig, who retired from RCA as a Fellow of the Technical Staff in 1967, joined the RCA Laboratories facsimile group in 1943, and made contributions to almost all major areas of the Electrofax system. In 1965, he received RCA's highest honor, the David Sarnoff Award for Outstanding Technical Achievement, and in 1968, he received the Society of Reproduction Engineers' Gold Medallion Achievement Award for his invention of Electrofax.

Three Labs scientists win best paper award

Christopher H. Strolle, Glenn A. Reitmeier and **Terrence R. Smith** of the Video Systems Research Laboratory, RCA Laboratories, received the 1981 Best Paper Award at the Society for Information Display Symposium-Exhibition held April 27-May 1, 1981 in New York City for: "Rotation of Instrumentation Images on a Raster-Scanned Display Utilizing Polar Coordinate Transformation." The award was presented at the 1982 SID Symposium held in San Diego, May 1982.

Royce elected Chairman

At the Montreal meeting of The Electrochemical Society, **Martin R. Royce,** Picture Tube Division, Lancaster, Pa., was elected Chairman of the newly formed Luminescence and Display Materials group. He will serve a two-year term of office. Mr. Royce will be responsible for conference planning, dissemination of scientific papers and the promotion of new interests and technologies amongst luminescence and display materials researchers in this country and abroad.

Kern is Society Chairman

Werner Kern of the Integrated Circuit Technology Research Laboratory, RCA Laboratories, was elected Chairman of the Dielectrics and Insulation Division of the Electrochemical Society. The elections were held during the national meeting of the Society in Montreal last May.

Paglione receives best paper award

Robert W. Paglione, Microwave Technology Center, RCA Laboratories, has received a best paper award for his paper "RF and Microwave Applicators for the Treatment of Cancer," presented at the IEEE AP/MTT-S Philadelphia Section, Benjamin Franklin 1981 Symposium on Antenna and Microwave Technology.

Cohen is a panel member

Marv Cohen, RCA Astro-Electronics, has become a member of the Future (Military) Space Concepts and Operations Panel of the AFSD/NSIE/AIAA Systems and Technology Workshop II.

Balzer was Chairman

Daniel L. Balzer, RCA Astro-Electronics, served as the Chairman for the Liquid Rocket Sessions at the AIAA/SAE/ASME 18th Joint Propulsion Conference.

Astro patent awards made

Robert Miller, Chief Engineer, RCA Astro-Electronics presented awards to three employees for filing patent applications. **Irv Brown** devised a method of maintaining geosynchronous satellite radiation of the earth. **Kern Phillips** and **Terry Tracy** designed an apparatus for reducing nutation of a momentum stabilized spacecraft.

Bob Miller (left), Chief Engineer, RCA Astro-Electronics with Irv Brown.

Patent-award winners Terry Tracy (left) and Kern Phillips (right) with Bob Miller (center), Chief Engineer, RCA Astro-Electronics.

Dr. Zworykin, RCA television pioneer, dies

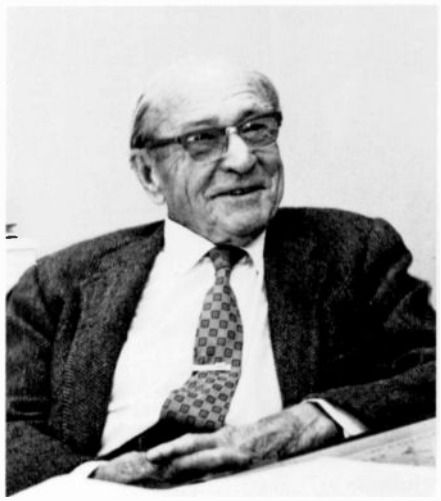

Dr. Vladimir K. Zworykin.

Television pioneer, Dr. Vladimir Kosma Zworykin died at the Princeton Medical Center on July 29, one day short of his ninety-third birthday.

Elected an Honorary Vice-President of the RCA Corporation upon his retirement in 1954, Dr. Zworykin was often called the "father of television." However, he declined the accolade, telling interviewers that hundreds contributed to television over many years. He preferred to compare television's development with the building of a ladder, explaining that as each engineer added a rung, "It enabled the others to climb a little higher and see the next problem a little better."

"Father" or not, there is no question that the achievement of practical television stems to a large extent from Dr. Zworykin's pioneering work in the 1920s and 1930s. His conception of the first practical TV camera tube, the iconoscope, and his development of the kinescope picture tube formed the basis for almost all important later advances in the field.

A Russian immigrant, he came to the United States after World War I and worked for Westinghouse in Pittsburgh from 1920 to 1929. It was there that he did some of his early work on television.

But it was not until he teamed up in 1929 with another Russian immigrant, Gen. David Sarnoff, later President and Chairman of RCA, that his television work got the management and financial backing that enabled Dr. Zworykin and the RCA scientists working with him to develop television into a practical system.

Both men never forgot their first meeting. In response to Gen. Sarnoff's question, Dr. Zworykin, thinking solely in research terms, estimated that the development of television would cost $100,000. Years later, Gen. Sarnoff delighted in teasing Dr. Zworykin by telling audiences what a "great salesman" the inventor was. "I asked him how much would it cost to develop TV. He told me $100,000, but RCA spent $50 million before we ever got a penny back from TV."

"He preferred to compare television's development with the building of a ladder . . . as each engineer added a rung, 'It enabled the others to climb a little higher and see the next problem a little better.' "

Dr. Zworykin was born on July 30, 1889, in Mourom, Russia, where his father owned and operated a fleet of boats on the Oka River. As the owner's son, he had the run of the ships and often played with the pushbuttons used to signal the engine room from the bridge. Thus, Dr. Zworykin would tell interviewers, he was intrigued with electrical communications well before he was 10 years old.

Dr. Zworykin in 1910. He studied with Boris Rosing at the Petrograd Institute of Technology.

Dr. Zworykin, in the mid-1920s, with an early version of the TV display tube (kinescope) that he invented.

Perhaps because of this interest in communications, his father sent him to the Petrograd Institute of Technology which awarded him an Electrical Engineering degree in 1912. At the institute, Dr. Zworykin studied under, and assisted, Professor Boris Rosing, to whom Dr. Zworykin credited both his decision to become a scientist and his special interest in television and electronics.

"It was not until he teamed up in 1929 with another Russian immigrant, Gen. David Sarnoff, that his television work got the backing it needed."

As early as 1906, Prof. Rosing believed that the solution to practical television was to be found, not in mechanical systems, but in the employment of cathode ray tubes. Dr. Zworykin's iconoscope and kinescope followed this line of reasoning.

In 1912, Dr. Zworykin entered the College de France in Paris, where he studied X-rays under the noted scientist

"His conception of the first practical TV camera tube, the iconoscope, and his development of the kinescope picture tube formed the basis for almost all important later advances in the field."

Dr. Zworykin with display of historic television tubes.

Professor Paul Langevin. His studies were interrupted by World War I and Dr. Zworykin had to return to Russia to serve in the Army Signal Corps. After the war, he came to the United States, becoming a citizen in 1924. He received a doctorate from the University of Pittsburgh in 1926.

Soon after arriving in the U.S., Dr. Zworykin joined the Westinghouse research staff and began investigations in the field of photoelectric emission. He also resumed his research in television. Dr. Zworykin became associated with RCA in 1929. He served as Director of the Electronic Research Laboratory, first in Camden, N.J., and from 1942 until his retirement in 1954, at Princeton, N.J.

In addition to TV, Dr. Zworykin applied his talents to a broad field of electronics and held more than 120 U.S. patents on developments ranging from gunnery controls to electronically controlled missiles and automobiles. Because of Dr. Zworykin's research activities, important devices such as various forms of secondary emission multipliers and image tubes were developed and perfected. The "Snooperscope" and "Sniperscope"—important military developments in World War II—were practical applications of research on infrared image tubes.

Dr. Zworykin's intensive study of electron optics directed his interest to the electron microscope. RCA's pioneering in the commercial development of the electron microscope typifies Dr. Zworykin's genius—not only his scientific expertise but his ability to attract and motivate good scientists.

In 1940, he hired a young Canadian graduate student, Dr. James Hillier, to work on the electron microscope. Dr. Hillier, who retired in 1977 as Executive Vice-President and Chief Scientist of RCA, decided to work for RCA because Dr. Zworykin recruited him with one question—how long would it take Dr. Hillier to build an electron microscope?—while other prospective employers engaged Dr. Hillier in theoretical discussions or emphasized their good working conditions and fringe benefits.

Working under Dr. Zworykin's guidance, it took Dr. Hillier little more than three months to build the first RCA electron microscope. Coincidentally, just three years after Dr. Zworykin was elected to the U.S. National Inventors Hall of Fame for his development of television, Dr.

(Continued on page 102)

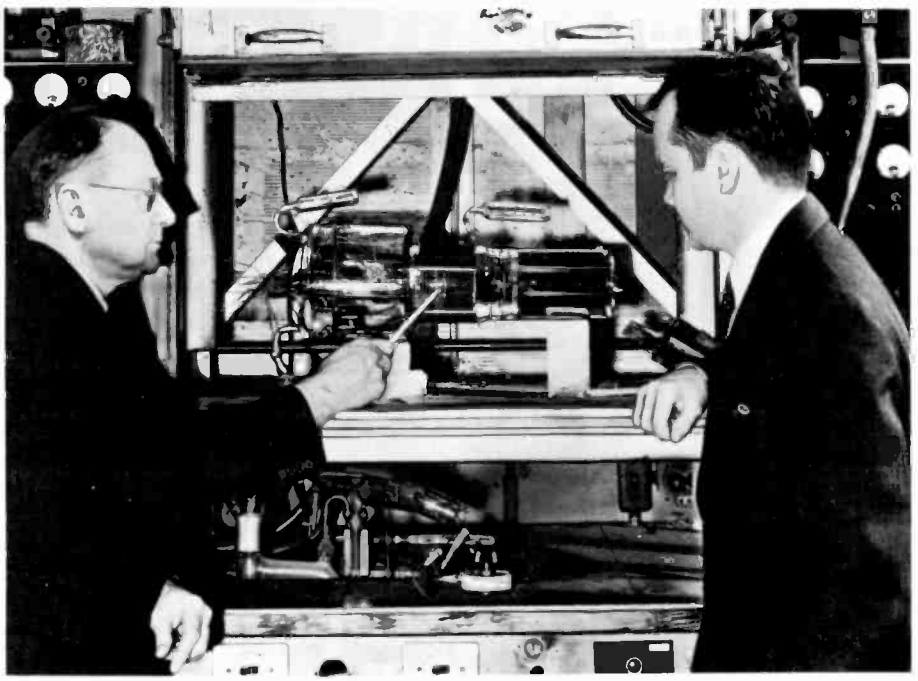

Two of RCA Victor's famous staff of television research engineers, Dr. Zworykin (left) and E.W. Engstrom, examine a new piece of equipment at Camden laboratories (circa 1939).

"RCA's pioneering in the commercial development of the electron microscope typifies Dr. Zworykin's genius—not only his scientific expertise but his ability to attract and motivate good scientists."

In Memoriam

Dr. Zworykin, or "The Doctor," which is the name by which many of us knew him, was unquestionably a great man; but I often wonder if any one of us, as an individual, is capable of appreciating the full measure of his genius. Like so many of the great people of history, The Doctor had breadth—breadth of interests, breadth of knowledge, of capabilities. He was a great inventor, but he was also an entrepreneur, a humanist, a practical psychologist, and a philosopher.

As you know, I was very close to The Doctor, both professionally and personally. I was always impressed by the visions that he constantly projected. After a while, I began to realize that his visions had a consistent theme—to use technology to enable people to do something that they wanted to do, but that they could not presently do.

His visions were not the idle daydreams of a gadgeteer. Yes, technical invention was usually the cornerstone of each of his visions, but the larger part of each vision was the outline of a complete plan for making it happen. When he explained his visions, technical people tended to hear only the technical parts. I was among those in the beginning. Business people heard only the business parts and so on. But with The Doctor, the vision was total. He dedicated his life to realizing those visions. For that, we ordinary mortals will forever be in his debt.

I would like to pass on a few personal thoughts regarding the breadth of The Doctor's personality. While The Doctor is notorious for his grossly inadequate estimate of the cost of developing television, his notoriety tends to mask the fact that he did sell the concept to General Sarnoff, and moreover, kept it sold in spite of delays and overruns.

In the laboratory, he had a very special ability to select or develop first-rate research workers. I was never sure whether he was good at selecting, or at developing, or both. It does not really matter. The fact is that there is a substantial roster of people from The Doctor's activities who have developed international reputations. Several of them are here today. There are several of us who remember The Doctor's daily visits to our laboratories, his suggestions, his needling, his discussions, his proddings. While at times he made us uncomfortable, and at times we even rebelled, the fact is, we ended up being better engineers and scientists and, on occasion, surprised even ourselves with our accomplishments. One part of his genius was his ability to inspire people to do better than their best.

He was completely impatient with bureaucracies in any form, and I used to believe he derived some kind of pleasure from finding ways to by-pass them. It was once my private story that he hired me on speculation and that it was not until I had been working for him for several months that I learned that I had no budget whatsoever. The Doctor had assumed, correctly, that it would take the accountants that long to catch up with him. I learned from that experience that his real passion was to remove any obstacle that stood in the way of "getting the job done."

In case you think that I am painting the picture of a superman, let me remind you that The Doctor was also very human. He was a good husband, as Katusha will attest, a good father and a good friend. His breadth also showed through in the wide range of his personal interests when away from his job. He had a plethora of friends from all walks of life that paralleled those interests: philosophers, writers, musicians, artists, politicians. Many, of course, were from the Russian community. Then, there were hunting companians, tennis opponents, and more. At one point in his life he even took a short excursion into flying his own plane. To be his friend was always an exhilarating experience.

Being human, he also had some foibles. As one example, he never quite believed that he had a heavy Russian accent. Yet on more than one occasion, when we had visitors at the Labs, I found myself translating for The Doctor even though he was speaking perfectly good English. I hope that these brief glimpses of The Doctor through one man's eyes have at least conveyed the message that I, for one, held him in the highest regard, not just as an illustrious inventor, but as a great man.

Dr. Zworykin has passed on. But I like to believe he died a happy man, having lived long enough to see the realization of his early great vision—to have technology take our eyes where our bodies cannot follow. While I cannot say whether he envisioned all the ramifications of the technology he initiated, I can say that the whole world is richer for his having lived.

—James Hillier
retired Executive Vice-President
and Chief Scientist of RCA

(Cont. from p. 100)

Hillier was elected in 1980 for his work on the electron microscope.

For a period of years following his 1954 retirement, Dr. Zworykin directed a Medical Electronics Center at the Rockefeller Institute in New York. In this capacity, as National Chairman of the Professional Group on Medical Electronics of the Institute of Radio Engineers, as Founder-President of the International Federation for Medical Electronics and Biological Engineering, and as Member of the Board of Governors of the International Institute for Medical Electronics and Biological Engineering Paris, he worked for the development of the use of electronic methods in medicine and the life sciences.

"He worked for the development of the use of electronic methods in medicine and the life sciences."

Mrs. Zworykin, Dr. Zworykin and Dr. Hillier with a portrait and citation presented to the "Doctor" at age 80.

Dr. Zworykin was often asked if, while working on television, he ever envisioned the worldwide entertainment media it became. He would reply that he hadn't, and credited Gen. Sarnoff with seeing TV as a new form of home entertainment. Dr. Zworykin would then go on to explain that in his early years he looked upon television as a system that would enable man to see things in places where his eyes couldn't reach. Thus, he was delighted with the first television pictures of the back side of the moon. And, when he visited the Jet Propulsion Laboratories in California to see the reception of pictures of Mars, he remarked, "This is what television is really for."

As he grew older, Dr. Zworykin curtailed his activities, spending winters in Florida, but never gave up his interest in scientific research. For many years, he was a Visiting Professor for the Center for Theoretical Studies and the Institute for Molecular and Cellular Evolution of the University of Miami in Florida. And he maintained an office at RCA Laboratories. Even at the age of 91, he would drive from his home in Princeton to his office in the David Sarnoff Research Center to read his large collection of scientific journals and reports.

In 1966, President Lyndon Johnson awarded him the United States' highest scientific honor, the National Medal of Science "for major contributions to the instruments of science, engineering and television, and for his stimulation of the application of engineering to medicine." Including the Medal of Science, Dr. Zworykin received virtually every major scientific honor among 27 major awards and numerous others from groups throughout the world. He was elected to such prestigious American societies as the National Academy of Sciences, the American Academy of Arts and Sciences, the American Philosophical Society, the American Association of the Advancement of Science, and the National Academy of Engineering.

Arnold Rose dies at age 66

Veteran packaging industry figure **Arnold Rose**, 66, of Menlo Park, Calif., died in his sleep of an apparent heart attack recently, a few days before he was scheduled to present a paper at the 32nd Annual Electronic Components Conference in San Diego, Calif.

Mr. Rose retired in 1978 from RCA after 37 years of service. He worked for a number of years at the Electron Tube Division in Lancaster and, after a brief hiatus, returned to the Semiconductor Division, then located in Harrison. Later he moved to Somerville, renamed the Solid State Division. He developed beam-lead technology at RCA, where he also made major contributions to the Trident and Safeguard programs. He had headed RCA's materials and processes laboratory and was manager of hybrid and packaging technology.

Co-workers remember Mr. Rose as a well-known man throughout the industry, whose calls to other companies would always elicit a cooperative exchange of information. He enthusiastically promoted new ideas in techniques and products, and participation in technical meetings and publications.

A manager of packaging system at Signetics for the past 3½ years, Mr. Rose conducted research in cavity package technology. Funds are being collected for a memorial in his honor to be awarded to young packaging scientists. Kenneth Picker, the fund coordinator, is a consultant and former director of Signetics' Advanced Technology Center. Information can be obtained from Dr. Picker at 19917 Merribrook Drive, Saratoga, Calif.

Technical excellence

Automated Systems technical excellence awards

Guyer

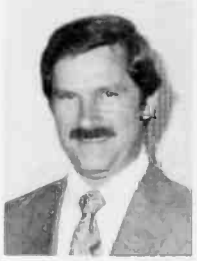
Fisher

Cortizas

The Burlington Technical Excellence Committee has selected for Individual Awards **Robert C. Guyer,** Senior Project Member, **Eldon M. Fisher,** Senior Project Member, and **Anthony P. Cortizas,** Senior Engineering Scientist.

Mini Laser Rangefinder. Cited for Technical Excellence is **Bob Guyer,** for optical/mechanical design work on the AN/PVS-X, Mini Laser Rangefinder. In five months, the Mini-LRF was transformed from a conceptual status to that of a completed engineering developmental model. Bob was responsible for the entire mechanical design and through his supervision of the optical supplier, Leitz, Canada, the optical design.

Bob demonstrated design excellence, high personal interest and diligence in the successful creation of the Mini-LRF on schedule.

Receiver synthesizer design for REMBASS. Cited for Technical Excellence is **Eldon Fisher,** for electronic design and development work on the REMBASS receiver synthesizer and data link. Eldon designed the UHF receiver synthesizer.

Eldon worked with technical experts from PM REMBASS at Fort Monmouth and RCA, Camden in establishing a realistic design specification. He designed all the circuits for the unit including: rf low-noise amplifiers, frequency multipliers, a high-speed digital frequency divider, active filters and clamps, a frequency limiter/discriminator and output buffers. The design work included use of advanced SOS digital ICs.

Eldon Fisher, by understanding and supporting the complete design and evaluation process, achieved technical excellence on the REMBASS Receiver Synthesizer design.

SIGMA project. Cited for Technical Excellence is **Tony Cortizas,** for significant professional achievements on the SIGMA project proposal. The SIGMA proposal was a joint involvement for Ford Aerospace and Communications Corporation (FACC), BDM Corporation and RCA in response to a competitive Army procurement request.

Tony made many contributions in the systems and communcations areas, but particularly outstanding were his contributions on the network-processing subsystem and the baseline system. He quickly became familiarized with the current fielded equipments, the desired distribution-processing objectives, and the state of the art and related technologies. Tony creatively applied this knowledge to addressing the major networking problems and formulating a network-processing subsystem-design approach. The understanding of the problem, and the design of this subsystem were of major importance in the overall technical approach.

First-quarter 1982 MSR award-winners announced

Harmening

Magness

Phillips

Wainwright

Bernie Matulis, Chief Engineer, Missile and Surface Radar, announced that the following award-winners will receive a commemorative desk plaque and a current text or reference book, and will be honored at a function next year.

W.A. Harmening—For outstanding contributions to the Advanced Tactical Radar proposal in the conception and verification of a unique antenna deployment design. His single-axis hinge solution permits storage of a complete two-faced array on a standard Army transport vehicle, with automatic deployment to the transmit position within 15 minutes. Verification of his unusual design was provided in a scale model of the proposed radar.

P.L. Magness—For design and development of a high-performance airborne S-band data transponder. Highly successful system testing conducted with the AN/SPY-1 radar has clearly demonstrated the feasibility of the system and has verified its applicability as a secure digital communications link virtually impervious to electronic countermeasures. His design has established a baseline for similar systems being proposed in new radar system developments.

D.A. Phillips—For important systems engineering contributions to the FAA Air Traffic Control Advanced Automation System. In assisting the FAA in its definition of overall requirements, Mr. Phillips demonstrated the value of systems engineering approaches to establishing system boundaries and then defining requirements within those boundaries. His work in this area has provided a structured approach to the FAA objectives of functional commonality and control center consolidation.

A.W. Wainwright—For his development of an on-line interactive programming system, "IO 8 BASIC," for use on Applicon Graphic Systems. His system permits users to program and interface with the Applicon directly in BASIC, without an external operating system, thereby providing self-documenting operator prompt and response programs. An early version of IO 8 BASIC has received immediate, enthusiastic acceptance throughout the Applicon user community.

Solid State Division awards for technical excellence

First-quarter 1982 technical excellence awards were given to the individuals shown on this page. Pictured below from left to right are:

Glen Shimomura
Joseph Harmon
Paul Sferrazza
Joseph Foy

As team contributors to the design of the CDP1804A, their efforts relative to device models, peripheral circuits, test analysis and design verification led to the successful development of the microprocessor designs.

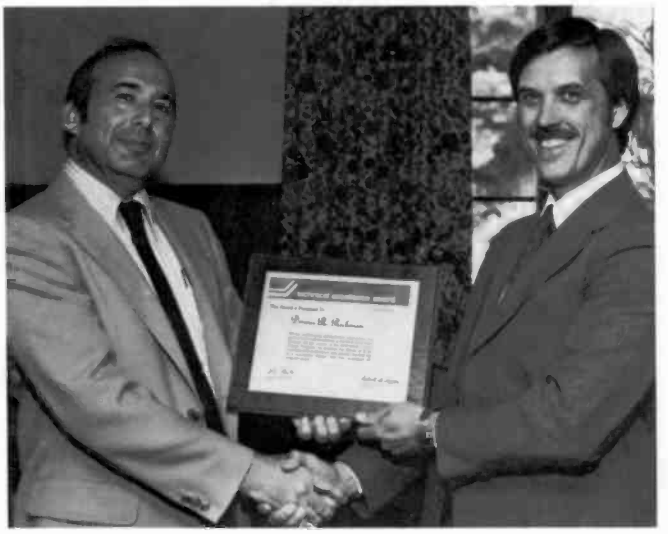

In the above picture **Dennis Richman** (right) is being presented his award by **Joel Overman** (left), Section Manager. As an individual contributor, Dennis directed and established new procedures that had a direct impact on the success of the CDP180A layout design program.

In the picture below, the outstanding team achievement of **Andrew Dingwall** (right) and **Victor Zazzu** (left) in the design and construction of the low-powered 8-Bit Flash Aid Converter has placed RCA in a leadership position in the development and production of digital TV.

In the picture above, the outstanding team achievements of **Richard Auerbach** (left) and **Howard Rifkin** (right) led to the successful development of the Sandra II General Mask Array Format Program. As a result of their efforts, significant increases have been achieved in mask specification productivity.

These recipients were selected by the Somerville Technical Excellence Committee based on the technical achievement, business value, and individual performance of each of their efforts.

Editorial Representatives

Contact your Editorial Representative at the TACNET numbers listed here to schedule technical papers and announce your professional activities.

Cablevision Systems

		TACNET
*John Ovnick	Van Nuys, California	534-3011

Commercial Communications Systems Division (CCSD)

*Bill Sepich	Camden, New Jersey	222-2156
Krishna Praba	Gibbsboro, New Jersey	222-3605
Andrew Billie	Meadowlands, Pennsylvania	228-6231

Consumer Electronics (CE)

*Eugene Janson	Indianapolis, Indiana	422-5208
Francis Holt	Indianapolis, Indiana	422-5217
Chuck Limberg	Indianapolis, Indiana	422-5117
Don Willis	Indianapolis, Indiana	422-5883
Byron Taylor	Indianapolis, Indiana	426-3247

Government Systems Division (GSD)

Advanced Technology Laboratories

*Merle Pietz	Camden, New Jersey	222-2161
Ed Master	Camden, New Jersey	222-2731

Astro-Electronics

*Frank Yannotti	Princeton, New Jersey	229-2544
Carol Klarmann	Princeton, New Jersey	229-2919

Automated Systems

*Paul Seeley	Burlington, Massachusetts	326-3095
Dale Sherman	Burlington, Massachusetts	326-2985

Government Communications Systems

*Dan Tannenbaum	Camden, New Jersey	222-3081
Harry Ketcham	Camden, New Jersey	222-3913

GSD Staff

*Ed Moore	Cherry Hill, New Jersey	222-5833

Missile and Surface Radar

*Don Higgs	Moorestown, New Jersey	224-2836
Jack Friedman	Moorestown, New Jersey	224-2112
Graham Boose	Moorestown, New Jersey	224-3680

National Broadcasting Company (NBC)

*Bob Mausler	New York, New York	324-4385

Patent Operations

Joseph Tripoli	Princeton, New Jersey	226-2992

Picture Tube Division (PTD)

*Ed Madenford	Lancaster, Pennsylvania	227-3657
Nick Meena	Circleville, Ohio	432-1228
Jack Nubani	Scranton, Pennsylvania	329-1499
J.R. Reece	Marion, Indiana	427-5566

RCA Communications

		TACNET
American Communications		
*Murray Rosenthal	Princeton, New Jersey	258-4192
Carolyn Powell	Princeton, New Jersey	258-4194
Global Communications		
*Dorothy Unger	New York, New York	323-7348

RCA Limited (Canada)

Bob McIntyre	Ste Anne de Bellevue	514-457-9000

RCA Records

*Greg Bogantz	Indianapolis, Indiana	424-6141

RCA Service Company

*Joe Steoger	Cherry Hill, New Jersey	222-5547
Ray MacWilliams	Cherry Hill, New Jersey	222-5986
Dick Dombrosky	Cherry Hill, New Jersey	222-4414

Research and Engineering

Corporate Engineering

*Hans Jenny	Cherry Hill, New Jersey	222-4251

Laboratories

Eva Dukes	Princeton, New Jersey	226-2882

"SelectaVision" VideoDisc Operations

*Nelson Crooks	Indianapolis, Indiana	426-3164

Solid State Division (SSD)

*John Schoen	Somerville, New Jersey	325-6467
Power Devices		
Harold Ronan	Mountaintop, Pennsylvania	327-1633 or 327-1827
Integrated Circuits		
Dick Morey	Palm Beach Gardens, Florida	722-1262
Sy Silverstein	Somerville, New Jersey	325-6168
John Young	Findlay, Ohio	425-1307
Electro-Optics and Power Devices		
John Grosh	Lancaster, Pennsylvania	227-2077
Solid State Technology Center		
Judy Yeast	Somerville, New Jersey	325-6248

***Technical Publications Administrators, responsible for review and approval of papers and presentations, are indicated here with asterisks before their names.**

POWERFUL COMPUTER AIDS make it possible to obtain accurate descriptions of microwave networks, using the simultaneous color display of all four S-parameters shown here in either rectangular or polar form. S-parameters, or complex scattering vectors, are related to the currents and voltages in two-port microwave networks. Researchers at RCA Laboratories (see article in this issue by Perlman, et al.) generated these plots by use of a highly interactive, user-oriented, automatic network analyzer system under the control of a software program named PLANA/1000 that they developed. The system is based on standard Hewlett Packard 8409 hardware, interfaced with an HP1000 disk-based minicomputer and a color-graphics subsystem.

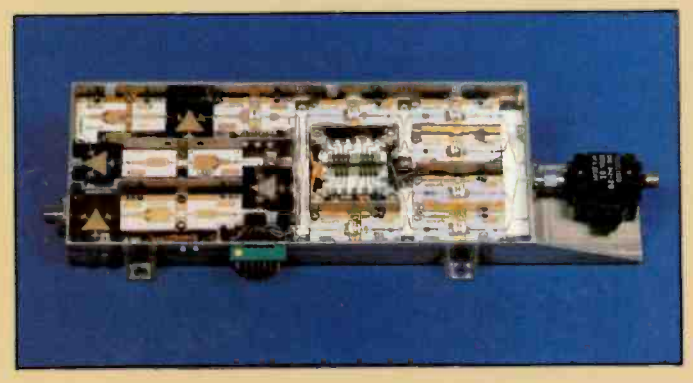

THE SOLID-STATE POWER AMPLIFIER (SSPA), a version of which is shown here, will power RCA's downlink satellite communications beginning with the Satcom bird scheduled for launch this Fall (see article in this issue by Wolkstein and LaPrade). RCA has decided to replace the standard C-band traveling-wave-tube amplifier (TWTA) with this SSPA because it performs better in all areas dependent on the linearity of power-transfer characteristics. Additional rf subcarriers can be accommodated by each SSPA channel in multicarrier service, thereby resulting in more revenue. Reliability and service life are expected to greatly exceed that of the TWTA.

RCA Engineer

A technical journal published by
Corporate Research and Engineering
"by and for the RCA engineer"

Bldg 204-2, Cherry Hill, NJ 08358
Forwarding and return postage guaranteed

BULK RATE
US Postage
PAID
Phila., Pa.
Permit No. 2906

LCTT EM MUSSELMANN
PO BOX 9
STRASBURG
PA 17579

Printed in the U.S.A.
Form No. RE-27-5